UNIVERSITY OF CAPE TOWN

ANGLO PLATINUM

Exploration of the mechanism of rhodium(III) co-precipitation with copper sulfide (at low rhodium concentrations) incorporating the cationic substitution reaction path

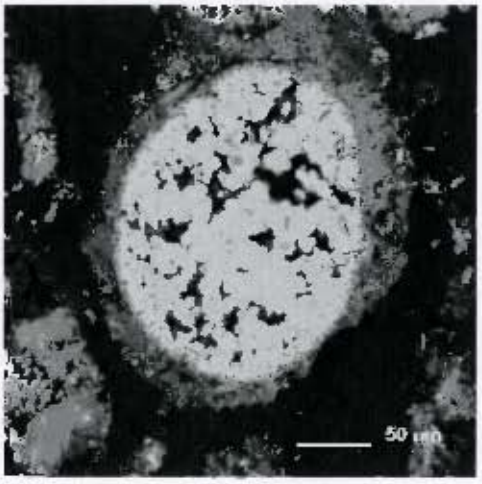

Barry Mc George
B.Sc. (Chem. Eng.)

Department of Chemical Engineering
University of Cape Town
Rondebosch
7700

Nov 2007

This half thesis is prepared in partial fulfilment of the requirements of the Taught Masters Degree in Hydrometallurgy

I certify that this thesis is my work. It has not been submitted to any other university for any other degree.

Signed by candidate

Barry Mc George

Nov 2007

Abstract

This study is a preliminary investigation into the mechanism and kinetics of Rh^{3+} co-precipitation with CuS upon aqueous thiosulphate addition to acidic base metal sulphate solutions, where Rh^{3+} concentration is two orders of magnitude lower than Cu^{2+}, over 50 – 150 °C. The heterogeneous cationic substitution has been identified as a new precipitation path in metal sulfide co-precipitation, namely, the reaction between more soluble, co-precipitated metal sulphide (CuS) and the less soluble cation in solution (Rh^{3+}), with the large K_{SP} difference providing the chemical driving force.

The analysis of the available literature, thermodynamic modelling and comparative kinetic studies of the specific reactions systems suggests the following simplified Rh co-precipitation mechanism (leaving out spectator ions):

$$Cu^{2+} + S_2O_3^{2-} + H_2O \rightarrow CuS + H_2SO_4 \quad (1)$$

$$2Rh^{3+} + 3S_2O_3^{2-} + 3H_2O \rightarrow Rh_2S_3 + 3H_2SO_4 \quad (2)$$

$$Cu^{2+} + (CuS)_x.nH_2S \rightarrow (CuS)_{(x+1)}.(n-1)H_2S + 2H^+ \quad (3)$$

$$Rh^{3+} + CuS.nH_2S \rightarrow CuRhS_2.(n-1)H_2S + 2H^+ + e^- \quad (4.1)$$

$$2Rh^{3+} + CuS.nH_2S \rightarrow CuRh_2S_4.(n-3)H_2S + 6H^+ \quad (4.2)$$

$$2Rh^{3+} + 3CuS_s \rightarrow Rh_2S_3 + 3Cu^{2+} \quad (5)$$

Initially, homogeneous reactions occur prior to perceptible nucleation (1)(2), which is then followed by heterogeneous crystal growth, (auto-)catalysed by the presence of the precipitated metal sulfides (3)(4). Rh^{3+} and Cu^{2+} compete for the available aqueous sulfide during the initial ionic precipitation (1)(2), where the bulk of the Rh precipitation occurs. When $[Rh^{3+}] << [Cu^{2+}]$, the overall $- r_{Cu(II)}$ (1)(3) >> $- r_{Rh(III)}$ (2)(4), consuming the available sulfide and limiting the amount of ionic Rh^{3+} precipitation. The CuS formed continues to precipitate Rh^{3+} via the cationic substitution reaction (5), resulting in the enrichment of Rh towards the edge of the CuS particles. As the ratio of aqueous sulfide to CuS is sufficiently decreased, the dominant reaction path switches from ionic precipitation to cationic substitution, which either takes the Rh precipitation to completion or stops the precipitation through the passivation of the CuS.

Temperature affects the reaction paths by affecting the relative ionic metal sulfide precipitation rates of the competing metals. At 50 – 95 °C, the large amount of aqueous Cu^{2+} effectively decreases the rate and extent of Rh co-precipitation, because the substitution reaction path is significantly slower that ionic precipitation; and the Rh passivates the CuS particle. At 150 °C, Cu^{2+} has negligible impact on the Rh precipitation rate and extent, where CuS formed has greater surface area and the substitution reaction takes the Rh precipitation to completion. The initial ionic co-precipitation rate is highly temperature sensitive and is probably chemical reaction controlled, while crystal growth and cationic substitution reactions over the middle period are independent of temperature, indicating a switch to mass transfer, particularly at 150 °C.

Barry Mc George,
PO Box 3187, Rustenburg, 2128
bmcgeorge@angloplat.com ; bmcgeorge789@gmail.com

Synopsis

This study is a preliminary investigation into the mechanism of rhodium(III) (Rh^{3+}) co-precipitation with copper sulfide (CuS) upon aqueous thiosulfate addition to synthetic, acidic base metal sulphate solutions, where the Rh^{3+} concentration is two orders of magnitude lower than the cupric ion (Cu^{2+}). Theoretical thermodynamic and comparative kinetic studies have been performed over 50 – 150 °C on the individual reaction paths in isolation and simultaneously during co-precipitation, namely:

1. **Ionic Rh^{3+} precipitation** with aqueous sulfide addition in the absence of Cu^{2+} in solution,
2. Rh^{3+} precipitation through the **cationic substitution** reaction of Cu^{2+} onto CuS previously precipitated,
3. Rh^{3+} and Cu^{2+} **co-precipitation** upon aqueous sulfide addition, occurring through paths 1 and 2.

The kinetics of the individual reaction systems and relative kinetics of simultaneous precipitation of Cu and Rh in the co-precipitation system are used to infer the dominant reaction path of the co-precipitation system.

At these conditions, thermodynamic modelling shows that ionic Rh^{3+} precipitation is completely selective over Cu^{2+} precipitation upon the addition of a sulfide-containing reagent, because Rh_2S_3 is significantly more insoluble than CuS. However, in practice, the selectivity is sometimes sacrificed for improved precipitation kinetics and extent by adding a large excess of sulfide above the Rh requirement. The excess sulfide is preferentially consumed by CuS precipitation, limiting the amount of ionic Rh precipitation.

The cationic substitution reaction:

$$2\ Rh^{3+}_{aq} + 3\ CuS_s \leftrightarrow\ Rh_2S_{3\,s} + 3\ Cu^{2+}_{aq} \qquad \Delta G_{rxn} = -160\ kJ/mol\ using\ HSC\ Chemistry^{®}$$

has a large chemical driving force owing to the large difference in solubility products of CuS and Rh_2S_3. This type of irreversible reaction path has not been considered in kinetic and mechanistic studies of metal sulfide co-precipitation reviewed in the literature. Thus, this study takes a novel approach.

Kinetic tests were performed under similar conditions in a batch pressure vessel at constant agitation and initial operating volume. A nitrogen atmosphere was maintained to prevent re-oxidation, particularly at elevated temperatures. The tests were designed specifically to maintain comparative precipitation kinetics of the various reaction systems, particularly the ratio of sulfide addition to Rh^{3+}, whether in the form of aqueous thiosulfate or previously precipitated CuS. Synthetic feed concentrations were approximately 13200 mg/l Cu^{2+}, 5500 mg/l Ni^{2+}, 15 g/l sulfuric acid and 90 mg/l Rh^{3+}. Aqueous sodium thiosulfate was added at 37 times the Rh requirement.

The measured Rh precipitation extent and modelled kinetics for the three systems at 95 and 150 °C are summarised in the illustration below. Kinetic modelling shows three distinctive precipitation periods, namely, the initial period showing very fast precipitation, the middle period approximated by pseudo first order kinetics and a final period showing a slow approach to completion, limited by passivation of the active surface, for all three systems. At 50 °C, an induction period precedes the initial period prior to perceptible nucleation. At atmospheric temperatures, the empirical logarithmic fit provides a better model of the data over the whole precipitation profile, including the initial precipitation and final passivation. At elevated temperatures, the pseudo first order model provides an almost perfect fit over the middle period and final period. These models are used to estimate the reaction rates.

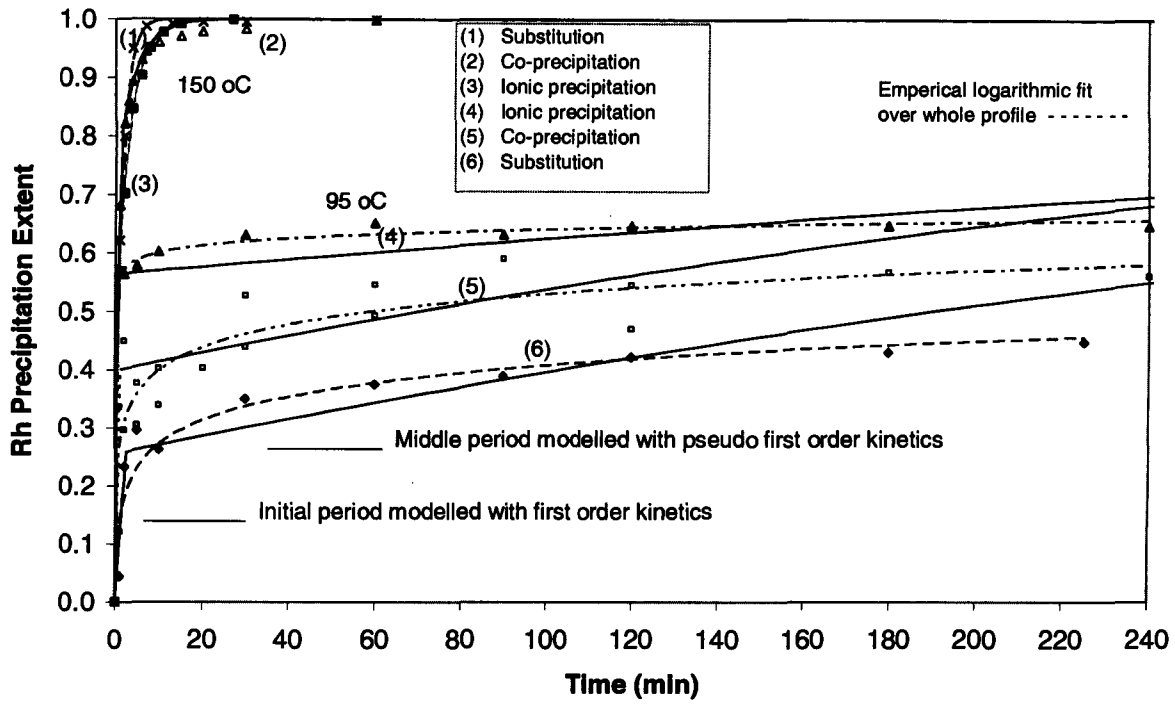

The bulk of Rh precipitation occurs during the initial period (1 – 2 min) for all three systems, primarily due to the large excess of sulfide being added. The initial rate decreases rapidly due to the consumption of the thiosulfate by decomposition to elemental sulfur in the ionic precipitation system, the consumption thiosulfate with CuS precipitation in the co-precipitation system and passivation of the CuS particles with increased Rh precipitation in the substitution reaction system. At 50 – 95 °C, the rate of Rh precipitation in the ionic precipitation system is significantly faster than the cationic substitution. As expected, the Rh precipitation rate in the co-precipitation system is between that of the ionic and substitution systems. At 150 °C, similar precipitation rates are observed for the three reaction systems and the dominant precipitation path in the co-precipitation system cannot be determined without the comparison of Rh distribution in the CuS.

The analysis of the available literature, thermodynamic modelling and comparative kinetic studies of the specific reactions systems suggests the following reaction mechanism for Rh co-precipitation with CuS:

$$Cu^{2+} + S_2O_3^{2-} + H_2O \rightarrow CuS + H_2SO_4 \quad (1)$$

$$2Rh^{3+} + 3S_2O_3^{2} + 3H_2O \rightarrow Rh_2S_3 + 3H_2SO_4 \quad (2)$$

$$Cu^{2+} + (CuS)_x.nH_2S \rightarrow (CuS)_{(x+1)}.(n-1)H_2S + 2H^+ \quad (3)$$

$$Rh^{3+} + CuS.nH_2S \rightarrow CuRhS_2.(n-1)H_2S + 2H^+ + e- \quad (4.1)$$

$$2Rh^{3+} + CuS.nH_2S \rightarrow CuRh_2S_4.(n-3)H_2S + 6H^+ \quad (4.2)$$

$$2Rh^{3+} + 3CuS_s \rightarrow Rh_2S_3 + 3Cu^{2+} \quad (5)$$

Initially, homogeneous reactions occur prior to perceptible nucleation (1)(2), which is then followed by heterogeneous crystal growth, (auto-)catalysed by the presence of the precipitated metal sulfides (3 and 4). Rh^{3+} and Cu^{2+} compete for the available aqueous sulfide during the initial ionic precipitation (1)(2), where the bulk of the Rh precipitation occurs. When $[Rh^{3+}] << [Cu^{2+}]$, the overall $-r_{Cu^{2+}}$ (1)(3) >> $-r_{Rh^{3+}}$ (2)(4), consuming the available sulfide and limiting the amount of ionic Rh^{3+} precipitation. The CuS formed continues to precipitate Rh^{3+} via the cationic substitution reaction (5), resulting in the

enrichment of Rh towards the edge of the CuS particles. As the ratio of aqueous sulfide to CuS is sufficiently decreased, the dominant reaction path switches from ionic precipitation to cationic substitution, which either takes the Rh precipitation to completion or stops the precipitation through the passivation of the CuS.

At 80 – 95 °C, at the relative concentrations of this study, Cu precipitation is 2 – 3 times faster than Rh on a relative basis, where the last 55 – 65 % of the Rh will have to precipitate via the cationic substitution reaction path, but passivation limits the overall precipitation extent, even at 37 times excess of the sulfide requirement of Rh. The presence of large amount of Cu^{2+} effectively decreases the rate and extent of Rh co-precipitation, because the substitution reaction path is significantly slower that ionic precipitation and passivation occurs. At 150 °C, Cu precipitation is only 30% faster than Rh, reducing the amount of precipitation via the substitution path to 10 – 20 %, taking the Rh precipitation to completion. Thus, at 150 °C, aqueous Cu^{2+} has negligible impact on the Rh precipitation rate or extent. The bulk of Rh precipitation occurs during the initial period, hence the initial precipitation conditions has a direct impact on the CuS carrying capacity and overall precipitation extent.

Mechanistic changes across the co-precipitation systems are expected with increasing precipitation extent, progressing from primary nucleation (1)(2) to crystal growth (3) and co-precipitation of the mixed sulfides (4), followed by cationic substitution (5). The rate-determining step probably switches from chemical reaction to mass transfer, particularly at 150 °C. This is supported by the excellent pseudo first order kinetics over the middle period and final period (R^2: 0.999 for ionic and substitution systems; 0.95 for co-precipitation). The fact that model holds true for ionic and co-precipitation systems, as well as substitution reaction systems, supports the argument that the systems are being controlled by the same rate-controlling step, namely, the mass transfer of Rh^{3+} to the surface, which is a **first order process.** This is supported by Roy's study of Ni and Cu co-precipitation at 150 °C, where the residence time of a turbulent pipe reactor required is 5 – 10 % of the 4-stage CSTR (Roy, 1961). At atmospheric temperatures, the near independence of precipitation rate and temperature over the middle period could result from passivation. Thus, specific mass transfer test work is required to verify mass transfer limitations over the initial period and middle period separately over atmospheric and elevated temperatures.

In order to achieve complete Rh recovery in the Rhodium Removal Section at Rustenburg Base Metals Refiners (Pty) Ltd, a process will have to be developed and designed to operate at elevated temperatures. Alternatively, mechanical activation of the precipitated CuS could be used to overcome the passivation at atmospheric temperatures. Knowledge of the rate-controlling step is critical for optimal design of a precipitation system and specific mass transfer investigations are required to quantify possible improved precipitation extent at more turbulent conditions.

In general, this work identifies an alternative precipitation path in the mechanism of metal sulfide co-precipitation. The heterogeneous cationic substitution reaction, with solubility differences providing the chemical driving force, must be considered when interpreting kinetics of co-precipitation mechanisms, particularly when co-precipitating a more insoluble metal sulfide at a much lower concentration from more soluble metal sulfides at a much higher concentration. The thermodynamic driving force (ΔG) is the dominant effect on selectivity when the concentrations are similar. In the co-precipitation mechanism, both the thermodynamics and overall relative kinetics must be taken into account. The relative difference in the metal sulfide solubility products and the relative concentrations affect the overall precipitation rate, which affects the selectivity of competing precipitation paths. It is speculated that the cationic substitution reaction could be an additional reaction path during the period before perceptible nucleation, where S-containing Cu complexes CuS, associates and amorphous clusters of CuS could be replaced by the Rh^{3+}, compared to ionic co-precipitation forming $CuRhS_2$.

Acknowledgements

I would like to acknowledge and sincerely thank the following people and organisations for their contributions towards this body of work:

Anglo Platinum for the opportunity of attending the masters program on a part time and full time basis with full company benefits and for sponsoring the experimental program.

Anglo Research team and facilities, particularly Hydrometallurgy and Chemistry Departments at Crown Mines campus and Mineralogy Department at Germiston campus, particularly Petra, Schultz, Kriba, Johann, Patricia (PV operating technition), Cathy and Doug.

Prof. Mike Nicol for presenting an excellent taught part of the Masters Degree in Hydrometallurgical, presented at University of Cape Town, and his comments in this study. I would certainly recommend the course to any chemical engineer working in the Hydrometallurgical field.

Prof. Alison Emslie Lewis for her supervision, technical expertise and patience.

Adjunct Prof. Peter Gaylard for convening the program, for his supervision and comments.

Zdenek Hofirek for his mentorship and technical expertise over the last 10 years and for providing translations of Russian papers.

Ester, Christine and Duncan, for their gracious proof-reading.

and dearest Caitlin, for her sweet patty cakes and support.

TABLE OF CONTENTS

ABSTRACT ii

SYNOPSIS iii

ACKNOWLEDGEMENTS vi

TABLE OF CONTENTS vii

LIST OF ILLUSTRATIONS x

NOMENCLATURE xv

1 INTRODUCTION 1

1.1 BACKGROUND 1
1.2 OBJECTIVES 2
1.3 APPROACH, SCOPE AND LIMITATIONS 3
1.4 THESIS OUTLINE 3

2 LITERATURE REVIEW 5

2.1 METAL SULFIDE (CO-)PRECIPITATION MECHANISM 5
2.2 RH PRECIPITATION THROUGH THE CATIONIC SUBSTITUTION REACTION 8
2.3 COVELLITE PRECIPITATION 10
2.4 HYPOTHESIS FOR RH CO-PRECIPITATION MECHANISM WITH CUS 11

3 THEORY 13

3.1 SULFIDE PRECIPITATION 13
3.1.1 Ionic precipitation 13
3.1.2 Cationic substitution 14
3.1.3 Metal sulfide co-precipitation 15

3.2 KINETIC MODELLING THEORY 15
3.2.1 Homogeneous ionic precipitation 16
3.2.2 Pseudo first order kinetics 16
3.2.3 Pseudo second order kinetics 17
3.2.4 Modelling the Arrhenius rate equation 17
3.2.5 Modelling heterogeneous ionic precipitation reactions 18
3.2.6 Cationic substitution reaction 20
3.2.7 Co-precipitation reaction 21
3.2.8 Calculation of the reaction rate 21

4 EXPERIMENTAL DESIGN 23

4.1 OVERVIEW 23
4.1.1 Thermodynamic study 23
4.1.2 Kinetic study 23

4.2 METHODOLOGY AND PROCEDURE 24
4.2.1 Feed preparation 24
4.2.2 General operating procedure 25
4.2.3 Ionic Rh precipitation procedure 26
4.2.4 Substitution reaction procedure 27
4.2.5 Rh co-precipitation with in situ CuS with sulfide addition procedure 27

4.3 SAMPLE PREPARATION 27
4.3.1 General filtration procedure 27

4.3.2 Solids preparation 28

4.4 EXPERIMENTAL EQUIPMENT 28
4.4.1 Pressure vessel batch reactor 28
4.4.2 Miscellaneous equipment 30

4.5 SPECIFIC TEST CONDITIONS 30
4.5.1 Calculated feed conditions 30
4.5.2 Specific test conditions 30
4.5.3 Analytical techniques and approach 32
4.5.4 Mineralogical techniques 32

5 CHEMISTRY AND THERMODYNAMIC MODELLING 33

5.1 CHEMICAL REACTIONS 33
5.1.1 Reducing the solution potential 34
5.1.2 Ionic precipitation using sodium thiosulfate addition 35
5.1.3 Rh precipitation through the substitution reaction 35
5.1.4 In situ Rh co-precipitation with CuS using thiosulfate addition 35
5.1.5 Rh precipitation through hydrolysis 36
5.1.6 Thiosulfate degradation 36
5.1.7 Alternative Rh precipitation through substitution with hydroxides and oxides 36

5.2 EH-PH DIAGRAMS OF S-CU-RH-H_2O SYSTEM 37
5.2.1 General Eh-pH diagram using all species in HSC Chemistry® 37
5.2.2 Metastable Eh-pH diagrams excluding sulfate ions 39
1. Temperature 41
2. Molality 42

5.3 EQUILIBRIUM SOLUTION CHEMISTRY MODELLING 43
5.3.1 Meta-stable system 43
1. Concentration Effect 43
2. Temperature Effect 43
3. Initial acid effect 45

5.4 DISCUSSION OF CHEMISTRY AND THERMODYNAMIC MODELLING 46

5.5 PROPOSED MECHANISM 46

6 KINETIC STUDY OF INDIVIDUAL SYSTEMS 47

6.1 ACCURACY OF MEASUREMENT 47
6.1.1 Solution analysis relative error 47
6.1.2 Solids analysis relative error 48
6.1.3 Post precipitation of Rh and Cu in solutions 49
6.1.4 Feed concentrations 50
6.1.5 Mass balance and metal accounting 52
6.1.6 Repeat tests and replicates 53
6.1.7 Sample volumes removed 54
6.1.8 Redox potential measurement 54

6.2 SUMMARY OF PRECIPITATION RESULTS 55
6.2.1 Final feed concentrations 55
6.2.2 Precipitation profiles 55

6.3 IONIC RH PRECIPITATION 58
6.3.1 Temperature effect 58
6.3.2 Stoichiometry 59
6.3.3 Stoichiometric thiosulfate addition 60

6.4 CATIONIC SUBSTITUTION 61
6.4.1 Temperature effect *61*
6.4.2 Cu leaching during substitution *61*
6.4.3 Stoichiometry *62*

6.5 RH CO-PRECIPITATION 64
6.5.1 Determining the appropriate precipitation profile results *64*
6.5.2 Temperature effect on Rh and Cu precipitation *66*
6.5.3 Comparison of Rh and base metal precipitation rates *67*
6.5.4 Selectivity of base metal precipitation *69*
6.5.5 Stoichiometry *70*
6.5.6 Rh distribution in CuS *71*

6.6 MODELLING KINETICS 75
6.6.1 Preliminary testing *75*
6.6.2 Testing for first or second order pseudo kinetics of the middle period *78*
6.6.3 Predicting the overall rate constant using Arrhenius Law *79*
6.6.4 Predicting the overall Cu rate constant using Arrhenius Law *82*
6.6.5 Kinetic model development *84*
6.6.6 Prediction of the reaction rates from the models *86*
6.6.7 Passivation limiting the precipitation extent *88*
6.6.8 Initial conditions affecting precipitation rate and overall extent *88*
6.6.9 Mechanistic changes *89*
6.6.10 Summary of kinetic modelling *90*

7 COMPARATIVE KINETICS 91

7.1 EVALUATION OF VALIDITY OF COMPARISON OF REACTION SYSTEMS 91

7.2 DISCUSSION 92
7.2.1 Comparative kinetics of reaction paths at 50 °C *92*
7.2.2 Comparative kinetics of reaction paths at 80 °C *94*
7.2.3 Comparative kinetics at 95 °C *96*
7.2.4 Comparative kinetics at 150 °C *97*
7.2.5 Comparative kinetics using solution basis *99*

7.3 SUMMARY OF COMPARATIVE KINETICS OF INDIVIDUAL SYSTEMS 100

8 RH CO-PRECIPITATION MECHANISM 101

8.1 MECHANISM 101
8.2 MECHANISTIC CHANGES 102

CONCLUSIONS 103

RECOMMENDATIONS 107

REFERENCES 109

APPENDICES ..... - 1 -

Appendices - Table of Contents

LIST OF ILLUSTRATIONS

List of Tables

Table 3.1: Solubility product (K_{SP}) using molar basis on metal 15

Table 4.1: Synthetic feed make-up concentrations calculated for various tests 24
Table 4.2: Pressure Vessel Specifications 28
Table 4.3: Calculated feed concentrations after reagent injection prior to reaction 30
Table 4.4: Specific test conditions 31
Table 4.5: Analytical method used for various elements 32

Table 5.1: Gibbs free energy of the various chemical reactions 34

Table 6.1: Standard deviation on solution assays for six repeat analyses 47
Table 6.2: Average standard deviation on concentrations from duplicate analyses 48
Table 6.3: Average standard deviation on solids concentrations 48
Table 6.4: Comparison of Rh designed, measured and predicted feed concentrations 51
Table 6.5: Comparison of predicted and measured concentrations for remaining elements after dilution 51
Table 6.6: Metal accounting comparison using theoretical and measured feed concentrations 53
Table 6.7: Feed concentrations used in the kinetic study analysis 55
Table 6.8a: Summary of Rh precipitation extent for all reaction systems (solid basis) 56
Table 6.8b: Summary of Rh precipitation extent for all reaction systems (solution basis) 56
Table 6.8c: Summary of Cu precipitation extent for all reaction systems (solids basis) 57
Table 6.8d: Rh precipitation rate calculated from modelled data for the middle period (solid basis) 57
Table 6.9: Measured ionic Rh precipitation stoichiometry ratios 59
Table 6.10: Measured ionic Cu precipitation stoichiometry with thiosulfate addition 62
Table 6.11: Measured Rh cationic substitution stoichiometry 63
Table 6.12: Relative Cu and Rh precipitation rate (solids basis) 68
Table 6.13: Measured Rh and Cu co-precipitation stoichiometry 70
Table 6.14: Rh precipitation first order kinetics linearisation constants over the initial and middle period (solids basis) 76
Table 6.15: Comparison of pseudo first and second order kinetics for middle period 78
Table 6.16: Calculation of initial rate constants assuming first order kinetics (solids basis) 80
Table 6.17: Determination of Arrhenius rate constants for the initial period over 50 – 95 °C and 95 – 150 °C 81
Table 6.18: Predicted overall initial reaction rate constant over the initial period for 50 – 95 °C 81
Table 6.19: Determination of Arrhenius rate constants for precipitation over the middle period for 50 – 95 °C and 95 – 150 °C 82
Table 6.20: Predicted and measured overall rate constant over the middle period for 50 – 95 °C 82
Table 6.21: Calculation of the initial rate constants of Cu precipitation (solids basis) 83
Table 6.22: Cu co-precipitation pseudo first order kinetics of the middle period (solids basis) 83
Table 6.23: Determination of Arrhenius rate constants for precipitation over the initial period 83
Table 6.24: Predicted and measured overall initial rate constant for 95 – 150 °C 83

Table 7.1: Cu precipitation comparison on terminal samples 91
Table 7.2: Rh precipitation comparison on terminal samples 92

List of Figures

Figure 4.1: Pressure Vessel System, showing temperature controller, magnetic drive of agitator, pressure gauge, sampling system with sample and nitrogen blow-back valves and cooling water. 29

Figure 5.1: Gibbs free energy for main Rh and Cu precipitation reactions over 0 – 200 °C 35

Figure 5.2: Eh-pH diagram of S-Cu-Rh-H_2O base case system for all speciation at 95 °C; upon reducing the potential with sulfide-containing reducing agent, Rh^{3+} first forms elemental Rh before converting to $RhS_{0.889}$, then Rh_3S_4 and Rh_2S_3; additional reduction will convert it back to Rh metal in the reverse sequence; at high oxidation potential, pH adjustment approaching 2 will convert Rh^{3+} to Rh_2O_3. Metal reduction is not noticed in practice and is an anomaly in the HSC calculation caused by the stability of the sulfate ion. 38

Figure 5.3: Eh-pH diagram of S-Cu-Rh-H_2O base case system for all speciation at 95 °C, only showing Rh_2S_3 dominant Rh speciation; upon reducing the potential with sulfide-containing reducing agent, Rh^{3+} first forms elemental Rh before converting to Rh_2S_3 and back to Rh metal; at high oxidation potential, pH adjustment approaching 0.2 will convert Rh^{3+} to Rh_2O_3, though in real systems Rh^{3+} is stable to pH < 3, probably due to complexation. Rh reduction to metal prior to forming a Rh sulfide is caused by an anomaly in HSC program due to the stability of the sulfate ion, which is not seen in practice. 38

Figure 5.4: Eh-pH diagram of S-Cu-Rh-H_2O metastable base case at 95 °C, particularly omitting species with sulfur of positive oxidation state and only including Rh_2S_3. Dashed lines indicate region of dominant ions in solution. Rh and Cu reduction from ion to metal no longer occurs. 39

Figure 5.5: EH-pH diagram of S-Cu-Rh-H_2O metastable system at 95 °C showing dominant Cu speciation, particularly omitting species with sulfur of positive oxidation state and only including Rh_2S_3. Cu reduction from ion to metal no longer occurs. 40

Figure 5.6: Eh-pH diagram of S-Cu-Rh-H_2O metastable system at 95 °C showing dominant Rh speciation, particularly omitting species with sulfur of positive oxidation state and only including Rh_2S_3. Rh reduction from ion to metal no longer occurs in the acidic pH. 40

Figure 5.7: Eh-pH diagram of S-Cu-Rh-H_2O metastable system, particularly omitting species with sulfur of positive oxidation state, combined for 25 and 150 °C, showing effect of temperature on Rh speciation. 41

Figure 5.8: Eh-pH diagram of S-Cu-Rh-H_2O system for metastable system at 95 °C with selected speciation, particularly omitting species with sulfur of positive oxidation state, at 95 °C, showing effect of Rh activity on Rh species distribution at molality of $1x10^{-4}$, $1x10^{-3}$ and $1x10^{-1}$ mol/kg; Rh^{3+} stability increases with decreasing molality. 42

Figure 5.9: Equilibrium composition with thiosulfate addition to 100 mg/l Rh containing 20 g/l Cu and 15 g/l sulfuric acid at 95 °C, showing equilibrium composition for meta-stable species; Rh precipitation with sulfide is completely selective over Cu precipitation. 44

Figure 5.10: Equilibrium composition with thiosulfate addition to 10 g/l Rh containing 20 g/l Cu and 15 g/l sulfuric acid at 150 °C, showing equilibrium composition for meta-stable species; Rh precipitation with sulfide is completely selective over Cu precipitation. 44

Figure 5.11: Equilibrium composition with thiosulfate addition to 10 g/l Rh containing 20 g/l Cu and 15 g/l sulfuric acid at 150 °C, showing equilibrium composition for meta-stable species; Rh precipitation with sulfide is completely selective over Cu precipitation. 45

Figure 5.12: Equilibrium composition with thiosulfate addition to base case with 100 mg/l Rh containing 20 g/l Cu and 0.1 g/l sulfuric acid at 95 °C, showing equilibrium composition for meta-stable species; Rh precipitation with sulfide is completely selective over Cu precipitation, irrespective of initial acid concentration; Rh precipitation is shifted right while acid concentration increases, thus acid plays a role in the Rh precipitation. 45

Figure 6.1: Ionic Rh precipitation at 50, 80, 95 and 150 °C, showing dominant temperature effect of increased Rh precipitation rate and extent with increasing temperature. Test conditions were kept constant, with sodium thiosulfate added at 37 times molar excess than stoichiometric requirement. 58

Figure 6.2: Ionic Rh precipitation at 150 °C, comparing stoichiometric sodium thiosulfate addition requirement against 37 times greater than stoichiometric requirement. Stoichiometric precipitation was significantly slower and incomplete. 60

Figure 6.3: Rh substitution with CuS at 50, 80, 95 and 150 °C, showing dominant temperature effect of increased Rh precipitation rate and extent with increasing temperature. CuS was prepared and added to simulate conditions of precipitating it in the ionic and co-precipitation tests. 61

Figure 6.4: Cu leaching profile at 50, 80, 95 and 150 °C, showing significant Cu release at 80 and 150 °C. 62

Figure 6.5: Cu co-precipitation at 50, 80, 95 and 150 °C, showing dominant temperature effect of increased Cu precipitation rate and extent with increasing temperature. 65

Figure 6.6: Cu co-precipitation at 50, 80, 95 and 150 °C, calculated from solid mass precipitated, assuming CuS, to avoid overestimation of Cu precipitation due to post-precipitation in filtrates; profiles illustrate that increasing temperature improves the Cu precipitation rate and extent 65

Figure 6.7a: Rh co-precipitation at 50, 80, 95 and 150 °C, showing dominant temperature effect of increased Rh precipitation rate and extent with increasing temperature. 66

Figure 6.7b: Cu and Rh co-precipitation profiles at 50, 80, 95 and 150 °C, calculated from solid mass precipitated; profiles illustrate that increasing temperature relatively increases Rh precipitation rate. 67

Figure 6.8: Rh and Cu ratio in solids for the substitution and co-precipitation systems over 50 – 150 °C, showing improved Rh selectivity with increasing temperature on final profiles. 69

Figure 6.9: EDX spectrum illustrating the relative proportions of Cu, Ni, S and Rh measured in a Rh-enriched area in #0-1 sample (Figure 1 in (Dinham, 2006)). 71

Figure 6.10: SEM back scattered image (BSE) and corresponding elemental distribution maps of a fine-grained CuS-O particulate in sample #0-1. Areas of epoxy in the mount appear black within the images. Although images are grainy, it is possible to see that Rh appears to occur at levels slightly above background throughout the CuS-O particulate (Figure 2 in (Dinham, 2006)).....72

Figure 6.11: Microprobe linescans show in Rh mass percent in the co-precipitated covellite formed in the thioform process at 95 °C; Rh distribution was measured at 5 um intervals over a number of particles, showing Rh mass % increasing towards the edges at 0 and 1. 73

Figure 6.12: Three dimensional Rh distribution over a cross-section of a covellite particle produced in the thioform process at 95 °C, showing enrichment towards the edge (Figure in Andrews, 2001).....73

Figure 6.13: First order model plot over the initial and middle precipitation regions of ionic and substitution systems at 95 °C; data approximating a straight line would follow first order kinetics; substitution showed initial fast first order kinetics, followed by slower pseudo first order kinetics, while ionic precipitation showed initially pseudo first order kinetics, followed by zero order kinetics (solids basis).....77

Figure 6.14: Initial and middle precipitation regions of ionic, substitution and co-precipitation systems at 95 °C, showing initial fast precipitation and the middle region modeled by first order kinetics (solids basis).....77

Figure 6.15: Comparison of the pseudo first and second order fits for elevated temperature, showing that first order model fitted the data of the ionic, substitution and co-precipitation systems. 79

Figure 6.16: Determination of activation energy and frequency factor for the initial period over 50 – 95 °C.....80

Figure 6.17: Modelling the precipitation profile for the initial and middle period using pseudo first order kinetics at 150 °C, providing an excellent fit of the measured data. 84

Figure 6.18: Modelling the precipitation profile for the initial and middle period using pseudo first order kinetics over 80 – 95 °C; the model does not predict the slow approach to completion after 120 min.....85

Figure 6.19a: Modelling the whole co-precipitation profile with an empirical logarithmic fit. 85

Figure 6.19b: Modelling the whole co-precipitation profile with an empirical logarithmic fit. 86

Figure 6.20a: Comparison of calculated Rh precipitation rates for ionic reaction system Rh over the middle period over 50 -150 °C, showing that the rate is fairly independent of temperature at atmospheric temperatures and increases significantly at 150 °C; rates tend towards zero precipitation prior to completion, showing passivation of the elemental sulfur occurring at atmospheric temperatures. 87

Figure 6.20b: Comparison of calculated Rh precipitation rates for substitution reaction system Rh over the middle period over 50 -150 °C, showing that the rate is fairly independent of temperature at atmospheric temperatures and increases significantly at 150 °C; rates tend towards zero precipitation prior to

completion, showing passivation of the CuS occurring at atmospheric temperatures. 87

Figure 6.20c: Comparison of calculated Rh precipitation rates for co-precipitation reaction system over 50 -150 °C over the middle period, showing that at the rate increased with increasing temperature; though the rates converged with increasing precipitation. 88

Figure 7.1a: Rh precipitation kinetic comparison for ionic, substitution and co-precipitation reaction paths at 50 °C with 37 times excess thiosulfate addition than Rh requirement; ionic precipitation is faster than cationic substitution, while co-precipitation kinetics were uncertain; Rh and Cu co-precipitation both had 9 min induction period; Cu precipitation. 94

Figure 7.1b: Comparative Rh precipitation kinetics ionic and substitution systems, calculated from an empirical logarithmic fit, against Rh precipitation extent, at 50 °C, showing faster ionic precipitation rate at a particular precipitation extent; rate approached zero at approximately 75 mg/l Rh 94

Figure 7.2a: Rh precipitation kinetic comparison for ionic, substitution and co-precipitation reaction paths at 80 °C, with 37 times excess thiosulfate addition than Rh requirement; Rh ionic precipitation rate and extent was greatest, followed by co-precipitation and then substitution reactions; after 120 min, ionic and co-precipitation rate and extent are similar; Rh precipitation is modelled with empirical logarithmic fit. 95

Figure 7.2b: Comparative Rh precipitation kinetics ionic, substitution and co-precipitation systems, calculated from an empirical logarithmic fit, against Rh concentration, at 95 °C, showing faster ionic precipitation rate at a particular precipitation extent; Rh precipitation stopped at 50, ~40 and 34 mg/l for substitution, co-precipitation and ionic systems, respectively. 95

Figure 7.3a: Rh precipitation kinetic comparison for ionic, substitution and co-precipitation reaction paths at 95 °C with 37 times excess thiosulfate addition than Rh requirement. Ionic precipitation rate and extent was greatest over the whole reaction period, followed by co-precipitation and cationic substitution; Rh precipitation is modelled with empirical logarithmic fit. 96

Figure 7.3b: Comparative Rh precipitation kinetics of ionic, substitution and co-precipitation systems, calculated from an empirical logarithmic fit, against Rh concentration, at 95 °C, showing faster ionic precipitation rate at a particular precipitation extent; Rh precipitation stopped at 50, ~40 and 34 mg/l for substitution, co-precipitation and ionic systems, respectively 97

Figure 7.4a: Rh precipitation kinetic comparison for ionic, substitution and co-precipitation reaction paths at 150 °C on solution basis, with 37 times excess thiosulfate addition than Rh requirement; initially, ionic precipitation is the slowest, a complete reversal from trends at atmospheric temperatures; substitution and co-precipitation are similar; Cu precipitation was almost complete after 4 min. Rh precipitation modelled with pseudo first order kinetics. 98

Figure 7.4b: Rh precipitation rate for the ionic, substitution and co-precipitation systems, calculated from pseudo first order kinetic model of the middle period, against Rh precipitation extent, at 150 °C, showing similar precipitation rates ionic and co-precipitation reaction systems, while substitution was surprisingly fastest; the linear line shows first order kinetics over this middle period. 98

NOMENCLATURE

ACRONYMS

ACRONYM	MEANING	ADDITIONAL INFORMATION
BMR	Base Metal Refinery	
CSTR	Continuously stirred tank reactor	
HSC Chemistry®	Thermodynamic calculation program	Chemical Reaction and Equilibrium software with extensive thermo-chemical database
EPR	Electron paramagnetic resonance spectroscopy	
EXAFS	Extended X-ray adsorption fine structure spectroscopy	Technique utilising measurement of variation (fine structure) of the X-ray absorption coefficient with energy in vicinity of one of the characteristic absorption edges of a particular element
ICP-OES	Inductively coupled plasma-optical emission spectroscopy	Analytical instrument
ICP-MS	ICP- mass spectroscopy	Analytical instrument
NA / NR	Not analysed / No result / Not applicable	Insufficient sample or not requested
OA	Oxidising agent	
PGM	Platinum Group Metals	In this reports context it refers to Pt, Pd and Rh
PV	Pressure Vessel	Batch reactor used for elevated pressure and temperature operation
RA	Reducing agent	
rpm	Revolutions per minute	
SEM	Scanning electron microscope	Hardware used
SEM EDX	SEM – Energy Dispersive X-ray spectroscopy	Technique used on SEM
SEM MLA	SEM – Mineral Liberation Analyser	MLA Software on SEM EDX automating the scanning procedure
Thioform	sodium formate and sodium thiosulfate	Mixture of reducing reagents used for PGM precipitation
XPS	X-ray photon spectroscopy	Technique analysing the first few molecular layers of surface of the particle, providing specific compound formation and surface phenomena
XAFS	X-ray adsorption fine structure spectroscopy	See EXAFS

ABBREVIATIONS

#	number
~	approximate(ly)
a/c	account or accounting
avg	average
calc'd	calculated
e-	electron
Eh-pH	Pourbaix diagram
Me	metal
meas.	measured
min	minute
rxn	reaction
Pptnn	precipitation
sig.	significant or significance
std. dev.	standard deviation

SYMBOLS

SYMBOL	MEANING	ADDITIONAL INFORMATION	Units
a_o	y-intercept of regression line	Used in statistical comparison of precipitation profiles using regression lines	
A_1	Slope of regression line	Used in statistical comparison of precipitation profiles using regression lines	
a	Aqueous	Denotes phase of ion/compound in reaction in HSC Chemistry ®	
aq	Aqueous	Denotes phase of ion/compound in reaction	
[A]	Concentration of A		mol/l or mass/l
{A}	Activity of A ion in solution		
C_A	Concentration for element or compound A		mol/l (or mass/l)
$C_{A,0}$	Concentration for element or compound A at time zero		mol/l (or mass/l)
Eh	Oxidation reduction potential	Values against hydrogen electrode, unless otherwise stated	
E_a	Activation energy		J/mol
ΔG	Change in Gibbs free energy		J/mol
ΔH	Change in Enthalpy		J/mol
k	Reaction rate constant for chemical reaction rate	Function of temperature using Arrhenius relationship	1/time (first order)
k^I	Pseudo reaction rate	Measured rate including constant	

	constant measured	concentration terms	
k_s	Reaction rate constant at solid surface		1/time (first order)
k_l	Mass transfer constant across boundary layer		1/time (first order)
k_o	Frequency factor (constant in Arrhenius relationship)	For first order reaction:	1/(time.gmol)
k_o^I	Pseudo frequency factor	The value includes the other constants in the rate equation	
K	Equilibrium constant	Of a reaction for the stoichiometry as written	
K	Temperature unit in Kelvin		
K_{SP}	Solubility product	$K_{SP} = \{Me^{2+}\}\{S^{2-}\}$ for reaction $MeS = Me^{2+} + S^{2-}$	
mV	milli volt	Electropotential	
mmol	milli mole		
MS	Mean square	Used in statistical comparison of precipitation profiles using regression lines	
MS_{res}	Mean square residual		
MS_{reg}	Mean square regression		
n	Number of points of regression line	Used in statistical comparison of precipitation profiles using regression lines	
pH	Negative log of the activity of the H^+ ion		
p(t)	Significance that the difference of the T-test is not real	1-p(t) is the significance or confidence that the difference is real	
p(F)	Significance of F-test that difference in variances of the are not real	1-p(F) is the significance difference is real	
$Q_{Rh,s}$	Rate of reaction of Rh at surface		mol / time
$Q_{Rh,liq}$	Rate of mass transfer Rh	Over the boundary layer	mol / time
r_A	Rate of reaction		mol / time
R	Universal gas constant	= 8.314	J/(gmol K)
R	Correlation coefficient	Gives the correlation between data and variable of the regression	
R^2	R squared	% of data explained by the model of data, $100 - R^2$ is the error	
s_1	Standard deviation		
s_1^2	Variance		
S^2	residual sum of squares of the regression	Used in statistical comparison of precipitation profiles using	

		regression lines	
SS	Sum of squares	Used in statistical comparison of precipitation profiles using regression lines	
SS_{tot}	Total sum of squares		
SS_{res}	Residual sum of squares		
SS_{reg}	Regression sum of squares		
$\{S^{2-}\}$	Activity of sulfide in solution		
s	Solid		
ΔS	Change in Entropy		J/K
t	Time	Profile time or precipitation ti	Min
t^{l}	Pseudo time	$t^{l} = t - t_d$	
t_d	Time delay	Time before first or second order model fits data of middle period	
t	t-distribution	Appropriate alternative to the normal distribution for small samples (n<40)	
T	Temperature		°C or K
µm	Micron		
X_A	Conversion of A	Fraction of A converted into product	

Elements and Compounds

Co	Cobalt	$Na_2S_2O_3.5H_2O$	Sodium thiosulfate pentahydrate
Co^{2+}	Cobaltous ion	Ni	Nickel
CoS	Cobalt sulfide	Ni^{2+}	Nickelous ion
$CuSO_4$	Copper	NiS	Nickel sulfide
Cu^{2+}	Cupric ion	$NiSO_4$	Nickel sulfate
CuS	Copper sulfide or covellite		
Cu_2S	Copper (I) sulfide	Rh	Rhodium
$CuSO_4$	Copper sulfide	Rh^{3+}	Rhodium (III) ion
$CuRhS_2$	Cu, Rh mixed sulfide compound	Rh_2S_3	Rhodium sulfide
		Rh_3S_4	Rhodium sulfide
Fe	Iron	Rh_2S_5	Rhodium sulfide
Fe^{2+}	Ferrous	Rh_9S_8	Rhodium sulfide
Fe^{3+}	Ferric	$Rh_2(SO_4)_3$	Rhodium sulfate
FeS	Iron sulfide		
		SO_4^{2-}	Sulfate ion
H^+	Proton	S^{2-}	Sulfide ion
HS^-	Bisulfide ion	$S_2O_3^{2-}$	Thiosulfate ion
H_2S	Hydrogen sulfide		
		Tl	Thallium
In	Indium	Tl_2S	Thallium sulfide
In_2S_3	Indium sulfide		

Me^{2+}	Metal (II) ion
Mn^{2+}	Manganese (II) ion
MeS	Metal sulfide
MnS	Manganese sulfide

Definitions

Atmospheric temperature	Temperature range of 50 - 95 °C in this study.
Cationic substitution	Cation exchange of more soluble Me cation in MeS with less soluble cation through an ion exchange mechanism.
Co-precipitation	Simultaneous precipitation of metals at conditions when both metals are insoluble.
Co-precipitation system	Tests designed for Rh and Cu co-precipitation with sulfide addition, occurring through ionic and substitution reaction paths.
Covellite	Copper sulfide compound CuS, better represented as Cu_3S_3, where Cu is actually cuprous ion (Cu^+).
Elevated temperature	Temperature greater than 100 °C. In this study the results at elevated temperature are applicable to temperature range around 150 °C.
Final period	Time period of the precipitation profile as precipitation extent tends to completion, where precipitation kinetics are very slow or have effectively stopped.
Ionic precipitation system	Tests designed for ionic Rh precipitation in the absence of base metal ions.
Ionic precipitation path	Ionic precipitation reaction during co-precipitation.
Induction period	Delay period before precipitation occurs due to homogeneous nucleation prior to precipitation.
Initial period	Initial period of precipitation used to comparative relative kinetics of various reaction systems, usually first 3 – 4 data points; at atmospheric temperature it is limited to 10 min reaction time, while at an elevated temperature.
Initial rate	Average initial reaction rate based on the first sample and / or second sample.
Middle period	Time period of the precipitation profile after the induction and/or initial period, where precipitation kinetics is modelled to pseudo first order or second order kinetics.
Reaction path	Predominant reaction occurring in the precipitation mechanism due to carious competing reactions OR Specific reaction in the multi-stage heterogeneous reactions.
Substitution system	Tests designed cation exchange of Rh^{3+} with Cu^{2+} in CuS.
Substitution path	Cation exchange of Rh^{3+} with Cu^{2+} in previously precipitated CuS in co-precipitation system.
Solids basis	Analysis performed on predicted solution concentrations calculated from the solid precipitation profile measured (however,

	at 150 °C, solution concentration used in basis).
Solution basis	Analysis performed on measured solution concentrations, excluding profiles which showed a large amount of post precipitation, which used the solids basis (however, at 50 °C, solid basis used due to excessive post precipitation. concentration used in basis)

Chapter One

1 INTRODUCTION

This study is a preliminary investigation into the mechanism of rhodium (Rh) co-precipitation with copper sulfide (CuS) under conditions where Rh^{3+} is two orders of magnitude lower than cupric ion. The effect of temperature over 50 – 150 °C on the Rh co-precipitation kinetics and mechanism is of particular interest. Knowledge of the reaction kinetics and mechanism is required for process development, design and optimisation.

1.1 Background

During PGM refining, converter mattes and other feed material containing Platinum Group Metals (PGMs) are separated from base metals using selective, oxidative leaching of the base metals in acidic mediums, where some PGM dissolution can occur. Alternatively, the base metals and PGMs are purposefully leached into solution for downstream separation and recovery. The choice between cementation, reduction, ionic precipitation and other techniques like solvent extraction and ion exchange will be dependent on process stream conditions, purpose of recovery and the overall process economics.

A number of production processes utilise selective metal sulfide precipitation techniques to separate base metals by exploiting the difference in their solubility products (Roy, 1961) (Tuominen and Groenquist, 1969) (Joris, 1969) (Harris *et al.*, 1977). Similarly, production processes specific to PGM precipitation from base metals are also available. Barkan and Greiver (1977a) developed the process for separation of PGMs from anode slime leach solution using elemental sulfur at elevated temperatures. Johnson Matthey developed the Thioform Process for recovery of dissolved PGMs from waste streams by precipitating the PGMs using a mixture of sodium thiosulfate and sodium formate reagent (thioform), however the process has never been published (Payne, 1978). The thioform technology was implemented into Anglo Platinum's Precious Metal Refinery in Rustenburg on acid and basic effluent streams in chloride medium. Afterwards, the process was adapted and retrofitted into Rustenburg Base Metal Refiners on a pressure leach solution containing high concentrations of base metal sulfates (Mc George, 2000). More recently, the PLATSOL process uses a similar PGM recovery process by adding sodium hydrogen sulfide (NaSH) to precipitate dissolved PGMs from the base metal leach solution in a mixed sulfate and chloride medium (Dreisinger *et al.*, 2001) (Ferron *et al.*, 2001) (Fleming *et al.*, 2000).

The PGM co-precipitation mechanism with base metal sulfides was speculative within Johnson Matthey and Anglo Platinum. The literature reviewed in this study showed that only a few kinetic studies were performed on metal sulfide co-precipitation (Roy, 1961) (Joris, 1969) (Barkan and Greiver, 1977a) (Bryson and Bjisterveld, 1991), highlighting general lack of knowledge on the mechanism, which is surprising in view of the many production applications. This is particularly relevant to the Rhodium Removal Process at RBMR, where Platinum Group Metals (PGMs) are recovered from a process stream by co-precipitating the valuable metals with CuS. Rh is precipitated from a leach solution containing 10 – 50 mg/l Rh, 30 – 35 g/l Cu, 90 – 110 g/l Ni, 1 g/l Co, 2 – 5 g/l Fe and 5 – 20 g/l sulfuric acid

concentration by adding approximately 20 g/l sodium thiosulfate pentahydrate, to force Cu and Rh sulfide co-precipitation, precipitating 40 – 60 % of the Rh within 3 hrs. This process has to be optimised to maximise PGM precipitation, preferably by improving the selectivity of PGM precipitation over the base metals. PGMs not recovered from this stream are ultimately treated through a less profitable toll-refining route.

At these conditions, both base metals and PGM sulfides are insoluble upon the addition of sulfide, thus ionic precipitation would occur through primary nucleation and secondary nucleation processes. Thermodynamic modelling shows that ionic Rh^{3+} precipitation is selective over Cu^{2+} precipitation upon the addition of a sulfide-containing reagent. This is due to the large difference between the solubility products of Rh_2S_3 and CuS. However, in practice, selectivity decreases due to relative kinetic effects. In some production processes, selectivity is purposefully sacrificed for improved precipitation kinetics and precipitation extent by adding a large excess of sulfide above the Rh requirement. Experience from the development of the Rhodium Removal Process showed that the large amount of cupric ion consumed the sulfide immediately, thus possibly limiting the amount of ionic Rh precipitation. However, a significant amount of Rh continued to precipitate.

One possible explanation for this continued precipitation is that additional Rh precipitates through a cation exchange reaction in the heterogeneous phase, referred to in this study as the substitution reaction. This reaction path was not considered in previous co-precipitation studies and the possible role of this bulk sulfide in the precipitation mechanism was not understood.

For the Rhodium Removal system, where the solubility product for Rh_2S_3 is approximately 20 – 47 orders of magnitude smaller than CuS, Rh^{3+} should precipitate onto the CuS surface via the reaction:

$$2Rh^{3+}_{aq} + 3CuS_s \rightarrow Rh_2S_{3\,s} + 3Cu^{2+}_{aq} \quad \Delta G_{rxn} = -160 \text{ kJ/mol using HSC Chemistry®} \qquad (1.1)$$

The Gibbs free energy of -160 kJ/mol over 0 – 200 °C is a very large driving force for the chemical reaction, indicating that the reaction would be fast and irreversible.

1.2 Objectives

The objective of the current study is to expand the current understanding of the Rh co-precipitation with CuS using sodium thiosulfate in a system containing Rh^{3+} concentrations two orders of magnitude lower than the base metal over 50 – 150 °C.

The specific objectives are to:

1. Demonstrate that Rh precipitates through a cationic substitution reaction,
2. Measure the relative kinetics of ionic Rh precipitation against substitution reaction at constant sulfide addition,
3. Determine which precipitation reaction path dominates in Rh co-precipitation mechanism,
4. Measure the effect of temperature on the mechanism,
5. Attempt to fit the kinetics to an appropriate model,
6. Discuss implications of findings on the development and optimisation of the Rh precipitation process.

1.3 Approach, Scope and Limitations

This study has been performed through a comparative study of the relative kinetics of the independent reaction systems, namely:

1. **Ionic Rh precipitation** with sulfide addition in the absence of Cu^{2+} in solution,
2. Rh precipitation through the cationic **substitution reaction** [1] of Cu in CuS previously precipitated in the absence of Cu^{2+} in solution, and
3. **Rh co-precipitation** with CuS formed ***in situ*** upon sulfide addition, probably occurring through ionic and substitution reaction paths,

by performing batch tests on the various systems at the similar conditions and measuring the relative Rh precipitation kinetics and extent at 50, 80, 95 and 150 °C under a nitrogen atmosphere.

The investigation is limited to the recovery of low concentrations of Rh^{3+} from synthetic solutions containing Cu and Ni sulfates and sulfuric acidic with concentrations two orders of magnitude greater than Rh. Sodium thiosulfate, which is used in the Rhodium Removal Section at RBMR, is used as the sulfide-containing reagent, as it has a lower toxicity than sodium sulfide. Reaction time is limited to 300 minutes.

1.4 Thesis Outline

Firstly, literature specific to metal sulfide precipitation is reviewed, covering ionic precipitation, cationic substitution reactions, co-precipitation, focusing on mechanism and kinetics. Studies specific to CuS co-precipitation and ionic CuS precipitation mechanism are then presented. This leads to the development of the hypothesis for the dominant reaction path during Rh co-precipitation with CuS, which is followed by the approach and specific tests, designed to answer the key questions.

Chemistry of the proposed system is provided and verified with thermodynamic calculations using HSC Chemistry® software package. Phase diagrams are constructed and solution equilibrium chemistry is modelled and discussed. Kinetic studies of the independent systems are presented and compared. Kinetic modelling is performed to gain an understanding of the mechanisms involved. Relative kinetics of the various reaction paths are compared. This leads to the development of the the Rh co-precipitation mechanism. General conclusions are drawn with respect to the Rh co-precipitation mechanism, kinetics and mechanistic changes, as well as the implications of these findings on process development and optimisation. Finally, recommendations are made.

[1] The metathesis term, which seems to be a favourable term used to describe the reaction 1.1 in literature covering the development of hydrometallurgical development of Ni pressure leaching (Hofirek and Kerfoot, 1992) (Rademan et al., 1999), has purposefully not been used owing to the definition of the metathesis reaction, which in some cases excludes reactions not involving electron transfer or heterogeneous reactions. The ion exchange term describing the type of chemical reaction itself is confusing, as this term has become an industrial term describing ion exchange technology, where ion exchange sites are fixed to a solid substrate. In this thesis the term cationic **substitution** has been selected to describe the metathesis or ion exchange or cation exchange reaction with the purpose of specifically including the heterogeneous reactions and electrochemical reactions. The other terms are used to specify the situation more specifically or to use the terms used in the paper being cited.

Chapter Two

2 LITERATURE REVIEW

Literature covering co-precipitation of metal sulfides is very limited, particularly literature specific to the Rh and CuS co-precipitation system. Thus, literature of similar metal sulfide precipitation systems has been reviewed, where findings would be applicable to the Rh precipitation system. The literature is presented by initially describing the current understanding of the co-precipitation mechanism and cationic substitution reaction separately. Ionic precipitation of metal sulfides is then covered.

This leads to the development of the proposed mechanism of Rh co-precipitation with CuS, showing that the co-precipitation mechanism also occurs through a cationic substitution reaction path, which involves a novel approach.

Additional detail on some of the key papers with additional comments and implications of the findings on this study is attached in Appendix C. Included in Appendix C is a number of additional references of literature related to the general study of metal sulfide (co-) precipitation, that are not specifically referred to in this thesis.

2.1 Metal sulfide (co-)precipitation mechanism

The introduction section mentions that only a limited number of kinetic studies have been performed on metal sulfide co-precipitation (Roy, 1961) (Joris, 1969) (Barkan and Greiver, 1977a) (Bryson and Bjisterveld, 1991), showing that there is no conclusive description of co-precipitation mechanism in the literature. This is surprising in view of the many metal sulfide precipitation applications in production. However, a number of related papers provide valuable insights into the co-precipitation mechanism.

Kolthoff and Moltzau (1935) attribute the "induced" co-precipitation of metal sulfides to the metal sulfides' strongly adsorbent properties towards H_2S, HS^- and S^{2-}, where the more soluble metal is "carried down" with less soluble metal sulfide, under conditions where the more soluble metal would not precipitate if it were there alone. Post-precipitation is given as the primary mechanism for of the induced precipitation, which is promoted by the strong adsorption H_2S. The induced precipitation process involves an exchange mechanism, where cations leave the solution and replace the hydrogen ions in the adsorbed H_2S on the metal sulfide, releasing the equivalent amount of acid. The study highlights the autocatalytic effect or catalytic effect of metal sulfides during ionic precipitation. This (auto-)catalysed ionic precipitation would obviously affect the co-precipitation kinetics and mechanism due to the metal sulfides' strongly adsorbent properties towards H_2S, HS^- and S^{2-}, which increases the precipitation rate at the surface, promoting crystal growth and reducing primary nucleation.

Rudnev and Malofeyeva (1964) show that thallium co-precipitation with a number of precious metal sulfides and indium co-precipitation with CuS occurs by forming chemical compounds in a microdisperse system of solid solutions of one sulfide in another. The later is very similar to the Rh co-precipitation with CuS, but the ratio of In:Cu is 1:1, while this study the Ration of Rh:Cu is 1:100. The dependence of co-precipitation on adsorption has been

studied by adding previously precipitated PGM sulfides to the thallium solution. Sulfide precipitates washed free from H_2S co-precipitated significantly less thallium (5-15 times) than unwashed precipitates, while washed sulfides added to a sulfuric acid solution containing H_2S, approximately half the thallium co-precipitated compared to the unwashed sulfides. In an attempt to understand the amount of adsorbed H_2S on the co-precipitation of thallium, PdS and Ag_2S adsorbs similar amounts of H_2S, but thallium is not co-precipitated on the Ag_2S. They conclude that H_2S, HS^- and S^{2-} adsorption on the sulfide surface is a necessary condition, but not the only condition, for co-precipitation of cations. In addition, thallium is entrained in previously precipitated Ru_2S_3 to the same extent as the co-precipitated system, probably due to the highly porous metal sulfide adsorbing the H_2S, HS^- and S^{2-}. X-ray diagrams show that the compound for Tl^+ co-precipitated onto previously precipitated Ru_2S_3 is $TlRu_2S_6$ rather than Tl_2S on the Ru_2S_8 surface. In their system, thallium co-precipitation with Rh_2S_3 via the reaction:

$$Tl^+ + Rh_2S_3.nH_2S \rightarrow TlRh_2S_4.(n-1)H_2S + H^+$$

where, Tl_2S has a similar K_{SP} as CuS. Similarly, it is assumed that if Rh^{3+} is to co-precipitate with CuS via the analogous reaction in the presence of H_2S, HS^- and S^{2-}:

$$Rh^{3+} + CuS.nH_2S \rightarrow CuRhS_2.(n-1)H_2S + 2H^+ + e^-$$

and / or,

$$2Rh^{3+} + CuS.nH_2S \rightarrow CuRh_2S_4.(n-3)H_2S + 6H^+$$

Rudnev and Malofeyeva (1964) and Kolthoff and Moltzau (1935) studies do not specifically cover the precipitation of the less soluble cation (Rh^{3+}) with the previously precipitated metal sulphide (CuS) in the absence of adsorbed H_2S, HS^- and S^{2-}. This study focuses on the co-precipitation of the less soluble metal (Rh^{3+}) with the more soluble metal due to the relative concentrations in the feed solution, which can precipitate through an cation exchange reaction, covered in Section 2.2.

Roy (1961), in the development of selective Ni and Co sulfide precipitation using H_2S at elevated temperatures, studied the kinetics and mechanism of Co and Ni precipitation. The reaction switches from zero order with respect to Ni and Co concentration in the initial period, where the bulk of the metal has precipitated under mass transfer of H_2S, to first order kinetics towards the end of precipitation. Roy (1961) suggests that it is probably limited by mass transfer of Ni^{2+} to the sulfide surface, because faster kinetics were observed in the turbulent pipe reactor pilot plant compared to four agitated CSTRs in series, which corresponds with the measured first order kinetics. Roy (1961) shows the catalytic effect of seeding Ni precipitation using hydrogen sulfide with finely powdered metallic Ni, Fe or recycled product, supporting the metal sulfide catalytic effect demonstrated by Kolthoff and Moltzau (1935).

Barkan and Greiver (1977a) studied the precipitation of PGMs from the dissolution of anode slimes by adding elemental sulfur at elevated temperatures. The solution, obtained from leaching of Ni electrowinning slimes, consists of 200 – 220 g/l sulfuric acid, 50 g/l Cu+Ni, 120 mg/l Rh, 40 mg/l Ru, 20 mg/l Ir, 140 mg/l Te and 100 mg/l Se. Rh precipitation is completed at ~200 °C and ~3 hours. Increasing the sulfur addition within the range of 5 – 30 g/l increases the rate of PGM precipitation, though extensive PGM precipitation occurring at minimum sulfur consumption. Metals are precipitated in the following sequence: Rh, Ru, Te and finally Ir. The precipitate contains 4% PGMs, 2 – 3 % Se and Te, with CuS making up the bulk. This PGM co-precipitation system is very similar to the current system being studied in this research work, but the co-precipitation mechanism is not discussed.

Barkan and Greiver (1977a) have shown that PGMs start precipitating at temperatures lower than predicted by their thermodynamic calculations for the individual sulfides, but do not offer

reasons for this phenomenon. Based on this literature review and findings presented in this thesis, three possible reasons are offered:

- Catalytic effect of the CuS precipitated (Kolthoff and Mautzau, 1935),
- Cationic substitution of PGMs with CuS, providing an alternative path for precipitation,
- Formation of mixed sulfides (Rudnev and Malofeyeva, 1964).

Techniques for concentrating PGMs from sulfate and chloride solutions by exploiting the collection properties of base metal sulfides for PGMs have been developed by Russian analytical chemists in the 1970's. These systems are also similar to the Rh co-precipitation system currently being studied. Base metal sulfides are either added directly (Dragavtseva *et al.*, 1977) (Mateeva, 1977) (Sinicyn *et al.*, 1977) or co-precipitated *in situ* from various sulfide-containing precipitating agents (Pshenitsyn and Prokof'yeva, 1958) (Myasoedova *et al.*, 1977) (Pavlenko *et al.*, 1974) (Shorikov *et al.*, 1986). At the correct operating conditions, complete PGM removal is possible.

Pshenitsyn and Prokof'yeva (1958) investigated the use of thiourea for qualitative separation of PGMs from solutions, particularly Rh and Ir, where PGM complexing with thiourea occurs. Upon heating selective PGM sulfide precipitation occurs through hydrolysis at elevated temperatures between 120 –190 °C. Low concentrations of Fe, Ni and Se do not interfere with the analytical method, while Cu, Pb and Sn are partially co-precipitated. This system differs from the current system being studied because the pH is significantly higher and thio complexing is not expected in this Rh and Cu co-precipitation system.

Shorikov *et al.* (1986) precipitated Ru directly from synthetic solution not containing base metals with polysulfides (NaS_x), where 99.3 - 99.7% precipitation occurred in 60 – 90 min reaction time over 80 – 100 °C. This system is similar to the ionic Rh precipitation system in the current study. A large sulfur excess was added at a ratio of S:Ru of 29 – 32 on molar basis. Significant reduction in metal transfer to precipitate occurs at a pH > 2 – 3 due to thio-complexing in solution. Acidification decomposes the thio salts, which precipitated the Ru sulfides and sulfur. This raises the concern that thiosulfate degradation could occur with the 15 g/l acid in the current study and a similar excess was added to overcome the problem.

Bryson and Bijsterveld (1991) studied the kinetics of co-precipitating manganese (Mn) and cobalt (Co) sulfides from synthetic solutions by adding ammonium sulfide in an attempt to understand the basic mechanisms controlling the removal of the Co impurity. This system is similar to the current system being studied, as the relative concentrations of the Mn and Co are similar to Cu and Rh. Additional excess aqueous sulfide is added in this industrial process to improve overall precipitation extent at the expense of Co selectivity. They show that MnS precipitation approximates first order kinetics, while precipitation of CoS shows three kinetic regions, namely, an induction period where little precipitation is observed, followed by rapid precipitation and finally a very slow approach to equilibrium. Seeding the reactor with metal sulfide precipitate from previous runs eliminates the induction period completely. It is expected that the Rh and Cu co-precipitation system would provide similar kinetics if it is operated at the same ambient temperature.

Increasing the temperature increases the base metal or PGM metal sulfide precipitation kinetics significantly (Roy, 1961) (Pshenitsyn and Prokof'yeva, 1958) (Myasoedova *et al.*, 1977), where at high temperatures this induction period does not occur. This is supported by findings during process development work of the Rh Removal Section at RBMR (Mc George, 2000). The large dependence of precipitation kinetics on temperature indicates that the co-precipitation reaction would probably be chemical reaction controlled (Levenspiel, 1972).

2.2 Rh precipitation through the cationic substitution reaction

Russian analytical chemists developed analytical techniques for concentrating PGMs from sulfate and chloride solutions by exploiting the collection properties of base metal sulfides.

Dragavtseva *et al.* (1977) and Mateeva *et al.* (1977) collected PGMs onto mechanically activated FeS and NiS. Sulfides not activated show significantly less dissolution in the cation exchange reaction, demonstrating the expected relationship between increased surface area and PGM precipitation extent in this heterogeneous reaction. Complete dissolution of the base metal through PGM precipitation shows that, at these conditions, the PGM sulfide passivate the base metal sulfide if sufficient surface area is available.

Dragavtseva *et al.* (1977) developed an analytical technique for extracting PGMs from solutions containing hydrochloric acid using activated pyrrhotite. The pyrrhotite was activated through fine milling and added to the solutions and agitated at room temperature in order to precipitate PGMs. FeS dissolution kinetics increases with increasing milling time and Pd precipitation kinetics increases with this increase in activation. Limiting precipitation capacity appeared to be ~2300 mg Pd/g FeS. Pyrrhotite precipitation capacity for Pt and Rh is measured at approximately two orders of magnitude lower than Pd and Os. Based on the experimental data they propose that the mechanism of PGM precipitation is a multistage process consisting of precipitation of sulfides, reduction to elemental form by ferrous ion, as well as surface adsorption on pyrrhotite and precipitated PGM sulfides side-by-side. Adsorption increases with increasing valence of adsorbed PGMs. Mateeva *et al.* (1977) show that complete FeS dissolution is achievable within 15 – 30 min, whilst not-activated FeS only achieves 15% dissolution in the same time. NiS dissolution proceeds at a significantly slower rate. Pyrrhotite effectively removes Os, Pd, Pt and Rh, whilst NiS removes Os, Pd and Pt, but no Rh. Sinicyn *et al.* (1977) contradict the finding of no Rh precipitation on NiS, who later show that Rh precipitation can occur on NiS.

Sinicyn *et al.* (1977) studied the factors influencing Rh removal from sulfate solutions using iron hydroxide and sulfides of Cu and Ni. For all adsorbents, a rapid increase in adsorption rate is noticed with increasing temperature. Difference in behaviour of adsorbents in pH range of 1-2 was measured, which could be used for quantitative Rh removal using metal sulfides in the presence of Fe. The various parameters studied are temperature, reaction or contact time, pH, quantity of precipitate and solution, and Rh concentration in solution. Sinicyn *et al.* postulate that the adsorption mechanism is based on chemical ion exchange, since physical adsorption rate would decrease with temperature. They noticed that the higher the difference between the PGM and base metal solubility products was, the higher the PGM precipitation rate. These papers clearly demonstrate that metals with lower solubility precipitate onto more soluble metal sulfides through some form of cation exchange mechanism, thought the mechanisms proposed are not formally proven.

These PGM precipitation reactions onto metal sulfides are similar to metathesis or cation exchange reactions described in the chemistry of Ni pressure leaching (Hofirek and Kerfoot, 1991) (Rademan *et al.*, 1999), for example:

$$NiS + Cu^{2+} \rightarrow Ni^{2+} + CuS$$

$$Ni_3S_2 + 2Cu^{2+} \rightarrow 2Ni^{2+} + Cu_2S + NiS$$

These cation exchange reactions are supported by findings of research performed on the mechanism of copper activation of mineral sulfides in froth flotation (Allison, 1982) (Sutherland and Wark, 1955) (Bushnell and Krauss, 1961) and water treatment for removal of heavy metals (Phillips and Krauss, 1964). Allison (1982) and Sutherland and Wark (1955) confirm that CuS precipitation occurs through cation exchange by primarily measuring the

stoichiometry of the reactions, with the driving force for the reaction coming from lower solubility of the CuS sulfide product. Nicol (1984), using potentiostatic and cyclic-voltametric measurements, shows that cation replacement in the metal sulfide can also occur through an electrochemical mechanism involving the anodic oxidation of the metal sulfide coupled to the cathodic reduction of sulfur in the presence of copper ions.

Evidence showing that cation exchange can occur through an electrochemical mechanism does not imply that it does occur. The potentiostatic and cyclic-voltametric measurements experiments themselves may have forced the conditions for the mechanism to be electrochemical. Rather, Nicol's work highlights that the cation exchange reaction is not necessarily a simple ion exchange and could involve an electrochemical mechanism. The actual mechanism may be important, but it is inconsequential to the overall chemical reaction, as the overall effect would remain a cation exchange process.

In the comprehensive "adsorption" study of cation precipitation with various precipitated base metal sulfides in an amorphous form, Philips and Krauss (1964) state that even though the possibility of conversion is a function of the relative stabilities of the sulfides, neither the rate of reaction nor the conversion seem to be related to the relative solubilities. The nature of the solid and the rate of diffusion of the cation are presumably more important factors. This is contrary to the findings of Sinicyn *et al.* (1977), where larger solubility product differences caused faster PGM precipitation kinetics. The contradiction can be explained by the fact that the reaction systems of the two studies were performed under completely different fluid dynamics and temperatures. Phillips and Krauss' findings are related to adsorption column at 25 °C, where the reaction rate was slow and diffusion may have been the rate-controlling step i.e. the driving force of the rate-controlling step is not related to the relative solubilities. In comparison, Sinicyn *et al.* findings were determined at 100 °C. This Russian paper does not clearly describe the agitation regime, though it was probably performed in a well-agitated reactor, where the rate-controlling step would probably be chemical reaction. At these conditions, the chemical driving force is directly related to the difference in solubility products. From this comparison, it could be inferred that temperature, and possibly agitation, could have an impact on the rate-controlling step. Thus, at certain conditions, the rate-controlling step could change from chemical reaction to mass transfer, which can have a significant impact on the design and operation of the co-precipitation system.

Increasing the temperature increases the cation exchange kinetics (Dragavtseva *et al.*, 1977) (Mateeva *et al.*, 1977) (Sinicyn *et al.*, 1977). The temperature effect on kinetics would indicate that the substitution reaction is chemical reaction controlled (Levenspiel, 1972).

Previous researchers into the co-precipitation mechanism overlooked the possibility of cationic substitution reaction describing some of the co-precipitation phenomena. For example, Bryson and Bijsterveld (1991) omitted to consider the cationic substitution of Mn^{2+} in the precipitated MnS by the less soluble Co^{2+} reaction to explain the precipitation kinetics and mechanism. Seeding the system with MnS could have eliminated the Co induction period by immediately precipitating through the cationic substitution reaction rather than through the catalytic effect of the seed during ionic precipitation. Cobalt's very slow precipitation kinetics in the third region could possibly be caused by passivation of the MnS reactive surface during the cationic substitution.

This study takes a novel approach of incorporating the possible cationic substitution reaction into the co-precipitation mechanism. This cationic substitution reaction is confirmed in the precipitation results presented in Section 6.3.

2.3 Covellite precipitation

The elucidation of a mechanism of Rh co-precipitation on CuS requires the study of the mechanism of ionic CuS precipitation alone. It is postulated that the ionic Rh precipitation would occur through a similar precipitation mechanism as CuS. A summary of pertinent papers in the order of the oldest to most recent is discussed below.

Mosselmans *et al.* (1995) have studied the structural changes undergone by amorphous CuS precipitates by X-ray adsorption spectroscopy when precipitated from solution. They show that the precipitate contains only Cu(I) and ages to covellite, but the initial form is dependent on the concentration of Cu(II) solution. Low concentration solutions give rise to brown sol, while more concentrated solutions produce a black floc, which has a close Cu-Cu interaction. Precipitation occurs at 10 °C.

Pattrick *et al.* (1997) studied the structure of amorphous CuS precipitated from aqueous solutions at 5 °C using X-ray adsorption. They revealed the existence of a metastable primitive structure that ages to amorphous covellite. Extended X-ray adsorption fine structure spectroscopy (EXAFS) demonstrates the presence of the sulfide (S_2-groups) and a Cu-S interaction; the latter is not found in covellite. Cu L_3-edge spectra reveals only Cu(I) to be present in all precipitates formed. X-ray photon spectroscopy (XPS) confirms the Cu(I) and reveals three types of S, namely, S^{2-}, S_2^{2-} and a very Cu deficient sulfide or HS^-. Upon aging, the primitive structure transforms into covellite by reordering the S_2- and Cu_3S-CuS_3 layers. The timing of the electron transfer between S and Cu is said to either take place in solution such that $6Cu(I) + 3S_2^{2-}$ precipitates or in the solid phase after CuS precipitation. Pattrick *et al.* are not sure when the reduction to Cu(I) occurred.

Volkov *et al.* (1988) studied the mechanism for the formation of CuS nanoparticles by *in situ* reactions in Poly(acrylic acid)-poly(vinyl alcohol) polymer matrix using UV-vis and IR spectroscopy, X-ray diffraction and gravimetric analysis. They describe the whole process of the formation of the CuS disperse phase nanoparticles involving the following stages: forming S-containing Cu complexes (within 1.5-2 min), appearance of various associates through coalescence of complexes and already formed associates, followed by growth the associates yielding sufficiently densely packed volume structures or CuS amorphous clusters (10 – 40 min), and finally, the interaction of the clusters through a coagulation and coalescence form the crystalline CuS particles. Increasing the temperature of precipitation causes a rapid increase in nanocrystallite formation. The surface metal atoms remain bound with the functional groups of the polymer matrix through all stages of the nanoparticle formation.

Luther *et al.* (2002) used a number of experimental techniques to clarify when Cu(II) reduction occurs in CuS precipitation at 25 °C. During cluster formation from Cu_3S_3 ring condensation, the release of some Cu(II) back into solution indicates that this electron transfer between Cu(II) and the S^{2-} occurs after the Cu-S bond formation and higher order cluster formation. Electron paramagnetic resonance (EPR) spectroscopy data analysis confirms that the covellite mineral formed contains only Cu(I) and that the Cu(I) forms in solution. Mass spectrometry data on covellite and laboratory prepared solid and solution CuS materials indicate Cu_3S_3 six-membered rings form in solution. The rings are the building blocks for aqueous CuS molecular clusters, which lead to CuS precipitation, better presented as copper (I) disulfide (Cu_2S_2). Frontier molecular orbital analysis for Cu(II) and sulfide indicate that an outer sphere electron transfer is symmetry forbidden, which is consistent with electron transfer occurring after the Cu-S bond formation via an inner-sphere process.

In hydrometallurgical processes, Van Hille *et al.* (2005) highlight two difficulties experienced in sulfide precipitation, namely, the formation of fine particles due to primary nucleation, aggregation and attrition, which is caused by low solubilities and high supersaturation levels,

and high localised sulfide concentration caused the formation of polysulfide complexes, consuming the sulfide reagent, which compromises metal removal. In the mixed Ni/Co system, Lewis (2006) reduces fines formation by reducing the local super-saturation by multiplying the feed points over the fluidised bed reactor. In contrast, fines formation in the CuS system cannot be avoided due to high super-saturation caused by a more insoluble CuS. The findings were applicable to precipitation at room temperatures.

At higher temperatures (60 - 95 °C), experience from the Rhodium Removal Section development test work and plant operation at RBMR shows that CuS precipitation upon thiosulfate addition initially turns the solution to a murky, colloidal green/brown colour within the first second, which rapidly converts to a dark brown or black covellite precipitate within approximately two seconds. The particle size distribution has a D_{50} of approximately 20 µm, with some particles being as large as 100 µm. These particles have been produced in a continuous stirred tank reactor, where more crystal growth can occur.

2.4 Hypothesis for Rh co-precipitation mechanism with CuS

The Rh co-precipitation mechanism proposed for Rh concentration two orders of magnitude lower than Cu is as follows:

1. Reduction of solution oxidation potential with reducing agent,
2. Ionic precipitation of CuS with sodium thiosulfate through primary nucleation,
3. Ionic Rh precipitation, catalysed by CuS precipitate, possibly forming mixed sulfide compounds,
4. Rh^{3+} cationic substitution of Cu^{2+} in the preferentially precipitated CuS, in the absence of aqueous or adsorbed sulphide, leaching Cu^{2+}back into solution.

It is proposed that co-precipitation occurs predominantly through the substitution reaction path in the heterogeneous phase, as a large amount of Cu^{2+} preferentially consumes the available sulfide ion. Operating temperature may affect the relative amount by changing the overall relative ionic precipitation kinetics of Cu^{2+} and Rh^{3+}. Rh co-precipitation can be approximated by pseudo first order kinetics during large excess of aqueous sulfide addition.

Chapter Three

3 THEORY

3.1 Sulfide precipitation

3.1.1 Ionic precipitation

Habashi (1999) in his textbook on hydrometallurgy briefly describes sulfide precipitation and this is summarised below.

Ionic precipitation reactions have the general equation:

$$yMe^{x+} + xA^{y-} \rightarrow Me_yA_{x(s)} \qquad (3.1)$$

where

A^{y-}	anion with negative charge y
Me^{x+}	metal with positive charge x
$Me_yA_{x(s)}$	Metal compound precipitate

Sulfide precipitation kinetics are usually fast because the precipitate formed has low solubility and is attracted together by electrostatic forces (Habashi, 1999).

For Cu and Rh ionic precipitation pertinent to this study:

$$Cu^{2+} + S^{2-} \rightarrow CuS_s \qquad (3.1a)$$

$$2Rh^{3+} + 3S^{2-} \rightarrow Rh_2S_{3\,s} \qquad (3.1b)$$

The solubility product (K_{SP}) is given by:

$$K_{SP,\,Mes} = \{Me^{2+}\}\{S^{2-}\} \qquad (3.2)$$

for the reaction: $MeS \rightarrow Me^{2+} + S^{2-}$

where $\{Me^{2+}\}$ activity of metal ion
$\{S^{2-}\}$ activity of sulfide ion

This gives the equilibrium relationship between the activity of the metal ion and sulfide ion with the precipitated metal sulfide, which is defined as unity. The K_{SP} of base metal and heavy metal sulfides are very small; hence the materials are very insoluble. The K_{SP} at 25 °C in water for Rh_2S_3 and other metal sulfides like CuS are summarised in Table 3.1 in Section 3.1.2. Rh_2S_3 ranges from 10^{-53} - 10^{-83}.

The chemical driving force for pure, ionic metal sulfide precipitation is given by the thermodynamic relationship:

$$\Delta G = -RT \ln(K_{SP})$$

where ΔG is the Gibbs free energy (chemical driving force),
R is the universal gas constant and
T is the absolute temperature

The negative ΔG implies that the reaction occurs to the right. The large negative number implies that the reactions can be taken as irreversible.

There are a number of possible Rh sulfide compounds that could form. Rh_2S_3 compound is precipitated as a black powder upon addition of hydrogen sulfide to Rh chloride solutions (Griffith, 1967). Rh_2S_5, Rh_3S_4, and Rh_9S_8, as well as Rh_2S_3, are included in the HSC Chemistry® database. The later compounds require the ionic precipitation to undergo electrochemical reactions during the ionic precipitation.

An increase in precipitation temperature leads to and increase in the primary nucleation rate (Söhnel and Garside, 1992), which will lead to more particle formation, with relatively less crystal growth, causing finer particles with more total surface area.

3.1.2 Cationic substitution

The general definition for metathesis reaction, or sometimes called exchange reactions or double decomposition reactions, is a chemical reaction between two compounds in which parts of each are interchanged to form two new compounds, illustrated by the following reaction:

$$AB + CD = AD + CB \qquad (3.3)$$

The general cation exchange / substitution / metathesis reaction in metal sulfides in a sulfate medium is given by:

$$Me^{I}SO_{4\,aq} + Me^{II}S_{\,s} \rightarrow Me^{I}S_{\,s} + Me^{II}SO_{4\,aq} \qquad (3.4)$$

where Me^{I} is less soluble than Me^{II}, and thus the solubility product, $K_{SP,I}$, is smaller than $K_{SP,II}$ and Me^{I} replaces Me^{II}. It can be shown that the ΔG_{rxn} is always negative if $Me^{II}S$ is less soluble than $Me^{I}S$. In Chapter 5, the ΔG of Rh^{3+} cation exchange with CuS is calculated as a large negative number, thus showing that the reaction is favourable.

For the Rh substitution reaction:

$$Rh^{3+} + 1.5CuS \rightarrow Rh_2S_{3\,s} + 1.5Cu^{2+} \qquad (3.5)$$

The reaction equilibrium constant is given by

$$K = \frac{\{Cu^{2+}\}^{3/2}\{CuS\}}{\{Rh^{3+}\}\{Rh_2S_3\}} = \frac{\{Cu^{2+}\}^{3/2}}{\{Rh^{3+}\}} = \frac{K_{Rh_2S_3}}{K_{CuS}\sqrt{K_{CuS}}}$$

where activities of the solids are unity activity of the sulfide in (3.2) cancel out.

The chemical driving force for metal sulfide substitution is given by the thermodynamic relationship:

$$\Delta G = -RT\ln\left(\frac{K_{Rh_2S_3}}{K_{CuS}\sqrt{K_{CuS}}}\right)$$

where ΔG is the Gibbs free energy (chemical driving force),

R is the universal gas constant and
T is the absolute temperature

Table 3.1 provides a summary of solubility products of metal sulfides relevant to this study or cited in the literature. The data highlights the various solubility differences of the various metal sulfides.

Table 3.1: Solubility product (K_{SP}) using molar basis on metal

Reference	Rh_2S_3	Rh_3S_4	Rh_9S_8	Rh_8S_{15}	$Rh_{10}S_{23}$	CuS	Cu_2S	NiS	FeS	CoS	MnS	Tl_2S	In_2S_3	Ag_2S
Kalthoff and Moltzau (1935)						$1x10^{-18}$ - $1x10^{-20}$		$1x10^{-05}$						
Monhemius (1977)						$1x10^{-36}$	$2x10^{-48}$	$1x10^{-21}$	$2x10^{-19}$		$5x10^{-14}$			
Thomas (1964)	$1x10^{-53}$ - $1x10^{-57}$													
http://www.ktf-split.hr						$8x10^{-37}$		$4x10^{-20}$	$8x10^{-19}$	$5x10^{-22}$	$3x10^{-14}$	$6x10^{-22}$	10^{-73}	$8x10^{-51}$
HSC database	$7x10^{-84}$	$2x10^{-79}$	$6x10^{-67}$	$2x10^{-85}$	$3x10^{-88}$	$4x10^{-37}$	$2x10^{-24}$	$1x10^{-22}$	$1x10^{-17}$	$1x10^{-43}$	$4x10^{-14}$			
HSC References	Knacke'91	Knacke'91, Mills'74	Mills'74	Mills'74	Mills'74	Knacke'91, Glushko'96, Landolt' 00	Barin'89 SGTE'94 Landolt' 00	Barin'93	Barin'93 Slop'96	Ruzinov75 Glushko96 Landolt' 00	Kosola'86 Barin'95, Landolt' 01			

Note: HSC calculated data had to be adjusted to a per mole basis of metal ion precipitated for direct comparisons

A more general qualitative order of metal sulfide solubility from most soluble to least soluble is given by: FeS <ZnS <NiS <CoS <PbS <CdS <CuS <Ag_2S <HgS <Ir_2S_3 <Rh_2S_3 <PtS_2 <RuS_2 <OsS_2 <Au_2S_3 (Thomas, 1964).

The cationic substitution precipitation path has not been described in the general precipitation theory reviewed.

3.1.3 Metal sulfide co-precipitation

The general co-precipitation reaction is approximated by (Rudnev and Malofeyeva, 1964):

$$Me^{I}SO_{4\,aq} + Me^{II}S.nH_2S \rightarrow Me^{I}Me^{II}S_2.(n-1)H_2S + 2H^+ + SO_{4\,aq} \qquad (3.6)$$

For Rh co-precipitation with CuS in the presence of H_2S, HS^- and S^{2-}:

$$Rh^{3+} + CuS.nH_2S \rightarrow CuRhS_2.(n-1)H_2S + 2H^+ + e^- \qquad (3.7a)$$

or,

$$2Rh^{3+} + CuS.nH_2S \rightarrow CuRh_2S_4.(n-3)H_2S + 6H^+ \qquad (3.7b)$$

In the absence of H_2S in solution cationic substitution reactions in Section 2.2 and 3.1.2. An increase in precipitation temperature should lead to faster primary nucleation (Söhnel and Garside, 1992), leading to finer particles with more surface area.

3.2 Kinetic modelling theory

This section is based on Chapter 3 of Levenspiel's book on Chemical Reaction Engineering, assuming homogeneous reaction kinetics is applicable, and Chapter 12 for heterogeneous fluid particle reactions (Levenspiel, 1972).

3.2.1 Homogeneous ionic precipitation

During the initial stage of MeS precipitation the reaction would take place in the homogeneous solution phase with reaction:

$$2\ Rh^{3+} + 3\ S_2O_3^{2-} + 3\ H_2O \rightarrow Rh_2S_{3\,s} + 3\ H_2SO_{4\,aq}$$

The reaction rate may be a function in the form of

$$-r_{Rh} = -\frac{dC_{Rh}}{dt} = -1.5\frac{dC_{Na_2S_2O_3}}{dt} = kC_{Rh}{}^{x}C_{Na_2S_2O_3}{}^{y}$$

where k is the overall rate constant
$x+y$ order of reaction.

3.2.2 Pseudo first order kinetics

For ionic Rh precipitation in the bulk phase (or heterogeneous reaction can be approximated by homogeneous reaction kinetics):

$$2\ Rh^{3+} + 3\ S_2O_3^{2-} + 3\ H_2O \rightarrow Rh_2S_{3\,s} + 3\ H_2SO_{4\,aq}$$

Assuming excessive thiosulfate addition,

$$-r_{Rh} = -\frac{dC_{Rh}}{dt} = k_1 C_{Rh} \qquad (3.8)$$

where $k_1 = C_{Na_2S_2O_3}\ k$

k_1 is the apparent or pseudo rate constant
k is the rate constant

Separating and integrating over $[Rh]_0$ to [Rh] over time = 0 to t provides

$$-\ln\frac{C_{Rh}}{C_{Rh,0}} = k_1 t \qquad (3.9)$$

Plotting $-\ln\frac{C_{Rh}}{C_{Rh,0}}$ *vs* t gives a straight line with slope k_1 going through the origin if the kinetics are first order.

However, if the y-intercept is greater than zero, while a significant linear relationship is maintained, then this shows that there is a delay before the first order kinetic relation applies. Graphically, this delay is the time required to shift the linear fit to the right to pass through the origin. Mathematically, this is performed by using the first data point of the linear fit after the delay, showing the linear relationship as the pseudo feed sample, making this time pseudo time zero.

$$-\ln\frac{C_{Rh}}{C_{Rh,0}} = k_1 t^{l} \qquad (3.10)$$

where $t^{l} = t - t_d$

t^{l} pseudo or apparent time
t_d time delay before model fits first order kinetics.

3.2.3 Pseudo second order kinetics

When $Na_2S_2O_3$ is added in excess it would effectively remain constant and the rate equation will reduce to pseudo second order, assuming *x* equals 2.

$$-r_{Rh} = -\frac{dC_{Rh}}{dt} = k_1 C_{Rh}^{\ 2} \qquad (3.11)$$

where $k_1 = C_{Na_2S_2O_3}\ k$

Separating and integrating over $C_{Rh,o}$ to C_{Rh} over time = 0 to time = t provides

$$\frac{1}{C_{Rh}} - \frac{1}{C_{Rh,0}} = \frac{1}{C_{Rh,0}}\frac{X_{Rh}}{1-X_{Rh}} = k_1 t \qquad (3.12)$$

The reaction is second order if plotting "$\frac{1}{C_{Rh}}$ vs t" gives slope k_1 and intercept $\frac{1}{C_{Rh,0}}$.

For a time delay t_d,

$$\frac{1}{C_{Rh}} - \frac{1}{C_{Rh,0}} = k_1 t^{l} \qquad (3.13)$$

where $t^{l} = t - t_d$

3.2.4 Modelling the Arrhenius rate equation

The rate constant temperature dependence is modelled using the Arrhenius Law, where.

$$k = k_0 e^{-Ea/RT} \qquad (3.14)$$

where

k	overall rate constant
k_o	frequency factor
E_a	activation energy
R	universal gas constant
T	temperature in Kelvin

Taking natural log on both sides of the equation, gives the linear relationship:

$$\ln(k) = \ln(k_0) - \frac{E_a}{R}\frac{1}{T} \qquad (3.15)$$

Plotting ln (k) against 1/T provides the activation energy and frequency factor constants,

where E_a = slope * R

k_0 = exp(y-intercept)

For pseudo first or second order relation, where the thiosulfate concentration is in excess and effectively remains constant, the measured rate constant is given by:

$$k_1 = C_{Na_2S_2O_3}\, k = (C_{Na_2S_2O_3})_o\, k_o^{I}\, e^{-Ea/RT} \qquad (3.16)$$

The reaction rate constant is given by:

or $k = k_1 / C_{Na_2S_2O_3}$ where concentration is in mol/l

Applying the above procedure would measure the pseudo rate constant (k_1) and the exponential of the y-intercept would provide the pseudo frequency factor (k_o^I) and

$$k_o = k_o^I / (C_{Na_2S_2O_3,O})$$

Modelling C_{Rh} for a specific, initial $C_{Rh,0}$ and constant $C_{Na_2S_2O_3}$ and temperature over time:

$$C_{Rh} = C_{Rh,0} \exp(-k_1 t) \qquad (3.17)$$

3.2.5 Modelling heterogeneous ionic precipitation reactions

As soon as precipitation occurs through crystal growth at the surface, the process then switches to a more complex heterogeneous reaction system involving a number of process steps.

The process steps are:

1. Rh^{3+} diffuses from the bulk solution through the boundary layer to the surface of the CuS particle,
2. $S_2O_3^{2-}$ S^{2-}, HS^- and H_2S_{aq} diffuse from the bulk solution through the boundary layer to the surface of the CuS particle,
3. Additional macro and micro pore diffusion can occur into the CuS particle,
4. Adsorption of the cations and anions onto the CuS solid surface,
5. Ionic chemical reaction on the surface, depositing Rh sulfides,
6. Diffusion of cations produced from the reaction e.g. H^+ back to bulk solution.

The overall kinetics would be determined by the rate-controlling step. The appropriate model and rate-controlling step would have to be evaluated, which is probably the reverse of the shrinking core model for small, spherical particles, auto catalysed by the metal sulfide precipitated.

3.2.6 Cationic substitution reaction

This heterogeneous reaction,

$$2\,Rh^{3+}{}_{aq} + 3CuS_{\,s} \rightarrow Rh_2S_{3\,s} + 3Cu^{2+}{}_{aq}$$

would pass through a number of sub-processes provided in Section 3.2.5. The overall kinetics is determined by the rate-controlling step. However, in this particular case the CuS is added in large excess, thus the surface area could be assumed constant. At these conditions the overall reaction kinetics may be approximated by homogeneous, pseudo first order kinetics.

Very fast Rh precipitation kinetics at the surface could lead to Rh^{3+} concentration at the CuS surface approaching zero and the reaction rate could switch to diffusion control across the boundary layer. Assuming constant area, at steady state the reaction rate at the surface is equal to the mass transfer rate-controlling step.

For first order reaction kinetics at the surface, mass transfer rate is given by:

$$Q_{Rh,liq} = k_{Rh,l}\,(C_{Rh,b} - C_{Rh,s}) \qquad (3.18)$$

where

$Q_{Rh,liq}$	rate of Rh consumed in the liquid
$C_{Rh,b}$	Rh concentration in the bulk solution
$C_{Rh,s}$	Rh concentration at the surface
$k_{Rh,l}$	mass transfer co-efficient over the boundary layer

The rate of Rh consumption at the reaction site at the surface is:

$$Q_{Rh,s} = -\,k_s\,C_{Rh,s} \qquad (3.19)$$

where

$Q_{Rh,s}$	rate of Rh consumed at the surface of the solid
$Q_{Rh,s}$	Rh concentration at the surface
$k_{Rh,s}$	chemical reaction constant of the surface reaction

At steady state $Q_{Rh,s} = Q_{Rh,liq}$

thus

$$k_{Rh,l}\,(C_{Rh,b} - C_{Rh,s}) = -\,k_s\,C_{Rh,s} \qquad (3.20)$$

Solving 3.20 for $C_{Rh,s}$ and substituting back into 3.18, as it cannot be measured, provides the overall equation for the rate of Rh precipitation:

$$Q_{Rh,liq} = -\,k_{overall}\,C_{Rh,b} \qquad (3.21)$$

which is a first order relationship.

$k_{overall}$ is a function of k_s ,k_L and a_{CuS} and will remain constant only if a_{CuS} is in large excess, effectively remaining constant. If a_{CuS} decreases, then the measured $k_{overall}$ will decrease as well, effecting the first order kinetics.

Thus plotting the rate of Rh consumption at a particular solution concentration against that Rh solution concentration should give a straight line through the origin.

Mass transfer limiting process is supported by finding by Roy (1961) at elevated temperatures, which showed that precipitation rate and extent increased from the agitated

batch reactor to the turbulent pipe reactor, as well as measuring first order towards precipitation completion.

3.2.7 Co-precipitation reaction

This reaction involves simultaneous ionic precipitation and substitution reaction and its kinetic modelling would more than likely correspond with the kinetic modelling of the dominant individual path.

3.2.8 Calculation of the reaction rate

The rate of Rh precipitation ($-r_{Rh}$) at a particular time was estimated by differentiating the model of the precipitation extent, where:

$$-r_{Rh} = C_{Rh,o}\,(dX_{Rh}/dt) \qquad (3.22)$$

For (pseudo) first order kinetic model:

$$-r_{Rh} = k_{measured} \cdot C_{Rh}$$

where $k_{measured}$ is the overall rate constant for the middle period and C_{Rh} is the actual concentration measured.

For the precipitation data at atmospheric temperatures, the logarithmic function ($y = a\ \ln(x) + b$) in Fig 6.19, where:

y = Rh precipitation extent (X_{Rh})
x = time (t), and
a , b = constants of the logarithmic fit

$-r_{Rh}$ at a particular time was calculated by:

$$\begin{aligned} -r_{Rh} &= C_{Rh,o}\,(dX_{Rh}/dt) \\ &= C_{Rh,o} \cdot d/dt(a\ \ln(t)) \\ &= C_{Rh,o} \cdot a/t \end{aligned} \qquad (3.23)$$

and the Rh concentration at time (t) is estimated from the model by:

$$C_{Rh} = C_{Rh,o}\,X_{Rh} = C_{Rh,o}\,(a\ \ln(t) + b) \qquad (3.24)$$

Chapter Four

4 EXPERIMENTAL DESIGN

4.1 Overview

The approach taken is divided into a theoretical thermodynamic study of the proposed chemistry and a practical study measuring the relative kinetics.

4.1.1 Thermodynamic study

Thermodynamic properties of the various chemical reactions have been calculated for the ΔH, ΔS, ΔG, K and logK over 0 – 200 °C using HSC Chemistry® chemical reaction and equilibrium software package, which has an extensive thermo-chemical database. This shows whether the reactions are possible from a thermodynamic perspective and gives a measure of the expected driving force for the chemical reaction.

Eh-pH equilibrium diagrams and equilibrium compositions diagrams have been generated for the S-Cu-Rh-H_2O systems at elemental concentrations pertinent to this study, namely, 20 g/l Cu, 100 mg/l Rh and 10 g/l S. The diagrams provide the stable region of the various possible compounds with respect to the electropotential of solution and pH. The effect of temperature and Rh concentration on the system is shown. The modelling is performed for all the species in the HSC database and then for selected species providing a more realistic metastable case.

Equilibrium compositions diagrams have been generated for the S-Cu-Rh-H_2O system over various thiosulfate addition amounts to the same solution composition. The relative amount of the ions and compounds formed at equilibrium are calculated at 95 °C and 150 °C, Rh concentration 100 mg/l and 10 g/l. The effect of initial acid concentration is studied. The modelling is performed for all species and compared to the metastable case.

The thermodynamic study is limited by the fact that thermodynamics predicts whether something is possible. However, the fact that something is possible does not imply that it actually will occur at an appreciable rate. Kinetic effects must be taken into consideration and kinetic models cannot be created without actual measurement of the process.

4.1.2 Kinetic study

In order to determine the dominant reaction path for Rh co-precipitation with CuS, the kinetics and extent of Rh precipitation through the ionic precipitation and substitution reaction were measured in isolation and compared to the combined effect during co-precipitation.

Synthetic feedstock solutions were produced individually for each test from analytical quality reagents in order to achieve approximately 100 mg/l Rh^{3+} concentration with base metal

sulfates and sulfuric acid concentrations approximately two orders of magnitude higher. The calculated make-up feed concentrations are provided in Table 3.1.

The tests were designed specifically to keep all the variables constant, particularly the ratio of sulfide addition to Rh ion, whether in the form of thiosulfate or previously precipitated CuS, in order to be able to compare the relative kinetics of the various systems. All the kinetic test work was performed in the same batch pressure vessel, at constant agitation and initial operating volume. Additional steps taken to ensure comparable test conditions are provided in the Section 4.3.

Reaction profiles over time were generated at 50, 80, 95 and 150 °C to evaluate the effect of temperature on the reaction path, as well as measure the activation energies for the three reactions. Thus a total of 12 kinetic tests were performed at specific test conditions provided in Section 4.5. Up to 11 samples of ~100 mL each were taken for each precipitation profile, which reduced the original volume by up to a maximum of 25%.

The batch pressure vessel operates as a closed bomb, thus the pressure was controlled manually. All tests were performed under a nitrogen atmosphere to avoid re-oxidation of the metal sulfide precipitate, particularly at elevated temperatures. The system was purged with nitrogen to strip the oxygen from the water during the heat-up phase at atmospheric temperatures. Temperature was controlled using an automatic temperature controller using an on/off electrical heating jacket and on/off cooling water in a submerged cooling coil.

Mineralogical studies would provide a comparison of the distribution of Rh substituted and co-precipitated in the CuS and specific compound formation to assist in determining the dominant reaction path.

4.2 Methodology and Procedure

4.2.1 Feed preparation

The feedstock for each individual test was prepared by weighing out the required base metal salts and acid as per the calculated requirements and added to 5.2 L demin water, which included the Rh solution volume if it were added up front. Rh volume was accurately pipetted from the 10 g/l $Rh_2(SO_4)_3$ standard stock solution. Concentrations are provided in Table 4.1.

Table 4.1: Synthetic feed make-up concentrations calculated for various tests

Element	Units	Calculated Concentrations			
		Path 1	Path 2a	Path 2b	Path 3
		Ionic Rh pptn	CuS pptn	Substitution	*In situ* co-pptn
Rh(III) as $Rh_2(SO_4)_3$	mg/l	96	0	0	96
Cu(II) as $CuSO_4$	g/l	0	14.2	0	14.2
Ni(II) as $NiSO_4$	g/l	0	5.5	0	5.5
Fe(II) as $FeSO_4$	g/l	0	0	0	0
H_2SO_4	g/l	15	15	15	15
Na^+ as Na_2SO_4	g/l	0	0	0	0
K^+ as K_2SO_4	mg/l	1000	1000	1000	1000

A number of precautions were taken to assist troubleshooting or to simplify the system. Potassium was added as a tie element to adjust concentrations for any dilution effect from filtration or errors or concentration effect from elevated temperature operation, particularly flashing off samples. Iron, which is normally in plant leach solutions, was not added to the feed solutions, to avoid iron hydrolysis reactions at elevated temperatures, as well as post precipitation in the filtrate samples. This simplified the system, as iron oxides and hydroxides can precipitate PGMs (Chapter 5) (Barkan and Greiver, 1977b).

Sodium thiosulfate was injected at temperature in the ionic and co-precipitation test, as well as CuS preparation in part (a) of the substitution reaction, while Rh was injected at the desired temperature to the CuS slurry in part (b) of the substitution reaction. The starting point of the reaction is defined as time zero (t=0) at the point of reagent injection.

Prior to reagent injection, a feed sample was taken at the desired operating temperature to compare the analysis with the design value. This extracted feed sample and subsequent reagent injection with flush water caused dilution and the actual feed concentrations at time zero had to be calculated (Table 4.3 in Section 4.5.1). Comparison of the measured value with the design value, as well as taking cognisance of the metal accounting, was used to estimate whether gross errors had occurred in the feed make-up procedure.

4.2.2 General operating procedure

The pressure vessel was operated as per the Anglo Research standard operating procedure by a Pressure Vessel (PV) operating technician.

The PV was purged with nitrogen (99.9%) during heat up prior to sealing the vessel before elevated temperatures were reached. The total pressure is a sum of the steam partial pressure achieved at the operating temperature and the nitrogen pressure supplied. The agitator speed was set at approximately 400 rpm. The temperature was automatically controlled at the desired setpoint. For atmospheric temperature tests, pressure was supplied from the nitrogen source to remove samples. At elevated temperatures the additional nitrogen pressure was supplied above the steam vapour pressure to approximately 5 bar.

Prior to sampling, the sampling line was blown clean using nitrogen, which provided the required pressure for sampling as well. The sampling system and the injection system shared a small portion if the same line into the PV, consisting of the sampling dip pipe, the sampling valve and bend to the quick-coupling connection. It was thus imperative to take a flush sample to avoid or reduce contamination of the feed sample and first profile sample. The flush sample volume was measured and recorded. Afterwards, approximately 100 mL feed sample was taken and the volume recorded. The sample blow-back procedure was deemed to be sufficient for the subsequent profile samples.

The injector bomb and flexible tubing was first purged of air before adding the reagents and sealing the system. At the desired operating temperature, reagents were injected using nitrogen of at least 2 bar greater than the PV operating pressure. The reagents were injected in spurts over a couple of seconds. In the case of injecting Rh^{3+} solution, the 50 mL of Rh solution was immediately chased by 100 – 150 mL of demin water. This wash water was carefully poured on top of the Rh solution in order to wash all the reagents off the walls.

Samples were taken through an open, cooled sampling system into a measuring cylinder i.e. the elevated temperature samples were flashed off across the sampling valve. The volume of the slurry was recorded prior to immediate filtration on a 0.45 micron Millipore system. General procedures for filtration are described in the Sample Preparation in Section 4.3.

No more than 11 samples of approximately 100 mL were taken from the PV, thus the volume did not drop below 4 litres or 75% of the original volume. Reducing the agitation was considered as a measure to compensate for the increase in power input per unit volume due to the drop in operating level. However, the calculations showed that the agitation speed had to be reduced by 1 rpm per 100 mL sample and the agitation speed control was not sensitive enough to achieve this. In most cases, the speed reduced by more than 1 rpm and could not be increased as it was already operating at maximum power output.

At the termination time, a large sample, usually around 900 mL, was taken from the PV prior to switching to cooling. This filtrate sample was filtered immediately and used for the solution sample for assay purposes. The system was rapidly cooled after taking this final sample to avoid additional precipitation during the PV cooling and dismantling time. This delay time was approximately 15-25 min for the elevated temperature tests, though it had no impact on the Rh solids, as the initial, representative filtration sample showed that Rh precipitation was already complete. In the atmospheric temperature tests, the delay before final filtration was significantly less. The mass balance data shows that additional precipitation was insignificant, as these reactions had already terminated.

Ideally, the redox measurement would have been taken on the slurry prior to filtration, however, the instrument had a very slow response time and the delay would affect the kinetic results. This redox was thus measured on all the filtrate samples at the end of the test.

When changing from one reaction path regime to another extra cleaning precautions were taken to remove all precipitate from the walls and internals of the PV.

Deviations from these general procedures are highlighted in the specific procedures for the three reaction path tests described below.

4.2.3 Ionic Rh precipitation procedure

During co-precipitation, CuS forms immediately, providing the catalyst for ionic Rh precipitation. Thus, in order to maintain comparable kinetic regime, the Rh ionic precipitation reaction was seeded with an inert metal sulfide to eliminate the induction period of primary Rh nucleation.

In the feed preparation, 20 mg of PdS was added to the feed solution, which is 1.5% of the expected maximum Rh_2S_3. The seed was prepared in a 1L glass beaker with magnetic stirring at stoichiometric palladium chloride and thiosulfate addition and 85-95 °C. Details of this test (#0-3) are attached in Appendix B.4 log sheet. The Rh solution was added up front into the feed solution for test no. 1 – 4. The general procedures were then followed.

Unfortunately, in the elevated temperature test (#4), 75% of the Rh in the feed precipitated during the long heating phase to reach 150 °C, which probably precipitated through hydrolysis. The #4 test results were discarded and replaced with results from an adapted procedure to eliminate the precipitation (#4R). The PdS seed was not available for the repeat test. To eliminate this precipitation through hydrolysis, Rh solution was injected at 150 °C. The bomb was then flushed and prepared for the thiosulfate injection within a few minutes. The feed sample was then taken after an initial flush sample and only then was the thiosulfate injected. This procedure was followed in the co-precipitation precipitation at 150 °C as well.

4.2.4 Substitution reaction procedure

For the particular temperature, say 95 °C, first, in part (a) of the test, the CuS was precipitated under the same conditions as co-precipitation test at 95 °C, forming a precipitate with the same characteristics as the co-precipitation test, for example pore size and surface area. Sodium thiosulfate was injected at temperature to produce the same amount of CuS as the co-precipitation test. Profile samples could not be taken, as this would remove sulfide from the system. The final slurry was filtered and then washed with water acidified to a pH of 2 to remove Cu^{2+}, HS^- and S^{2-}. The wet solids were repulped in the acidified water, re-filtered and stored in this water before commencing part (b) of the test.

For part (b) of the substitution reaction, the feedstock was made to desired concentrations and the test started as per the general procedure. Rh was not added to the feed solution to avoid the substitution reaction occurring during the heating phase. Base metal salts were not added to the solution so that the leaching of Cu^{2+} during cationic substitution reaction would be easier to detect. The feed sample was taken to obtain a background Cu^{2+} concentration. Unfortunately, this removed some of the sulfide in the form of CuS from the system and test co-precipitation tests (no. 9 – 12) were adjusted accordingly. The Rh^{3+} solution was injected at desired temperature at time zero, which was the start of the actual Rh precipitation profile. The first profile sample part (b) of the test was particularly vulnerable to Rh contamination.

4.2.5 Rh co-precipitation with *in situ* CuS with sulfide addition procedure

The general procedure was followed and at temperature, the required mass of dissolved sodium thiosulfate is injected to co-precipitate CuS and Rh_2S_3 directly.

Unfortunately, taking a feed sample in 5b – 8b, some sulfide in the form of CuS was removed from the system and thus the thiosulfate addition to the co-precipitation test no. 9 – 12 was reduced accordingly.

4.3 Sample Preparation

4.3.1 General filtration procedure

The sample slurry volume was read off the measuring cylinder within an accuracy of 2 mL prior to filtration. Approximately 20% of the slurry was filtered and the filtrate was used to wet and wash the filter system and discarded. Filtration continued immediately afterwards. The filtrate sample was then taken from this solution and the solids were washed with demin water on the Millipore filtration system. Two Millipore systems were used to cope with the frequent sampling.

The final bulk filtration was performed on the same dual Millipore system using the same procedure. A large 900 mL sample was taken from the PV prior to cooling at the terminal time for the filtrate sample. The remainder of the slurry was filtered once the PV was cool enough to disassemble.

In test 5a – 8a it was imperative to remove unreacted sulfides, bisulfide and adsorbed H_2S from the CuS and thus the solids were replupled in demin water with a pH of 2 for additional washing. It was unlikely that the amount was significant, because the large excess of Cu^{2+} would have precipitated onto it.

4.3.2 Solids preparation

Samples were generally air-dried overnight to reduce the possibility of oxidation and then placed in an oven controlled at temperature <55 °C to drive off the final moisture, but ensuring that significant oxidation of the sulfide would not occur. In some cases the solids were placed directly into the oven.

Filter paper and containers masses were pre-determined on a 3-point decimal scale. The dry solids and filter paper were weighed on the same scale and the dry masses were calculated by difference. In some cases the container masses were included as well.

4.4 Experimental equipment

4.4.1 Pressure vessel batch reactor

The experimental equipment is presented in Figure 4.1. Pressure vessel equipment specifications are provided in the Table 4.2 below.

Table 4.2: Pressure Vessel Specifications

Type	Parr series 4550, 7.5 L floor stand reactor
Material of Construction	Titanium grade 4 shell and sleeve, Ti grade 2 internal tubing (cooling coil, sample line, agitator shaft and blades), Flexible hosing lined with PFA
Temperature Control	Parr series 4842 temperature controller (external electric heating jacket and internal, submerged cooling coil). Two thermocouples inserted into Ti thermowell.
Pressure Control	Manual pressure control, Pressure gauge for indication. Maximum delivery pressure set at regulator, PV vented manually.
Agitator	6-flat blade, double impeller, 85 mm diameter, 15 mm height, 130 mm between impellers (centre to centre), and approximately 40 mm off the bottom. Variable speed drive with magnetic coupling.
Gas supply	Connected to 99.9% nitrogen gas cylinder
Injector bomb	200 mL volume reagent injection system using N_2 pressure.
Sampler	50 mL sample volume with concentric pipe heat exchanger with cooling water

The sampler was positioned near the bottom of a well-agitated vessel; thus it is fair to assume that representative samples were taken. The sampler and the bomb were connected to the PV sampling line using easy, male-and-female connections for fast change-over, thus the systems shared the same line, valve and submerged sample line.

The bomb consists of 1 inch tubing with a volume of $\pm$ 200 mL connected to nitrogen pressure source. The bomb had isolation valves at the bottom and top, as well as a vent valve.

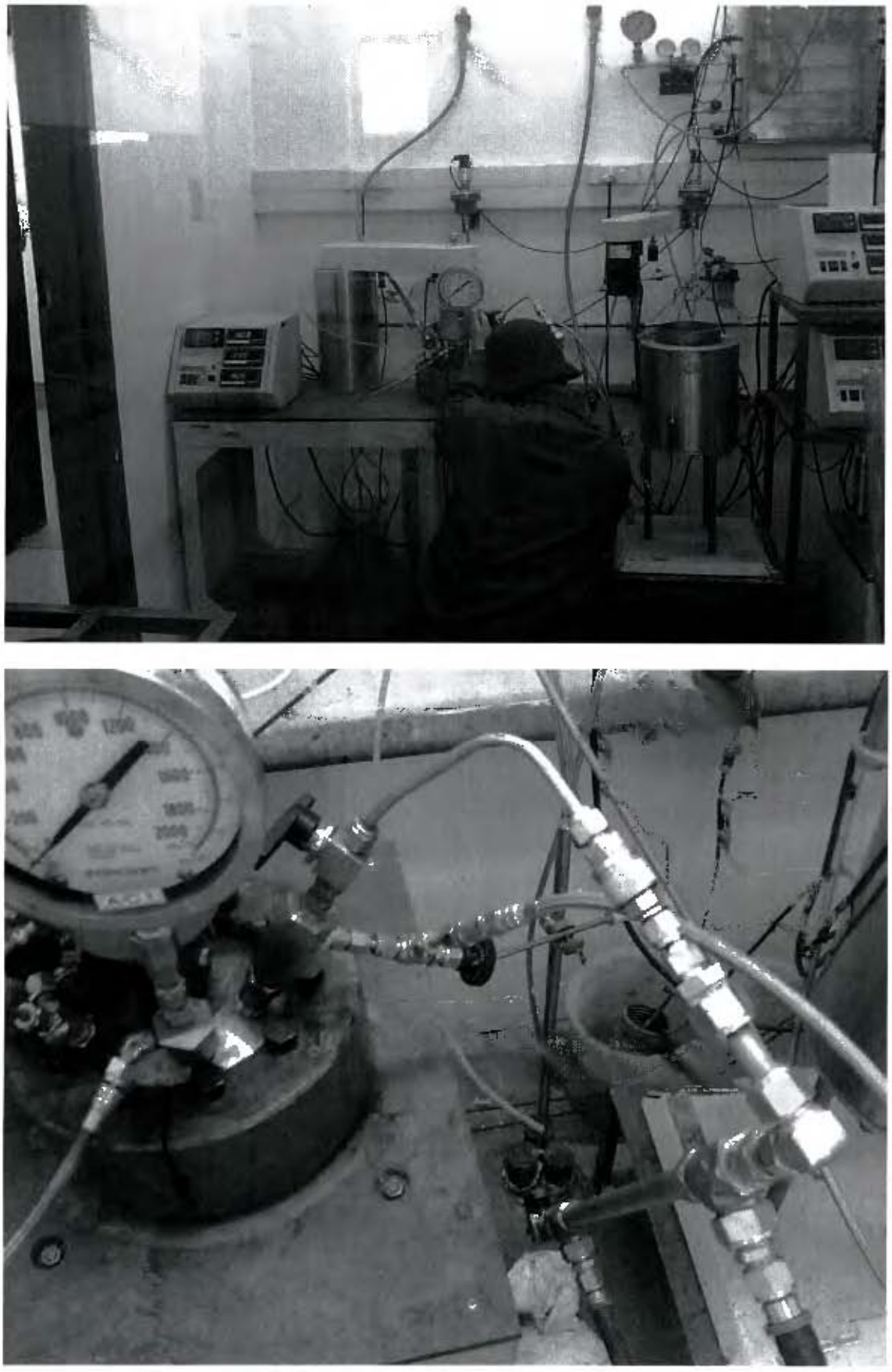

Figure 4.1: Pressure Vessel System, showing temperature controller, magnetic drive of agitator, pressure gauge, sampling system with sample and nitrogen blow-back valves and cooling water.

4.4.2 Miscellaneous equipment

Filtration equipment used for samples and bulk final slurry filtration was a Millipore filtration system using 0.45 µm filter paper and Buchner flask with vacuum achieved from a dedicated vacuum pump.

The Eh meter used was a Meterlab™ PHM220 with a Pt electrode in 3 molar KCl referenced to Ag/AgCl.

4.5 Specific Test Conditions

4.5.1 Calculated feed conditions

Make-up feed conditions are provided in Table 4.1 above. The make-up concentrations differ from the initial concentration at time zero due to the removal of the initial feed sample and dilution through reagent injection. The actual feed concentrations calculated for each specific test for the condition after reagent injection prior to reactions occurring are presented in Table 4.3.

Table 4.3: Calculated feed concentrations after reagent injection prior to reaction

Test #	Cu mg/l	Ni mg/l	H_2SO_4 g/l	Na mg/l	K Mg/l	Rh mg/l	Solids g/l
1	0	0	14.4	2264	963	93	0
2	0	0	14.4	2264	963	93	0
3	0	0	14.4	2264	963	93	0
4	0	0	14.4	2264	963	93	0
4R	0	0	14.4	2264	963	93	0
5a	13216	5118	13.4	2183	929	0	
5b	0	0	15.1	0	971	93	4.67
6a	13312	5156	13.5	2199	936	0	0
6b	0	0	14.5	0	971	93	4.67
7a	13217	5119	13.4	2183	929	0	0
7b	0	0	14.0	0	936	90	4.50
8a	13216	5118	13.9	2183	929	0	0
8b	0	0	14.4	0	962	92	4.62
9	13217	5119	13.9	2099	929	89	0
9R	13726	5316	14.4	2180	965	93	0
10	13223	5121	13.9	2100	929	89	0
11	13217	5119	13.9	2099	929	89	0
11R	13217	5119	13.9	2099	929	89	0
12	13217	5119	13.9	2099	929	89	0

The reason for the slight variations in the calculated values are due to varying volumes of flush and feed samples prior to reagent addition. In the case of acid concentration some variation was caused by small errors in make-up concentrations.

4.5.2 Specific test conditions

Specific test details, like masses of reagents added, sample volumes, measured solids concentrations, redox profiles etc, are provided in the log sheet, assays and mass balance

tables in Appendix B.4. The specific test conditions, namely, the operating temperature, form of CuS, design and actual calculated Rh concentration after injection and sampling times of the profile, are summarised in Table 4.4.

Sulfide addition ratio to initial Rh concentration in the ionic reactions was 4.5% higher than the ratio of the substitution and co-precipitation reactions due to an experimental design oversight caused by the feed samples of 5b - 8b. The ionic tests #1-3 had already been completed before the problem was realised.

In all cases, the sulfide excess was very high and it is unlikely that this slight increase would have an effect on the overall Rh precipitation kinetics.

Table 4.4: Specific test conditions

Test #	Description	Temperature [°C]	CuS Form	Rh conc [mg/l] Design calc'd	Rh conc [mg/l] Calc'd at injection	Time Profile [min]
	Miscellaneous:					
0-1	Scouting test: co-precipitation	150	ppt *in situ*	50	51	None
0-2	Rh_2S_3 seed production stoichiometric sulfide addition	150	No CuS	192	189	0, 1, 2, 5, 10, 30, 60, 120, 180, 240, 245
0-3	Produce PdS	85-95	No CuS	1000	1000 mg/l Pd	None
	Kinetic tests:					
1	Ionic Rh precipitation (PdS seed)	50	No CuS	96	93	0, 1, 2, 6, 12, 30, 60, 120, 180, 240, 300
2	Ionic Rh precipitation (PdS seed)	80	No CuS	96	93	0, 1, 2, 5, 10, 30, 60, 120, 180, 240
3	Ionic Rh precipitation (PdS seed)	95	No CuS	96	93	0, 1, 2, 5, 10, 30, 60, 120, 180, 240
4	Ionic Rh precipitation (PdS seed)	150	No CuS	96	93	0, 1, 2, 4, 7, 10, 20, 30, 60
4R	Ionic Rh precipitation (Not seeded)	150	No CuS	96	93	0, 1, 2, 4, 6, 8, 11, 15, 27
5a	CuS precipitation	50	ppt *in situ*			
5b	Substitution reaction	50	Add 5a ppt	96	93	0, 1, 2, 5, 10, 30, 60, 90, 120, 180, 240, 290
6a	CuS precipitation	80	ppt *in situ*			
6b	Substitution reaction	80	Add 6a ppt	96	93	0, 1, 2, 5, 10, 30, 60, 90, 120, 180, 240
7a	CuS precipitation	95	ppt *in situ*			
7b	Substitution reaction	95	Add 7a ppt	96	90	0, 1, 2, 5, 10, 30, 60, 90, 120, 180, 225
8a	CuS precipitation	150	ppt *in situ*			
8b	Substitution reaction	150	Add 8a ppt	96	92	0, 1, 2, 4, 7, 13, 20, 30, 60
9	Cu and Rh co-precipitation *in situ*	50	ppt *in situ*	96	89	0, 1, 2, 5, 10, 30, 60, 90, 120, 180, 240, 300
9R	Cu and Rh co-precipitation *in situ*	50	ppt *in situ*	100	93	0, 1, 2, 5, 10, 30, 60, 90, 120, 180, 240
10	Cu and Rh co-precipitation *in situ*	80	ppt *in situ*	96	89	0, 1, 2, 5, 10, 30, 60, 90, 120, 180, 240
11	Cu and Rh co-precipitation *in situ*	95	ppt *in situ*	96	89	0, 1, 2, 5, 10, 30, 60, 90, 120, 180, 240
11R	Cu and Rh co-precipitation *in situ*	95	ppt *in situ*	96	89	0, 1, 2, 5, 10, 20, 30, 60, 120
12	Cu and Rh co-precipitation *in situ*	150	ppt *in situ*	96	89	0, 1, 2, 3, 4, 6, 7, 10, 20, 30, 60

Note: ppt = precipitate ; pptn = precipitation ; R implies repeat of that test #

4.5.3 Analytical techniques and approach

Analytical techniques used for the Rh, Cu, S, K, Na and sulfuric acid are provided in Table 4.5. Anglo Research Laboratory performed the analysis according to accredited laboratory standards. The Analytical Department measured various elements randomly in duplicate.

Table 4.5: Analytical method used for various elements

Method for element	Element
ICP-MS (solution)	Rh , K
ICP-MS (solid)	Rh, K
ICP-OES (solution)	Cu, Ni
ICP-OES (solid)	Cu, Ni
Leco (solids)	S
Free Acid	Titration
Atomic Adsorption (solution)	Na

Generally, the feed and final solutions and final solids were analysed in duplicate. In some cases, the solutions visually showed post-precipitation after filtration and it was requested that these samples be treated through digestion procedure to perform a total stream analysis. Precipitation profile results in Chapter 6 show that the total stream analysis was not performed by the laboratory.

The accuracy and precision of the analytical techniques were measured towards the end of the test program by re-submitting two solutions for 5 additional analyses to determine the standard deviation and relative error associated with the analysis.

Insufficient solids were produced in the profile samples for analytical analysis. Generally, only the final solids were analysed, thus a mass balance and metal accounting could only be calculated on the final samples.

4.5.4 Mineralogical techniques

Precipitated compound form and distribution was measured using Scanning Electron Microscope (SEM) using Energy Dispersive X-ray (EDX) spectroscopy and Mineral Liberation Analyser (MLA) on preliminary material produced at 150 °C.

The electron microprobe technique with its higher resolution was the preferred mineralogical technique for characterisation of the trace concentrations, providing quantitative measurement of Rh distribution in the CuS cross-section. However, the instrument was not available at the time of the study.

X-ray Photon Spectroscopy (XPS) would have analysed the first few molecular layers of surface of the particle, providing specific compound formation and surface phenomena, but this was not performed due to budget and time constraints.

Unfortunately, only preliminary mineralogy was performed in this study using SEM-EDX due to time and budget constraints.

Chapter Five

5 CHEMISTRY AND THERMODYNAMIC MODELLING

5.1 Chemical reactions

Proposed chemistry for the various reaction paths is provided below. Thermodynamic values are calculated for ΔH, ΔS, ΔG, K and logK over 0 – 200 °C for the reactions using HSC Chemistry®. The tabulated data is attached in Appendix A.1, while the chemical reactions and their respective ΔGs are summarised in Table 5.1. The ΔG of the main reactions as a function of temperature is illustrated in Figure 5.1. ΔG is calculated through

$$\Delta G = - RT \ln(K)$$

where ΔG is the change in Gibbs free energy
R universal gas constant
T temperature
K equilibrium constant of the reaction

The aquo, sulfato or aquo-hydroxo solution speciation or complexes are not in the HSC Chemistry® database; thus the pure Rh^{3+} ion form has been used. Complexing would increase the stability of the ion and reduce the Gibbs free energy for the reactions by affecting the equilibrium constants. However, for the same Rh^{3+} complex speciation, the difference in the ΔG of various reaction comparisons would probably remain the same as the differences presented in Table 5.1.

The chemistry is discussed under the following sections:

1. Reducing the solution mixed potential,
2. Ionic precipitation using thiosulfate addition (without redox reactions),
3. Ionic precipitation using thiosulfate addition (with redox reactions),
4. Cationic substitution (without redox reactions),
5. Cationic substitution (with redox reactions),
6. Rh hydrolysis,
7. Thiosulfate degradation.

Table 5.1: Gibbs free energy of the various chemical reactions

No.	Reactions (using HSC database)	Delta G (kJ/mol Me^{x+}) @		
		50 °C	100 °C	150 °C
	Reducing the solutions mixed potential			
5.1	$4\ Fe_2(SO_4)_3 + Na_2S_2O_3 + 5H_2O \rightarrow Na_2SO_4 + 8\ FeSO_4 + 5\ H_2SO_4$	-50	-56	-62
5.2	$4\ Fe_2(SO_4)_3 + CuS + 4H_2O \rightarrow 8\ FeSO_4 + CuSO_4 + 4\ H_2SO_4$	-36	-42	-48
5.3	$12\ Fe_2(SO_4)_3 + Rh_2S_3 + 12H_2O \rightarrow 2RhSO_4 + 24\ FeSO_4 + 12H_2SO_4$	-23	-28	-34
	Ionic precipitation using sodium thiosulfate addition			
5.4	$Rh_2(SO_4)_{3\ aq} + 3\ Na_2S_2O_{3\ aq} + 3\ H_2O \rightarrow Rh_2S_{3\ s} + 3\ Na_2SO_{4\ aq} + 3\ H_2SO_{4\ aq}$	-333	-338	-341
5.5	$CuSO_{4\ aq} + Na_2S_2O_{3\ aq} + H_2O \rightarrow CuS_s + Na_2SO_{4\ aq} + H_2SO_4$	-112	-114	-116
	Ionic precipitation with redox reactions			
5.6a	$3\ Rh^{3+} + 4.125\ S_2O_3^{2-} + 4.625\ H_2O \rightarrow Rh_3S_4 + 9.25\ H^+ + 4.25\ SO_4^{2-}$	-315	-320	-323
5.6b	$4\ Rh^{3+} + 3\ S_2O_3^{2-} + 7\ H_2O \rightarrow 4\ Rh + 2S + 14\ H^+ + 4\ SO_4^{2-}$	-164	-170	-171
5.6c	$2.667\ Rh^{3+} + S_2O_3^{2-} + 5\ H_2O \rightarrow 2.667\ Rh + 10\ H^+ + 2\ SO_4^{2-}$	-143	-148	-149
5.6d	$9\ Rh^{3+} + 9.378\ S_2O_3^{2-} + 14.877\ H_2O \rightarrow Rh_9S_8 + 29.754\ H^+ + 10.755\ SO_4^{2-}$	-263	-268	-270
5.6e	$8\ CuSO_{4\ aq} + 5\ S_2O_3^{2-} + 9\ H_2O \rightarrow 4\ Cu_2S_s + 18\ H^+ + 6\ SO_4^{2-}$	-77	-79	-81
5.6f	$2\ Rh^{3+} + 4\ S + 4\ H_2O \rightarrow Rh_2S_3 + 8H^+ + SO_4^{2-}$	-247	-251	-249
	Cationic substitution (without redox reactions)			
5.7a	$Rh_2(SO_4)_{3\ aq} + 3CuS_s \rightarrow Rh_2S_{3\ s} + 3CuSO_{4\ aq}$	-167	-168	-167
5.7b	$Rh_2(SO_4)_{3\ aq} + 3NiS_s \rightarrow Rh_2S_{3\ s} + 3NiSO_{4\ aq}$	-288	-299	-287
5.7c	$2\ Rh^{3+} + 3\ Cu_2S \rightarrow 2\ Rh_2S_3 + 6\ Cu^+$	-74	-87	-97
	Cationic substitution (with redox reactions)			
5.8a	$24\ Rh^{3+} + 33\ CuS + 4\ H_2O \rightarrow 8\ Rh_3S_4 + 33\ Cu^{2+} + 8H^+ + SO_4^{2-}$	-161	-164	-167
5.8b	$6.547\ Rh^{3+} + 6.82\ CuS + 4H_2O \rightarrow 6.547Rh_9S_8 + 6.82Cu^{2+} + 8H^+ + SO_4^{2-}$	-146	-150	-149
5.8c	$2\ Rh^{3+} + 3\ CuS \rightarrow 2\ Rh + 3\ S + 3\ Cu^{2+}$	-39	-43	-44
	Rh hydrolysis			
5.9	$2Rh^{3+} + 3\ H_2O \rightarrow Rh_2O_3 + 6H^+$	-16	-34	-46
	Thiosulfate degradation			
5.10	$S_2O_3^{2-} + H_2O \rightarrow H_2S(g) + SO_4^{2-}$	-24	-28	-32
5.11	$3\ S_2O_3^{2-} + H_2SO_4 \rightarrow 4\ S + H_2O + 3\ SO_4^{2-}$ (acid consumption)	-74	-72	-71
5.12	$2Rh^{3+} + 3\ S_2O_3^{2-} \rightarrow Rh_2S_3 + 3\ SO_3(g)$	-94	-116	-138
	Cationic substitution with oxides and hydroxides			
5.13a	$Fe(OH)_3 + 2\ Rh^{3+} \rightarrow Rh_2O_3 + Fe^{3+} + 3H^+$	-16	-20	-22
5.13b	$Fe_2O_3 + 2\ Rh^{3+} \rightarrow Rh_2O_3 + 2Fe^{3+}$	-5	-3	+2
5.13c	$1.5\ Cu(OH)_2 + 2Rh^{3+} \rightarrow Rh_2O_3 + 1.5Cu^{2+} + 3H^+$	-45	-53	-58
5.13d	$3\ CuO + 2Rh^{3+} \rightarrow Rh_2O_3 + 3Cu^{2+}$	-71	-75	-76
5.14	$2Rh^{3+} + 4S + 4H_2O = Rh_2S_3 + 8H^+ + SO_4^{2-}$	-247	-251	-249

5.1.1 Reducing the solution potential

The solution mixed potential must first be reduced into the stable region of the desired metal sulfide for precipitation to occur, otherwise the oxidising species, normally ferric or oxygen, would re-oxidise these metal sulfides back into solution. In plant solutions, sufficient sodium thiosulfate must be added to reduce all the ferric to ferrous. ΔG increases in the negative direction with increasing temperature, thus the reactions would be more favourable at higher temperatures and probably faster from a thermodynamic perspective. As expected, reducing ferric with CuS has a larger negative ΔG, as it is more soluble and would leach first. Aqueous Na_2S provides greater ΔG than thiosulfate addition for ferric reduction.

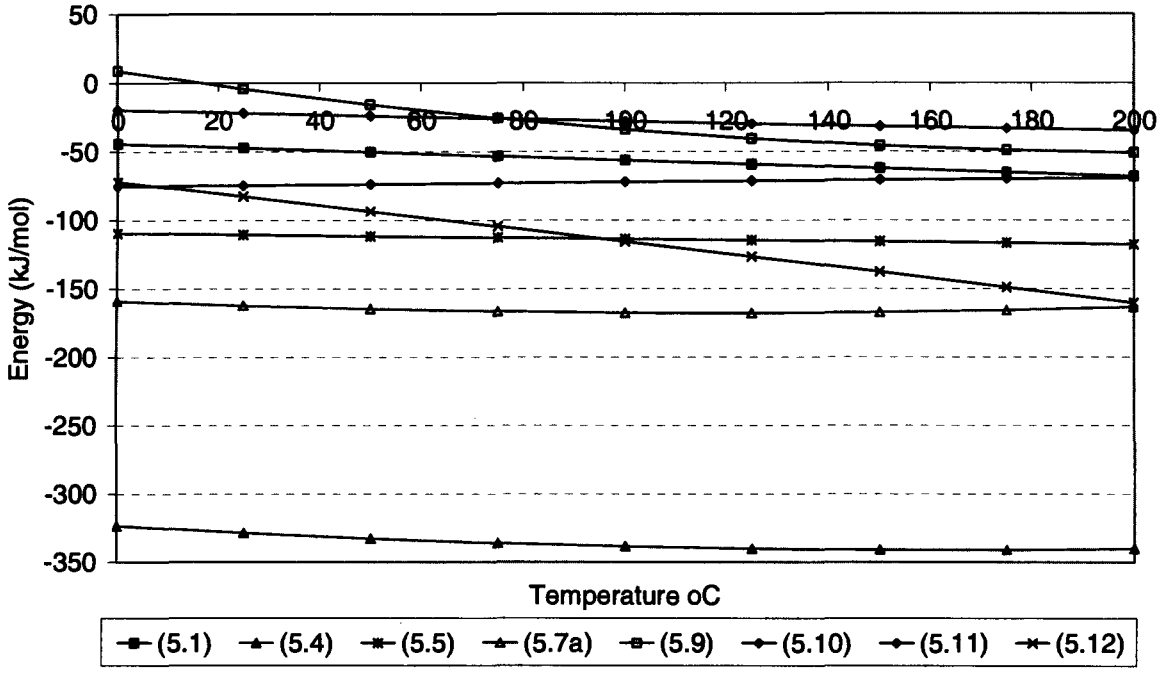

Figure 5.1: Gibbs free energy for main Rh and Cu precipitation reactions over 0 – 200 °C

5.1.2 Ionic precipitation using sodium thiosulfate addition

The driving force for the reactions is nearly independent of temperature, thus from a thermodynamic perspective, temperature has an insignificant effect on the reaction. Rh and S formation is the least favourable precipitate compared to Rh sulfides. From a thermodynamic perspective, the most favourable precipitate is Rh_2S_3, followed by Rh_3S_4 and Rh_9S_8 ($RhS_{0.889}$).

5.1.3 Rh precipitation through the substitution reaction

Indirect Rh precipitation through cation exchange or substitution reaction is evaluated for reactions with and without redox reactions. The large, negative ΔG shows that the reactions are irreversible. The driving force for the reactions is nearly independent of temperature, thus from a thermodynamic perspective, temperature would have an insignificant effect on the reaction. As expected, the ΔG of Rh substitution on NiS is significantly greater than that of CuS substitution, because of a larger solubility product difference with Rh sulfide. Similar to ionic precipitation, Rh and S formation is the least favourable precipitate compared to Rh sulfides, followed by Rh_9S_8 and then Rh_3S_4. The most favourable reaction is the formation of Rh_2S_3. Also, the ΔG of Rh ionic precipitation in Figure 1 is significantly larger than that of the substitution reaction.

5.1.4 In situ Rh co-precipitation with CuS using thiosulfate addition

Ionic precipitation of Cu and Rh could possibly occur as a mixed sulfide compound. Thermodynamic data was not available for this variable, as mixed sulfide and thermodynamic calculations have not been performed. Ionic Rh and Cu precipitation in co-precipitation would occur through ionic and substitution reaction paths described in Section 5.1.2 and 5.1.3.

The ΔG of Rh ionic precipitation is significantly larger than the substitution reactions (Fig. 5.1). Thus from a thermodynamic perspective, Rh precipitation in the Rh and Cu co-precipitation system would favour the ionic precipitation path over the substitution reaction path.

5.1.5 Rh precipitation through hydrolysis

ΔG of reaction becomes negative above ~18 °C; thus the Rh hydrolysis would be possible from a thermodynamic perspective. The relatively small value implies that the reaction probably would not occur as fast as the sulfide system. The significance of the hydrolysis reaction would be measured by the amount of oxygen detected in the residue, ensuring that no surface oxidation occurs.

5.1.6 Thiosulfate degradation

The ionic precipitation results demonstrate that a large amount of acid is consumed during the ionic precipitation tests with the precipitate being high in sulfur. This leads to investigating a number of probable reactions that would consume the thiosulfate sulfide, consume acid, and generate hydrogen sulfide and SO_2 / SO_3 gases detected in the air during the kinetic tests.

Thiosulfate hydrolysis can produce H_2S gas (5.10), while acid can break down thiosulfate and precipitate elemental sulphur (5.11). Also, the ionic precipitation of Cu^{2+} and Rh^{3+} generates acid with thiosulfate precipitation, possibly forming an intermediate SO_3 product (5.12), which in turn reacts with water to form H_2SO_4. Thus, aqueous sulfide precipitation potential could be lost to sulphur precipitation and gas loss to the vapour space, and eventually to the atmosphere during venting. Thiosulfate decomposition does not occur in the CuS precipitation and co-precipitation tests at the same extent, as the bulk of the thiosulfate is consumed immediately during Cu^{2+} precipitation.

5.1.7 Alternative Rh precipitation through substitution with hydroxides and oxides

Analogous to Rh precipitation with sulfides in the substitution reaction, Rh could precipitate onto base metal hydroxides and oxides formed at higher pHs. ΔG of reaction calculations produce negative values, excluding Fe_2O_3 reaction, which would only occur at a temperature less than 125 °C. The chemical driving force for these reactions is an order of magnitude less than the sulfide substitution reactions, thus the reaction would not occur as fast as the sulfide system. Free acid would also dissolve the oxide precipitates and thus sufficiently high pH would be required.

5.2 Eh-pH diagrams of S-Cu-Rh-H_2O system

Pourbaix diagrams and equilibrium composition diagrams have been generated for the S-Cu-Rh-H_2O systems using HSC Chemistry® to study the effect of temperature and concentrations on the system. The diagrams have been generated at Cu and S of 0.3 molality (mol/kg water) and Rh of 0.001 mol/kg. This is approximately 20 g/l Cu, 100 mg/l Rh and 10 g/l S. The purpose of presenting the diagrams is to illustrate the:

1. Eh and pH conditions of formation for the Rh and Cu sulfide compounds and types of compounds,

2. Effect of temperature on the system,

3. Effect of molality or ion activity on the system.

The exercise is first performed by selecting all species in the HSC program, which creates unrealistic diagrams not experienced in practice (Section 5.2.1). Selecting the sulfate species causes an anomaly in the diagrams due to the stability of the sulfate ion (Section 5.2.2). This anomaly of metal alloy precipitation occurring before metal sulfide precipitation is eliminated by not selecting any sulfur-containing species with a positive oxidation state and limiting the Rh sulfide species to Rh_2S_3. The aquo or sulfato or chloro or aquo-hydroxo complexes are not in the HSC Chemistry® database; thus the pure ion form has been used. Rh complexing would increase the stability region of the ion and reduce the driving force for the reaction.

5.2.1 General Eh-pH diagram using all species in HSC Chemistry ®

The general Eh-pH diagram for all species at 95 °C is illustrated in Figure 5.2. To improve readability, this diagram has been deconstructed into Eh-pH diagram of Rh-dominant species in Figure 5.3. This provides a simplified illustration of the anomaly of Rh^{3+} first being reduced to elemental Rh before being oxidised back to Rh_2S_3. Additional reduction converts it back to Rh metal. Rh^{3+} is hydrolysed at a pH of 1 to precipitate Rh_2O_3. This occurs at a higher pH in practice, probably due to Rh complexing in solution increasing the stability region of the Rh^{3+} ion.

This is an anomaly caused by the stability of the sulfate ion affecting the calculation of the HSC Chemistry® program and is eliminated in the metastable Eh-pH diagrams in the Section 5.2.2 by not including S species with a positive oxidation state (personal communication with M. Nicol).

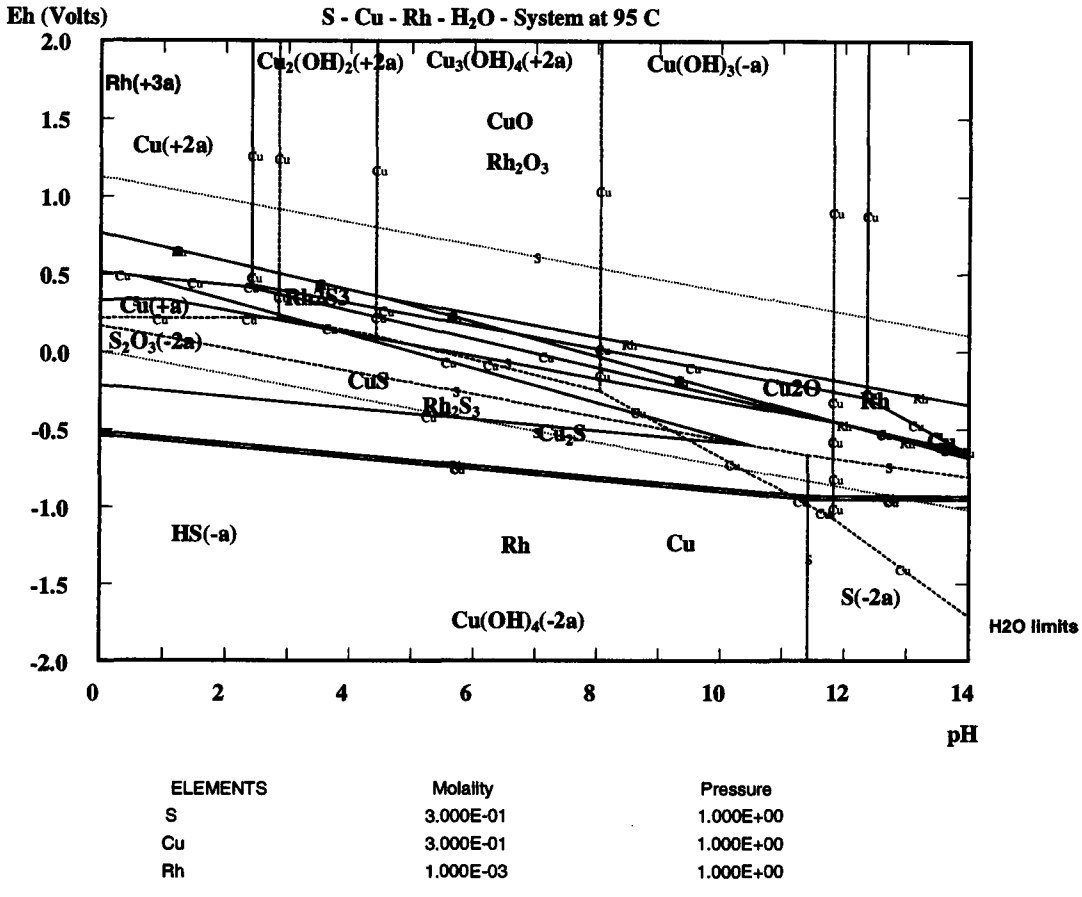

Figure 5.2: Eh-pH diagram of S-Cu-Rh-H_2O base case system for all speciation at 95 °C; upon reducing the potential with sulfide-containing reducing agent, Rh^{3+} first forms elemental Rh before converting to $RhS_{0.889}$, then Rh_3S_4 and Rh_2S_3; additional reduction will convert it back to Rh metal in the reverse sequence; at high oxidation potential, pH adjustment approaching 2 will convert Rh^{3+} to Rh_2O_3. Metal reduction is not noticed in practice and is an anomaly in the HSC calculation caused by the stability of the sulfate ion.

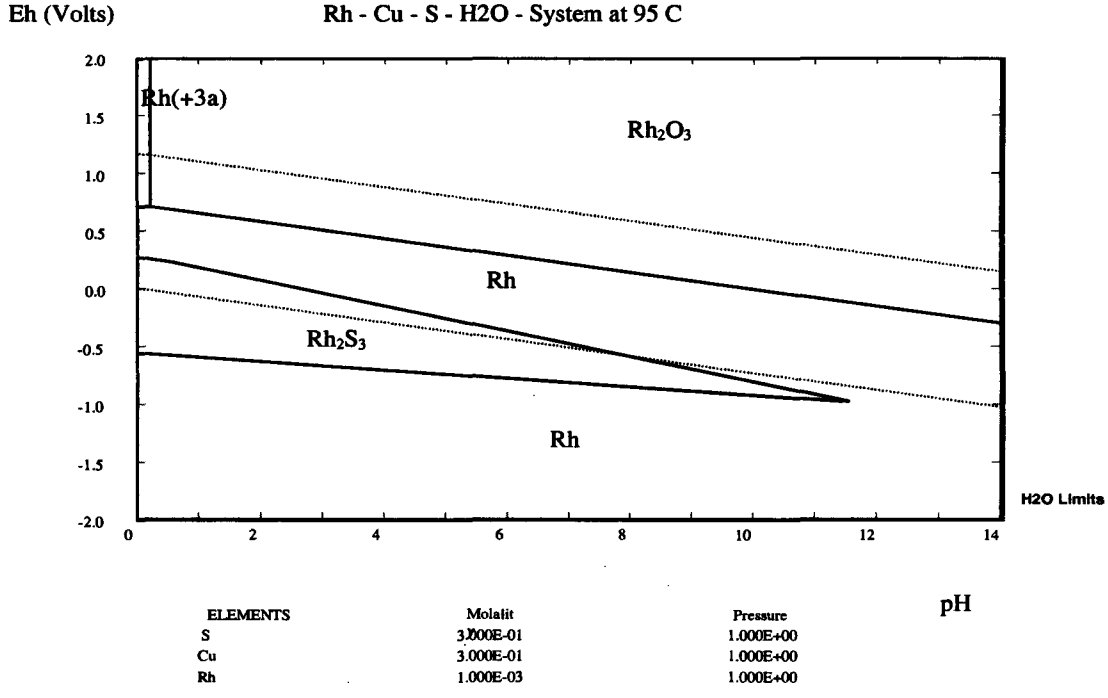

Figure 5.3: Eh-pH diagram of S-Cu-Rh-H_2O base case system for all speciation at 95 °C, only showing Rh_2S_3 dominant Rh speciation; upon reducing the potential with sulfide-containing reducing agent, Rh^{3+} first forms elemental Rh before converting to Rh_2S_3 and back to Rh metal; at high oxidation potential, pH adjustment

approaching 0.2 will convert Rh^{3+} to Rh_2O_3, though in real systems Rh^{3+} is stable to pH < 3, probably due to complexation. Rh reduction to metal prior to forming a Rh sulfide is caused by an anomaly in HSC program due to the stability of the sulfate ion, which is not seen in practice.

5.2.2 Metastable Eh-pH diagrams excluding sulfate ions

Some of the Eh-pH diagrams are repeated for systems with selected species and particularly omitting sulfate ions containing S with a positive oxidation state. The species selected are:

Cu, CuO, Cu_2O, $Cu(OH)_2$, CuS, Cu_2S, Rh, RhO, Rh_2O, Rh_2O_3, Rh_2S_3, S, Cu^{2+}, Cu^{+}, CuO_2^{2}, $CuOH^{+}$, $Cu(OH)_3^{-}$, $Cu(OH)_4^{2-}$, Cu_2OH^{3+}, $Cu_2(OH)_2^{2+}$, $Cu_3(OH)_4^{2+}$, $Cu(OH)O^{-}$, $HCuO_2^{-}$, HS^{-}, Rh^{3+}, S^{2-}, $S_2O_3^{2-}$

The diagrams demonstrate that Rh and Cu ions precipitate as metal sulfide upon sulfide addition, and only with further reduction does it get reduced to a metal. The sulfide ion activity is affected by the pH. Temperature and molality effects are presented and discussed. Additional metastable diagrams are provided in Appendix A.2.

Figure 5.4 is de-constructed into various main elements for readability in Figure 5.5 and 5.6. The main sulphur speciation is presented in Appendix A.2.

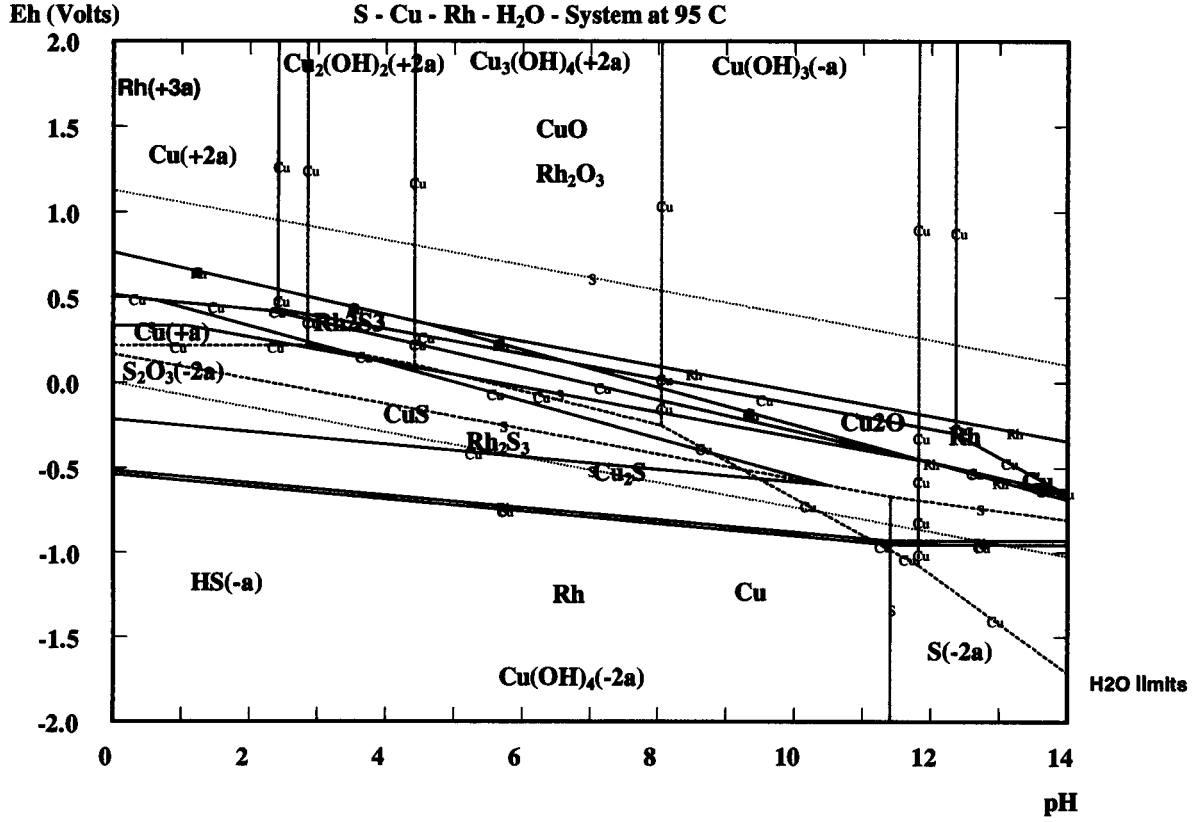

ELEMENTS	Molality	Pressure
S	3.000E-01	1.000E+00
Cu	3.000E-01	1.000E+00
Rh	1.000E-03	1.000E+00

Figure 5.4: Eh-pH diagram of S-Cu-Rh-H_2O metastable base case at 95 °C, particularly omitting species with sulfur of positive oxidation state and only including Rh_2S_3. Dashed lines indicate region of dominant ions in solution. Rh and Cu reduction from ion to metal no longer occurs.

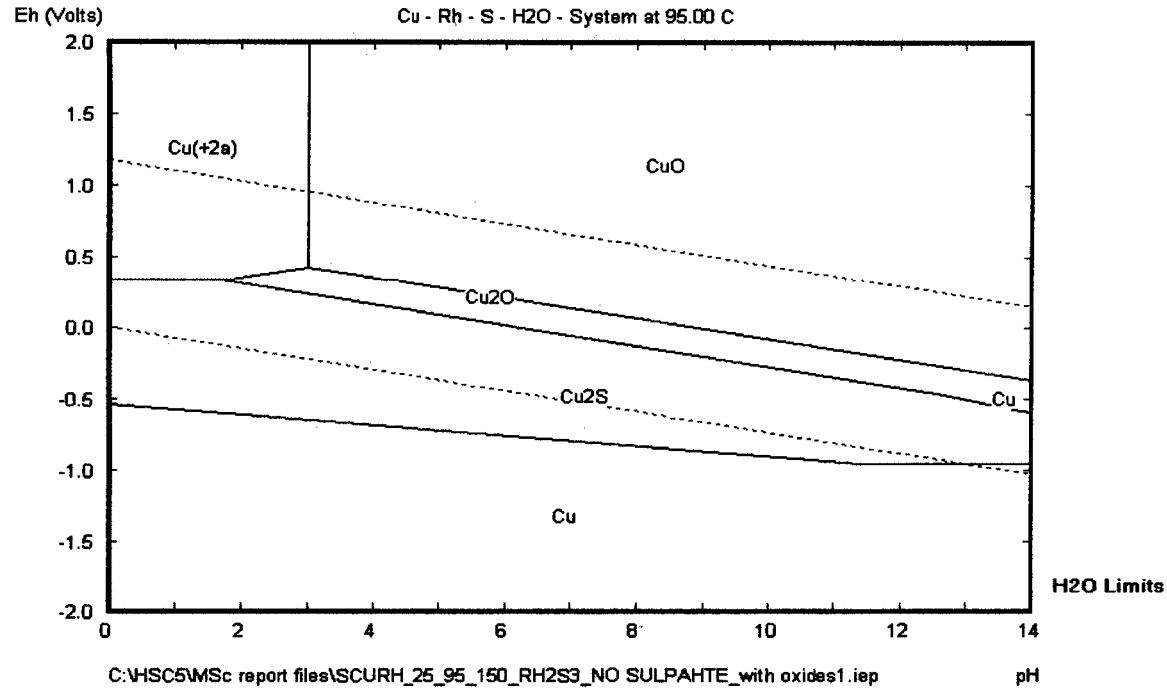

ELEMENTS	Molality	Pressure
S	3.000E-01	1.000E+00
Cu	3.000E-01	1.000E+00
Rh	1.000E-03	1.000E+00

Figure 5.5: EH-pH diagram of S-Cu-Rh-H_2O metastable system at 95 °C showing dominant Cu speciation, particularly omitting species with sulfur of positive oxidation state and only including Rh_2S_3. Cu reduction from ion to metal no longer occurs.

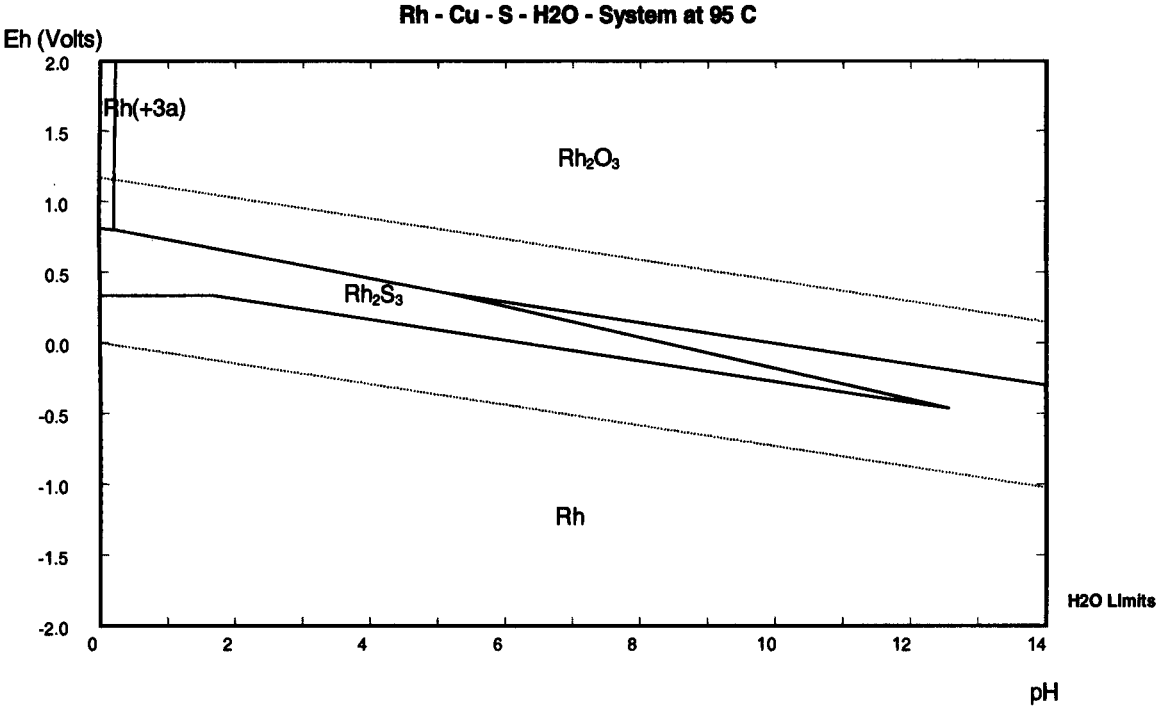

ELEMENTS	Molality	Pressure
S	3.000E-01	1.000E+00
Cu	3.000E-01	1.000E+00
Rh	1.000E-03	1.000E+00

Figure 5.6: Eh-pH diagram of S-Cu-Rh-H_2O metastable system at 95 °C showing dominant Rh speciation, particularly omitting species with sulfur of positive oxidation state and only including Rh_2S_3. Rh reduction from ion to metal no longer occurs in the acidic pH.

1. Temperature

The effect of temperature on the S-Cu-Rh-H_2O system for the metastable case is provided in Figure 5.7.

Higher temperature shifts the metal sulfide stability region down and left at high pH and shifts the stability region up at low pH. The increase in temperature increases the Rh^{3+} stability region at higher pH, which corresponds with higher PGM dissolution at higher temperatures.

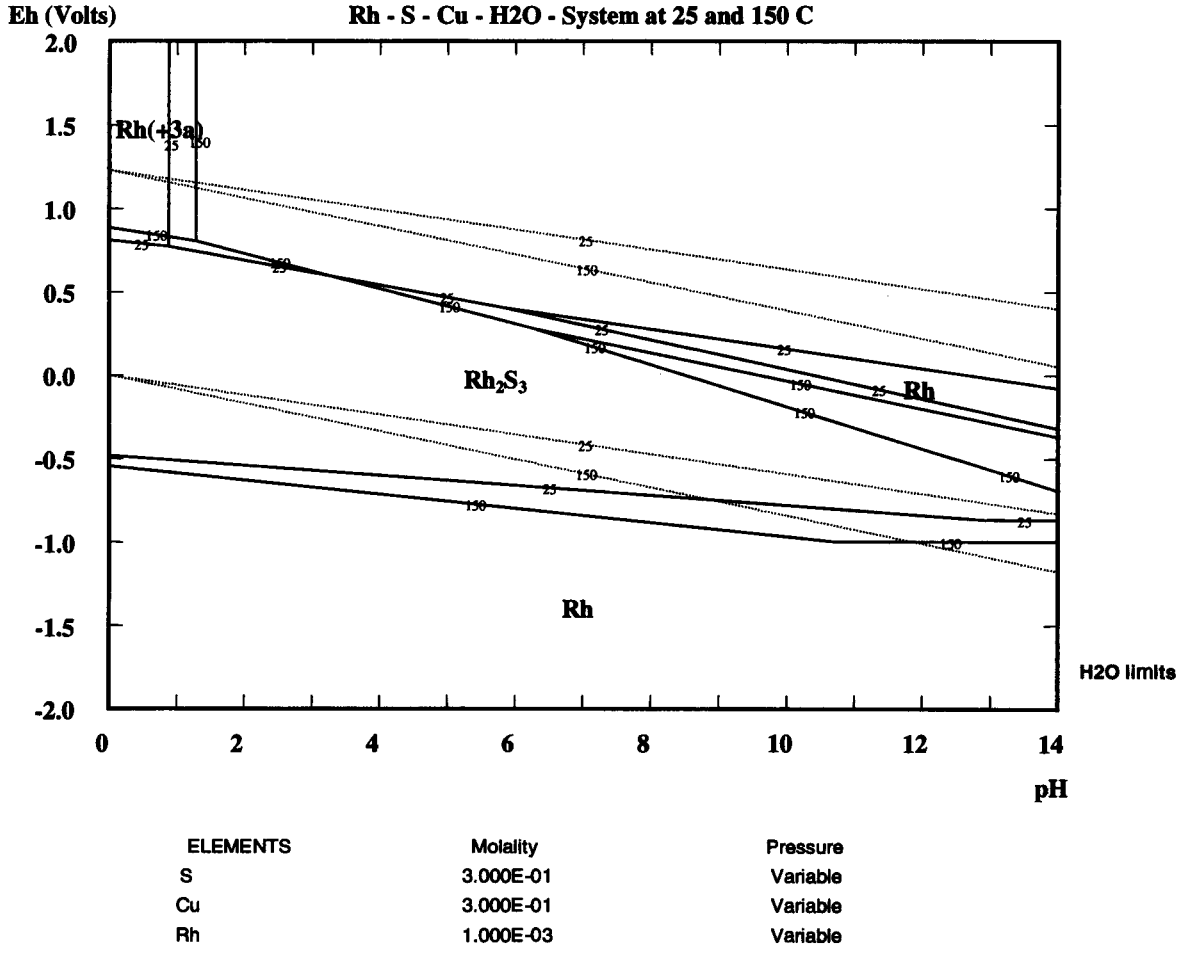

Figure 5.7: Eh-pH diagram of S-Cu-Rh-H_2O metastable system, particularly omitting species with sulfur of positive oxidation state, combined for 25 and 150 °C, showing effect of temperature on Rh speciation.

Rh ion stability increases in the pH direction with increasing temperature. Rh ion stability decreases with increasing temperature on the electropotential axis, implying that PGMs would start precipitating earlier at higher temperatures upon addition of the reducing agent.

2. Molality

At 95 °C, the effect of varying Rh molality on Eh-pH diagram only showing dominant Rh species is demonstrated in Figure 5.8 diagram. Molality is varied over the following ranges:

1. S: 0.001, 0.01 and 1 mol/kg
2. Cu: 0.001, 0.01 and 1 mol/kg
3. Rh: 0.0001, 0.001 and 0.1 mol/kg

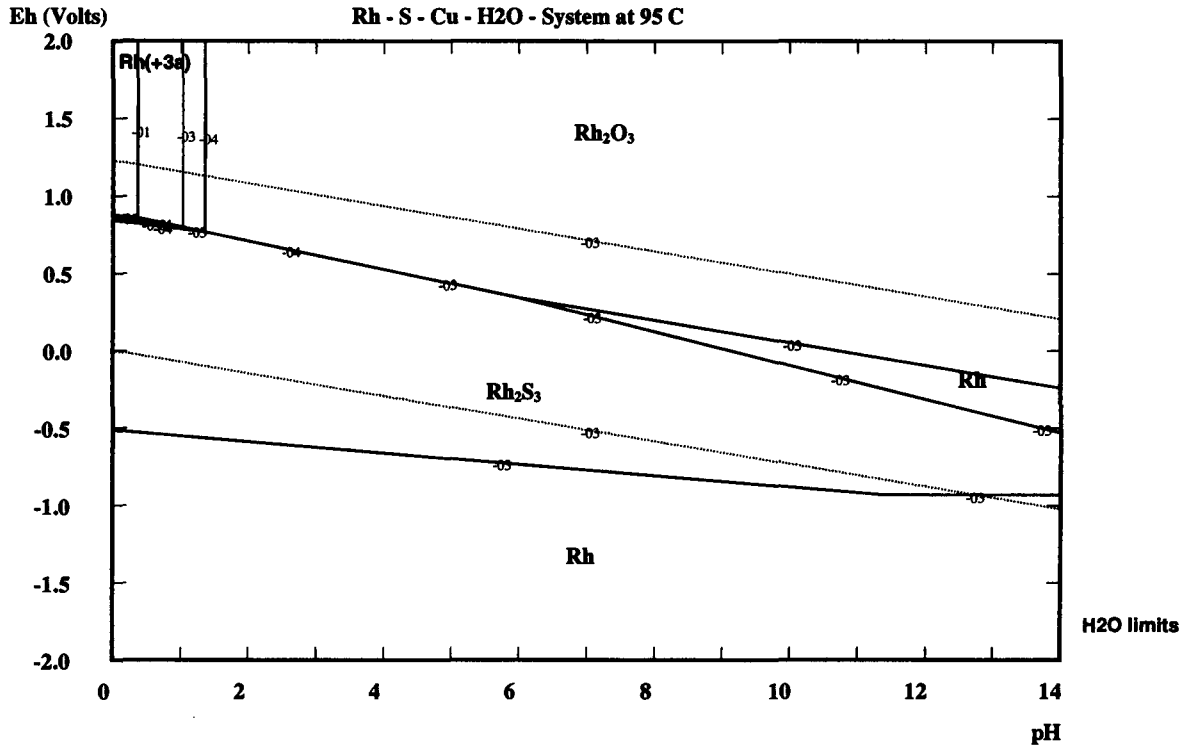

ELEMENTS	Molality	Pressure
S	3.000E-01	1.000E+00
Cu	3.000E-01	1.000E+00
Rh	Variable	1.000E+00

Figure 5.8: Eh-pH diagram of S-Cu-Rh-H_2O system for metastable system at 95 °C with selected speciation, particularly omitting species with sulfur of positive oxidation state, at 95 °C, showing effect of Rh activity on Rh species distribution at molality of $1x10^{-4}$, $1x10^{-3}$ and $1x10^{-1}$ mol/kg; Rh^{3+} stability increases with decreasing molality.

Rh^{3+} ion stability increases with decreasing Rh ion molality (or activity) in the pH direction and increases very slightly in the Eh direction. This implies that Rh^{3+} ion is hydrolysed or precipitated with hydroxide with more difficulty at lower concentrations. At lower Rh concentrations, additional reducing reagent is required to reduce the solution potential to precipitate Rh_2S_3. This implies that it becomes more difficult from a thermodynamic perspective to precipitate the Rh while its concentration is decreasing.

5.3 Equilibrium solution chemistry modelling

HSC Chemistry® is used to calculate the equilibrium amount of the various ions and compounds upon thiosulfate addition to the feed solution, studying the following:

1. Temperature of 95 °C and 150 °C,
2. Rh concentration 100 mg/l and 10 g/l,
3. Select all solid species compared to meta-stable species,
4. Effect of acid concentration.

It is important to note that solution speciation does not include solution complexation effects.

5.3.1 Meta-stable system

Equilibrium composition diagrams for metastable sulfides at 100 mg/l and 10 g/l Rh at 95 and 150 °C are provided in Figure 5.9 – 5.11. The diagrams are reproduced without any species containing sulfur with oxidation state above zero, and limiting the Rh sulfide species to Rh_2S_3 in Section 5.3.2. This eliminates the anomaly of Rh and Cu being reduced by the sulfide directly to metal. The effect of Rh concentration, temperature and initial acid concentration is studied. The base case including all speciation is provided in Appendix A.3.

1. Concentration Effect

Figures 5.9 and 5.10 show that Rh sulfide precipitation with thiosulfate addition is completely selective over CuS precipitation over 0.1 – 10 g/l Rh.

2. Temperature Effect

Figure 5.10 and 5.11 comparison shows that Rh sulfide precipitation with thiosulfate addition is completely selective over CuS precipitation at 95 and 150 °C.

The equilibrium compositions are not significantly affected by temperature. This can be explained by the fact that the reaction equilibriums are nearly independent of temperature (see ΔG calculations in Section 5.1). Thus, the equilibrium lines would shift on the Eh-pH diagram, but the relative equilibrium amounts would remain constant on the equilibrium line.

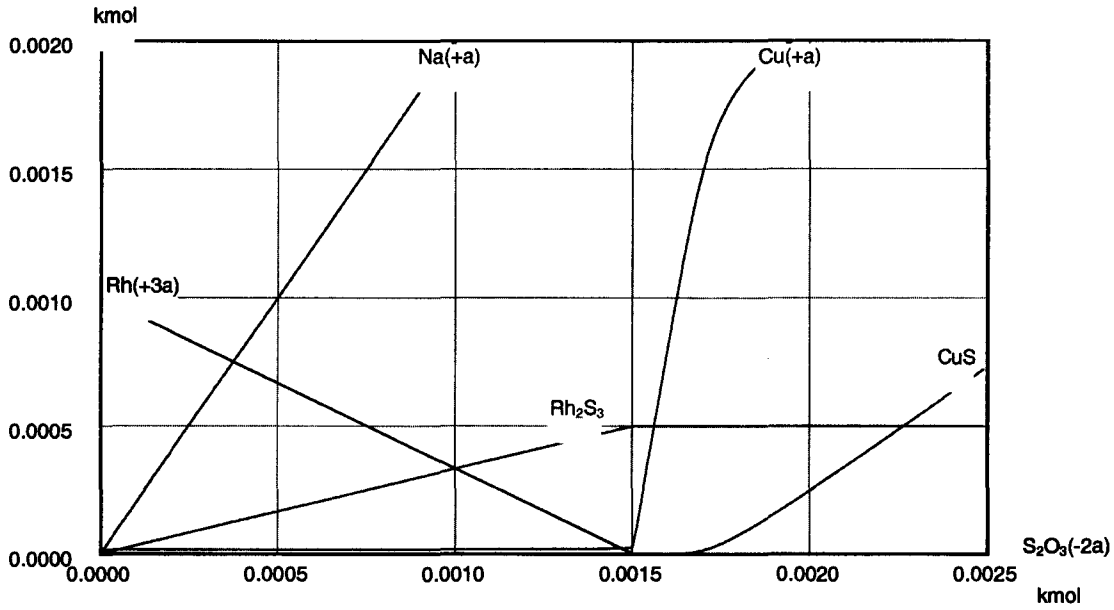

Figure 5.9: Equilibrium composition with thiosulfate addition to 100 mg/l Rh containing 20 g/l Cu and 15 g/l sulfuric acid at 95 °C, showing equilibrium composition for meta-stable species; Rh precipitation with sulfide is completely selective over Cu precipitation.

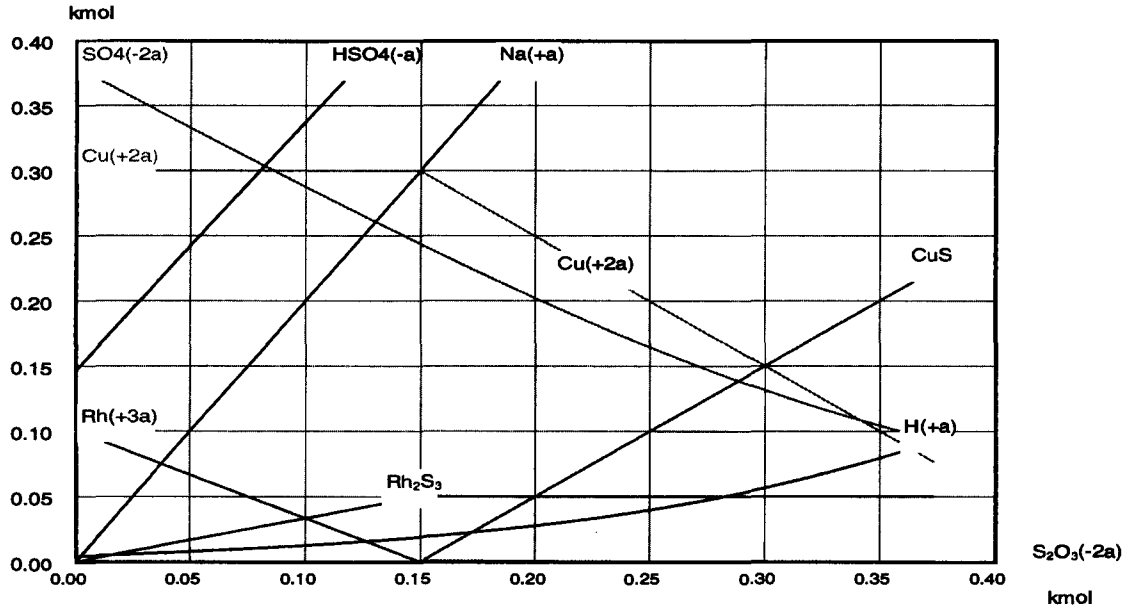

Figure 5.10: Equilibrium composition with thiosulfate addition to 10 g/l Rh containing 20 g/l Cu and 15 g/l sulfuric acid at 95 °C, showing equilibrium composition for meta-stable species; Rh precipitation with sulfide is completely selective over Cu precipitation.

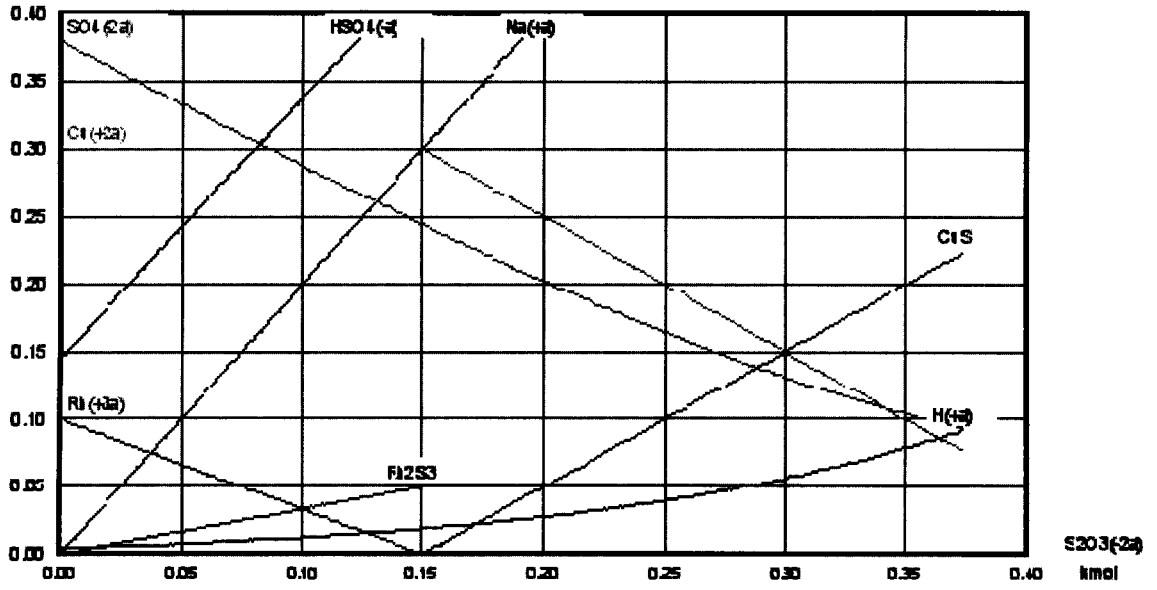

Figure 5.11: Equilibrium composition with thiosulfate addition to 10 g/l Rh containing 20 g/l Cu and 15 g/l sulfuric acid at 150 °C, showing equilibrium composition for meta-stable species; Rh precipitation with sulfide is completely selective over Cu precipitation.

3. Initial acid effect

The base case is repeated for a system with 0.001 mol/kg acid. The same compositions and order of precipitation is determined, illustrated in Figure 5.12.

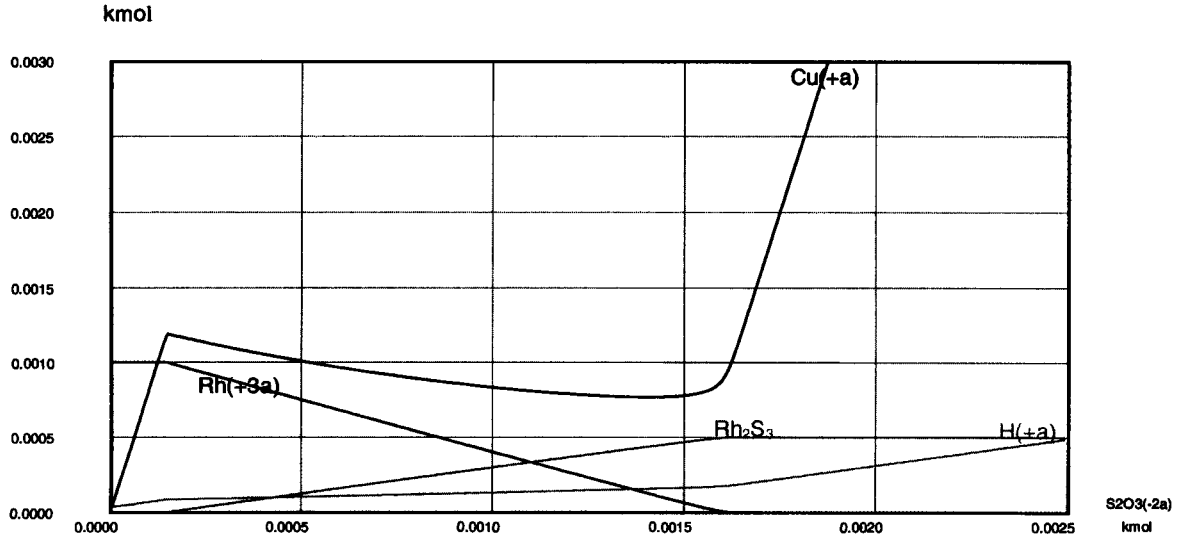

Figure 5.12: Equilibrium composition with thiosulfate addition to base case with 100 mg/l Rh containing 20 g/l Cu and 0.1 g/l sulfuric acid at 95 °C, showing equilibrium composition for meta-stable species; Rh precipitation with sulfide is completely selective over Cu precipitation, irrespective of initial acid concentration; Rh precipitation is shifted right while acid concentration increases, thus acid plays a role in the Rh precipitation.

As expected, initial acid has insignificant effect on Rh precipitation selectivity for this perfect system, which is already completely selective. However, HSC Chemistry cannot calculate any equilibrium points at zero initial acid. A delay in Rh precipitation also occurs, thus acid must play a role in the mechanism. The cuprous ion (Cu^+) is preferentially formed prior to acid generation.

5.4 Discussion of chemistry and thermodynamic modelling

The ΔG of reactions prove that the reactions are thermodynamically possible for the three systems and possible alternative chemistries. The metastable Eh-pH diagrams show various Rh sulfide compounds, though the most stable compound is Rh_2S_3, which forms through ionic precipitation or cationic substitution. Other reactions involving electrochemical reactions are possible, but less favourable due to smaller ΔG of reactions.

The sulfate ion (or all species with a positive S oxidation state) have to be excluded from the Eh-pH modelling to avoid the anomaly caused by the HSC Chemistry® program, where it erroneously predicts that the thiosulfate or sulfide ion would reduce Rh^{3+} directly to metal before precipitating as a sulfide. This anomaly is caused by the stability of the sulfate ion in the HSC Chemistry® program (Nicol, 2006).

Increasing the temperature increases the stability region of the Rh^{3+} ion in the pH direction but reduces the Rh^{3+} stability region in the Eh direction. Thus, upon the addition of the thiosulfate reducing agent, Rh^{3+} starts precipitating as a sulfide at a higher Eh i.e. elevated temperature favours Rh precipitation.

Equilibrium composition calculations show that Rh^{3+} precipitation is completely selective over Cu^{2+} precipitation upon thiosulfate addition for low and high Rh concentrations, though in practice this selectivity could be forfeited by bulk concentration effects on precipitation kinetics. Temperature has insignificant effect on the equilibrium, while a minimum amount of acid is required for the reaction to occur, indicating that acid could be involved in the mechanism.

Rh^{3+} ion stability increases with decreasing Rh ion molality in higher pH direction and increases very slightly in the Eh direction. Rh requires additional thiosulfate to reduce the Eh for Rh_2S_3 precipitation. This implies that it would become more difficult from a thermodynamic perspective to completely precipitate the Rh.

5.5 Proposed mechanism

The chemistry suggests the following simplified reaction mechanism for Rh co-precipitation with CuS:

$$Cu^{2+} + S_2O_3^{2-} + H_2O \rightarrow CuS + H_2SO_4 \quad (1)$$

$$2Rh^{3+} + 3\ S_2O_3^{2-} + 3\ H_2O \rightarrow Rh_2S_{3\,s} + 3\ H_2SO_4 \quad (2)$$

$$2Rh^{3+} + 3\ CuS \rightarrow Rh_2S_3 + 3Cu^{2+} \quad (3)$$

Cu^{2+} and Rh^{3+} compete for the available aqueous sulfide available in the thiosulfate via reactions (1) and (2). Once the CuS has precipitated, Rh^{3+} continues to precipitate onto the CuS via the cationic substitution reaction (3), which competes against Rh ionic precipitation (2).

For ionic Rh precipitation in the absence of Cu^{2+}, thiosulphate degrades with acid, precipitating sulfur, upon which Rh^{3+} continues to precipitate:

$$H_2SO_4 + S_2O_3^{2-} \rightarrow 4\ S + H_2O + 3\ SO_4^{2-} \quad (4)$$

$$2\ Rh^{3+} + 4\ S + 4\ H_2O \rightarrow Rh_2S_3 + + 8H^+ + SO_4^{2-} \quad (5)$$

In this system, Rh^{3+} ionic precipitation competes with acid in the thiosulfate degradation via reactions (2) and (4). The precipitated S continues to precipitate the Rh^{3+} onto the surface, thus ionic precipitation reaction (2) also competes with reaction (5).

Chapter Six

6 KINETIC STUDY OF INDIVIDUAL SYSTEMS

Solids assays and solution assays are presented in Appendix B.3.1 and in Appendix B.3.2, respectively. This includes Cu, Ni, K, Na, H_2SO_4 and Rh concentrations, replicates and repeat analyses, as well as finalised average concentrations utilised in the subsequent comparative study and kinetic modelling. Statistical analysis on assays is attached in Appendix B.3.3. The individual test results are summarised in the log sheets in Appendix B.4, which include actual test details and observations, finalised average concentrations used in data analysis, mass balance calculations, metal accountabilities and stoichiometric ratio calculations. The precipitation profiles are illustrated in Appendix B.5. Details of the kinetic modelling of the various systems are presented in Appendix B.6. Summary of detailed results are provided in various sections below, covering accuracy of measurements and results of the individual systems.

6.1 Accuracy of measurement

6.1.1 Solution analysis relative error

The accuracy of the solution analysis was measured by evaluating the random duplicate analyses generated in the laboratory procedure and specific multiple repeat analyses on two filtrate solutions. These analyses are presented in Appendix B.3.2, where descriptive statistics has been performed to calculate the relative errors. The results are summarised in Table 6.1 and 6.2.

A high Rh concentration filtrate solution (Rh-9R-240) and low concentration filtrate solution (Rh-3-240) were re-analysed on a later day for five additional repeats for Rh, Cu, Ni and acid. The results in the Table 6.1 show that the Rh concentration assay alone has a large relative error, even though it is determined using the very accurate Inductive Coupled Plasma – Mass Spectroscopy (ICP-MS) technique.

Table 6.1: Standard deviation on solution assays for six repeat analyses

Element	Average (mg/l)	Std deviation (mg/l)	Relative error (Std dev. / Avg) %
Rh – low	25	1.2	5.0
Rh – high	93	2.3	3.3
Cu	11247	231	2.0
Ni	6447	350	5.4
Acid	17.9 g/l	0.4	2.5

Table 6.2 shows that the average random duplicate assays for Rh, Cu, Ni, Na, and acid provide similar relative errors as Table 6.1.

Table 6.2: Average standard deviation on concentrations from duplicate analyses

Element	Concentration range (mg/l)	Count	Average (mg/l)	Std deviation (mg/l)	Relative error (Std dev. / Avg) %
Rh – low	0 – 1	4	0.5	0.04	8.0
Rh – high	10 – 100	53	65	2.7	4.2
Cu – Low	30 – 120	5	77	0.6	0.7
Cu – High	8000 – 15000	10	11808	142	1.2
Na	~2000	4	2042	6	1.7
K	~1000	14	1158	8	0.3
Acid	10 – 20 g/l	25	17 g/l	0.3 g/l	0.2

This large error on Rh analysis causes a significant amount of noise in the precipitation profiles. Rh and Cu post-precipitation in the filtrate samples are shown to be a concern over the initial ionic and co-precipitation systems and over the whole profile at low temperatures, which is addressed in detail in Section 6.1.3. The above repeat analyses show that this post precipitation phenomenon does not occur on the final profile solutions, supported by reasonable final metal accountabilities presented in Section 6.1.5.

In future work, the reason for this high relative error must be determined and resolved prior to commencement of the kinetic study. If the error persists, then additional sample analysis replicates, as well as duplicate test runs, would be required to improve the accuracy and significance of the overall results.

Rigorous comparative statistics have to be applied to the profiles to ensure that the differences in the results are actually significant, which is covered in Chapter 7.

6.1.2 Solids analysis relative error

Solid assay random duplicates are presented in Appendix B.3.1 with the average standard deviation and relative error summarised in Table 6.3.

Table 6.3: Average standard deviation on solids concentrations

	Count	Average	Std dev.	Relative error (Std dev. / Avg) %
Cu	5	56	1.5	3.4
S	6	40	1.0	3.3
Rh	11	1.5	0.2	12

The relative error of 12% on Rh in the CuS is very high. The source of this error needs to be identified before commencing future work, though Section 6.1.1 indicates that the error could possibly occur in the final ICP measurement. Even though the overall solids analysis has a large relative error associated with it, the general precipitation trends with regards to

temperature and relative kinetics within the various precipitation systems are still maintained. This is probably because final solids are analysed in duplicate to quadruplicate.

6.1.3 Post precipitation of Rh and Cu in solutions

Post precipitation of metal with unreacted aqueous sulfide in the sample filtrates has been noticed in ionic and co-precipitation systems, but only at atmospheric temperatures over the period of low precipitation extents. This is caused by higher amounts of unreacted aqueous sulfide being present in the filtrates due to lower aqueous sulfide consumption over this period. This causes the overestimation of metal precipitation extent and under-accounting of metal in the precipitate over the initial period of ionic and co-precipitation at atmospheric temperatures.

An attempt to stop post precipitation by oxidising the sulfide ion has been unsuccessful. Adding hydrogen peroxide only partially oxidises the unreacted aqueous sulfide, causing the precipitation of elemental sulfur. This is an inadequate method, as PGMs can precipitate onto elemental sulfur (Chapter 5) (Barkan and Greiver, 1977a). The laboratory was instructed to perform a total sample analysis by re-dissolving post-precipitated material. Precipitation profiles show that the analytical laboratory did not perform this total stream analysis adequately, as post precipitation phenomena were measured in the precipitation profiles.

This post precipitation in the filtrates does not affect the solids analysis, as the samples are filtered immediately. Thus, the Rh and Cu solution concentrations are re-calculated by subtracting the estimated amount of metal measured in the precipitate from the initial feed. The calculation assumes that metal content in the final solid sample is constant over the whole profile, which is a fair assumption for the ionic and co-precipitation systems. Insufficient mass has been collected for individual solid profile analyses. The procedure provides more realistic Rh precipitation profiles for ionic and co-precipitation systems at 50 °C and Cu solution profiles over the initial period at all temperatures. The final solids are analysed in duplicate to quadruplicate to achieve accurate solids analyses. This is reflected in the mass balance and metal accounting presented in Section 6.5.1.

Comparative kinetics at elevated temperatures (#4, #8b and #12) are performed on the same solution basis, because of excessive solid mass loss caused by precipitation onto the PV internals (#4b). This is not a problem, as the solutions samples do not show any post precipitation due to the high precipitation extents. As expected, the substitution system (#5b - 8b) does not show post precipitation, as there is no aqueous sulfide in the filtrates. In any case, insufficient sample mass over the substitution reaction profiles prohibits the prediction of Rh concentrations and the solution concentrations are used. The remaining profiles (#1-#3 and #9-#11) are recalculated from the solids basis to maintain the same basis within each profile, as well as maintaining the same basis for comparison between systems at any particular temperature.

The measured and predicted final solution assays are compared in Table B5.5 and B5.6 in Appendix B5. The calculated concentrations shift by similar amounts at atmospheric temperatures, thus the relative kinetics between the various temperatures for each reaction system or the relative kinetics of the individual systems at a particular system do not change. To confirm the relative kinetic findings, the comparative kinetic exercise is repeated at solution concentrations (see section 7.5.5).

6.1.4 Feed concentrations

Ideally, feed concentration for each test should be equal for a perfect comparison. However, slight variations in the extracted volume of the feed sample at temperature and the injected volumes cause some variation in the actual initial concentrations.

Analytical errors in measured feed values have a major impact on overall analysis. It is thus important to ensure that accurate feed concentrations are used in the subsequent mass balances, individual and comparative kinetic study and kinetic modelling. However, the measured feed concentrations had a large relative error of analysis (Section 6.1.1). Unfortunately, some of the feed analyses were not performed in duplicate and the analysis could be within ± 5% range. Mass balances show that some specific feed concentrations measured were probably not correct. The error associated with pipetting the Rh requirement into the synthetic feed make-up or Rh injection procedure at temperature is significantly less than the average relative error associated with the solution assay.

Actual feed concentrations at the starting point have been calculated from the measured values to take into account the dilution effect of reagent injection and flush water. The dilution factor is calculated from the actual volumes extracted for the feed sample at temperature and the volume of reagent and flush water injected at the start of the test. Not taking the dilution effect into account would cause an overestimation of metal precipitation owing to the different concentration basis. These factors are calculated in Appendix B.2. In addition, the feed samples of the substitution reaction system cannot be taken, as this would remove sulfide from the system and compromise the comparative study. Hence, the initial concentration at time of reagent injection has to be calculated from the feed preparation, feed sample and injection volumes.

Thus, replacing the measured concentrations with predicted feed concentrations was considered for all the reaction system profiles in order to improve the accuracy of the results. This would also maintain the same basis for comparison by treating all the precipitation profile analyses in the same manner. The predicted and measured concentrations before and after dilution effects are compared in Table 6.4 and 6.5. The concentrations are similar enough to ensure that gross error does not occur during the feed preparation procedures and the calculated concentrations can be trusted. On this basis, test #4 was repeated (discussed in Section 6.1.6). Differences are primarily due to the large analytical error described in Section 6.1.1, as well as error induced during the synthetic feed make-up procedure. Metal accounting over each profile is also used as an additional check (Section 6.1.5).

Table 6.4: Comparison of Rh designed, measured and predicted feed concentrations

Test #	Description	Rh conc [mg/l]	Rh conc [mg/l]	Rh conc [mg/l]	Rh conc [mg/l]
		Design before injection	Calculated at injection (theoretical)	Measured before injection	Calculated at injection (on measured)
1	Ionic Rh precipitation	96	92.6	98.9	95.3
2	Ionic Rh precipitation	96	92.6	93.6	90.2
3	Ionic Rh precipitation	96	92.6	96.9	93.3
4	Ionic Rh precipitation (discarded)	96	92.6	26.8	25.8
4R	Ionic Rh precipitation	96	92.6	102	98.4
5a	CuS precipitation	0	0	0.3	0.3
6a	CuS precipitation	0	0	0.2	0.2
7a	CuS precipitation	0	0	0.3	0.3
8a	CuS precipitation	0	0	0.1	0.0
5b	Substitution reaction	96	93.3	0.2	0.2
6b	Substitution reaction	96	93.4	0.1	0.1
7b	Substitution reaction	96	90.0	< 0.05	< 0.05
8b	Substitution reaction	96	92.5	< 0.05	< 0.05
9	Cu and Rh co-precipitation *in situ*	96	89.3	103	99.4
9R	Cu and Rh co-precipitation *in situ*	100	96.2	111	107
10	Cu and Rh co-precipitation *in situ*	96	89.4	104	100
11	Cu and Rh co-precipitation *in situ*	96	89.3	102	98.3
11R	Cu and Rh co-precipitation *in situ*	96	89.3	96.2	92.6
12	Cu and Rh co-precipitation *in situ*	96	89.3	81.5	78.6

Table 6.5: Comparison of predicted and measured concentrations for remaining elements after dilution

Test	Cu		Ni		H_2SO_4		K	
#	Predicted	measured	predicted	measured	predicted	measured	predicted	measured
	mg/l	mg/l	mg/l	mg/l	g/l	g/l	mg/l	mg/l
1	0	7	0	8	14.4	14.9	963	1145
2	0	9	0	8	14.4	14.9	963	1127
3	0	35	0	NR	14.4	16.1	963	1147
4	0	75	0	NR	14.4	15.2	963	1177
4R	0	4	0	< 2	14.4	17.1	963	931
5a	13216	12902	5118	5760	13.4	16.2	929	935
6a	13312	12450	5156	5650	13.5	16.3	936	894
7a	13217	13705	5119	5700	13.4	16.4	929	915
8b	13216	13552	5118	6800	13.9	15.4	929	NR
5b	0	35	0	NR	15.1	14.6	971	963
6b	0	85	0	NR	14.5	13.2	971	959
7b	0	112	0	NR	14.0	14.9	936	903
8b	0	73	0	NR	14.4	15.1	962	1150
9	13217	12940	5119	5460	13.9	15.5	929	1084
9R	14236	13120	5513	5540	15.0	15.4	1001	1186
10	13223	12800	5121	5540	13.9	15.5	929	1109
11	13217	13290	5119	6000	13.9	15.8	929	1014
11R	13217	12460	5119	5360	13.9	14.2	929	1058
12	13217	12760	5119	5550	13.9	14.6	929	980

The predicted feed concentration improves the overall mass balance considerably, particularly on systems which have problematic feed analysis (Table 6.6). These specific cases are discussed below to support the argument of replacing the measured values with theoretical feed concentrations.

Measured feed concentrations of 9 and 9R are based on a single analysis and the predicted feed values improve the overall mass balance by 10% absolute. Test #12 measures Rh concentration as significantly lower than the expected theoretical value, where metal accounting shows 19% more Rh in the precipitated solids than the original feed. Based on this analysis, the 82 mg/l is repeated, which produces an 88 mg/l estimate prior to dilution. This new analysis reduces the over-accounting to 15%, taking the dilution effect into account. The theoretical diluted value of 89 mg/l reduces the over-accounting to 9%, which is in line with the 8% over-accounting of copper in the same test i.e. the Rh accounting is aligned with the general systematic error of the test. The 109% accountability is also similar to metal accounting of the substitution reaction #8b operating at the same temperature and #11, operating under the same co-precipitation system. Thus, the theoretical feed value would make these direct comparisons more realistic as well. In addition, the comparison of #1 and #9R is particularly sensitive to the different feed concentrations of the measured values, because the predicted profiles (Section see 6.1.3) show low precipitation extents.

Hence, based on the above evidence and arguments, the theoretical diluted value replaces the actual measured diluted value in subsequent mass balances, individual and comparative kinetic study and kinetic modelling. The approach taken is to replace all the Rh feed values in order to maintain the same basis in the comparative study.

The study uses the measured feed concentrations of the remaining elements and acid analyses. This is because the relative analytical error on these analyses is significantly smaller than Rh and the adjustment is not required. In this case, the measured values are more appropriate. The final feed values used in this study are summarised in Table 6.7.

6.1.5 Mass balance and metal accounting

Rh and Cu metal accounting is used as an important measure of the accuracy of the individual kinetic profiles. Limitations on the sample volume on the kinetic profile limit the mass of solids removed per sample. Thus, it is only possible to perform the metal accountabilities on the final sample.

The Rh metal accounting in this study is defined as:

$$\% \text{ Rh a/c} = (\text{mol Rh in final soln} + \text{mol Rh in final solids}) / (\text{Rh at time} = 0)\ \%$$

Overall metal accounting is calculated in the mass balance log sheets in Appendix B.4. The summary in Table 6.6 shows the Rh and Cu accountabilities on measured and predicted feed samples after taking the dilution effect into account.

Table 6.6: Metal accounting comparison using theoretical and measured feed concentrations

Test #	Predicted Feed		Measured Feed		Improvement in metal accounting**	
	Rh a/c %	Cu a/c %	Rh a/c %	Cu a/c %	Rh a/c %	Cu a/c %
1	90	NA	88	NA	+2	NA
2	88	NA	88	NA	0	NA
3	90	NA	90	NA	0	NA
4	NR	NA	NR	NA	NR	NA
4R	39	NA	37	NA	+2	NA
5b	97	NA	NR	NA	NR	NA
6b	99	NA	NR	NA	NR	NA
7b	102	NA	NR	NA	NR	NA
8b	113	NA	NR	NA	NR	NA
9	97	101	87	104	+10	+3
9R	99	88	90	96	+9	-6
10	109	91	97	94	-6	-3
11	105	97	96	96	-1	+1
11R	105	97	102	103	-3	0
12	109	104	119	108	+10	+4

** Improvement in metal accounting when changing feed basis from measured feed concentration to predicted feed concentration ; Note: '+' = improvement in mass balance i.e. closer to desired 100% ; NR= no result ; NA = not applicable

Rh is under-accounted for in the ionic precipitation reactions (#1 - #3), mainly due to solids loss caused by precipitation on the PV walls and internals, while ionic precipitation at elevated temperature experiences excessive precipitation onto the PV internals and a total solid mass cannot be measured. Cu is under-accounted in co-precipitation system due to solids loss as well.

Utilising the predicted feed conditions generally improves the Rh metal accountabilities, while Cu accountabilities remain relatively unchanged. Accountabilities are similar for ionic and substitution systems for both feed values, but significantly different on the co-precipitation system. The general improvement in specific test runs and relatively unchanged accountabilities in the other tests support the argument for using predicted feed values, as it improves the accuracy of the overall relative kinetic study.

6.1.6 Repeat tests and replicates

Test #11 has been repeated and produces a similar Rh precipitation profile within the expected relative error of the analytical analysis on the solution and solids basis. The data sets have been combined for kinetic modelling and relative kinetic comparisons. This provides additional confidence for the comparison of the remaining profiles, assuming this total error remains constant.

Test #4 has been repeated due to a large amount of Rh precipitating during the heat-up phase, probably caused by hydrolysis reactions. The Rh feed concentration at 150 °C measured at time zero is 25 mg/l, showing that approximately 75% of the Rh precipitates during heating phase onto the internals prior to reagent addition. The repeated test has been adapted to inject Rh at 150 °C, sample the feed and then inject thiosulfate at time zero (#4R).

This approach has been applied to the other systems at 150 °C as well (#8b and #12). Test #4 results have been discarded from the comparative study.

Test #9 has been repeated because the precipitate extent at 50 °C is similar to extent at 80 °C. This is contrary to the findings of all the reaction systems, which show a clear relationship between increasing temperature causing an increase in precipitation rate and extent. The repeat test (#9R) has produced the expected relative precipitation trends with regards to temperature and relative kinetics of the various reaction systems, which supports the argument for discarding test #9 results. However, the mass balance on test #9 and 9R is reasonable (~90%), which indicates that the results for each test could be real (Table 6.6). The profiles have been re-evaluated using the solids basis to eliminate the post precipitation effect (see Section 6.1.3). However, this has comparison only eliminated the anomaly over the initial period. The final precipitation extent of #9 is still significantly greater than #9R and similar to ionic precipitation at 50 °C (#1). As #9R is the more likely result, the calculated Rh concentration is used in the subsequent comparative kinetic study and kinetic modelling. However, the dubious results of #9 cannot be discarded outright and additional confirmatory test work is required to confirm relative kinetics at 50 °C. This is discussed in more detail under the co-precipitation results in Section 6.5.

6.1.7 Sample volumes removed

In order to maintain constant conditions over the precipitation profile, the sample volume has had to be limited to ensure that the volume removed would remain within acceptable limits of the initial volume. The final volumes of the tests are within 71 – 83% of the initial volume. The impact of this volume reduction on the dimensionless power number is insignificant, where the agitation rate has had to be reduced by 1 rpm. The agitator controller is not this sensitive. Thus, if the reaction rate were mass transfer controlled, the varying volume and power input into agitation would not impact on overall precipitation kinetics significantly.

6.1.8 Redox potential measurement

The redox profiles are provided in the individual test log sheets in Appendix B.4 and the individual redox profiles are illustrated attached in Appendix B.5.

The readings have been taken on the filtered solutions after the test for two reasons. There would have been insufficient time to read the value prior to filtration, as it would cause significant delay before filtration, where precipitation would continue and affect the overall kinetic results. Also, the instrument does not produce good replicate results and the whole solution profile set is measured in succession to provide at least comparative readings within each profile. The varying feed readings of very similar solutions show that, generally, the redox profiles cannot be compared to each other, though the relative change within a particular profile is reasonable.

Generally, ionic precipitation is between 200 – 300 mV (against Ag/AgCl) and substitution and co-precipitation between 400 – 500 mV after the sulfide addition. Redox decreases rapidly upon thiosulfate or CuS addition and generally increases slightly over time over the precipitation profile.

6.2 Summary of precipitation results

6.2.1 Final feed concentrations

The final feed concentrations used in this kinetic study are summarised in Table 6.7. As described in Section 6.1.4 and 6.1.5, the actual measured values adjusted for dilution effects are used for Cu, Ni, H_2SO_4, Na and K, while predicted values are used for the Rh, because it is a more accurate approach.

Ideally the comparative study would prefer equal feed samples. Table 6.7 shows that the feed concentrations are similar enough to maintain the integrity of the study. In addition, the extent of metal precipitation is calculated as a fraction of the feed value, thus eliminating the small shift in the concentration profiles due to the varying feed values.

Table 6.7: Feed concentrations used in the kinetic study analysis

Test #	Cu mg/l	Ni mg/l	H_2SO_4 g/l	Na g/l	K Mg/l	Rh mg/l
1	8	9	15.4	NR	1189	92.6
2	9	9	15.5	NR	1170	92.6
3	36	NR	16.7	NR	1191	92.6
4	78	NR	15.8	10	1222	92.6
4R	4	< 2	17.7	10	965	92.6
5a	12902	5755	16.2	24	935	0
6a	12450	5649	16.3	17	894	0
7a	13705	5701	16.4	10	915	0
8a	13552	6799	15.4	NR	NR	0
5b	35	NR	14.6	9	963	93.3
6b	85	NR	13.2	3	959	93.4
7b	112	NR	14.9	7	903	90.0
8b	73	NR	15.1	11	1150	92.5
9	13405	5657	16.1	22	1123	89.3
9R	13595	5744	16.0	31	1229	96.2
10	13265	*5737*	16.1	NR	1150	89.4
11	13789	6229	16.4	16	1052	89.3
11R	12952	5575	14.8	18	1100	89.3
12	13228	5756	15.1	16	1016	89.3

6.2.2 Precipitation profiles

Summary of Rh extent using the solids basis and solution basis is provided in Table 6.8a and 6.8b, respectively. In each basis, the measured solution concentrations are used for the substitution system and tests at elevated temperature. Cu precipitation extent using the solids basis is provided in Table 6.8c. Concentration data summary is tabled in Appendix B.5. It is reiterated that switching from the solution basis to the solids basis does not change the relative precipitation extents significantly (See Table B.5.6).

Table 6.8a: Summary of Rh precipitation extent for all reaction systems (solid basis)

Test #	Temp	Rh precipitation extent [%]							
	°C	1 min	2 min	~5 min	10 min	30 min	60 min	120 min	240 min
Ionic system (solids basis)									
#1	50	9	10	14	16	18	19	19	20
#2	80	34	41	44	48	49	49	51	50
#3	95	56	56	58	60	63	65	65	65
#4R **	150	57	70	85	97	100	100	100	100
Substitution system (solution basis)									
#5b **	50	0	0	0	1	2	11	10	17
#6b **	80	1	3	11	9	9	30	33	34
#7b **	95	4	23	30	26	35	38	42	45
#8b **	150	62	80	95	99	100	100	100	100
Co-precipitation system (solids basis)									
#9	50	0	0	1	5	28	30	30	30
#9R	50	0	0	0	0	3	5	6	5
#10	80	26	28	28	29	33	35	45	NR
#11	95	34	28	38	40	53	55	55	56
#11R	95	12	30	31	34	44	49	47	NR
#12 **	150	68	82	89	96	98	100	100	100

Note: ** measured solution basis

Table 6.8b: Summary of Rh precipitation extent for all reaction systems (solution basis)

Test #	Temp	Rh precipitation extent [%]							
	°C	1 min	2 min	~5 min	10 min	30 min	60 min	120 min	240 min
Ionic system (solution basis)									
#1 *	50	9	10	14	16	18	19	19	20
#2	80	23	25	24	36	35	47	53	62
#3	95	33	43	45	55	56	65	70	74
#4R	150	57	70	85	97	100	100	100	100
Substitution system (solution basis)									
#5b	50	0	0	0	1	2	11	10	17
#6b	80	1	3	11	9	9	30	33	34
#7b	95	4	23	30	26	35	38	42	45
#8b	150	62	80	95	99	100	100	100	100
Co-precipitation system (solution basis)									
#9 *	50	0	0	1	5	28	30	30	30
#9R *	50	0	0	0	0	3	5	6	5
#10	80	19	14	9	17	18	24	32	36
#11	95	12	14	8	13	21	32	43	51
#11R	95	9	10	11	15	28	34	42	NR
#12	150	68	82	89	96	98	100	100	100

Note: * profiles calculated using precipitated Rh in solids profile due to post precipitation in samples (see Section 6.1.3)

Table 6.8c: Summary of Cu precipitation extent for all reaction systems (solids basis)

Test #	Temp	Cu precipitation extent [%]							
	°C	1 min	2 min	~5 min	10 min	30 min	60 min	120 min	240 min
Co-precipitation system									
#9	50	0	0	0	0	3	16	17	17
#9R	50	0	0	0	0	3	6	14	12
#10	80	15	16	15	16	19	20	25	100
#11	95	14	19	16	17	22	23		
#11R	95	6	16	16	18	21	23		
#12 *	150	23	25	25	25	26	26		
		Cu precipitation extent on maximum precipitation [%]							
#9	50	0	0	0	2	17	94	102	100
#9R	50	0	0	0	0	24	51	112	100
#10	80	15	16	15	16	19	20	25	100
#11	95	61	82	69	74	97	100		
#11R	95	28	67	69	77	92	100		
#12 *	150	88	95	97	97	99	100		

Note: * profiles calculated using precipitated Rh in solids basis

Table 6.8d: Rh precipitation rate calculated from modelled data for the middle period (solid basis)

Test #	Temp	Rh precipitation rate ($-r_{Rh}$) [mg/min/L]							
	°C	1 min	2 min	~5 min	10 min	30 min	60 min	120 min	240 min
Ionic system (solids basis)									
#1	50	2.0	1.0	0.33	0.17	0.07	0.03	0.02	0.01
#2	80	2.5	1.2	0.49	0.25	0.08	0.04	0.02	0.01
#3	95	1.7	0.9	0.35	0.17	0.06	0.03	0.01	0.01
#4R **	150	11.3	7.8	3.0	0.80	0.01			
Substitution system (solution basis)									
#5b **	50	0	0	0	0.51	0.17	0.08	0.04	0.02
#6b **	80	5.6	2.8	1.1	0.56	0.19	0.09	0.04	0.02
#7b **	95	5.4	2.7	1.1	0.54	0.18	0.09	0.05	0.02
#8b **	150	19.7	10.4	2.6	0.50	0.25	0.05		
Co-precipitation system (solids basis)									
#9R	50	0	0	0	0.07	0.04	0.02	0.01	
#10	80	2.9	1.4	0.6	0.29	0.10	0.03	0.02	
#11	95	3.8	1.9	0.8	0.38	0.13	0.06	0.03	0.02
#11R	95	6.2	3.1	1.2	0.62	0.21	0.10	0.05	
#12 **	150	6.7	3.8	1.8	0.83	0.36	0.03		

Note: ** measured solution basis; 50 – 95 °C: data modelled to empirical logarithmic function; 150 °C: pseudo first order kinetics

The precipitation profiles of the various systems are presented and discussed for each individual system in the sections to follow, while comparative kinetics between the systems is discussed in Chapter 7.

The Rh precipitation rate presented in Table 6.8d is calculated as described in Section 3.2.8 and illustrated and discussed in Section 6.6.6.

6.3 Ionic Rh precipitation

6.3.1 Temperature effect

Ionic Rh precipitation has been performed at various temperatures at constant conditions, particularly sodium thiosulfate addition at 13.5 g/l, which is 37 times greater than the Rh requirement (see 'Actual Concentrations' in Appendix B.2). Rh precipitation profiles are illustrated in the Figure 6.1. The Rh precipitation rates are calculated from the kinetic model developed in Section 6.6 and illustrated in Figure 6.20a and Appendix B.5.

The precipitation profiles show a clear relationship of increasing Rh precipitation kinetics and extent with increasing temperature. After 10 min reaction time, approximately 16% Rh precipitation occurred at 50 °C compared to 97 % at 150 °C. At 240 min, 20, 62, 74 and 100% Rh precipitation occurs at 50, 80, 95 and 150 °C, respectively. Comparative statistics in Chapter 7 shows that the differences in the profiles are significant.

Incomplete precipitation at atmospheric temperatures at this large excess of thiosulfate addition indicates that passivation has occurred onto the elemental sulfur formed during thiosulfate decomposition (section 6.3.2). Passivation is discussed in more detail in Section 6.6.

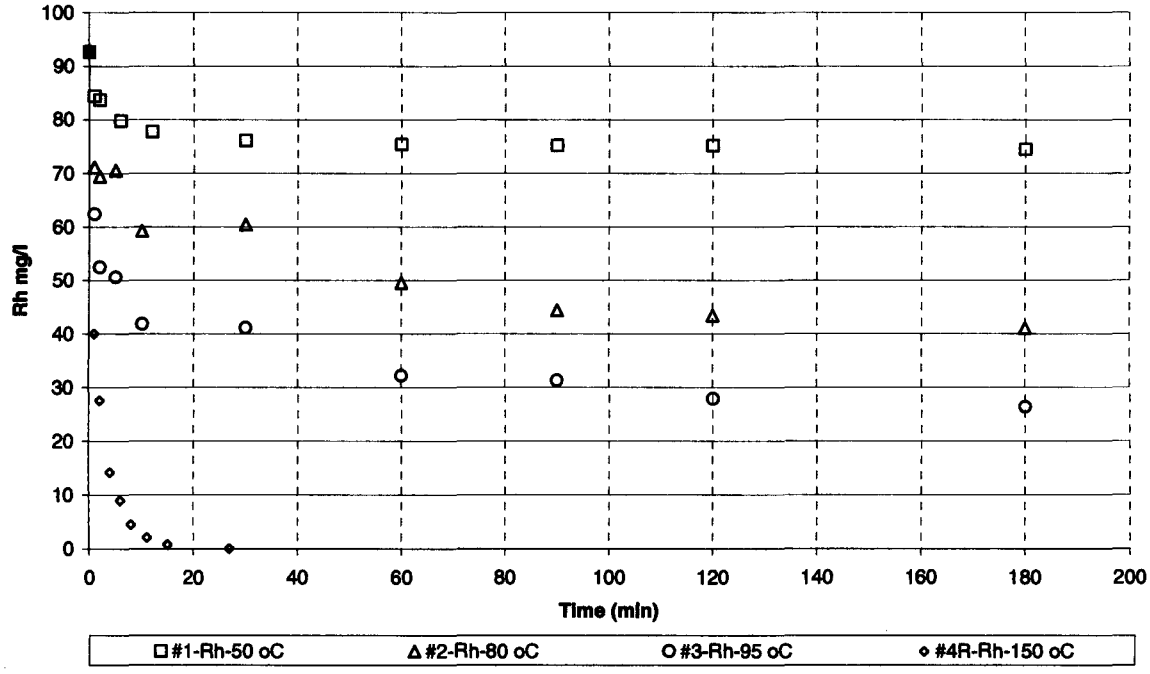

Figure 6.1: Ionic Rh precipitation at 50, 80, 95 and 150 °C, showing dominant temperature effect of increased Rh precipitation rate and extent with increasing temperature. Test conditions were kept constant, with sodium thiosulfate added at 37 times molar excess than stoichiometric requirement.

The chemical reaction step at the surface is usually much more sensitive to temperature than the physical steps (Livenspiel, 1972); thus the sensitivity of this ionic reaction system to temperature indicates that the reaction is chemical reaction controlled rather than mass transfer or diffusion controlled.

6.3.2 Stoichiometry

Measured molar ratios are calculated in log sheet and mass balance tables in Appendix B.4. Molar ratios of various elements and / or compounds are summarised in the Table 6.9.

Table 6.9: Measured ionic Rh precipitation stoichiometry ratios

Test #	Molar ratios of compounds			
	Acid / S %	S / Na %	Acid / Na %	Rh / Acid %
1	95	89	94	0.7
2	86	88	87	1.5
3	90	82	85	1.7
4R	99	88	98	1.8
Average	92	87	91	1.4
Expected	25	133	33	67

Note:
Acid / S = H_2SO_4 consumed / S in solids ; S / Na = S in solids / $Na_2S_2O_3$ added ; Acid / Na = H_2SO_4 generated / $Na_2S_2O_3$; Rh / Acid = Rh precipitated from solution / acid consumed ; 100% is a 1:1 mole ratio

The ratios of specific tests or the average ratios are compared to the expected ratios, which are based on the expected ionic precipitation without redox reaction chemistry presented in Chapter 5. Acid consumption and S precipitation is in great excess of the stoichiometric Rh precipitation. Acid must have been consumed mainly through thiosulfate degradation to elemental S, where 3 mols of sodium thiosulfate would produce 4 mol S, as per the reaction below:

$$3\ S_2O_3^{2-} + H_2SO_4 = 4\ S + 3\ SO_4^{2-} \qquad (5.11)$$

Complete Rh precipitation at elevated temperatures shows that sufficient thiosulfate was added initially to maintain the required excess for the comparative study. The 92% average ratio shows less S precipitated than the maximum 4/3 or 133%. Thus not all the excess thiosulfate degrades and sufficient sulfide is left for Rh precipitation. Some potential S precipitation is lost to H_2S gas detected in the atmosphere, possibly formed through thiosulfate hydrolysis in reaction 4.10.

Acid consumed is significantly more than the expected ~25% from thiosulfate degradation, which must have occurred through additional acid consumption reaction/s not considered in the thermodynamic study. Some potential acid formation could have been lost to SO_2 / SO_3 gas formed in reaction 4.12, which escaped the vapour space and eventually the system during sampling.

The comparative kinetic tests have been partially compromised by this degradation, as Rh can precipitate onto the elemental sulfur as Rh sulfide (reaction 5.7f) (Barkan and Greiver, 1977a) would be slower than nucleation and crystal growth. However, ionic precipitation remains the fastest precipitation system when compared to substitution and co-precipitation at 50 – 95 °C, thus it does not affect the general relative kinetic comparison.

Temperature does not seem to affect the overall stoichiometry, thus it does not affect the selectivity of the various reactions taking place.

6.3.3 Stoichiometric thiosulfate addition

The comparison of ionic Rh precipitation kinetics and extent at elevated temperatures for excess thiosulfate addition and stoichiometric requirement is illustrated in the Figure 6.2. Both precipitation profiles demonstrate fast initial precipitation kinetics, slowing down over the second period and followed by a slow approach to completion.

Initial rate of precipitation of excess addition is almost double that of the stoichiometric addition at half the feed concentration, highlighting the effect of Rh^{3+} and S^{2-} concentration on overall precipitation rate. Complete precipitation only occurs with excess sulfide addition. The incomplete Rh precipitation during the stoichiometric reaction can mainly be explained by the thiosulfate degradation reactions, whether sulfide precipitation potential is lost to H_2S and SO_2 / SO_3 gases, or acid digestion. This again demonstrates the need for excess sulfide in the comparative kinetic study.

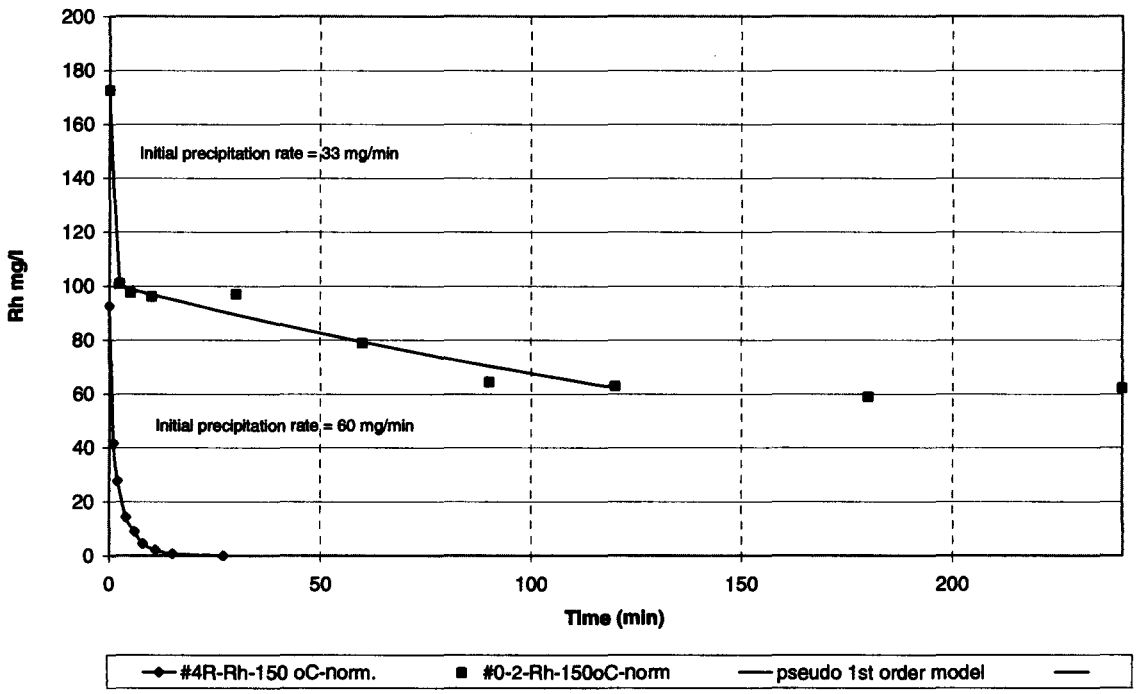

Figure 6.2: Ionic Rh precipitation at 150 °C, comparing stoichiometric sodium thiosulfate addition requirement against 37 times greater than stoichiometric requirement. Stoichiometric precipitation was significantly slower and incomplete.

6.4 Cationic substitution

6.4.1 Temperature effect

Rh precipitation kinetics on CuS increases significantly with increasing temperature. The precipitation profiles are illustrated in Figure 6.3. The Rh precipitation rates are calculated from the kinetic model developed in Section 6.6 and illustrated in Figure 6.20b and Appendix B.5.

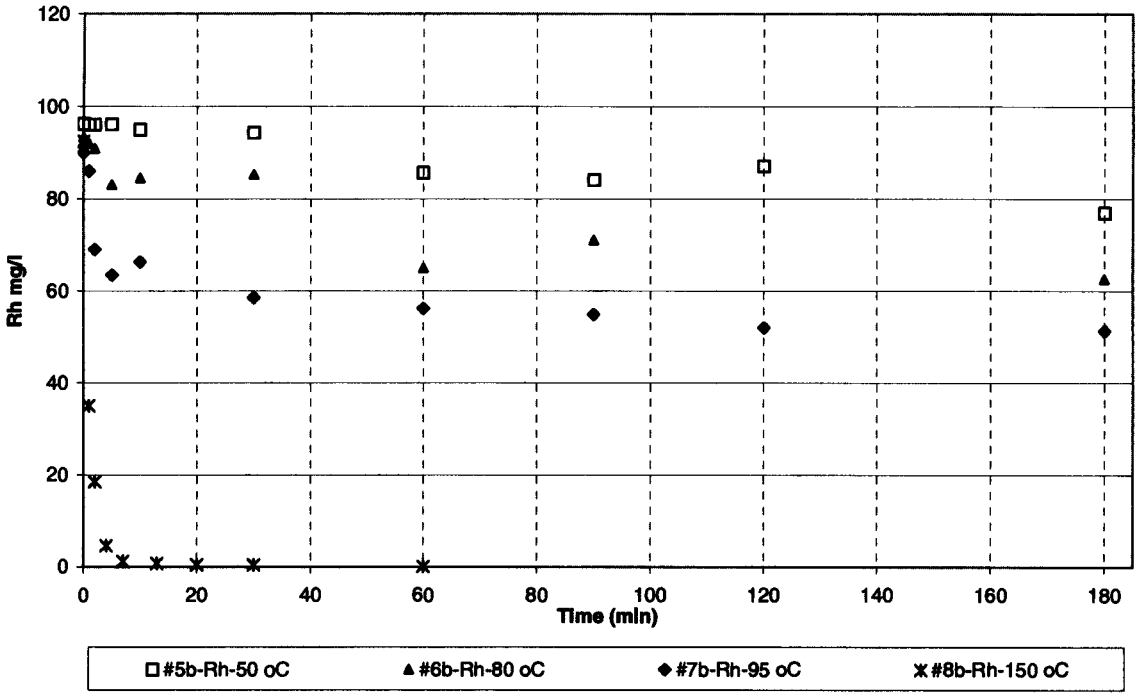

Figure 6.3: Rh substitution with CuS at 50, 80, 95 and 150 °C, showing dominant temperature effect of increased Rh precipitation rate and extent with increasing temperature. CuS is prepared and added to simulate conditions of precipitating it in the ionic and co-precipitation tests.

In the substitution reaction system after 10 min reaction time, Rh precipitation is 1% at 50 °C, while almost complete precipitation occurs at 150 °C. At 240 min, 17, 34, 45 and 100 % Rh precipitation occurs at 50, 80, 95 and 150 °C, respectively. The extent and rate increases significantly with increasing temperature, indicating that this reaction is chemical reaction controlled. However, the surface area of the previously precipitated CuS increases with increasing temperature; thus the controlling step cannot be deduced from temperature alone. Incomplete precipitation at atmospheric temperatures at this large excess of CuS indicates that passivation occurs, which is discussed in Section 6.6.

An induction period of ~10 min occurs before Rh precipitation is noticeable. It cannot be due to thio-complexation, as no thiosulfate is added to the system.

6.4.2 Cu leaching during substitution

The Cu leaching from CuS with Rh^{3+} is illustrated in Figure 6.4. The fact that Rh precipitation occurs onto the CuS system has the implication that the interaction of the bulk metal sulfide on the valuable metal or impurity must be taken into consideration when attempting to

understand the co-precipitation mechanism. Only partial leaching is noticed at atmospheric temperatures, while approximately 44% of the expected Cu is leached at 150 °C. The ratio of Cu released per mol Rh precipitation is quantified and discussed in Section 6.4.3.

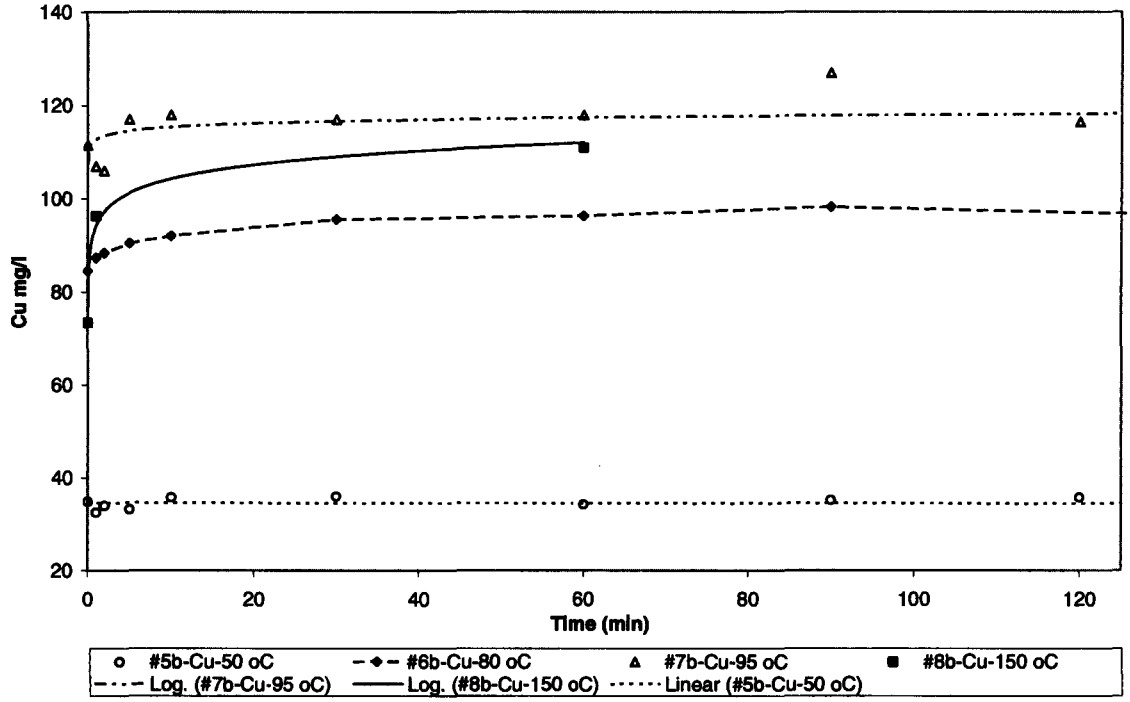

Figure 6.4: Cu leaching profile at 50, 80, 95 and 150 °C, showing significant Cu release at 80 and 150 °C.

6.4.3 Stoichiometry

Measured molar ratios are calculated in the log sheet and mass balance tables in Appendix B4. The ratios of various elements or compounds for ionic Cu precipitation are summarised in the Table 6.10 and Rh substitution ratios are summarised in Table 6.11.

Table 6.10: Measured Ionic Cu precipitation stoichiometry with thiosulfate addition

	Molar ratios of compounds on final samples (%)				
Test #	Cu / Na	Cu / S	Cu / Acid	Acid / Na	S / Na
5a	64	162	161	40	39
6a	29	115	73	39	60
7a	83	113 (7b data)	169	49	NA
8a	NA	87 (8b data)	NA	NA	NA
Average	59	119	134	43	50
Expected	100	100	44 – 100	100	100

Note:
Na = $Na_2S_2O_3.5H_2O$ added, measured by Na in final solution ; Cu / Na = Cu precipitated from solution / Na ; Cu / S = Cu to S in solid; Cu / Acid = Cu precipitated from solution / H_2SO_4 generated in solution ; Acid / Na = H_2SO_4 generated / $Na_2S_2O_3.5H_2O$ added ; S / Na = S in solids / $Na_2S_2O_3$ added; 100% is a 1:1 mole ratio

Molar ratios from solution chemistry show that Cu precipitates as CuS, however #5a in Table 6.10 indicates some possible Cu_2S formation. Cu to S ratio in the solids of part (b) in Table

6.11 confirms CuS formation. The moles of Cu precipitated against the moles or thiosulfate added ion approached the ratio of one, but complete precipitation does not occur. The solution stoichiometry is affected by the acid consumption reaction and acid balance cannot be used to confirm various reactions.

Table 6.11: Measured Rh cationic substitution stoichiometry

Test #	Molar ratios of compounds on final samples (%)		
	Cu leached / Rh ppt	(Cu+Rh) / S (solids)	Rh ppt / acid
5b	17	78	13
6b	30	115	1
7b	6	114	1
8b	66	89	3
Average	30	99	4.6
Expected	150	100	0

Note:
Na = $Na_2S_2O_3.5H_20$; S =elemental S or S^{2-} ; Acid = H_2SO_4 generated; (Cu+Rh) / S = total metal to sulfide in solids; 100% is a 1:1 mole ratio

Table 6.10 shows that only partial Cu^{2+} release occurs during Rh precipitation through substitution. At atmospheric temperatures, Cu released into solution over the amount of Rh precipitation averages at 30% basis points of the expected 150% for the substitution reaction i.e. only 20% of the expected Cu release. At 150 °C, the Cu release increases to 44% of expectations.

Possible explanations for partial Cu leaching into solution are:

1. Sulfide-containing ions have not been sufficiently washed off the precipitated CuS, causing some ionic precipitation at the surface, forming Rh,Cu mixed sulphide (Rudnev and Malofeyeva, 1964),

2. Alternative Rh compounds have formed, leaching different stoichiometric quantities of Cu via reaction 5.8a - 5.8c

Additional test work is required to confirm the release of Cu during cationic substitution. The tests should be designed independently from the comparative kinetic study to ensure sufficient background Cu in solution to saturate the CuS surface. Secondly, the ratio of Rh^{3+} to CuS should be increased to concomitantly increase the amount of Cu^{2+} release.

It must be highlighted that the actual release of Cu^{2+} is of lesser importance than the fact that Rh actually precipitated onto the CuS.

6.5 Rh co-precipitation

6.5.1 Determining the appropriate precipitation profile results

Problems with accuracy of the measurement of the Rh precipitation profiles are discussed in Section 6.1, highlighting relatively high analytical error and post precipitation in the samples. The specific impact on the co-precipitation system results is discussed in more detail below, highlighting the most appropriate data selected for the subsequent comparative kinetic study.

- **Rh precipitation at 50 °C**

Section 6.1.6 describes the results of duplicate co-precipitation tests producing very different results for solution and solid profiles, though both tests have similar metal accounting of 90%. Additional confirmatory test work would be required to confirm relative kinetic comparisons at 50 °C. Only the ionic and substitution reactions can be compared with any confidence.

- **Cu precipitation over 50 – 150 °C**

Figure 6.5 shows that, at 80 – 150 °C, a rapid decrease in concentration occurs over the first two samples, followed by a rapid increase in concentration, before decreasing steadily to completion. There are a number of possible explanations and counter arguments for this phenomenon:

1. Cu is released back into solution on 80 – 150 °C profiles by Rh precipitation through cationic substitution; however, the amount of Rh precipitated does not account for all the Cu release, particularly at 150 °C.

2. Initially two samples were contaminated with residual thiosulfate from the injection procedure, as discussed in Section 6.2.2, which would explain the release of Rh as well; however, flush samples would have reduced this contamination on the first sample and probably eliminated it on the second sample.

3. Post precipitation of Cu and Rh in the initial samples, as discussed in Section 6.1.3, is the most likely cause.

The predicted Cu concentrations based on solid profiles are presented in Figure 6.6. This eliminates the excessive releaching of Cu back into solution, confirming that it is mainly caused by the post precipitation phenomenon. This suggests that the laboratory did not provide adequate total stream analysis. However, a small release still occurs, probably due to cationic Rh substitution, as well as possible thiosulfate contamination.

Unfortunately, the comparison of the measured and predicted Cu concentration data presented in the log sheets in Appendix B.4 shows that the predicted concentrations underestimate the Cu precipitation towards the end of each precipitation profile, probably due to solid loss during the test procedure, as discussed in Section 6.1. This is illustrated by comparing Figure 6.5 and 6.6. Thus, it is important to maintain the same comparative basis within each profile, as well as comparing the profiles at various temperatures. Hence, the solids basis is used for the comparative kinetic study and modelling.

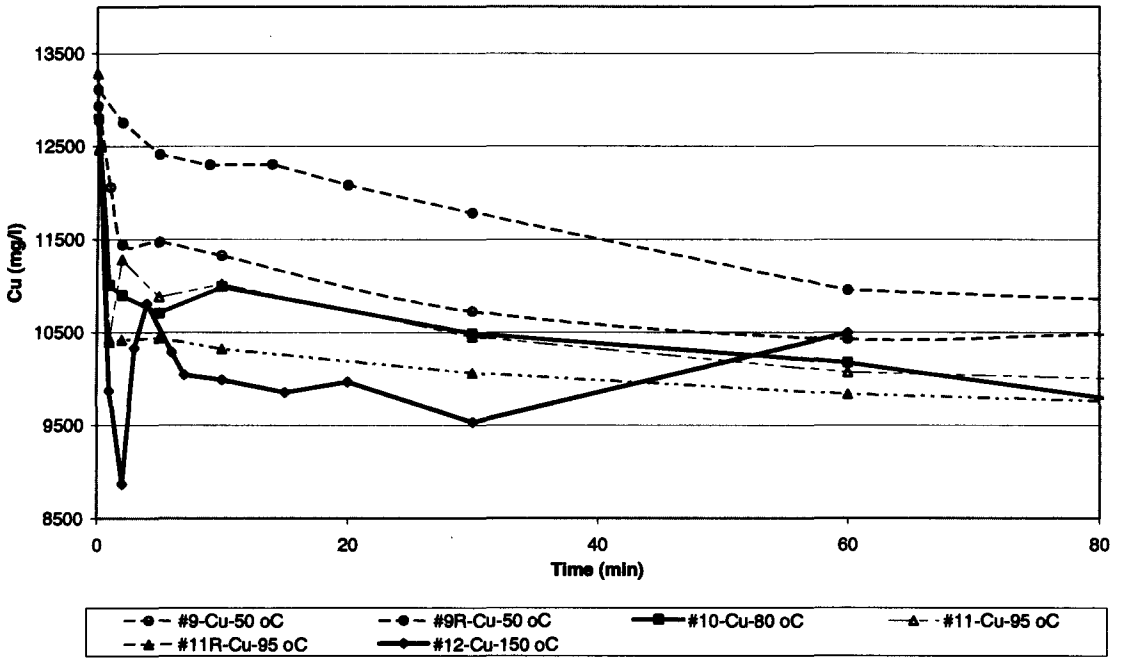

Figure 6.5: Cu co-precipitation at 50, 80, 95 and 150 °C, showing dominant temperature effect of increased Cu precipitation rate and extent with increasing temperature.

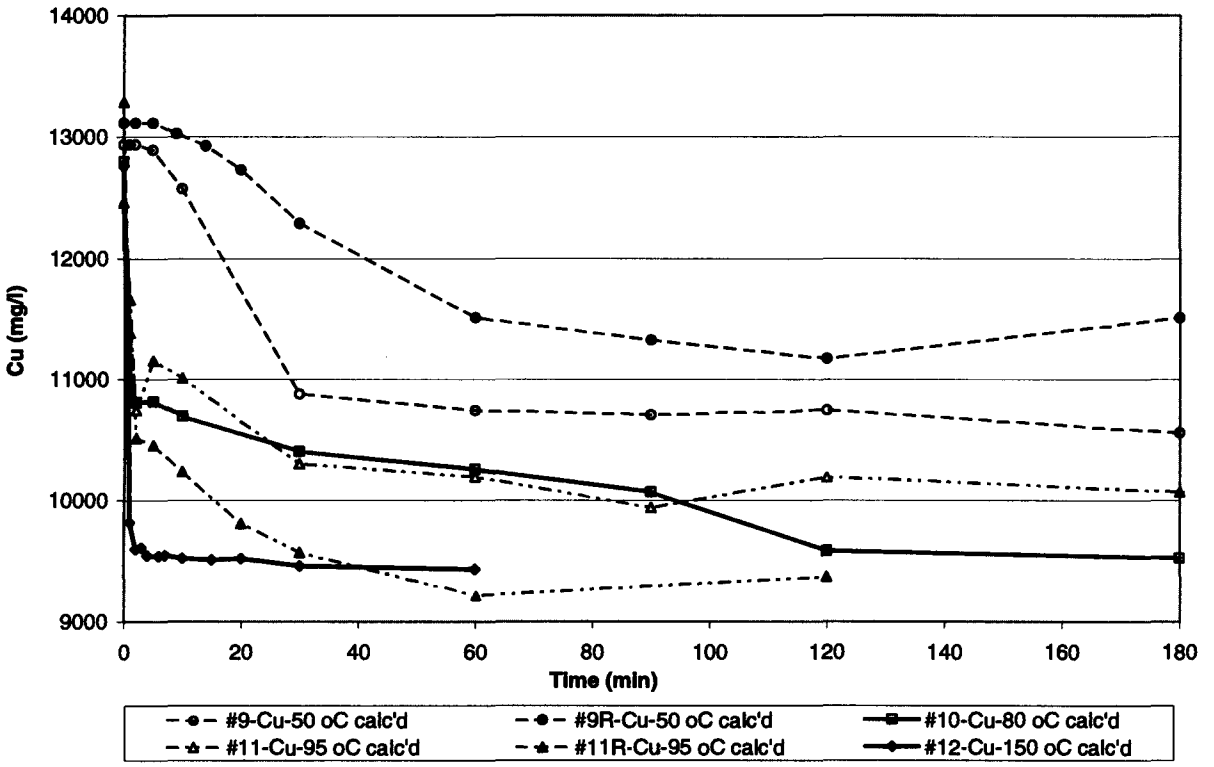

Figure 6.6: Cu co-precipitation at 50, 80, 95 and 150 °C, calculated from solid mass precipitated, assuming CuS, to avoid overestimation of Cu precipitation due to post-precipitation in filtrates; profiles illustrate that increasing temperature improves the Cu precipitation rate and extent .

6.5.2 Temperature effect on Rh and Cu precipitation

Figure 6.5 and 6.6 illustrates the rate of Cu precipitation during co-precipitation concomitantly increasing with temperature. Thus, the reactions are probably chemical reaction controlled. Similar overall precipitation extent occurs at 95 – 150 °C, while significantly slower precipitation kinetics and extent occurs at 50 °C. The solids basis shows that Cu precipitation at 50 °C experiences an induction period of approximately 5 min before precipitation is visible. This would be due to the time required for the homogeneous reactions prior to nucleation and crystallisation. Precipitation rate is effectively immediate at 80 °C and above. Rh precipitation also shows this induction period.

Similarly, effect of temperature on Rh co-precipitation is illustrated in the Figure 6.7, showing that Rh precipitation kinetics and extent increases significantly with increasing temperature. After 5 min reaction time, insignificant precipitation occurs at 50 °C, compared to 89% at 150°C. At 240 min, 5 – 30, 36, 51 and 100 % Rh precipitation occurs at 50, 80, 95 and 150°C, respectively. The precipitation profile at 50 °C on #9 and 9R shows that Rh precipitation occurs at the same time as Cu precipitation. Either the relative ionic precipitation rates are the same or the formation of CuS triggers Rh precipitation.

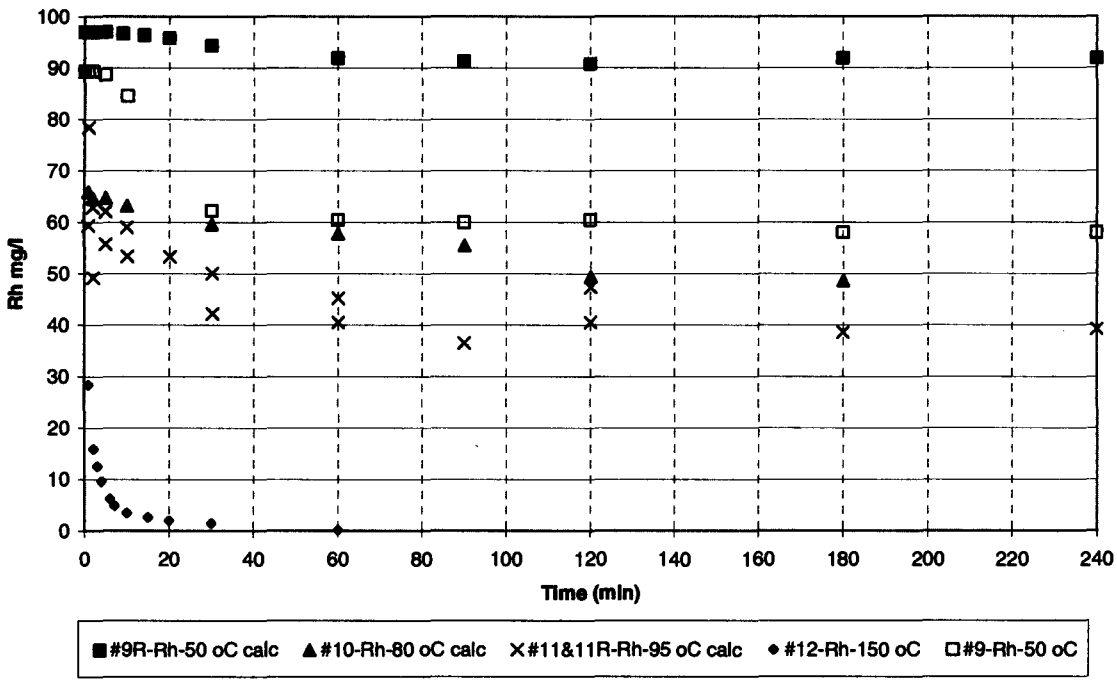

Figure 6.7a: Rh co-precipitation at 50, 80, 95 and 150 °C, showing dominant temperature effect of increased Rh precipitation rate and extent with increasing temperature.

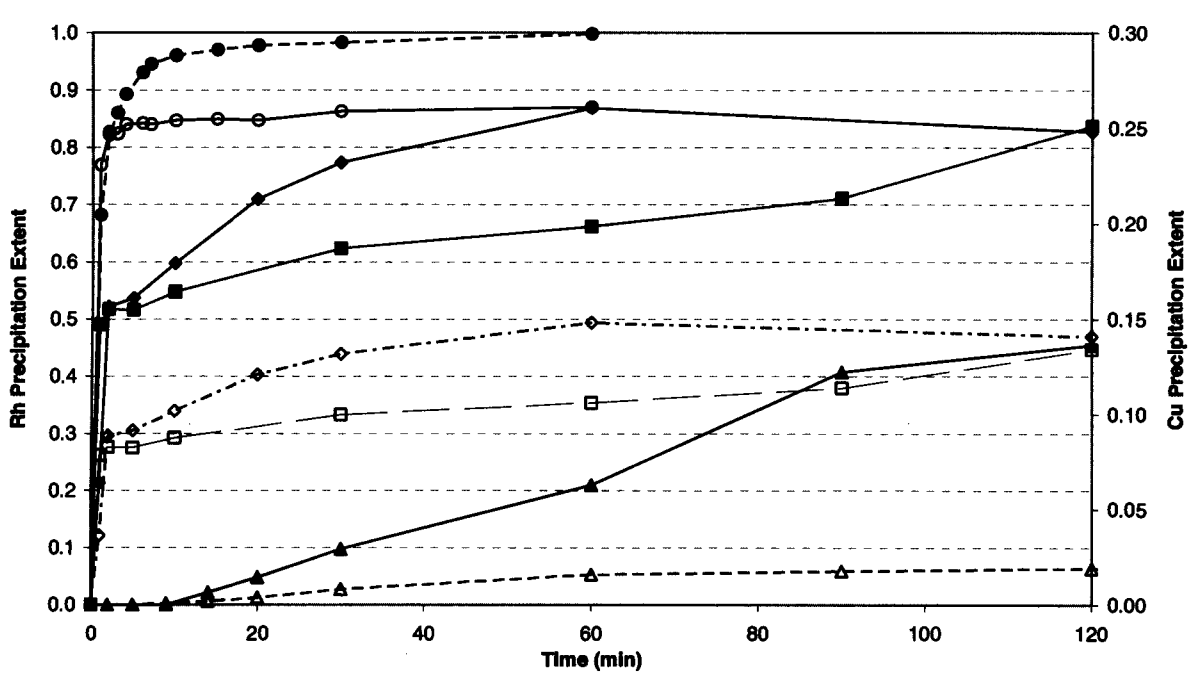

Figure 6.7b: Cu and Rh co-precipitation profiles at 50, 80, 95 and 150 °C, calculated from solid mass precipitated; profiles illustrate that increasing temperature relatively increases Rh precipitation rate.

Comparative statistics of the precipitation profiles in Chapter 7 shows that the difference of separation between 80 and 95 °C is significant on the solids basis, but are similar on the solution basis. It is believed that this disparity is due to the post precipitation. The co-precipitation reaction systems' sensitivity to temperature over the initial period shows that Rh co-precipitation is probably chemical reaction controlled.

The precipitation rate of Rh and Cu is compared in Figure 6.7b, showing the relative precipitation rate over the first 120 min. At 50 °C, Cu experiences approximately 10 min induction period before relative slow Cu precipitation commences, while Rh precipitation does not occur over the first 20 min. At 150 °C, Cu precipitation is slightly faster than Rh precipitation. Cu precipitation is completed after the 3 minutes, while Rh precipitation is approximately 85% completed. At 80 °C, the relative rate of Cu and Rh precipitation is in between 50 and 150 °C. The ratio of the relative precipitation rates is presented in Table 6.12 in Section 6.5.3.

At atmospheric temperatures, the Rh precipitation was incomplete, probably due to passivation of the CuS, which is discussed in Section 6.6.

6.5.3 Comparison of Rh and base metal precipitation rates

Aqueous sulfide is required to precipitate Rh through the ionic reaction path in the co-precipitation mechanism. If the aqueous sulfide is preferentially consumed, then Rh continues to precipitate through the cationic substitution with Cu^{2+} in CuS described in Section 6.5.2. Relative kinetics of various precipitating metals is compared to gain an understanding of the co-precipitation reaction mechanism. The extent of Cu precipitation is used as an indication of the amount of aqueous thiosulfate available for ionic Rh precipitation.

Relative kinetics of various precipitating metals, namely, Rh, Cu and Ni, is compared to gain an understanding of the co-precipitation reaction mechanism by comparing the following:

1. Initial absolute precipitation rates,

2. Relative precipitation rates on a normalised basis (Table 6.12) (Figure 6.7b),

3. Ratio of Cu to Rh in the co-precipitated solids (Figure 6.8).

From an absolute perspective, the initial rate of Cu precipitation is over two orders of magnitude higher than Rh over 80 -150 °C. Initial rates measured are ~40-50 mmol Cu/min compared to ~0.1-0.6 mmol Rh/min. This can be explained by the fact that Cu concentration is two orders of magnitude greater than Rh. The extent of Cu precipitation is used as an indication of the amount of aqueous thiosulfate available for ionic Rh precipitation. On an absolute basis, CuS precipitation consumes the bulk of the aqueous thiosulfate (sulfide) ion, limiting the amount of ionic Rh precipitation. Once the aqueous sulfide is depleted, Rh would continue to precipitate through the cationic substitution reaction.

Final Cu precipitation extents normalised to the maximum precipitation extent of 26% are compared to Rh precipitation extents. The ratio of Cu extent to Rh extent is presented in Table 6.12. A ratio of one implies that the precipitation extents are equal from a relative perspective. A higher ratio shows that Rh precipitation is less selective than copper from a relative respective.

Table 6.12: Relative Cu and Rh precipitation rate (solids basis)

Test #	Temp °C	1 min	2 min	~5 min	10 min	30 min	60 min	120 min	240 min
#9	50	-	-	0.0	0.4	0.6	3.1	3.3	3.3
#9R	50	-	-	-	0.0	8.8	9.7	17.4	18.8
#10	80	2.2	2.2	2.2	2.2	2.2	2.2	2.2	-
#11	95	1.8	3.0	1.8	1.8	1.8	1.8	-	-
#11R	95	2.3	2.3	2.3	2.3	2.1	2.0	-	-
#12	150	1.3	1.2	1.1	1.0	1.0	1.0	-	-

Table 6.12 shows that the ratio increases with decreasing temperature i.e. Rh precipitation selectivity decreases with decreasing temperature. At 50 °C, Rh overall selectivity decreases with reaction time, as more Cu preferentially precipitates. However, at 95 °C the ratio decreases only slightly with reaction time, while at 150 °C, Cu precipitation is only marginally faster than Rh from a relative perspective.

At 50 °C, the induction period of 5 - 9 min is noticed for Cu and Rh, where precipitation occurs simultaneously, with Cu precipitation being relatively faster than Rh. Either the relative ionic precipitation rates are the same or the formation of CuS triggers Rh precipitation.

An alternative approach to quantifying precipitation selectivity is the ratio of Cu and Rh in the solids against temperature for each reaction system. Figure 6.8 shows that Rh selectivity improves with increasing temperature, mainly because of additional Rh precipitation relative to a constant Cu content.

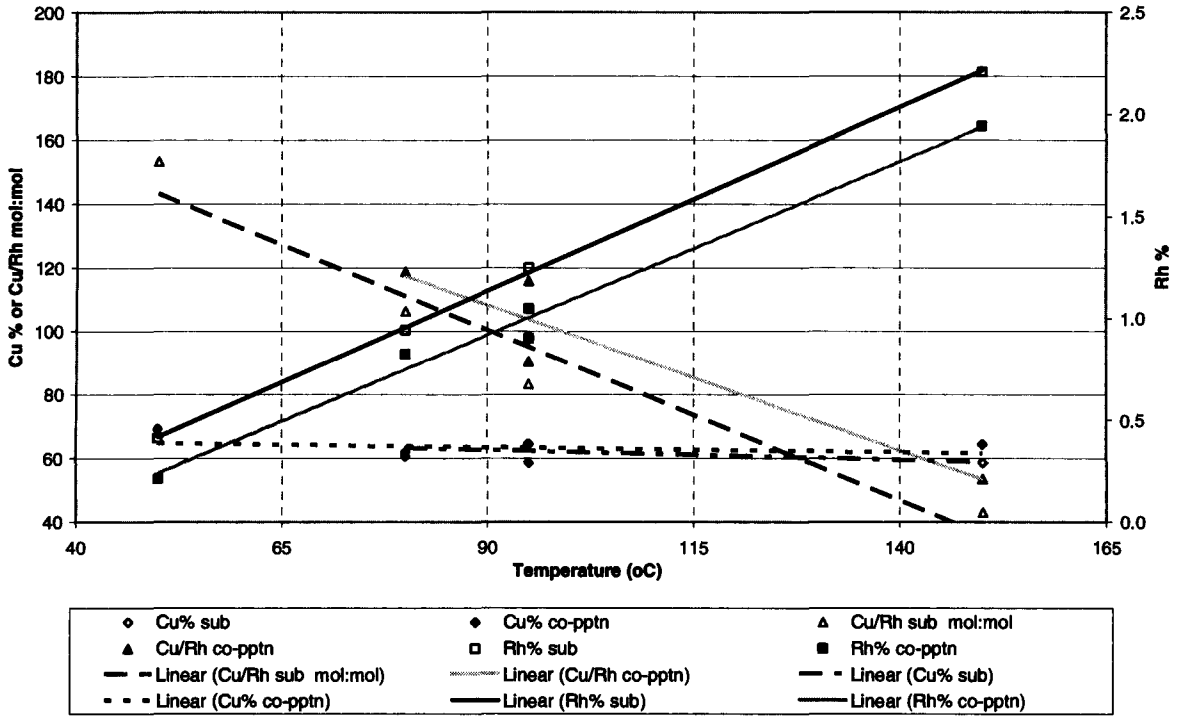

Figure 6.8: Rh and Cu ratio in solids for the substitution and co-precipitation systems over 50 – 150 °C, showing improved Rh selectivity with increasing temperature on final profiles.

In summary, Rh precipitation selectivity decreases with decreasing temperature and relatively more Rh in the feed would have to precipitate through the substitution reaction path for complete Rh precipitation.

6.5.4 Selectivity of base metal precipitation

Assays in the log sheets in Appendix B.4 shows that Cu precipitation is almost completely selective over Ni precipitation (0.05-0.08% Ni detected on solids). This would be expected from a thermodynamic perspective, where CuS is significantly more insoluble than NiS. In this case, the Ni concentrations are in the same order of magnitude as Cu and kinetic effects do not come into play. Thus, the overall Cu precipitation rate is significantly faster than Ni due to the chemical driving force.

Alternative findings would be expected if the relative concentrations of Cu and Ni were significantly different. If Cu concentration had been relatively low compared to Ni, then by the same argument, Cu would co-precipitate with Ni while attempting to achieve complete Cu removal. This would likely occur due to overall Ni precipitation kinetics being faster than copper, similar to the Rh and Cu co-precipitation system currently being studied. If Cu were not present, then Rh precipitation selectivity over Ni could possibly improve over that of Cu owing to the thermodynamic effect of a larger difference in metal sulfide solubility products. Ni would probably still precipitate due to metal concentrations affecting kinetics if the solution potential is reduced enough.

If the Cu^{2+} concentration is decreased sufficiently to reduce the overall Cu precipitation to a rate similar or slower than Rh^{3+}, then one would expect Rh^{3+} precipitation to become selective over Cu^{2+}. If Cu concentration is low relative to Rh, then complete selectivity would probably occur due to thermodynamic and kinetic effects. Confirmatory test work is required

for specific systems, as the relative kinetics of the individual metals is dependent on their concentrations.

In general, both the thermodynamics and overall relative kinetics must be taken into account when predicting the response of co-precipitation systems. The relative difference in the metal sulfide solubility products and the relative concentrations affects the overall precipitation rates, which has a direct effect on precipitation selectivity and the co-precipitation mechanism. The kinetic effect has the greatest impact on selectivity if the concentration differences are large enough.

6.5.5 Stoichiometry

Stoichiometric calculations are performed using both the solution and solid profiles. The molar ratios between compounds and elements summarised in the Table 6.13 supports expected ionic Cu and Rh precipitation with CuS formation. The ratio of metal precipitation to thiosulfate addition shows nearly complete metal sulfide addition occurs. The solids show slightly lower ratios, probably due to some solids being under-accounted (see Table 6.6).

The ratio of S precipitated against thiosulfate indicates that some thiosulfate is lost to H_2S and SO_3 gas with increasing temperature, causing relatively less CuS precipitation. Test #9R shows incomplete sulfide precipitation and it is expected that some of the sulfide has possibly been complexed with the base metals in solution. This could possibly be a function of the unknown acid-consuming reaction being a function of temperature.

Acid stoichiometry remains unconfirmed, probably due to acid consumption reactions described in ionic precipitation section. Acid consumption seems to increase with increasing temperature.

Table 6.13: Measured Rh and Cu co-precipitation stoichiometry

	Basis	(Cu+Rh) / Na	(Cu+Rh) / Acid %	(Cu+Rh) / S	Acid / Na	S / Na
9R	Solution	67	148		45	
	Solids	50		131		38
10	Solution	120	122		99	
	Solids	96		96		100
11R	Solution	85	73		117	
	Solids	97		106		92
12	Solution	71	47		150	
	Solids	101		110		91
Average	Solution	86	98		103	86
	Solids	86		111		86
Expected		~100	~100	~100	~100	~100

Note:
Cu+Rh metal precipitated from solution for solution basis and Cu+Rh measured in precipitate for solids basis ; Na = $Na_2S_2O_3.5H_2O$ added, measured by Na in final solution ; S = elemental S or S^{2-} in solids ; Acid / Na = H_2SO_4 generated / $Na_2S_2O_3.5H_2O$ added ; S / Na = S in solids / $Na_2S_2O_3$ added, , measured by Na in final solution ; 100% is a 1:1 mole ratio

6.5.6 Rh distribution in CuS

1. Elevated temperatures

Preliminary mineralogical analysis has been performed at Anglo Research Mineralogy Department using the SEM-EDX/MLA technique on the co-precipitation scouting test (#0-1). This precipitate is produced at 150 °C under conditions similar to test #12, though the initial Rh concentration is lower at 50 mg/l.

Dinham (2006) has reported that extremely fine-grained, spongy particulates of less than 3 µm diameter precipitated CuS are found throughout the sample. These CuS particulates are not exclusively covellite as produced in the production plant CSTR at 95 °C (Andrews, 2001); instead, approximately half of the CuS particulates contain a few percent of oxygen incorporated in the crystal structure. Neither the CuS nor the CuS-O particulates have aggregated to the levels observed in plant samples.

A small number (< 10 grains) of the fine-grained CuS aggregates contain small areas of higher backscatter. Analyses of these areas indicate slightly elevated Rh concentrations of up to 2.0 ± 0.4 wt % (Dinham, 2006). Figure 6.9 illustrates an EDX spectrum obtained on a Rh-enriched area within a CuS particulate, illustrating the relative proportions of Cu, S and Rh. In many cases the areas of Rh distribution are small, potentially smaller than the estimated 2 – 3 µm beam size of the SEM.

SEM mapped images are then run to confirm the single point results on Rh-rich areas. Figure 6.10 presents an example of such a mapping, containing O, S, Rh, Ni and Cu distribution within a particular grain.

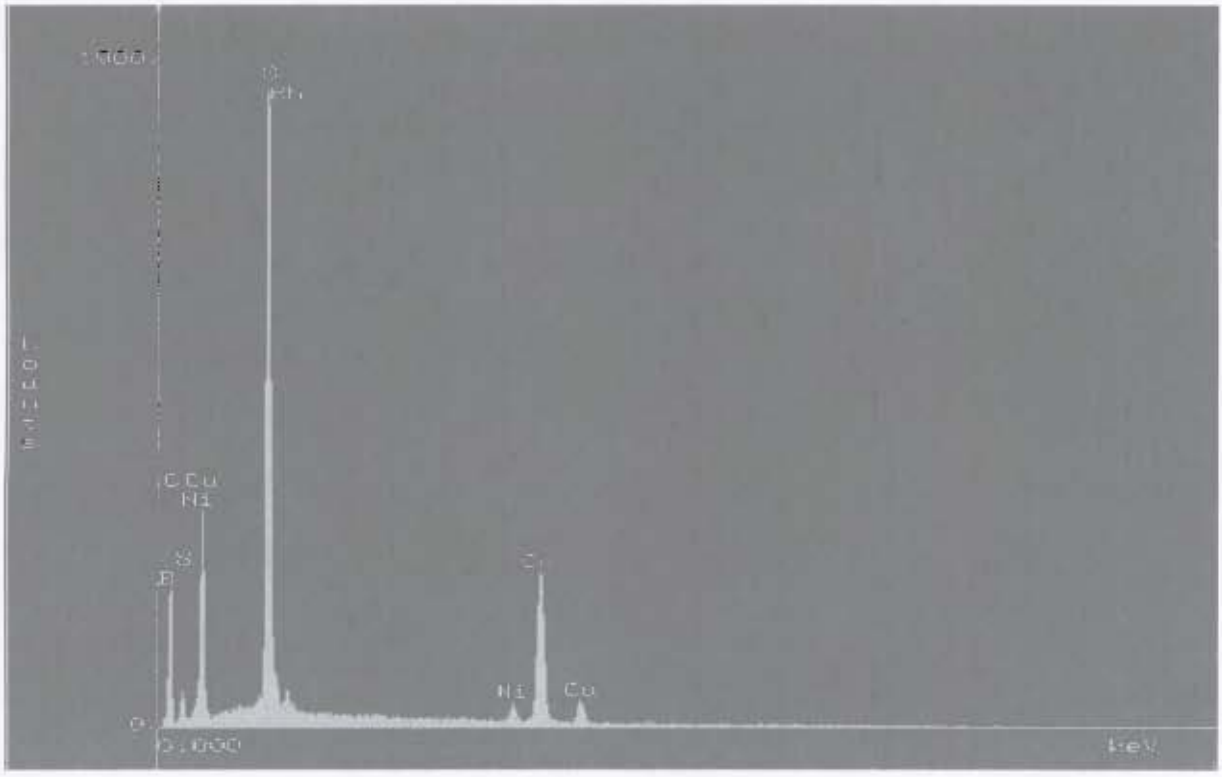

Figure 6.9: EDX spectrum illustrating the relative proportions of Cu, Ni, S and Rh measured in a Rh-enriched area in #0-1 sample (Figure 1 in (Dinham, 2006)).

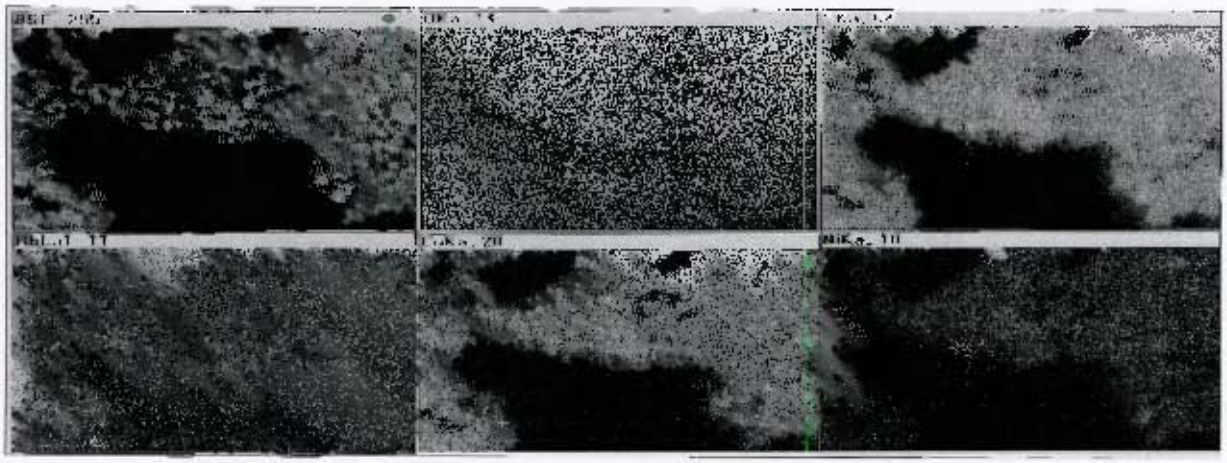

Figure 6.10: SEM back scattered image (BSE) and corresponding elemental distribution maps of a fine-grained CuS-O particulate in sample #0-1. Areas of epoxy in the mount appear black within the images. Although images are grainy, it is possible to see that Rh appears to occur at levels slightly above background throughout the CuS-O particulate (Figure 2 in (Dinham, 2006)).

These maps indicate that higher than background Rh levels seem to occur throughout the entire mapped particulate. Dinham (2006) concludes that Rh is found to be randomly distributed at slightly higher than background levels in selected CuS or CuS-O grains.

Dinham (2006) suggests that it would be unlikely that the Rh can be mapped using electron microprobe techniques, unless coarser material that is neither oxidised nor porous can be produced. This implies that this technique is not ideal for precipitate formed at elevated temperatures and alternative techniques would have to be used.

2. Rh co-precipitation in CuS at atmospheric temperatures

SEM-EDX/MLA and microprobe techniques would have been used to compare the Rh distribution in the CuS for the substitution and co-precipitation systems. This was originally part of the scope of this work, but it was not performed due to budget and time constraints. A previous Rh distribution study commissioned by the author using the microprobe technique on samples produced in the Rhodium Removal Section at RBMR in a CSTR at 95 °C shows the following (Andrews, 2001):

1. Distinctive sulfide mineral (Cu, Pd, Rh, Ru, S) containing ~ 10 % Rh,
2. Rh substitution in covellite particles; some CuS contains up to 1.5 % Rh,
3. Rh enrichment towards the edge of the covellite particles.

Data from the measurements taken approximately 5 µm apart over a number of CuS particles of varying size has been normalised to the fraction away from the edge. Plotting Rh percent against the normalised distance clearly demonstrates this average enrichment in the Figure 6.11. Linescans shown in three-dimensional graph in Figure 6.12 illustrate the Rh distribution over the cross-section of one particular particle, also showing enrichment towards the sides. This enrichment on the outer surface of the CuS could lead to passivation.

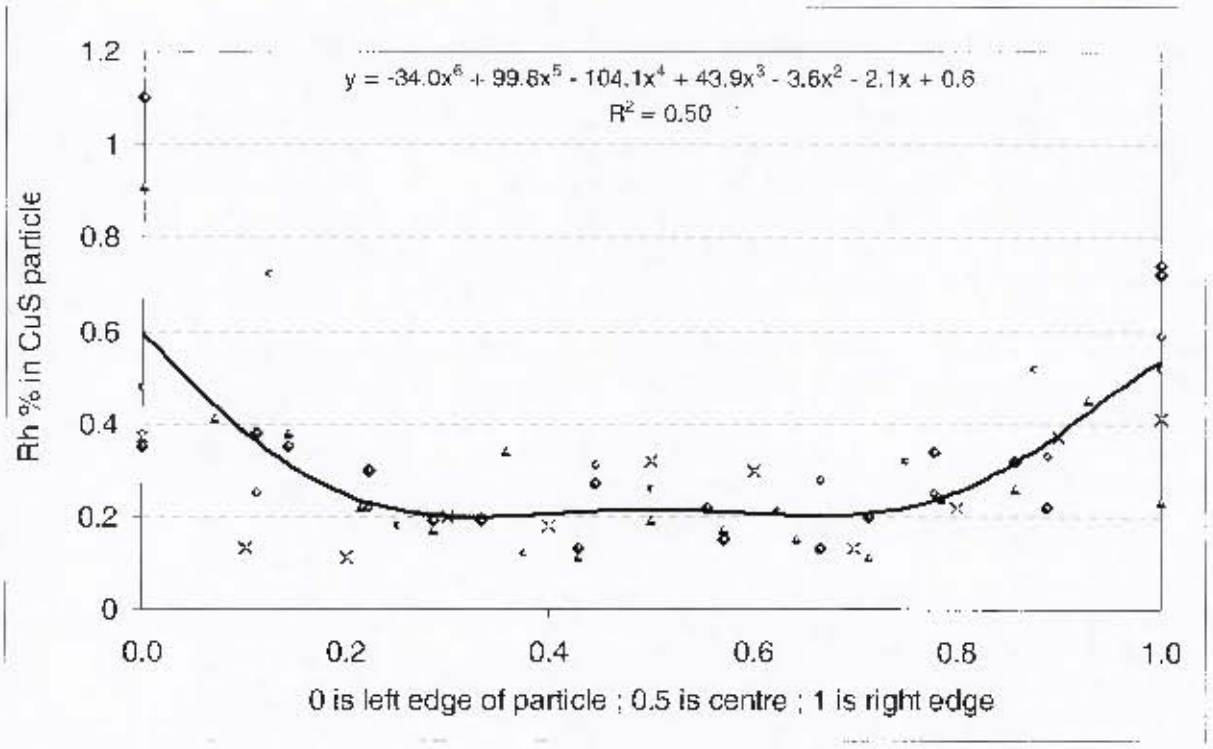

Figure 6.11: Microprobe linescans show in Rh mass percent in the co-precipitated covellite formed in the thioform process at 95 °C; Rh distribution was measured at 5 um intervals over a number of particles, showing Rh mass % increasing towards the edges at 0 and 1.

Figure 6.12: Three dimensional Rh distribution over a cross-section of a covellite particle produced in the thioform process at 95 °C, showing enrichment towards the edge (Figure in Andrews, 2001).

3. Interpretation of mineralogical results of Rh distribution

Plant samples have been produced at 95 °C, while the preliminary material in this study is precipitated at 150 °C. The change in the microstructure can be explained by the high super-saturation and faster precipitation kinetics at higher temperatures, causing finer material to form through more primary nucleation.

The actual background concentration is estimated from the stoichiometry calculations at 1.2% Rh, assuming complete Rh precipitation occurred (Appendix B.4). This is a fair assumption based on compete Rh precipitation in test #12. The very small number of particles found to contain Rh at 2.0% implies that the rest of the CuS sample must have contained the randomly distributed Rh at the background concentration near 1.2%, though the particles are too small to be detected. The oxygen in the CuS possibly indicates that a small amount of metal could have precipitated through the hydrolysis reactions or it simply occurred through post-oxidation of the solids during drying.

The increased Rh concentration towards the edge of the co-precipitated covellite particle indicates that Rh precipitated through the heterogeneous substitution reaction. Ionic precipitation, catalysed by the CuS, could also take place; however, the aqueous sulfide concentration would have been low due to the immediate aqueous sulfide consumption through CuS precipitation. The Rh in the centre probably results from ionic precipitation, however, substitution throughout the crystal growth or diffusion of Rh into the centre could also explain this.

Rh distribution in the co-precipitated covellite must be compared to the covellite in the substitution system to quantify the dominant reaction path in co-precipitation. If Rh passivates the outer surface of the CuS in the substitution system, thereby limiting the amount of Rh precipitating inside the particle, then the relative distribution of Rh in the co-precipitated covellite will indicate the amount of Rh precipitating through each reaction path. The rate of Rh distribution from the outside to the centre would provide valuable insight into when the reaction path occurs. If Rh diffuses appreciably into the porous CuS particles in the substitution reaction system and precipitates throughout the CuS particle, then it becomes more difficult to predict the dominant reaction path in co-precipitation. A direct comparison of the Rh distribution in substituted and co-precipitated CuS on a time basis would show the relative kinetics of the two independent systems. The relative kinetics would be used to infer a dominant reaction path in co-precipitation. For example, if mineralogy confirms that the substitution reaction is significantly slower than ionic precipitation, then one could infer that most of the Rh in the centre of the CuS would have precipitated ionically, as aqueous sulfide would still have been present. Alternatively, some Rh could have precipitated by the substitution reaction occurring in the homogeneous phase before crystalline CuS had formed.

4. Additional mineralogical analysis required

SEM-EDX/MLA and microprobe techniques should be used on the atmospheric precipitates of this study to confirm previous results and show Rh distribution in the CuS for the various reaction systems. Dinham (2006) recommends two alternative analytical techniques which may provide further information on the mode of occurrence of Rh for atmospheric and elevated temperatures:

1. X-ray Photoelectron Spectroscopy (XPS) is capable of analysing the first few molecular layers of a mineral surface, providing compositional analysis of the surface, oxidation and bonding stages of the same element.

2. X-ray Absorption Fine Structure (XAFS) spectroscopy, which is an elemental speciation technique that utilises the measurement of the variation (fine structure) of the X-ray absorption coefficient with energy in the vicinity of one of the characteristic absorption edges of a particular element, though it is expensive with a lengthy waiting list.

These techniques are used by some researchers in the study of CuS formation described in the literature review.

6.6 Modelling Kinetics

Kinetic modelling has been primarily performed to understand the mechanism of individual reaction systems, particularly the co-precipitation system. The development of an accurate, predictive model is of secondary importance and used only to test the validity of the selected model. The error in the analytical measurement is not accurate enough to produce accurate kinetic data like activation energy of overall rate constants. However, the kinetic data is certainly accurate enough to produce comparative results.

Another key reason for modelling the kinetic data is to produce linear regression lines, preferably using a fundamental model, to compare the precipitation extent of the various precipitation profiles on a rigorous, statistical basis. This is addressed in Chapter 7.

The kinetic modelling is initially performed on the predicted Rh solution concentrations using the solids basis described in Section 6.3. This is followed by repeating the modelling using the measured solution concentrations as an additional check. Calculated kinetic modelling data is attached in Appendix B.6.

6.6.1 Preliminary testing

The kinetic data modelling shows three distinctive precipitation periods for each precipitation system, namely, the initial period showing extremely fast precipitation, the middle period approximated by first or second order kinetics and a final period showing a slow approach to completion (Figure 6.13 - 6.14).

Definitions of the various precipitation regions used in this study are provided below:

1. The induction period is the delay time before perceptible nucleation occurs i.e. reactions in the homogeneous phase prior to solid precipitation.
2. The initial period of precipitation is defined as the period where very fast precipitation occurs, which is usually complete after 1 – 2 min. The comparative kinetic study in Chapter 7, the initial period is extended up to 5 min to provide sufficient data points for the comparisons. At 50 °C, the induction period precedes the initial period, while at 80 -150 °C, the induction period is not noticed.
3. The middle period is time period of the precipitation profile after the induction and/or initial period, following pseudo first order kinetics at a significantly slower rate.
4. The final period of the precipitation profile, where precipitation extent tends to completion, showing very slow kinetics or effectively stopped.
5. The initial rate is limited to the first sample of the solids profile using the solids basis.

For each reaction system, modelling of the first two periods together, the linear regression line provides good correlation with the kinetic models; however, the lines are shifted from the origin, breaching the requirement for first order kinetics. This shifts the predicted concentration away from the measured values. Table 6.14 summarises overall rate constant measured and quality of the linear fit. Quality of the first order kinetic model fit increases with increasing temperature, however, the shift increases as well. Generally, the shift is caused by significantly faster precipitation kinetics in the first few samples than over the middle period. Figure 6.13 - 6.14 illustrates the various periods and change in kinetics at 95 °C.

Table 6.14: Rh precipitation first order kinetics linearisation constants over the initial and middle period (solids basis)

Test #	Temperature K	Data range Min	Slope k (min^{-1})	y-intercept	Significance of correlation R P(t{R})	Coeff .of variance R^2
			Ionic			
1	323	0 – 30	4.78E-03	0.08	0.08	0.59
2	353	0 – 30	6.51E-03	0.51	0.13	0.59
3	368	0 – 60	3.82E-03	0.85	0.00	0.90
4R	423	0 – 13	2.82E-01	0.66	0.00	1.00
			Substitution			
5b	323	0 – 180	1.20E-03	0.002	0.00	0.90
6b	353	0 – 180	2.10E-03	0.074	0.01	0.76
7b	368	0 – 120	3.39E-03	0.20	0.01	0.64
8b	423	0 – 15	3.20E-01	1.23	0.03	0.85
			Co-precipitation			
9R	323	0 – 60	9.89E-04	0.00	0.00	0.99
10	353	0 – 180	1.77E-03	0.33	0.00	0.95
11&11R	368	0 – 120	3.97E-03	0.43	0.00	0.49
12	423	0 – 13	1.61E-01	1.5	0.00	0.87

Thus, the middle period has to be modelled using pseudo kinetics described in Section 3.2.2 to take the fast precipitation of the initial period into account. The initial fast kinetics would indicate that a mechanistic change has been occurring from the initial to middle period. Initially Rh would precipitate through homogeneous nucleation, followed by heterogeneous crystal growth, while towards the end of the precipitation extent Rh precipitation would be dominated by the cationic substitution reaction. These precipitation processes would certainly go through different precipitation mechanisms and possibly different orders of reaction.

However, the reason for the initial fast kinetics rapidly decreasing is primarily due to the pseudo rate constant ($k_1 = C_{Na_2S_2O_3}.k$) rapidly decreasing. For the ionic precipitation system, significant thiosulfate degradation occurs (Section 6.2.1), mainly through reaction with acid within the first minute. In this case, this reduction in the aqueous thiosulfate ion was the more likely cause for this rapid decrease in the precipitation rate. Rh would continue to precipitate onto the elemental sulfur (via reaction 5.14), but it is expected that this heterogeneous reaction would be significantly slower than ionic precipitation and the overall rate constant would decrease. In the co-precipitation system, the CuS precipitates preferentially to thiosulfate degradation, but it too shows a large initial rate constant over 80 - 150 °C, which rapidly decreases after the first few minutes. In this case, Rh would continue to precipitate on the precipitated CuS and for similar reasons the rate constant would decrease.

For the substitution reaction, where the thiosulfate ion is not present, the system still shows very fast initial precipitation and a rapid decrease. In this scenario, the surface area for precipitation would decrease with increased precipitation extent. The decrease in the measured rate constant could possibly be due to Rh passivating the CuS. This passivation could be extended to the cationic substitution reaction path in the co-precipitation system.

Figure 6.14 shows that the data has to be modelled with pseudo kinetics to take the very different kinetic regimes into account, though an empirical log fit provides a reasonable fit for the whole precipitation profile (Fig. 6.19a and 6.19b).

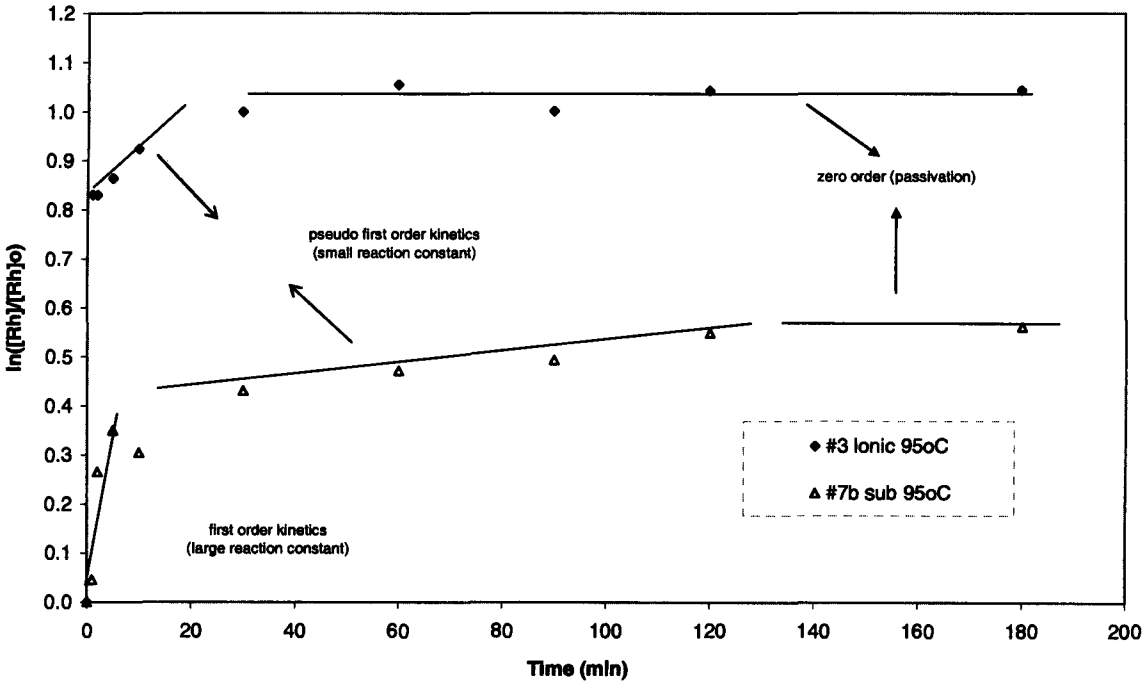

Figure 6.13: First order model plot over the initial and middle precipitation regions of ionic and substitution systems at 95 °C; data approximating a straight line would follow first order kinetics; substitution showed initial fast first order kinetics, followed by slower pseudo first order kinetics, while ionic precipitation showed initially pseudo first order kinetics, followed by zero order kinetics (solids basis).

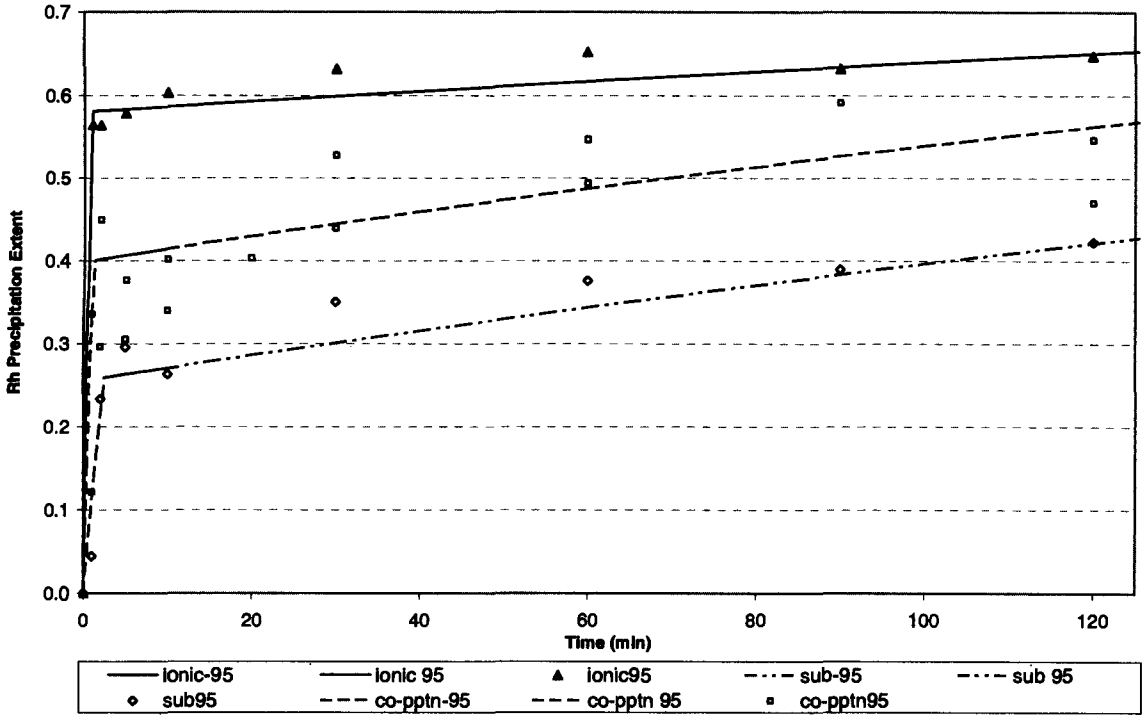

Figure 6.14: Initial and middle precipitation regions of ionic, substitution and co-precipitation systems at 95 °C, showing initial fast precipitation and the middle region modeled by first order kinetics (solids basis).

6.6.2 Testing for first or second order pseudo kinetics of the middle period

Modelling the kinetics after the initial precipitation period is performed by forcing the first sample of the middle period to effectively become the pseudo feed sample at pseudo time zero and recalculate model data according to the theory presented in Chapter 3. This provides the appropriate linear fit and required intercepts for the pseudo first order fit of the rate constant. This pseudo fit must not be confused with the pseudo first order rate constant caused by excess sulfide addition. Graphically, this is equivalent to shifting the first order model right until the line passes through the origin and any additional induction period.

Test #	1	2	3	4R	5b	6b	7b	8b	9R	10	11	11R	12
Time delay (min)	12	2	2	2	30	5	2	1	14	1	1	1	1

At 50 °C long induction periods are noticed before precipitation occurs. The middle period is then modelled to pseudo first and second order kinetics to determine the more appropriate model. The data fit is provided in Table 6.15. The pseudo kinetics shifted the y-intercept towards the origin, as well as shifting the predicted model towards the measured data.

Table 6.15: Comparison of pseudo first and second order kinetics for middle period

Test #	Temperature °C	Data range min	Slope k (min^{-1})	y-intercept	Sig. of R P(t{R})	Coeff. Of var. R^2	Slope k (min^{-1})	y-intercept	Sig. of R P(t{R})	Coeff. of var. R^2
			Ionic – 1st order				Ionic – 2nd order			
1	50	12 – 30	2.08E-04	0.01	0.03	0.75	2.74E-06	0.01	0.03	0.75
2	80	2 – 120	1.17E-03	0.07	0.03	0.65	1.41E-05	0.02	0.05	0.50
3	95	2 – 120	1.53E-03	0.06	0.03	0.64	4.26E-05	0.03	0.03	0.65
4R	150	2 – 11	2.84E-01	0.04	0.00	1.00	4.72E-02	-0.02	0.01	0.90
			Substitution – 1st order				Substitution – 2nd order			
5b	50	30 – 180	1.12E-03	0.03	0.05	0.78	1.08E-05	0.01	0.01	0.82
6b	80	5 – 180	1.79E-03	0.004	0.04	0.71	2.45E-05	0.01	0.03	0.72
7b	95	2 – 120	2.10E-03	0.05	0.00	0.87	3.56E-05	0.02	0.00	0.89
8b	150	1 – 7	5.64E-01	0.10	0.01	0.99	1.36E-01	-0.06	0.04	0.93
			Co-precipitation – 1st order				Co-precipitation – 2nd order			
9R	50	14 – 180	5.51E-04	0.01	0.00	0.89	5.91E-06	0.01	0.00	0.89
10	80	1 – 120	2.14E-03	0.01	0.00	0.97	3.72E-05	0.02	0.00	0.96
11& 11R	95	1 – 60	2.66E-03	0.11	0.01	0.49	6.06E-05	0.02	0.00	0.54
12	150	1 – 6	2.36E-01	0.01	0.00	0.998	0.02528	0.06	0.01	0.990

At atmospheric temperature, the first and second order models give a very similar fit of the data; thus the actual order of the reaction is uncertain. At elevated temperatures, the first order model provides a significantly better fit for the ionic and substitution reactions systems. This is illustrated in Figure 6.15. The pseudo first and second order calculated modelling data for the middle period are attached in the Appendix B.6.3.

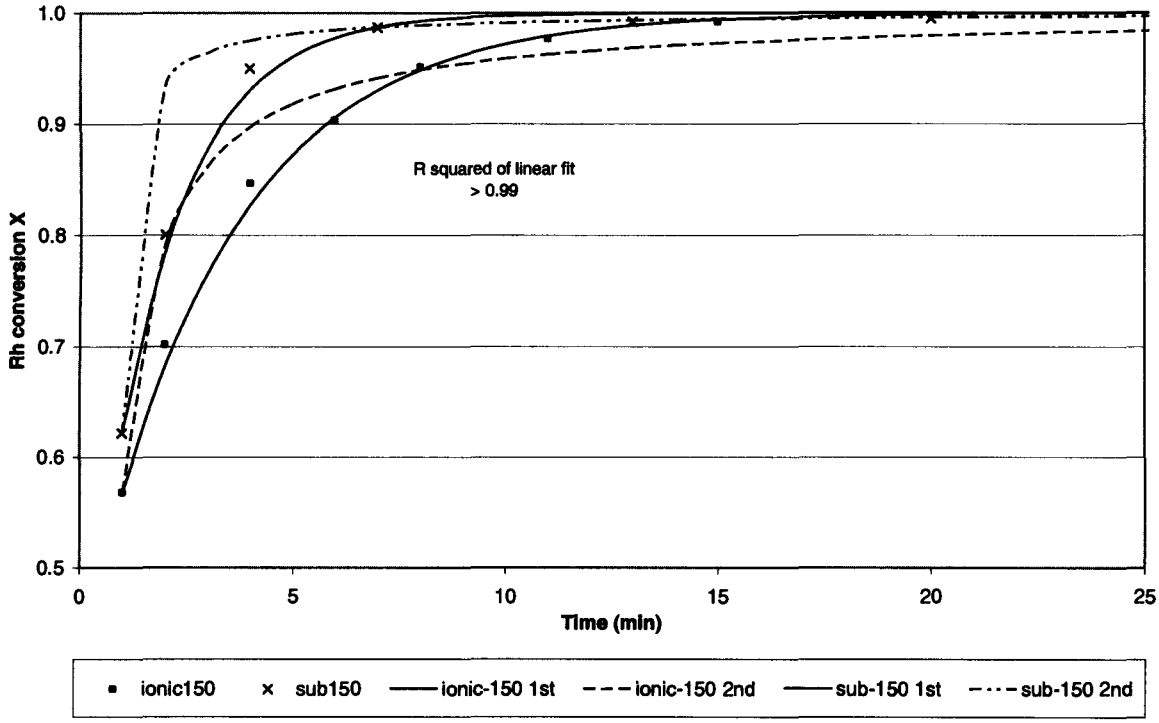

Figure 6.15: Comparison of the pseudo first and second order fits for elevated temperature, showing that first order model fitted the data of the ionic, substitution and co-precipitation systems.

6.6.3 Predicting the overall rate constant using Arrhenius Law

➢ Measuring E_a for initial period

The preliminary testing in Section 6.1.1 shows that the initial precipitation rate is significantly faster for all three reaction systems. Because of thiosulfate degradation and possible CuS passivation, the initial rate constant is modelled to the Arrhenius relationship, assuming first order kinetics, where the initial thiosulfate concentration is known. The activation energy and frequency factor is determined separately over 50 – 95 °C and 95 – 150 °C because of the possible mechanistic change from atmospheric to elevated temperature, which would change the activation energy.

Table 6.16 provides the calculated rate constant from the initial sample point, usually at 1 min.

Table 6.16: Calculation of Initial rate constants assuming first order kinetics (solids basis)

	Ln ([Rh]/[Rh]$_0$) (1)	Time (min) (2)	k $_{measured}$ (3)= (1) / (2)	[$S_2O_3^{2-}$] or [CuS]$_o$ (4)	k_{rxn} (3)/(4)*1000	Ln(k_{rxn})
				(mmol/l)		
1	0.09	1	0.093	49.2	1.9	0.64
2	0.42	1	0.421	49.2	8.5	2.15
3	0.83	1	0.831	49.2	16.9	2.83
4R	0.84	1	0.840	49.2	17.1	2.84
5b	0.00	1	0.002	50.3	0.04	-3.18
6b	0.01	1	0.015	50.3	0.3	-1.23
7b	0.05	1	0.046	48.4	0.9	-0.06
8b	0.97	1	0.971	50.3	19.3	2.96
9	0.001	1	0.001	45.7	0.02	-3.82
9R	0.00	2	0.001	45.7	0.01	-4.51
10	0.30	1	0.304	49.2	6.2	1.82
11	0.41	1	0.409	45.7	9.0	2.19
12	1.15	1	1.146	45.7	25.1	3.22

The rate constant of the reaction is determined by dividing the overall measured constant by the initial thiosulfate concentration or initial CuS concentration, assuming it is constant over this short period. The E_a and k_o are determined by plotting ln(k) against 1/T in Figure 6.16. The atmospheric and overall temperature ranges are compared in Table 6.17.

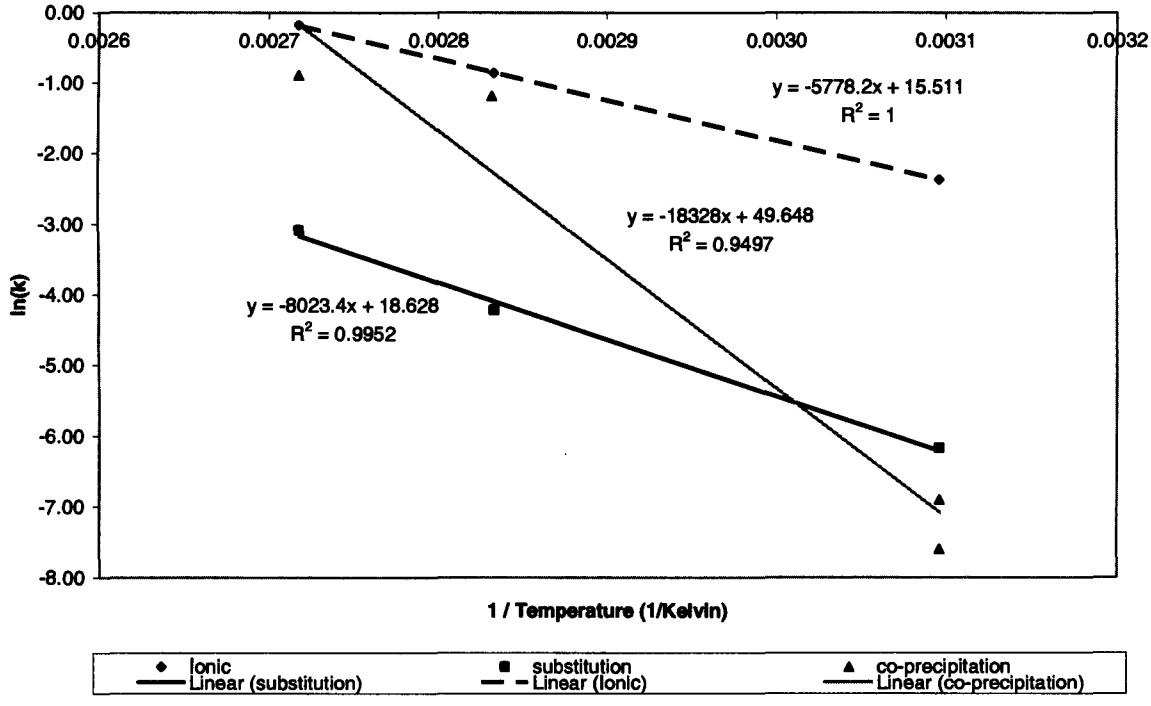

Figure 6.16: Determination of activation energy and frequency factor for the initial period over 50 – 95 °C.

Table 6.17: Determination of Arrhenius rate constants for the initial period over 50 – 95 °C and 95 – 150 °C

	Ionic	Substitution	Co-precipitation	Ionic	Substitution	Co-precipitation
	50 – 95 °C			95 – 150 °C		
-Ea/R	-5778	-8023	-18328	-31	-8662	-2916
$Ln(k_o)$	15.5	18.6	49.6	-0.1	20.4	7.0
p(t{R})	0.004	0.044	0.025	--	--	--
R^2	1.000	0.995	0.950	--	--	--
Activation energy (E_a) [kJ]	48	67	152	0	72	24
Frequency factor measured (k_o^I) [1/(min.gmol)]	5.45E+06	6.67E+01	3.65E+21	9.03E-01	7.20E+01	1.13E+03
Frequency factor for the reaction $k_o = k_o^I/[Na_2S_2O_3]$ [1/(min.gmol)]	9.76E+02	1.35E+03	3.09E+03	5.20E+00	1.46E+03	4.92E+02

Table 6.17 shows that activation energy measured for the substitution system is the same for atmospheric and elevated temperature, indicating that a mechanistic change possibly does not occur i.e. the same reaction path is followed. For the ionic precipitation system, an E_a of zero for 95 to 150 °C is measured because the initial rate constants are similar i.e. the initial rate constant is independent of temperature. As expected, the co-precipitation system, the E_a for 95 to 150 °C is significantly less than that of 50 – 95 °C, somewhere in between the ionic and substitution systems. The straight line fits fir 50 - 95 °C are good to excellent and the Arrhenius equation is used to predict the rate constant of the reaction. Table 6.18 shows that the predicted and measured reaction rate constants are similar for the ionic and substitution system, while the co-precipitation is not modelled accurately.

As expected, the modelled data from 50 – 95 °C does not predict the measured rate at elevated temperatures for the ionic and co-precipitation systems, as mechanistic changes are occurring, as the middle period rate constant is significantly smaller than the initial rate constant. However, the atmospheric temperature model did predict the initial rate constant at 150 °C for the substitution reaction system. This again implies that a mechanistic change does not occur from atmospheric to elevated temperatures in the substitution reaction.

Table 6.18: Predicted overall initial reaction rate constant over the initial period for 50 – 95 °C

Temperature	Predicted rate constant of reaction [min^{-1}]			Measured rate constant of reaction [min^{-1}]		
K	Ionic	Substitution	Co-precipitation	Ionic	Substitution	Co-precipitation
323	1.9	0.04	0.019	1.9	0.04	0.02
353	8.7	0.33	2.1	8.5	0.29	6.2
368	16.9	0.87	19.1	16.9	0.94	5.2
423	130	14.3	12360	17.1	19.3	25.1

➢ **Measuring E_a for the middle period at atmospheric temperatures**

Table 6.19 provides the activation energy and apparent frequency factor for the middle period modelled by pseudo first order kinetics over 50 – 95 °C and 95 and 150 °C. Due to the initial thiosulfate degradation the thiosulfate concentration is not known (or the CuS surface area) and the actual frequency factor cannot be calculated. Table 6.20 shows that the measured and predicted rate constants are similar. Data is calculated in Appendix B.6.4.

Table 6.19: Determination of Arrhenius rate constants for precipitation over the middle period for 50 – 95 °C and 95 – 150 °C

	Ionic	Substitution	Co-precipitation	Ionic	Substitution	Co-precipitation
	50 – 95 °C			95 – 150 °C		
-Ea/R	-5155	-1677	-4327	-17168	-15836	-12715
$Ln(k_o)$	7	-2	6	39	37	29
p(t{R})	0.063	0.030	0.111	-	-	-
R^2	0.99	1.00	0.97	-	-	-
Activation energy (E_a) [kJ]	43	14	36	143	132	106
Frequency factor measured (k_o^I) [1/(min.gmol)]	1.70E+03	2.02E-01	3.79E+02	9.85E+16	1.01E+16	2.65E+12

Table 6.20: Predicted and measured overall rate constant over the middle period for 50 – 95 °C

Temperature	Predicted rate constant of reaction [min^{-1}]			Measured rate constant of reaction [min^{-1}]		
K	Ionic	Substitution	Co-precipitation	Ionic	Substitution	Co-precipitation
323	0.0002	0.0011	0.0006	0.0002	0.0011	0.0006
353	0.0008	0.0018	0.0018	0.0007	0.0018	0.0021
368	0.0014	0.0021	0.0030	0.0015	0.0021	0.0027

The modelled data from 50 – 95 °C does not predict the measured rate at elevated temperatures. This supports the fact that a mechanistic change occurs between atmospheric and elevated temperatures.

6.6.4 Predicting the overall Cu rate constant using Arrhenius Law

The same approach taken for modelling Rh is taken for Cu. First order rate constants for the initial period are calculated in Table 6.21. The constants of the straight line fits for the pseudo middle period are summarised in the Table 6.22. This shows that modelling the middle period to pseudo first order kinetics shifted the line to the origin. Cu precipitation also has an initial large rate constant, which rapidly decreases during the initial period.

Temperature has a small effect on initial precipitation rate between 80 and 95 °C. The initial precipitation rate almost doubles from 95 to 150 °C. This data is not modelled very well by the Arrhenius relationship. The change in the E_a from atmospheric temperature to elevated

temperature indicates that mechanistic changes are probably occurring as well. Detailed calculations are attached in Appendix B.6.4.

Table 6.21: Calculation of the initial rate constants of Cu precipitation (solids basis)

	Ln ([Rh]/[Rh]$_0$) (1)	Time (min) (2)	k meas. (3)= (1) / (2)	[$S_2O_3^{2-}$] or [CuS]$_o$ (4)	k_{rxn} (3)/(4)*1000	Ln(k_{rxn})
				(mmol/l)		
9	0.000	1	0.000	45.7	0.0	-
9R	0.000	2	0.000	45.7	0.0	-
10	0.16	1	0.159	49.2	3.2	1.17
11	0.15	1	0.154	45.7	3.4	1.22
12	0.26	1	0.262	45.7	5.7	1.75

Table 6.22: Cu co-precipitation pseudo first order kinetics of the middle period (solids basis)

Test no. #	Tempura-ture °C	Data range Min	Co-precipitation			
			Slope K	y-intercept ln(ko)	p(t{R})	Coeff .of variance R^2
9R	50	14 – 60	6.04E-04	0.0006	0.05	0.60
10	80	1 – 120	8.11E-04	0.0008	0.04	0.94
11	95	2 – 60	7.38E-04	0.0007	0.00	0.60
12	150	2 – 20	2.95E-04	0.0003	0.01	0.59

Table 6.23: Determination of Arrhenius rate constants for precipitation over the initial period

	Cu Co-precipitation		
	50 – 150 °C	50 – 95 °C	95 – 150 °C
-Ea/R	-7854	-16302	-1503
Ln(k_o)	18.5	43.2	2.2
p(t{R})	0.197	0.195	-
R^2	0.645	0.909	-
Activation energy (E_a) [kJ]	65	136	12
Frequency factor measured (k_o') [1/(min.gmol)]	1.04E+08	1.36E+02	1.25E+01

Table 6.24: Predicted and measured overall initial rate constant for 95 – 150 °C

Temperature	Co-precipitation overall rate constant [min^{-1}]		
K	Predicted (50 -150 °C)	Predicted (95 -150 °C)	Measured
323	0.003	0.09	0.001
353	0.023	0.13	0.16
368	0.056	0.15	0.15
423	0.90	0.26	0.26

6.6.5 Kinetic model development

The models are developed using the initial rate constants measured in section 6.6.3 for the initial period. In some cases this is slightly adjusted to fit the first few data points better (not just the initial point). This shifts the model of the middle period down if the initial rate is decreased. The delay period, t_d, defining the start of the pseudo fist order middle period, is also adjusted slightly to shift the pseudo model into to the data, essentially allowing the modelling of the initial and middle period simultaneously. The adequacy of the modelling is determined visually.

The models illustrate the initial and middle rate change, and the requirement for a pseudo modelling approach is summarised in Figure 6.17 and 6.18. The calculated data is presented in Appendix B.6. The pseudo first order modelling of the middle period provides an excellent fit of the data at 150 °C. Ideally, more samples are required over the initial period to improve the model. At 80 - 95 °C, the similar modelling exercise only approximates the data. The pseudo first order middle period over-predicts the precipitation extent after 120 min towards the final period, where a slow approach to completion occurs.

At atmospheric temperatures, the empirical logarithmic model fits the data better over all three precipitation periods by predicting fast, initial precipitation and a slow approach to completion (Figure 6.19). This empirical logarithmic model over-predicts Rh precipitation extent at 150 °C towards completion.

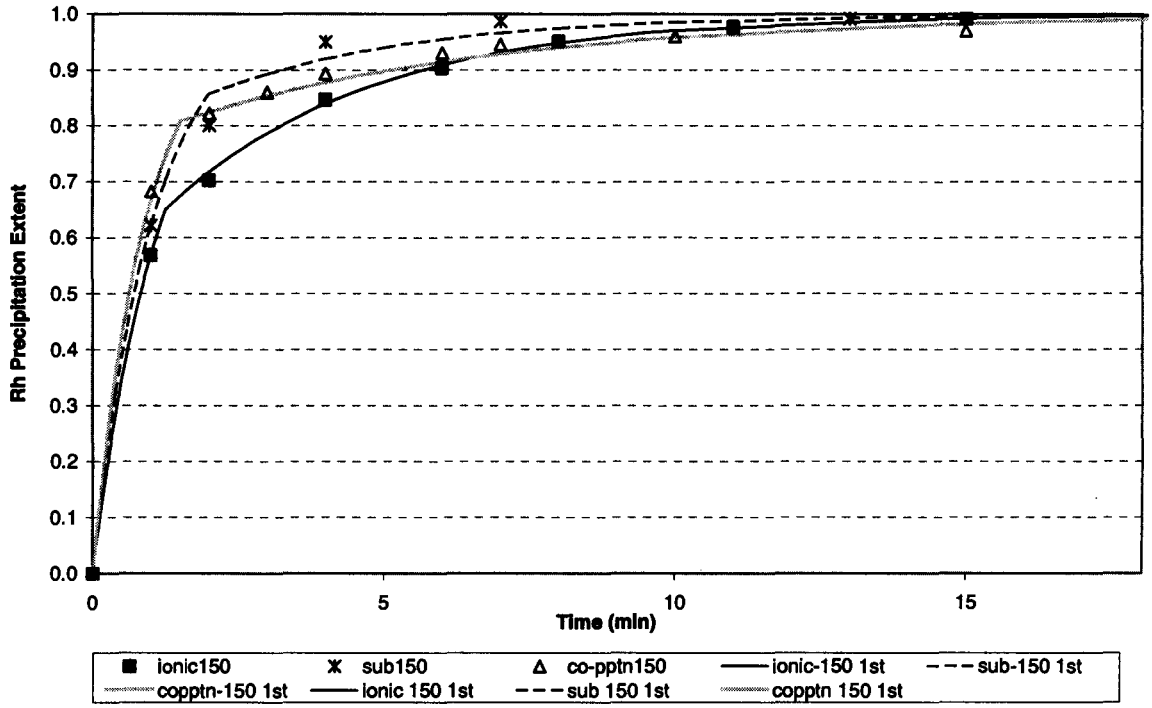

Figure 6.17: Modelling the precipitation profile for the initial and middle period using pseudo first order kinetics at 150 °C, providing an excellent fit of the measured data.

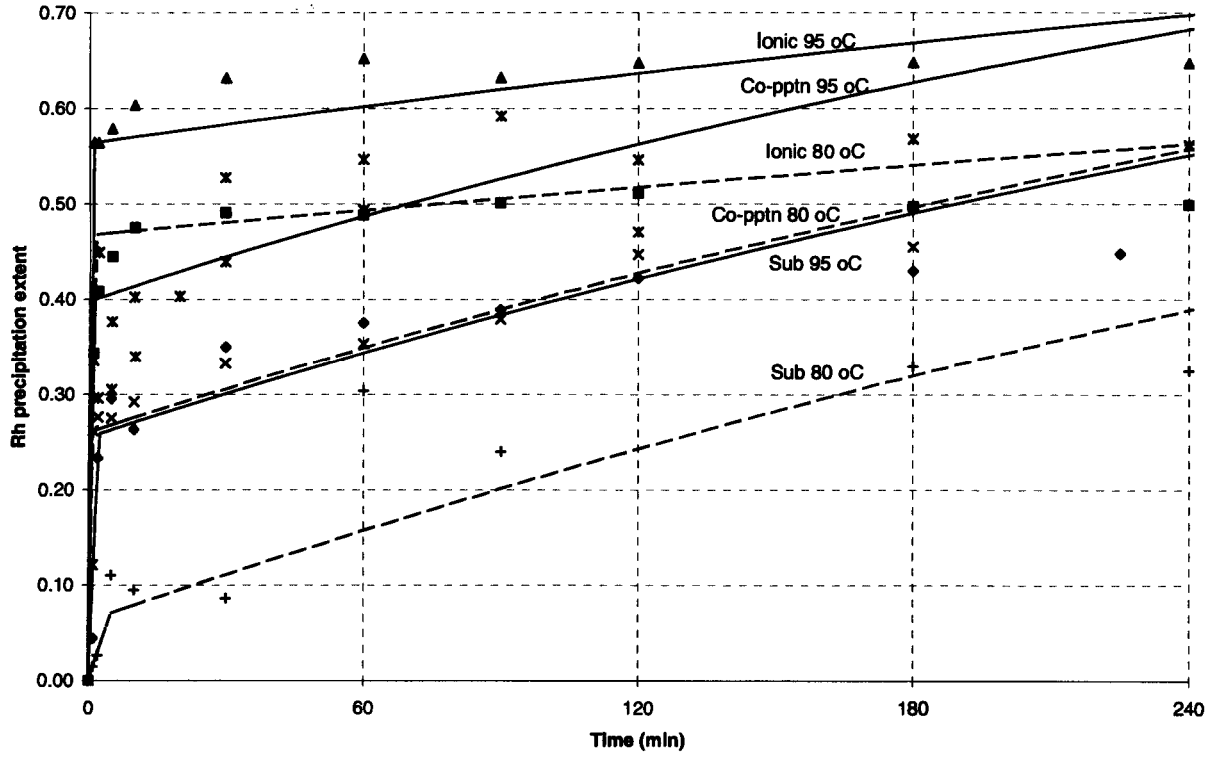

Figure 6.18: Modelling the precipitation profile for the initial and middle period using pseudo first order kinetics over 80 – 95 °C; the model does not predict the slow approach to completion after 120 min.

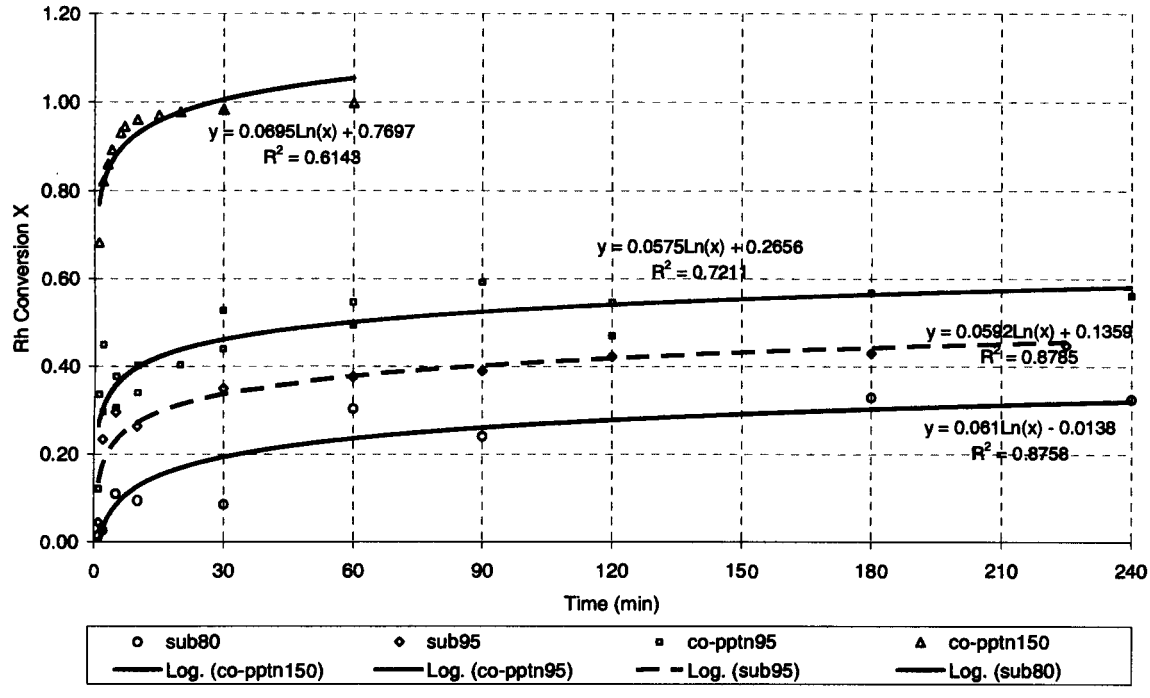

Figure 6.19a: Modelling the whole co-precipitation profile with an empirical logarithmic fit.

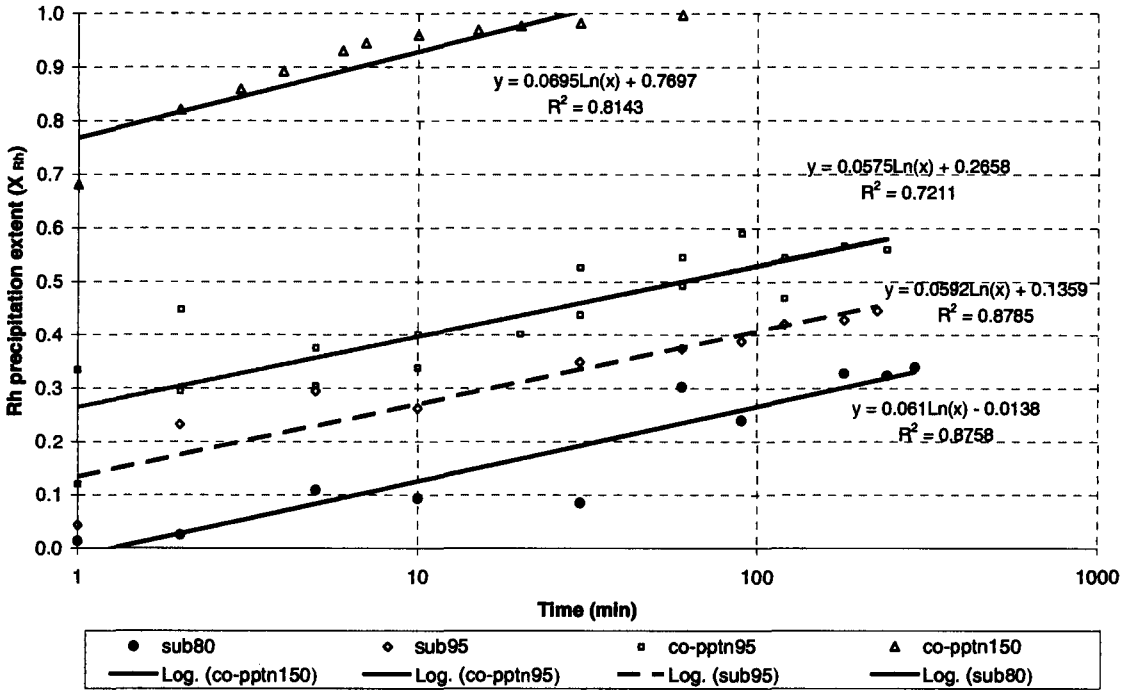

Figure 6.19b: Modelling the whole co-precipitation profile with an empirical logarithmic fit.

A table of the logarithmic constants for all the profiles is provided in Appendix B.6.5.

6.6.6 Prediction of the reaction rates from the models

The calculated Rh precipitation rates are illustrated in Figure 6.20a-c. The data is attached in Appendix B.5.

The Rh precipitation rate of the ionic and substitution reaction systems is fairly independent of temperature over the middle period. The rate of the co-precipitation system over the middle period increases with increasing temperature, but this dependence decreases with precipitation extent (or time). The implication of this on the mechanistic changes or changes in the rate-controlling step is discussed in the sections to follow. The comparison on a time basis is actually performed at different Rh concentrations or precipitation extents.

Figures in Appendix B.5 show the same comparisons as Fig. 6.20 on a concentration basis. The linear portions of the graphs indicate areas of (pseudo) first order kinetics, which highlights the change in order of reaction from one to zero due to passivation. Note that the rate is calculated from the empirical logarithmic fit for atmospheric temperatures and using the pseudo first order model for elevated temperature.

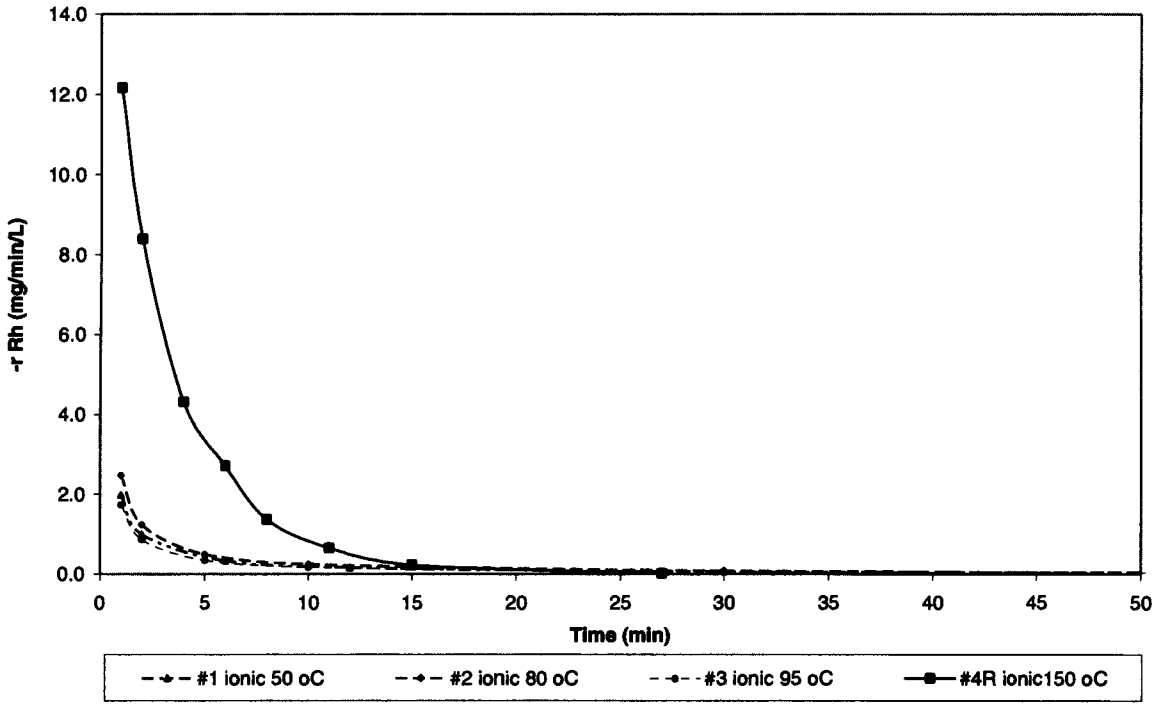

Figure 6.20a: Comparison of calculated Rh precipitation rates for ionic reaction system Rh over the middle period over 50 -150 °C, showing that the rate is fairly independent of temperature at atmospheric temperatures and increases significantly at 150 °C; rates tend towards zero precipitation prior to completion, showing passivation of the elemental sulfur occurring at atmospheric temperatures.

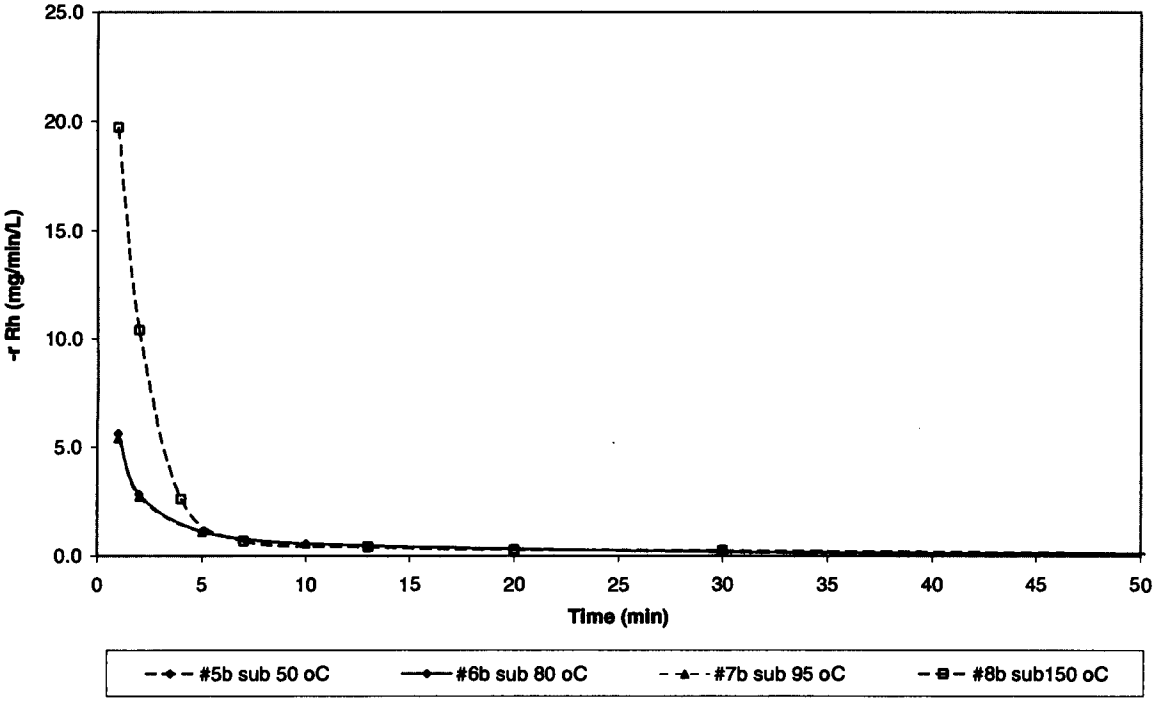

Figure 6.20b: Comparison of calculated Rh precipitation rates for substitution reaction system Rh over the middle period over 50 -150 °C, showing that the rate is fairly independent of temperature at atmospheric temperatures and increases significantly at 150 °C; rates tend towards zero precipitation prior to completion, showing passivation of the CuS occurring at atmospheric temperatures.

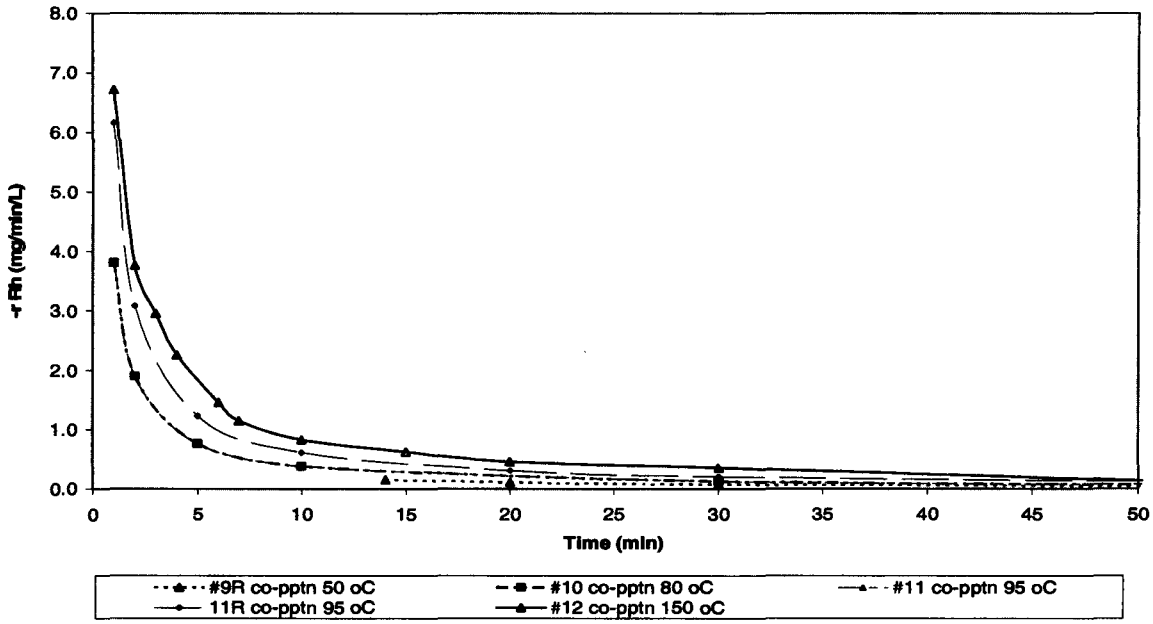

Figure 6.20c: Comparison of calculated Rh precipitation rates for co-precipitation reaction system over 50 -150 °C over the middle period, showing that at the rate increases with increasing temperature; though the rates converged with increasing precipitation.

6.6.7 Passivation limiting the precipitation extent

The pseudo first order models over-predict the precipitation extent over the final period at atmospheric temperature, probably due to surface passivation occurring. This is surprising, as the amount of sulfide or sulfur available in the solid phase approaches 37 times the stoichiometric Rh requirement. Empirical logarithmic models illustrated in fig. 6.19a and 6.19b provide a good data fit over the whole precipitation profile, including the period of passivation possibly occurring over the final period. For the ionic precipitation system, Rh would passivate the elemental sulfur (Section 6.3.2), while for the substitution and co-precipitation systems, Rh precipitation would passivate the CuS.

However, at 150 °C with the same excess sulfide addition, passivation does not limit the Rh precipitation in all three reaction systems. This is probably due to the significantly finer CuS or sulfur precipitate formed having a much greater surface area (Section 6.5.6). The greater Rh precipitation extent over the initial period also would have reduced the chance of passivation, as there is significantly less Rh to precipitate onto the elemental sulphur in ionic precipitation or CuS in substitution and co-precipitation.

The passivation phenomenon must be investigated further to determine whether CuS co-precipitated at low temperatures, having been passivated with Rh precipitation, can precipitate additional Rh at elevated temperatures. This will determine whether elevated temperatures can drive the surface reaction further by forcing more Rh into the CuS microstructure or release more Cu from the mixed sulfides formed on the surface or whether passivation is primarily a function of the surface area of CuS available.

6.6.8 Initial conditions affecting precipitation rate and overall extent

The precipitation kinetics show that the bulk of Rh that does precipitate occurs during the initial period for all three systems. After the initial period, additional Rh precipitation is limited by passivation of Rh on the reactive surface.

In the co-precipitation system, the conditions of the initial period determine the ionic precipitation rate of:

1. nucleation and crystal growth,
2. relative precipitation rates of the competing Cu and Rh precipitation, and
3. properties of the CuS formed, particularly surface area.

A high initial precipitation rate reduces the amount of Rh that has to precipitate through the cationic substitution reactions, thereby reducing the chance of passivation occurring. The surface area of the CuS determines the amount of Rh precipitation possible via the cationic substitution path, thus CuS formed at high temperatures would also have less chance of complete passivation occurring. Hence the initial precipitation conditions have a direct impact on the CuS carrying capacity for Rh.

6.6.9 Mechanistic changes

Mechanistic changes would be expected to occur over the ionic and co-precipitation systems profiles with increasing precipitation extent. Initially Rh would precipitate through homogeneous nucleation, followed by heterogeneous crystal growth, while towards the end of the precipitation extent Rh precipitation would be dominated by the cationic substitution reaction, possibly stopping the Rh precipitation through passivation of the CuS surface. These precipitation processes would certainly go through different precipitation mechanisms and possibly a different order of reactions.

The initial period of ionic and co-precipitation systems over 50 – 150 °C are probably chemical reaction controlled owing to the strong dependence of precipitation rate and extent on temperature. The increasing CuS surface area is the reason for the increased extent and rate increases significantly with increasing temperature of the substitution system.

At 80 – 95 °C, the order of the reaction of the middle period is not certain. For the ionic and co-precipitation systems, a number of precipitating paths would be occurring simultaneously and cationic substitution would also be hindered by CuS passivation, thus complicating the model and the order of reaction. The measured data quality also would have contributed to this. At 50 – 95 °C, the near independence of precipitation rate and temperature over the middle period indicates that the rate-controlling step possibly may change from chemical reaction to the diffusion of the Rh^{3+} across the boundary layer to the surface, which is less dependent on temperature. The mechanistic change is supported by the significant decrease in activation energy measured from the initial to the middle period, also indicating a change from chemical reaction to diffusion controlled. This is probably caused by the passivation of the surface area, forcing the rate-controlling step to switch from chemical reaction to mass transfer.

At 150 °C, where passivation does not occur, all three systems are modelled extremely accurately with pseudo first order kinetics over the middle period and final period with R^2 between 0.95 – 0.999. At elevated temperatures, diffusion of Rh^{3+} across the boundary layer to the metal sulfide surface could become the rate-controlling step when the chemical reaction at the surface is very fast. The fact that this holds true for ionic and co-precipitation systems, as well as substitution reaction systems, supports the argument that the systems are being controlled by the same rate-controlling step, namely, the mass transfer of Rh^{3+} to the surface, **which is a first order process**. This is supported by a study of Ni and Cu co-precipitation with sulfide, where the turbulent pipe reactor increases precipitation kinetics substantially above the agitated, batch reactor at the same operating temperature of 150 °C (Roy, 1961). Alternatively, the rate-controlling step from the initial to the middle period could have remained the chemical reaction at the surface, which also would have been pseudo first

order owing to the large surface area for Rh precipitation effectively remaining constant, maintaining a constant over reaction constant.

Specific mass transfer test work is thus required to verify mass transfer limitations over the crystal growth and cationic substitution reaction paths and quantify the increased precipitation extent possible with increasing turbulence. This should be performed independently on the initial and middle period, as well as the initial period over atmospheric and elevated temperatures at conditions where passivation will not occur.

6.6.10 Summary of kinetic modelling

Kinetic modelling bas been performed primarily to understand the mechanism of individual reaction systems, particularly the co-precipitation system, rather than to develop an accurate, predictive model.

The kinetics suggests a mechanistic change occurs on each individual profile over the three periods. A mechanistic change would be expected as precipitation changes from ionic nucleation to heterogeneous crystal growth or cation exchange reactions. In addition, the drastic decrease in Rh precipitation rate from the initial period to the middle period is mainly caused by the overall pseudo rate constant decreasing rapidly with the consumption of thiosulfate in the ionic and co-precipitation systems and passivation of the CuS particles in the substitution system. Thus, pseudo kinetic conditions created by adding a large excess of sulfide described in Section 3.4 do not hold.

The initial period requires additional data to improve the kinetic modelling, though the reaction rate constants are predicted from the initial rates. The middle period is partially modelled by pseudo first order kinetics for all three reaction systems at atmospheric temperatures, but over-predicts the removal towards the end, where passivation could be occurring. Contrary to this, almost perfect pseudo first order kinetics is measured at 150 °C, where passivation is not a concern due to the increased surface area of the finer CuS and the increased precipitation extent over the initial period. At atmospheric temperatures, the empirical logarithmic model provides an improved fit over the whole precipitation profile, predicting the fast initial precipitation and passivation. The overall pseudo rate constants are modelled to Arrhenius relationship, determining the activation energies and frequency factors for each reaction system. Predicted rate constants in most cases are reasonable.

At elevated temperatures, the rate-controlling step is believed to be the diffusion of Rh^{3+} across the boundary layer to the metal sulfide surface when the chemical reaction at the surface is very fast. The fact that this holds true for ionic and co-precipitation systems, as well as substitution reaction systems, supports the argument that the systems are controlled by the same mass transfer rate-controlling step. This is supported by a study of Ni and Cu co-precipitation with sulfide, where the turbulent pipe reactor increases precipitation kinetics substantially above the agitated, batch reactor at the same operating temperature of 150 °C (Roy, 1961).

Specific mass transfer test work is required to verify mass transfer limitations over the crystal growth and cationic substitution reaction paths and quantify the increased precipitation extent possible with increasing turbulence, as alternative explanations supporting chemical reaction controlled remain feasible. This should be extended to atmospheric temperatures, looking at the initial and middle periods independently, preferably at conditions where passivation will not take place.

Chapter Seven

7 COMPARATIVE KINETICS

The study of the independent precipitation systems in Chapter 6 shows that Rh co-precipitation with CuS can occur through ionic precipitation and cationic substitution reaction paths. Kinetic tests has been designed to compare the individual reaction paths of the independent, isolated systems in order to infer the dominant reaction path in the co-precipitation system. Most importantly, the amount of sulfide addition in the form of thiosulfate or CuS was constant and in large excess above the Rh requirement. However, due to thiosulfate degradation into S, H_2S or SO_3, this sulfide was lost from the liquid phase to the vapour space or precipitated as elemental sulfur. Thus, the test conditions are first evaluated to ensure constant conditions have been maintained.

The comparison of the precipitation kinetics of the various reaction systems are compared visually, taking the error of analytical analysis into account. The comparison is repeated over the initial, middle and final periods using the fundamental first order models determined in the individual kinetic studies on the precipitation data summarised in Table 6.1 and Table 6.25.

This section presents the validation of the comparison, description of the comparative statistical procedure and results, followed by the discussion of the relative kinetics at 50, 80, 95 and 150 °C using the solid precipitation basis. The comparison is repeated for the solution basis.

7.1 Evaluation of validity of comparison of reaction systems

Table 7.1 compares the amount of Cu precipitated in the ionic preparation reactions in 5a-8a (or mass CuS measured after the 'b' part) against Cu co-precipitated in 9-12 on a solid and solution basis.

Table 7.1: Cu precipitation comparison on terminal samples

Substitution	Cu precipitated		Co-precipitation
Test #	mmol/l	mmol/l	Test #
	Solid Basis		
5b	19	26	9R
6b	32	47	10
7b	34	47	11R
8b	43	51	12
	Solution Basis		
5b	44	43	9R
6b	21	66	10
7b	51	49	11R
8b	47	43	12

The comparison between Cu precipitation in substitution and co-precipitation are similar, particularly taking the large excess into account. Except for #6 and #10 at 80 °C, the solution chemistry shows similar amounts of CuS formed. The solid analyses indicated that #6 and #10 were indeed similar. In addition, the overall Rh precipitation extent in Table 7.2 is similar

for substitution and co-precipitation at specific temperatures, thus Rh precipitation does not affect the Cu precipitation results.

Table 7.2: Rh precipitation comparison on terminal samples

Test #	Rh precipitated Solid basis		Test #
	mmol/l	mmol/l	
5b	0.1	0.1	9R
6b	0.3	0.4	10
7b	0.4	0.4	11R
8b	1.0	0.9	12
	Solution basis		
5b	0.2	0.0	9R
6b	0.3	0.3	10
7b	0.4	0.4	11R
8b	0.9	0.9	12

In addition, at 150 °C, complete Rh precipitation occurs on all three systems after 60 min. This indicates that sufficient excess sulfide has been added to all the tests, making the comparative kinetic study valid from a number of perspectives:

1. Sufficient thiosulfate is added to overcome degradation in ionic precipitation.

2. Sufficient thiosulfate is added to precipitate sufficient CuS to not be affected by passivation of the CuS surface with precipitated Rh.

3. Thiosulfate degradation mainly forms elemental sulfur, which can also precipitate Rh, thus most of the sulfur is not lost from the system.

Thus, sufficient excess sulfide has been added to the comparative kinetic tests, making the various reaction paths comparable at any particular temperature.

The comparative study has been partially compromised by thiosulfate degradation due to Rh precipitation onto elemental sulfur (Barkan and Greiver, 1977a) being slower than the ionic precipitation with aqueous sulfide in this study. However, ionic precipitation remains the fastest precipitation system over 50 – 95 °C; thus, it has not compromised the relative comparison of the various paths. If thiosulfate degradation had not occurred, then even faster ionic precipitation would have been measured, probably similar to the initial precipitation rate.

7.2 Discussion

7.2.1 Comparative kinetics of reaction paths at 50 °C

Comparison of the precipitation extent against time for the three reaction systems at 50 °C is illustrated in Figure 7.1a. Similarly, the comparison is made using the calculated $-r_{Rh}$ against C_{Rh} and this illustration is attached in Figure 7.1b. This provides the reaction rate comparison at the same Rh concentration basis.

The low temperature reduces the Cu and Rh precipitation rate significantly. Ionic Rh precipitation shows the fastest precipitation kinetics and highest precipitation extent. The substitution reaction path had almost no Rh precipitation over the first 20 min, which increases to 17% overall after 240 min. Similarly, no Rh co-precipitates in the first 10 min,

with 5% after 240 min. The differences between the precipitation profiles are significant for both the initial and final period. It is expected that co-precipitation would be faster than substitution due to the ionic precipitation component, but this does not occur using 9R results (solids basis). The profile of #9 using the solids basis provides the expected result of co-precipitation being faster than substitution, but it is faster than the ionic precipitation as well. Additional test work is required to confirm comparative results at 50 °C.

As discussed in Section 6.5, the relative precipitation kinetics of Cu and Rh indicates that Rh precipitation at 50 °C would predominantly occur through cationic substitution reaction paths (#9 and #9R), but passivation of the surface would limit the overall precipitation extent.

This slow co-precipitation can possibly be explained through thiosulfate complexing (Van Hille *et al.*, 2005) with Cu^{2+} in solution prior to precipitation at this low temperature, limiting both Cu and Rh ionic precipitation. However, this is unlikely at this systems pH. In addition, some sulfide precipitation potential is lost to gas phase through H_2S and SO_2 / SO_3 formation and is lost from the system during sampling. This is supported by acid consumption over the first 10 min.

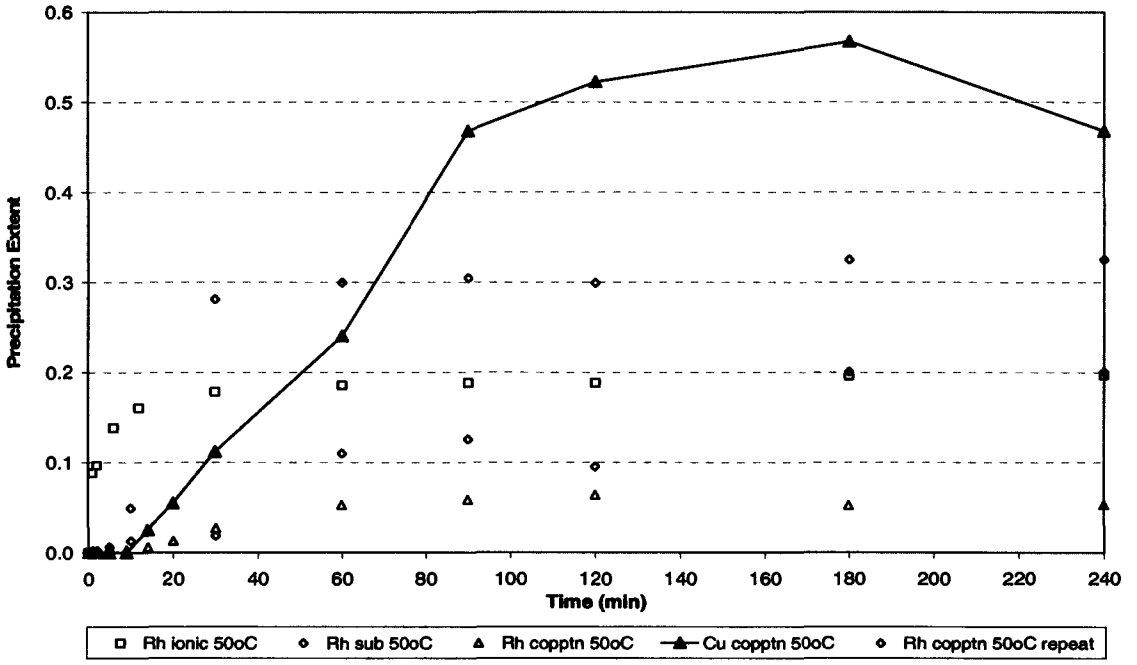

Figure 7.1.a: Rh precipitation kinetic comparison for ionic, substitution and co-precipitation reaction paths at 50 °C with 37 times excess thiosulfate addition than Rh requirement; ionic precipitation is faster than cationic substitution, while co-precipitation kinetics were uncertain; Rh and Cu co-precipitation both had 9 min induction period; Cu precipitation.

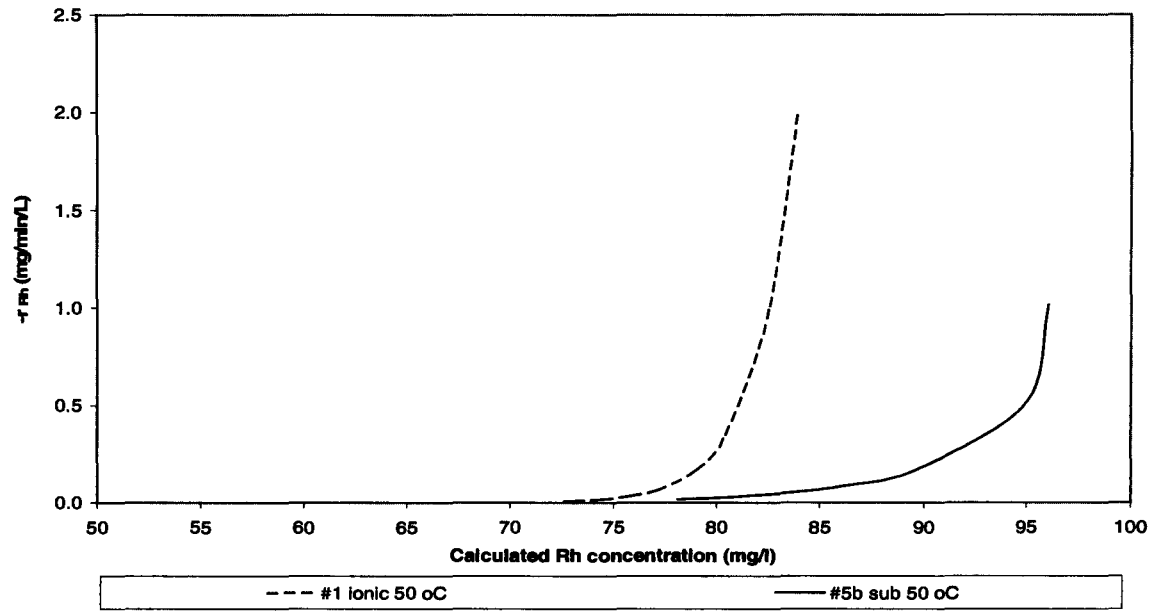

Figure 7.1b: Comparative Rh precipitation kinetics ionic and substitution systems, calculated from an empirical logarithmic fit, against Rh precipitation extent, at 50 °C, showing faster ionic precipitation rate at a particular precipitation extent; rate approached zero at approximately 75 mg/l Rh.

If #9 results are shown to be valid, the relative kinetics of the final period can be explained by the Rh precipitating predominantly through the ionic precipitation reaction path, as the overall precipitation extents are similar. However, the overall precipitation extent of #9R is similar to the substitution reaction system, indicating that in this scenario the predominant reaction path could be the substitution reaction. If both these results are valid, then this finding provides a possible technique to increase Rh precipitation selectivity at lower temperatures by controlling the reaction mechanism. Purposefully performing initial precipitation at low temperatures and increasing the temperature with increasing reaction time could possibly improve overall kinetics.

7.2.2 Comparative kinetics of reaction paths at 80 °C

Comparison of the precipitation extent against time for the three reaction systems at 80 °C is illustrated in Figure 7.2a. Similarly, the comparison is made using the calculated $-r_{Rh}$ against C_{Rh} and this illustration is attached in Figure 7.2b. Ionic precipitation system provides the fastest relative kinetics.

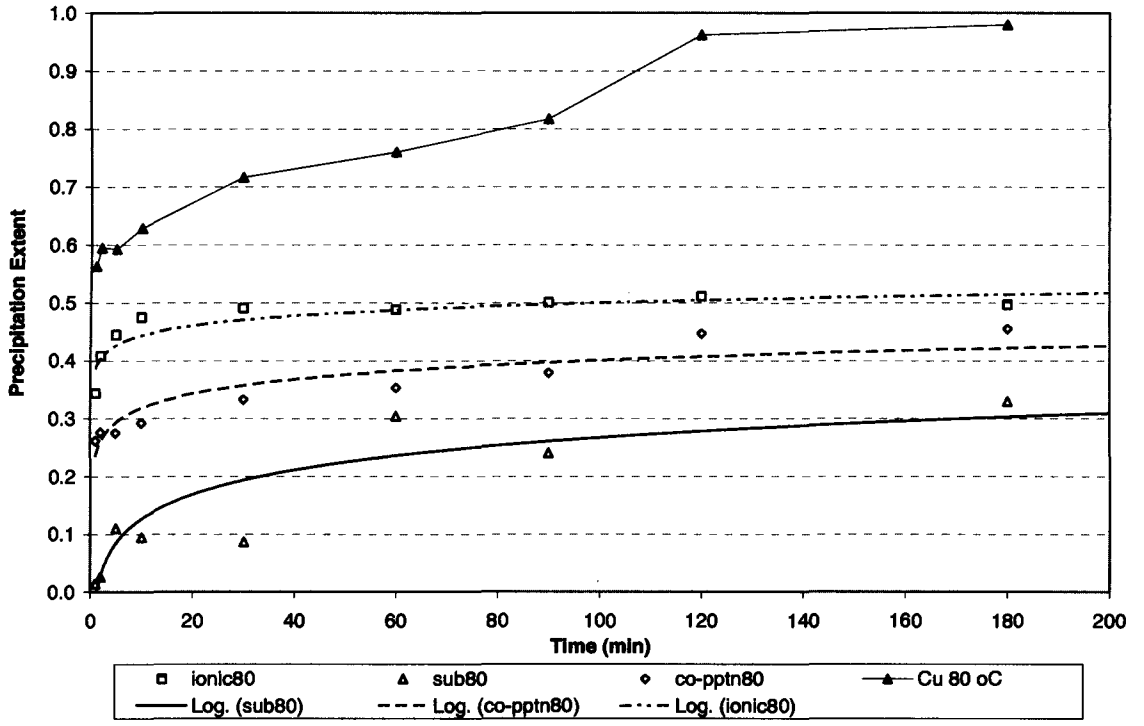

Figure 7.2a: Rh precipitation kinetic comparison for ionic, substitution and co-precipitation reaction paths at 80 °C, with 37 times excess thiosulfate addition than Rh requirement; Rh ionic precipitation rate and extent was greatest, followed by co-precipitation and then substitution reactions; after 120 min, ionic and co-precipitation rate and extent are similar; Rh precipitation is modelled with empirical logarithmic fit.

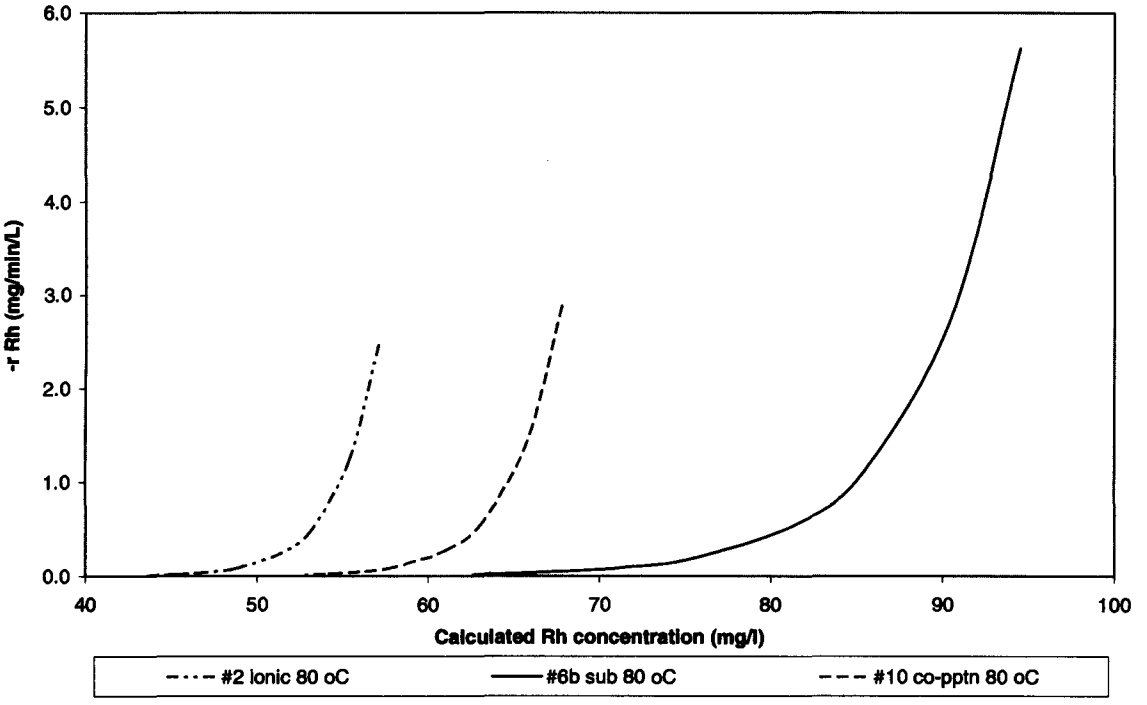

Figure 7.2b: Comparative Rh precipitation kinetics ionic, substitution and co-precipitation systems, calculated from an empirical logarithmic fit, against Rh concentration, at 95 °C, showing faster ionic precipitation rate at a particular precipitation extent; Rh precipitation stopped at 50, ~40 and 34 mg/l for substitution, co-precipitation and ionic systems, respectively.

The precipitation profiles show that over the initial 5 min, substitution is the slowest at ~10% Rh precipitation, while ~28% occurs in co-precipitation and 44% occurs through ionic precipitation. This falls within expectations, as some ionic precipitation would increase the co-precipitation rate. After 60 min, substitution and co-precipitation rate and extents are similar at 34% and 36%, respectively. This can be explained by the fact that once ionic Cu^{2+} precipitation is complete, thiosulfate would not be available for ionic Rh precipitation, but would continue precipitating through the cationic substitution.

The relative rate of Cu and Rh precipitation in the co-precipitation indicates that ionic precipitation could occur up to approximately 120 min (Fig 6.7b in Section 6.5.2 and Figure B.5.3 in Appendix B.5).

7.2.3 Comparative kinetics at 95 °C

Comparison of the three reaction paths at 95 °C is illustrated in Figure 7.3a and Figure 7.3b for X_{Rh} against reaction time and $-r_{Rh}$ against C_{Rh}, respectively.

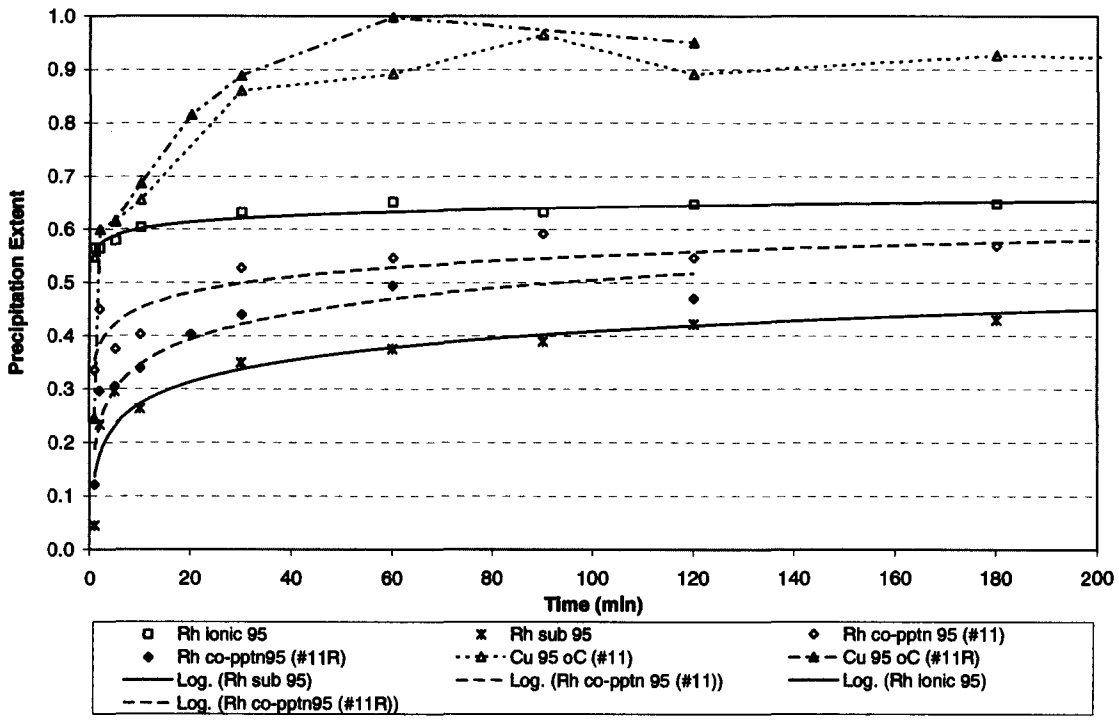

Figure 7.3a: Rh precipitation kinetic comparison for ionic, substitution and co-precipitation reaction paths at 95 °C with 37 times excess thiosulfate addition than Rh requirement. Ionic precipitation rate and extent was greatest over the whole reaction period, followed by co-precipitation and cationic substitution; Rh precipitation is modelled with empirical logarithmic fit.

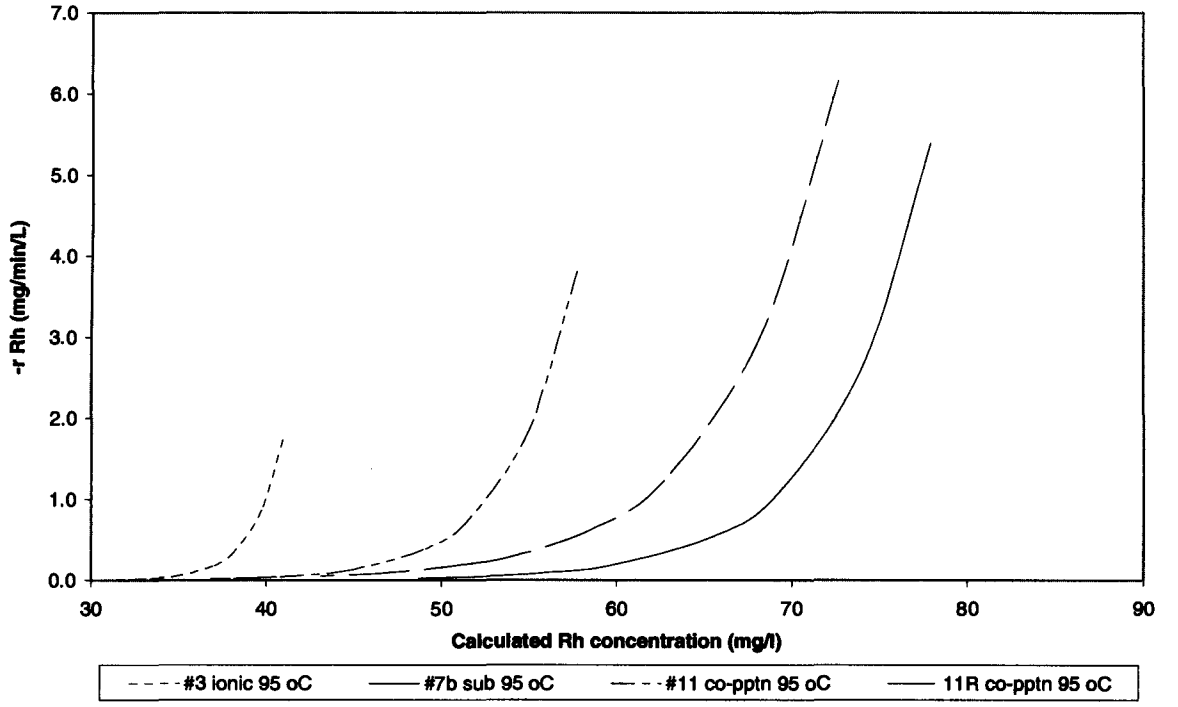

Figure 7.3b: Comparative Rh precipitation kinetics of ionic, substitution and co-precipitation systems, calculated from an empirical logarithmic fit, against Rh concentration, at 95 °C, showing faster ionic precipitation rate at a particular precipitation extent; Rh precipitation stopped at 50, ~40 and 34 mg/l for substitution, co-precipitation and ionic systems, respectively.

The ionic precipitation system remains the fastest. Rh co-precipitation is faster than substitution reaction over the whole period, probably due to ionic precipitation occurring. The relative rate of Cu and Rh precipitation in the co-precipitation (Fig 7.3b) indicates that ionic precipitation could occur up to approximately 30 – 60 min. Thus, a significant amount of Rh precipitation would have to occur through the substitution reaction path.

Thus, from the relative kinetics at atmospheric temperature, Rh co-precipitation occurs predominantly through ionic precipitation for the first ~50% precipitation extent, while the remainder would occur through cationic substitution, but passivation limits this amount.

7.2.4 Comparative kinetics at 150 °C

Comparison of the three reaction paths at 150 °C is illustrated in Figure 7.4a which shows that the three reaction systems give similar precipitation kinetics, particularly when taking the relative error on the solution assays into account. The empirical logarithmic fit is not as good as the pseudo first order model, thus the rate of Rh precipitation is calculated from:

$$- r_{Rh} = k_{measured} C_{Rh}$$

where $k_{measured}$ is used to fit the data over the middle period and C_{Rh} is calculated from the pseudo first order model.

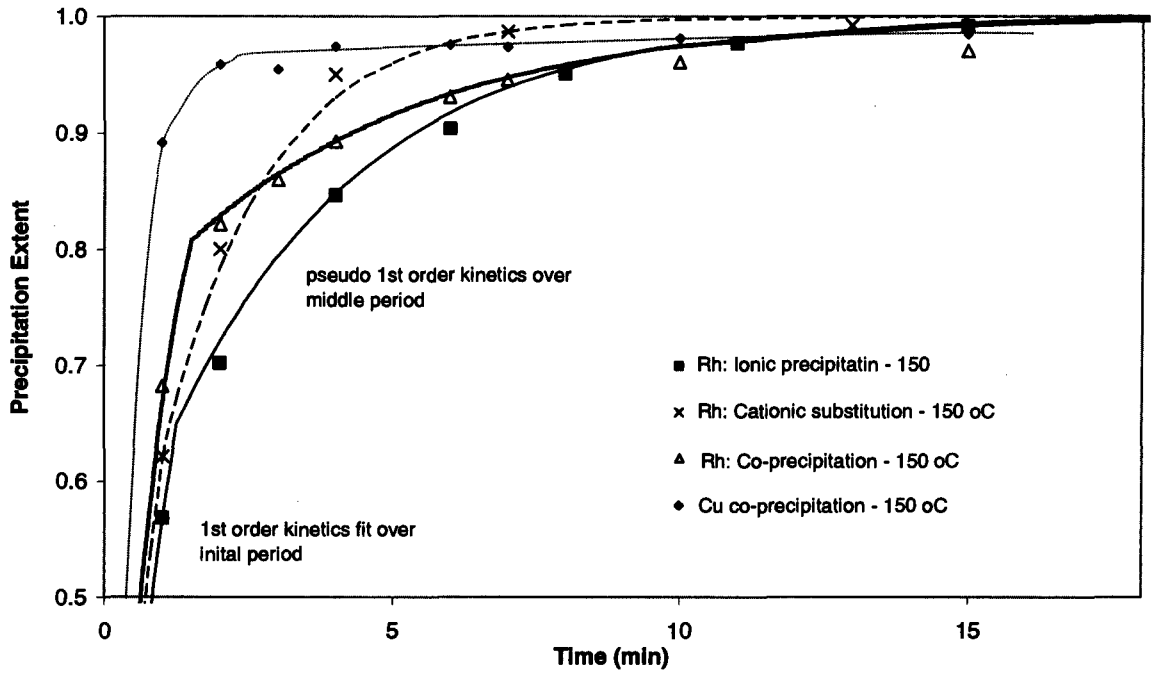

Figure 7.4a: Rh precipitation kinetic comparison for ionic, substitution and co-precipitation reaction paths at 150 °C on solution basis, with 37 times excess thiosulfate addition than Rh requirement; initially, ionic precipitation is the slowest, a complete reversal from trends at atmospheric temperatures; substitution and co-precipitation are similar; Cu precipitation was almost complete after 4 min. Rh precipitation modelled with pseudo first order kinetics.

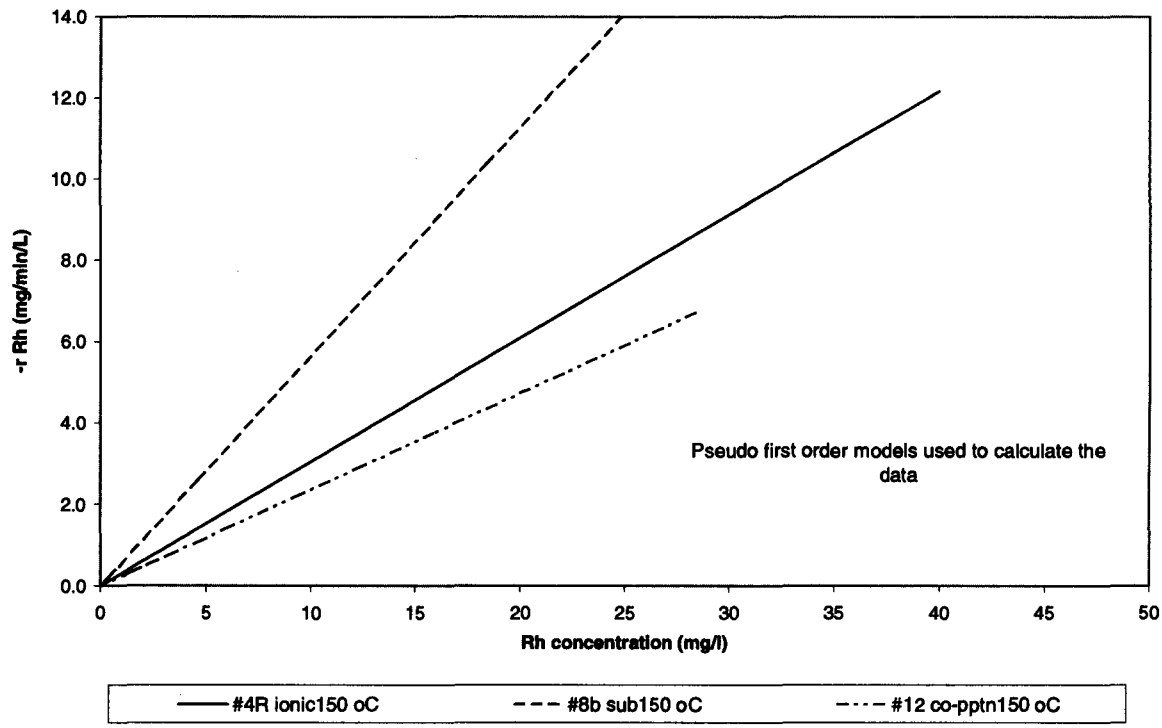

Figure 7.4b: Rh precipitation rate for the ionic, substitution and co-precipitation systems, calculated from pseudo first order kinetic model of the middle period, against Rh precipitation extent, at 150 °C, showing similar precipitation rates ionic and co-precipitation reaction systems, while substitution was surprisingly fastest; the linear line shows first order kinetics over this middle period.

The comparison of reaction rates of the three systems on a Rh concentration basis (Fig 7.4b) shows that the substitution reaction rate is the fastest, while the ionic and co-precipitation systems are similar. This is different to the findings at atmospheric temperatures. These switches can be explained through a number of possible reasons:

1. At this high temperature with very fast Rh and Cu precipitation kinetics, there is insufficient seed for ionic precipitation and Rh precipitation is delayed by the induction period prior to the auto-catalytic effect, which would occur immediately after some Cu precipitation during co-precipitation,

2. The rate-controlling step could switch to the release of sulfide from the thiosulfate, making cationic substitution relatively faster, as the CuS is immediately available for precipitation,

3. Thiosulfate degradation to elemental S could occur faster than at atmospheric temperature, thus reducing the aqueous sulfide activity even faster, thereby reducing ionic precipitation rate; Rh would continue to precipitate onto the elemental S at a slower rate,

4. The presence of Cu^{2+} in co-precipitation forces CuS precipitation prior to thiosulfate degradation, effectively reducing this degradation, explaining why co-precipitation is faster than ionic precipitation.

This indicates that the comparative conditions of the various systems at 150 °C are possibly not ideal. At best, one could infer that the differences in their relative kinetics are negligible, particularly taking the analytical error into account. This would be expected as the measured rates at a particular Rh concentration are equal for the ionic and substitution reaction systems, thus the co-precipitation system would also be expected to be similar.

The relative rate of Cu and Rh precipitation in the co-precipitation indicates that ionic precipitation could occur up to approximately 4 – 5 min. Approximately 90% of the Rh has already precipitated after 5 min, thus ionic precipitation probably dominates. However, simultaneous Rh precipitation through the substitution reaction could have occurred, though it could be quantified with the data in this study. The final 10% of Rh precipitation would occur through the cationic substitution reaction. Additional sampling within the first minute could reduce this ionic precipitation estimate and mineralogy determining the Rh distribution in the CuS would quantify the amount of ionic precipitation. Studying the relative Rh distribution in CuS could possibly quantify relative amounts (Section 6.5.6). Mineralogy would also give a visual picture of the CuS carrying capacity for substituted and co-precipitated material.

7.2.5 Comparative kinetics using solution basis

The analysis has been repeated on the solution basis. The results are presented in Appendix B.7. Generally, the comparative study produces similar results. However, at 80 and 95 °C, the substitution and co-precipitation rates are similar towards the end of the precipitation at each temperature. It is likely that post-precipitation causes the similar precipitation extents. The comparison of all the final precipitation extents on measured solution concentrations does not yield any changes to the relative kinetics.

7.3 Summary of comparative kinetics of individual systems

1. At atmospheric temperatures, on the time and concentration basis, the substitution reaction is significantly slower than ionic precipitation in the absence of aqueous Cu^{2+} over 50 – 95 °C. As expected, the co-precipitation rate is faster than the substitution rate due to the contribution of the faster ionic precipitation path.

2. At the elevated temperature of 150 °C, on the concentration basis and time basis, the rate of Rh precipitation for ionic and co-precipitation systems are similar, while substitution is the fastest. At best, one could infer that the small differences in the relative kinetics are negligible, particularly taking the overall analytical error into account. It is not possible to infer a dominant reaction path while aqueous sulfide is available without Rh distribution comparisons in the CuS.

Chapter Eight

8 RH CO-PRECIPITATION MECHANISM

8.1 Mechanism

The analysis of the available literature, thermodynamic modelling and comparative kinetic studies of the specific reactions systems, particularly the relative precipitation kinetics of Cu and Rh, suggests the following general, but simplified Rh and Cu sulphide co-precipitation mechanism:

$$Cu^{2+} + S_2O_3^{2-} + H_2O \rightarrow CuS + H_2SO_4 \quad (1)$$

$$2Rh^{3+} + 3\,S_2O_3^{2-} + 3H_2O \rightarrow Rh_2S_3 + 3H_2SO_4 \quad (2)$$

$$Cu^{2+} + (CuS)_x.nH_2S \rightarrow (CuS)_{(x+1)}.(n\text{-}1)H_2S + 2H^+ \quad (3)$$

$$Rh^{3+} + CuS.nH_2S \rightarrow CuRhS_2.(n\text{-}1)H_2S + 2H^+ + e^- \quad (4.1)$$

$$2Rh^{3+} + CuS.nH_2S \rightarrow CuRh_2S_4.(n\text{-}3)H_2S + 6H^+ \quad (4.2)$$

$$2Rh^{3+} + 3\,CuS \rightarrow Rh_2S_3 + 3\,Cu^{2+} \quad (5)$$

Initially, homogeneous reactions occurs prior to perceptible nucleation (1 and 2). Initially, homogeneous reactions occurs prior to perceptible nucleation, which is then followed by heterogeneous crystal growth (3) and co-precipitation (4), (auto-)catalysed by the presence of the precipitated metal sulfides. Rh^{3+} and Cu^{2+} compete for the available aqueous sulfide during ionic precipitation (1)(2)(3)(4). Selectivity of the aqueous sulfide is determined by the relative Rh and Cu precipitation rates of the individual paths, which are a function of ΔG, temperature affecting precipitation kinetics (and to a much lesser extent ΔG) and reacting ion activities.

The mechanism of ionic precipitation with $S_2O_3^{2-}$, through the formation of S^{2-}, HS^- and H_2S, which is affected by the solution pH is not covered. A number of side reactions in Table 5.1 are also possible, like formation of alternative Rh compounds and thiosulfate degradation reactions.

At the relative concentrations in this study, the overall Cu^{2+} precipitation rate is significantly faster than Rh^{3+}, consuming the available sulfide and reducing the amount of ionic Rh^{3+} precipitation possible. In the absence of Cu^{2+}, on a comparative basis, the ionic Rh precipitation (2 and 3) is significantly faster than cationic substitution (5). From this it is inferred that the co-precipitation system, during the period where aqueous sulfide and CuS is available, ionic Rh precipitation path (2 and 4) will dominate, until the ratio of aqueous sulfide to CuS is sufficiently decreased and Rh precipitates predominantly through the heterogeneous cationic substitution reaction path (5), either taking Rh precipitation to completion or stopping the precipitation through the passivation of the CuS. It is speculated that the cationic substitution reaction could be an additional reaction path during the period

before perceptible nucleation, where S-containing Cu complexes CuS, associates and amorphous clusters of CuS could be replaced by the Rh^{3+}, compared to ionic co-precipitation forming $CuRhS_2$.

At 80 – 95 °C, at the relative concentrations of this study, Cu precipitation is 2 – 3 times faster than Rh on a relative basis, where the last 55 – 65 % of the Rh will have to precipitate via the cationic substitution reaction path, but passivation limits the overall precipitation extent, even at 37 times excess of the sulfide requirement of Rh. The presence of large amount of Cu^{2+} effectively decreases the rate and extent of Rh co-precipitation, because the substitution reaction path is significantly slower that ionic precipitation and passivation occurs. At 150 °C, Cu precipitation is only 30% faster than Rh, reducing the amount of precipitation via the substitution path to 10 – 20 %, taking the Rh precipitation to completion. Thus, at 150 °C, aqueous Cu^{2+} has negligible impact on the Rh precipitation rate or extent. The bulk of Rh precipitation occurs during the initial period, hence the initial precipitation conditions has a direct impact on the CuS carrying capacity and overall precipitation extent.

It is speculated that the cationic substitution reaction could be an additional reaction path during the period before perceptible nucleation, where S-containing Cu complexes CuS, associates and amorphous clusters of CuS, where the Cu^{2+} would be replaced by the Rh^{3+}, in comparison to ionic co-precipitation forming $CuRhS_2$. This has not been considered in the co-precipitation literature reviewed.

8.2 Mechanistic changes

Mechanistic changes across the co-precipitation systems are expected with increasing precipitation extent (1)(2), progressing from primary nucleation to crystal growth (3) and co-precipitation of the mixed sulfides (4). The rate-determining step probably switches from chemical reaction to mass transfer, particularly at 150 °C. This is supported by the excellent pseudo first order kinetics over the middle period and final period (R^2: 0.999 for ionic and substitution systems; 0.95 for co-precipitation). The fact that model holds true for ionic and co-precipitation systems, as well as substitution reaction systems (5), supports the argument that the systems are being controlled by the same rate-controlling step, namely, the mass transfer of Rh^{3+} to the surface, which is a **first order process.** This is supported by Roy's study of Ni and Cu co-precipitation at 150 °C, where the residence time of a turbulent pipe reactor required is 5 – 10 % of the 4-stage CSTR (Roy, 1961). At atmospheric temperatures, the near independence of precipitation rate and temperature over the middle period could result from passivation. Thus, specific mass transfer test work is required to verify mass transfer limitations over the initial period and middle period separately over atmospheric and elevated temperatures.

The passivation phenomenon must be investigated further to determine whether CuS co-precipitated at low temperatures, having been 'passivated' with Rh precipitation, can precipitate additional Rh at elevated temperatures. This will determine whether temperatures can drive the surface reaction further by forcing more Rh into the CuS microstructure or release more Cu^{2+} from the mixed sulfides formed. Alternatively, typical passivation is occurring.

Chapter Nine

CONCLUSIONS

The analysis of the available literature, thermodynamic modelling and comparative kinetic studies of the specific reactions systems, particularly the relative precipitation kinetics of Cu and Rh and kinetic modelling leads to the following conclusions:

1. General mechanism

This work identifies an alternative precipitation path in the mechanism of metal sulfide co-precipitation. The heterogeneous cationic substitution reaction, with solubility differences providing the chemical driving force, must be considered when interpreting kinetics of co-precipitation mechanisms, particularly when co-precipitating a more insoluble metal sulfide at a much lower concentration from more soluble metal sulfides at a much higher concentration. In the co-precipitation mechanism, both the thermodynamics and overall relative kinetics must be taken into account. The relative difference in the metal sulfide solubility products and the relative concentrations affect the overall precipitation rate, which affects the selectivity of competing precipitation paths. The thermodynamic driving force (ΔG) is the dominant effect on selectivity when the concentrations are similar.

Temperature affects the mechanism by affecting the relative ionic metal sulfide precipitation rates of the competing metals. For this Rh co-precipitation system, with Rh^{3+} concentration two orders of magnitude lower than Cu^{2+}, at 50 - 95 °C, the presence of a large amount of aqueous Cu^{2+} effectively decreases the rate and extent of Rh co-precipitation, while at 150 °C, Cu^{2+} has negligible impact. Increasing temperature increases the amount of primary nucleation of the CuS, thereby increasing the active surface area available for precipitation through finer particle formation. This, in turn, increases the rate and extent of Rh precipitation, whether through catalysed crystal growth (ionic) or cationic substitution. The heterogeneous cationic substitution reaction is significantly slower than ionic precipitation (at 50 – 95 °C), thus the cationic substitution reaction path has the potential to slow down the overall Rh co-precipitation rate. Thus is the initial precipitation conditions that have the dominant effect on the overall Rh precipitation rate and extent.

2. Kinetic modelling and mechanistic changes

Kinetic modelling bas been performed primarily to understand the mechanism of individual reaction systems, particularly the co-precipitation system, rather than to develop an accurate, predictive model.

Kinetic modelling shows three distinctive precipitation periods, namely, the initial period showing very fast precipitation, the middle period approximated by pseudo first order kinetics and a final period showing a slow approach to completion, limited by passivation of the active surface, for all three systems. At 50 °C, an induction period precedes the initial period prior to perceptible nucleation. At atmospheric temperatures, the empirical logarithmic fit provides a better model of the data over the whole precipitation profile, including the initial

precipitation and final passivation. At elevated temperatures, the pseudo first order model provides an almost perfect fit over the middle period and final period.

Mechanistic changes are expected across the co-precipitation systems with increasing precipitation extent, progressing from primary nucleation to additional ionic precipitation through sulfide crystal growth and co-precipitation of the mixed sulfides. The rate-determining step probably switches from chemical reaction to mass transfer, particularly at 150 °C

Due to thiosulfate degradation or CuS passivation, the activation energies and frequency factors are estimated from the initial rate constants for each reaction system. Ionic precipitation, substitution and co-precipitation reactions are measured with an activation energy of 48 kJ, 67kJ and 135 kJ, respectively, over 50 – 95 °C and 0 kJ, 72 kJ and 38 kJ, respectively, over 95 – 150 °C. Thus, from a kinetic perspective, for ionic precipitation, the temperature has a small effect on initial Rh precipitation rate from 95 to 150 °C. The similar activation energies for the substitution reaction indicate that the reaction mechanism remains the same over 50 – 150 °C, while co-precipitation reaction mechanisms change to a relatively faster reaction path from 95 °C to 150 °C.

From a modelling perspective, the fact that the pseudo model holds true for ionic and co-precipitation systems, as well as substitution reaction systems, supports the argument that the systems are being controlled by the same rate-controlling step, namely, the mass transfer of Rh^{3+} to the surface, which is a **first order process.** This is supported by Roy's study of Ni and Cu co-precipitation at 150 °C, where the residence time of a turbulent pipe reactor required is 5 – 10 % of the 4-stage CSTR (Roy, 1961).

3. Passivation

The passivation phenomenon must be investigated further to determine whether true passivation is occurring or whether apparent passivation is a result of very slow kinetics. The pertinent question is whether CuS co-precipitated at lower temperatures, having been 'passivated' with Rh precipitation, can precipitate additional Rh at elevated temperatures. This will determine whether temperatures can drive the surface reaction further by forcing more Rh into the CuS microstructure and / or release more Cu^{2+} from the mixed sulfides formed.

4. Optimisation of the Rhodium Removal Process at RBMR

Maximising the Rh precipitation extent in the Rhodium Removal Section in RBMR is paramount, but not at the expense of additional base metal precipitation. Optimisation study is required to improve Rh precipitation selectivity, maximising the ratio of Rh to Cu in the mixed sulfide precipitate, but not at the expense of overall Rh precipitation extent. Reducing the sulfide addition rate or operating at lower temperatures would come at a cost of slower precipitation kinetics. A minimum amount of CuS may be required to ensure sufficient surface area for the reaction, as passivation is occurring. This heterogeneous reaction path must be taken into consideration when developing or designing such removal processes. Knowledge of this rate-controlling step is critical for optimal design of a removal system and specific mass transfer investigations are required to quantify possible improved precipitation extent at more turbulent conditions.

In the current atmospheric temperature plant, Rh precipitation extent could be improved by introducing mechanical activation of the CuS particle through particle breakage or attrition grinding to overcome the passivation phenomenon. This would maximise the usage of the

available CuS for Rh precipitation, reduce the fresh reagent addition and effectively improve the overall Rh selectivity. Multiple addition points for thiosulfate addition would increase Rh precipitation extent by promoting ionic precipitation during the initial nucleation period, where the bulk of the Rh precipitation occurs.

Alternatively, this process will have to be developed and designed to operate at elevated temperatures to maximise Rh precipitation, which would occur through increased ionic precipitation over the initial period, followed by complete removal of Rh due to the increased surface area of precipitated CuS. Multiple reagent addition points and the recycling of precipitate and mechanical activation would increase selectivity by reducing fresh reagent addition requirements.

Consideration should be given to precipitating the CuS at atmospheric temperatures to partially precipitate the Rh, followed by increasing the temperature to the optimum elevated temperature using a heat exchanger and turbulent pipe reactor. This is one method of avoiding possible localised reducing conditions when injecting the sulfide reducing reagent at elevated temperatures, which can cause stainless steel corrosion. This approach would probably come at the expense of Rh selectivity, as slightly more CuS would be required to ensure complete Rh precipitation, as less Rh will precipitate through the ionic precipitation path. Hence, more Rh would precipitate through the substitution reaction path, which is possibly limited by passivation of the CuS surface with Rh.

Chapter Ten

RECOMMENDATIONS

The following recommendations are suggested to improve the experiments:

1. Separate injection and sampling system to avoid contamination of first sample. Attempt to take more equal volumes of feed at temperature and inject more equal volumes of reagents and flush water to maintain the same feed basis.
2. Ensure that greater precision is received from the assay laboratory. Ensure that effective total solution stream analysis occurs to overcome post precipitation phenomenon or take larger samples and perform the comparative kinetic study on the solids precipitation profiles.
3. Allow initial CuS precipitation in part (a) of substitution reaction the same overall reaction time as the overall ionic precipitation reaction time at the same temperature, respectively and perform part (b) of the substitution reaction at the same base metal solution concentrations as co-precipitation.

The following recommendations are suggested to confirm results:

4. Repeat tests at 50 °C, particularly the co-precipitation system. Perform more duplicate precipitation profiles and take more samples within the first minute at elevated temperatures.
5. Perform cationic substitution reaction at sufficient background Cu^{2+} to saturate the CuS surface to ensure that no adsorbed H_2S, HS^- and S^{2-} is present and increase the ratio of Rh^{3+} to CuS to increase the amount of Cu^{2+} being released.
6. Monitor actual Cu^{2+} release during co-precipitation by starting with higher with higher Rh^{3+} concentrations.
7. Perform mineralogical studies on precipitate of the three systems to determine the solid compounds and Rh distribution in the CuS for the cationic substitution and co-precipitation using Scanning Electron Microscope with Energy Dispersive X-ray spectroscopy, Microprobe and X-ray Photon Spectroscopy.
8. Confirm the passivation phenomenon in more detail by determining whether CuS co-precipitated at low temperatures, having been 'passivated' with Rh precipitation, can precipitate additional Rh at elevated temperatures i.e. is passivation a function of CuS surface area alone or can elevated temperatures can drive the surface reaction further by forcing more Rh into the CuS microstructure or release more Cu^{2+} from the mixed sulfide compounds formed on the surface.

The following recommendations are suggested for plant optimisation:

9. Optimise the co-precipitation system operating at elevated temperatures by reducing the excess sulfide, but not at the expense of Rh precipitation extent and test the various configurations possible.

10. Confirm that the rate-controlling step at elevated temperatures over the initial and middle precipitation period is mass transfer for the three reaction systems and measure the possible increase in precipitation at turbulent pipe reactor conditions. Extend this test to atmospheric temperatures as well.

11. Revisit co-precipitation studies like Co co-precipitation from Mn electrolytic feed and consider the cationic exchange reaction to explain the mechanism.

REFERENCES

Allison, S.A. , Mintek, report M29, 30th April, (1982).

Andrews, L. , *"Rhodium and Ruthenium distribution in Rhodium press cake samples"*, Internal report Min. Rep. No. M/01/48, 8pp. (2001).

Barkan, V.Sh. and Greiver, T.N. , Izv. Vyshshykh Uchebnykh Zav., Tsvt.met., No.2 pp. 157-158. (1977)a (English translation).

Barkan, V.Sh. and Greiver T,N. , *"Coprecipitation of platinum metals with iron hydroxide"*, Russian Journal of Inorganic Chemistry , 22 (8), 1977. Translated from Zhurnal Neorganicheskoi Khimii, 22, 2197-2203 , (1977)b.

Bryson, A.W. and Bijsterveld, C.H. , *"Kinetics of the precipitation of manganese and cobalt sulfides in the purification of a manganese sulfate electrolyte"* , Elsevier Science, Hydrometallurgy, 27 , 75-84, (1991).

Bushnell C.H. and Krauss, C.J. , *"Copper activation of pyrite"*, Can. Min. Metall. Bull, 55, 314, (1962).

Dinham , Internal memorandum to K. Viljoen within Anglo Platinum , REF NO: R200600881 (M/05/148), (2006).

Dragavtseva, N.A., Avvakumov, E.G. and Mateeva, N.I., Tsvetnye Metally, No.6, pp.21-23 , (1977). Translated by Z. Hofirek (not published).

Dreisinger, D., Fleming, C.A., Ferron, C.J., and O'Kane, P.T., *"Hydrometallurgical treatment of base metal sulfide concentrates containing precious and platinum group metals."*,. www.polymetmining.com/press_releases/ technical_papers11_27_01.html , (2001)

Ferron, C.J., Fleming, C.A., O'Kane, P.T., and Dreisinger, D., *"Pilot plant demonstration of the PLATSOL process for the treatment of the Northmet copper-nickel PGM deposit"*, www.polymetmining.com/press_releases/ technical_papers2_27_01.html - 101k , (2001).

Fleming, C.A., Ferron, C.J., O'Kane, P.T., and Dreisinger, D., *"A process for the simultaneous leaching and recovery of gold, platinum group metals and base metals from ores and concentrates."*, EDP Congress, edited by P.R. Taylor, The Minerals, Metals and Materials Society, (2000).

Griffith, W.P. , *"The chemistry of the rarer Platinum metals (Os, Ru, Ir and Rh)"*, Interscience publishers, (1967).

Habashi, F. , *"Textbook of Hydrometallurgy"*, Metallurgie Extractive Quebec, (1999): Chapter 22.

Harris, M., Meyer, D.M. and Auerswald, K., The production of electrolytic manganese in South Africa, J. S. Afr. Inst. Min. Metallur. 77(7) (1977): 137-142.

Hofirek Z. and D. G. E. Kerfoot , *"The chemistry of the nickel-copper matte leach and its application to process control and optimisation"*, Hydrometallurgy, Volume 29, Issues 1-3, (1992) , Pages 357-381.

Joris, S., *"La cintetique de precipitation des sulferus de calbalt et de nickel par l'hydrogene sulfur."*, Bull. Soc. Chim. Belges, 78 (1969): 607-619.

Kolthoff, I.M. , J. Phys. Chem. 35 2711 (1931) In: Kolthoff, I.M. and Moltzau D.R., *"Induced precipitation and properties of metal sulfides"*, Chem. Rev. 17 (1935).

Kolthoff, I.M. and Moltzau D.R., *"Induced precipitation and properties of metal sulfides."* Chem. Rev. 17 (1935): 293-325.

Levenspiel, O., *"Chemical Reaction Engineering"* , 2nd ed., Wiley International , pg. 374 , (1972).

Luther III, G.W., Theberge, S.M. Rozan, T.F. , Richard, D., Rowkands C.C. and Oldroyn, A., Environ. Sci. Technol. 36, (2002): 394-402.

Mateeva, N.I., Dragavtseva, N.A., Antipov, N.I. and Avvakumov, E.G., Tsvetnye Metally, (1977), No. ?, pp.19-21. Translated by Z. Hofirek (not published).

Mc George, B. , *"Recovery of PGMs from MC Plant process liquors"*, Amplats Internal Refining Conference , RBMR Library, (2000).

Monhemius, A.J., *"Precipitation diagrams for metal hydroxides, sulfides, arsenates and phosphates"*, Trans. Inst. Min. Metall., 86 (1977):137-142.

Mosselmans J.W.F, Charnock, J.M., Garner, C.D., Pattrick R.A.D., and Vaughan, D.J., *"A XAS study of structural changes undergone by amorphous copper sulfides when precipitated from solution"*, Physica, Elsevier Science, B208&209, (1995), 609-610.

Myasoedova, G.V., Malofeeva, O.P., Shvoeva, E.V., Illarionova, S.B., Savvin, S.B. and Zolotov. Yu. A. V.I. Vernadskii Institute of Geochemistry and Analytical Chemistry, Academy of Sciences of the USSR. Translated from Zhural Analiticheskoi Khimii, Vol. 32, No.4, pp. 645-649, (1977).

Nicol M.J. , *"An electrochemical study of the interaction of copper(II) ions with sulfide minerals"*, In: Richardson P.E. , S. Srinivasan and R. Woods (Editors). Proceedings of the international symposium on electrochemistry in mineral and metal processing , The Electrochemical Society, Pennington, N.J., 1984 , *International Journal of Mineral Processing, Volume 17, Issues 3-4, July (1986), pp 152-168.*

Nicol M.J. , Personal communication , (2006).

Pattrick R.A.D Mosselmans J.W.F, Charnock, England, K.E.R., Helz, G.R., J.M., Garner, C.D.,., and Vaughan, D.J., Geochemica et Cosmochimica Acta, Pergamon, Vol.61. No.10, pp. 2023-2036, (1997).

Payne, J , Thioform (sulfide) recovery of values from MRR Royston effluent , Johnson Matthey Report, (1978).

Pavlenko, L.I., Malofeeva, G.I., Simonova, L.V. and Andryyushchenko, O.Yu. V.I. Vernadskii Institute of Geochemistry and Analytical Chemistry, Academy of Sciences of the

USSR. Translated from Zhural Analiticheskoi Khimii, Vol. 29, No.6, pp. 1122-1129, (1974).

Phillips, H.O. and Kraus, K.A., J. Chromat.,17, 549 (1964).

Pshenitsyn, N.K. and Prokof'yeva, Zhural Neoganicheskoi Khimii (J. of Inorganic Chem.), Vol. III. No.4, (1958), pp. 996-1001. English translation.

Payne, J , Thioform (sulfide) recovery of values from HRR Royston effluent Johnson Matthey Report, (1978).

Rademan J. A. M. , L. Lorenzen and J. S. J. van Deventer , *"The leaching characteristics of Ni–Cu matte in the acid–oxygen pressure leach process at Impala Platinum"*, Hydrometallurgy, Volume 52, Issue 3, June (1999), Pages 231-252.

Roy, T.K., *"Preparing nickel and cobalt concentrates."* , Ind. Eng. Chem., 53 (1961): 559-566.

Rudnev, N.A. and Malofeyeva G.I., *"Chemical compounds formed in the co-precipitation of cations with sulfides"*, Talanta, Pergamon Press Ltd., Vol.11 (1964) p.531-542.

Shorikov, Yu. S., Orlov, A.M. and Kornyushina, S.N. State scientific research and planning institute for the rear earth industry. Translate from: Zhural Prikladnoi Khimii, Vol. 59, No.3, pp. 496-499, (1986).

Sinicyn, N.M., Borisov, V.V., Dobronrabov. S.A. and Ladygo, A.S., Radiochimija, (1977), No.1, pp.27-29. Translated by Z. Hofirek (not published).

Söhnel, O. and Garside, J. , (1992) , "Precipitation basic principles and industrial applications", 1st Ed. , Butterworth-Heinemann , pp.

Sutherland, K.L. and Wark, I.W., *Principles of flotation*, Melbourne, Australian Inst. of Mining and Metallurgy, (1955), Chap. 9 and 10.

Thomas, R. Chem. App., *88*, 3 (1964). In: Sinicyn, N.M., Borisov, V.V., Tuominen, T. and Groenquist, P.O., *"Hyrogen sulfide as precipitation reagent in hydrometallurgy"*. , Ertzmetall., 22 (1969): 81-86.

Tuomien, T. and Groenqvist, P.C. , (1969) , Ertmetall. Vol 22, H5, pp.81-86.

Van Hille, R.P., Peterson, K.A., and Lewis, A.E., *Copper sulfide precipitation in fluidised bed reactor*, Chem. Eng. Science 60 , (2005), 2571-2578.

Volkov, A.V.; Moskvina, M.A.; Volynskii, A.L.; Bakeev, N.F.; Polymer Science, Ser.A, Vol.40 No.9, (1998) , p. 893-900.

APPENDICES

TABLE OF CONTENTS

APPENDIX A – THERMODYNAMIC CALCULATIONS ..... - 3 -

A.1. Gibbs free energy of reaction ..... - 3 -

1. Ionic CuS precipitation ..... - 4 -
2. Ionic Rh precipitation without redox reactions ..... - 4 -
3. Ionic Rh precipitation with redox reactions ..... - 5 -
4. Rh^{3+} precipitation through cation substitution reaction with CuS and NiS ..... - 5 -
5. Rh^{3+} precipitation through cation substitution reaction with redox reactions ..... - 6 -
6. Rh^{3+} precipitation through cation substitution with base metal oxides or hydroxides ..... - 7 -
7. Ferric reduction with sulfide addition ..... - 8 -
8. Ferric reduction with metal sulfide solids / precipitate ..... - 8 -
9. Thiosulphate decomposition to Sulphur and H_2S ..... - 8 -
10. Sulphur trioxide generation ..... - 8 -

A.2. Eh-pH Diagrams ..... - 9 -

1. Additional base case selecting all species at 95 °C ..... - 10 -
2. Additional metastable Eh-pH diagrams ..... - 12 -

A.3. Equilibrium Composition Diagrams ..... - 16 -

APPENDIX B – RESULTS ..... - 17 -

B.1. Miscellaneous ..... - 17 -

B.2. Experimental Design Details ..... - 18 -

B.3. Solid and Solution Assays ..... - 21 -

1. Solids Assays ..... - 21 -
2. Solution Assays ..... - 24 -
3. Statistics on Assays and Comparisons ..... - 31 -

1. Solution Assay Standard Deviations ..... - 31 -
2. Average and Standard deviations for Rh element analysed in replicate (two analyses) ..... - 32 -
3. Average and Standard deviations for other element analysed in replicate (two analyses) ..... - 33 -
4. Average and Standard deviations for Solid Assays repeats ..... - 34 -
5. Comparative statistics using T-Test ..... - 35 -

B.4. Log sheets, Assays and Mass Balance Tables ..... - 36 -

B.5. Leach Profiles ..... - 58 -

1. Summary of predicted and measured concentration values ..... - 58 -
2. Calculation of precipitation extent and reaction rates over middle period: (pseudo first order kinetics at 150 °C; logarithmic fit at 50 - 95 °C) ..... - 61 -
3. Precipitation profile graphical illustrations ..... - 63 -
4. Kinetics of systems on concentration basis ..... - 64 -

B.6. Kinetic Modelling ..... - 66 -

1. Kinetic calculation data (solids basis) ..... - 66 -
2. Kinetic calculation data (solution basis) ..... - 67 -
3. Comparison of pseudo first order and second order models over middle period ..... - 68 -
4. Modelling rate constant to Arrhenius relationship ..... - 69 -
5. Rh Modelling data ..... - 74 -

B.7. Individual and comparative results using solution basis ..... - 75 -

APPENDIX C – LITERATURE ..... - 77 -

APPENDIX A – THERMODYNAMIC CALCULATIONS

A.1. Gibbs free energy of reaction

Gibbs free energy of reaction (ΔG) is calculated using the HSC Chemistry® program for the proposed process chemistry. The reactions considered are:

- Ionic CuS precipitation
- Ionic Rh precipitation without redox reactions
- Ionic Rh precipitation with redox reactions

- Rh^{3+} precipitation through cation substitution reaction with CuS and NiS
- Rh^{3+} precipitation through cation substitution reaction with redox reactions
- Rh^{3+} precipitation through cation substitution with base metal oxides or hydroxides

- Ferric reduction with sulfide addition
- Ferric reduction with metal sulfide solids/precipitate
- Thiosulphate decomposition to Sulphur and H_2S

ΔG provides a measure of the thermodynamic driving force for the chemical reaction. ΔG values that are negative imply that the reactions proceed to the right, thus it is thermodynamically favourable. The large ΔG implies that the reaction goes to completion i.e. it is irreversible. The larger driving force would possibly increase kinetics.

All calculations are performed from 0 – 200 °C at 25 °C intervals for ionic precipitation and metathesis reactions. Values are calculated for $S_2O_3^{2-}$ precipitating agents, and in some cases compared to S^{2-} addition. HSC outputs a ΔG value for the balanced reaction, thus the basis changes as the stoichiometry changes. ΔG values have been re-calculated relative to an equivalent molar basis; thus the kJ/mol values in the last column are comparable. The K and log K values are calculated for the reaction stiochiometries as displayed in the reactions above the tables.

The calculations need to be performed for the complexed ion, but these species are not available in the HSC Chemistry® database. The negative ΔG values are expected to be reduced due to PGM complexing in solution, also reducing the precipitation kinetics.

1. Ionic CuS precipitation

Cu(+2a) + S2O3(-2a) + H2O = CuS + 2H(+a) + SO4(-2a)

T	deltaH	deltaS	deltaG	K	Log(K)	deltaG
C	kJ	J/K	kJ			kJ/mol Cu(2+)
0	-90	72	-110	8.86E+20	20.9	-110
25	-87	46	-111	2.53E+19	19.4	-111
50	-98	43	-112	1.20E+18	18.1	-112
75	-99	40	-113	8.64E+16	16.9	-113
100	-100	38	-114	8.66E+15	15.9	-114
125	-100	37	-115	1.15E+15	15.1	-115
150	-100	38	-116	1.93E+14	14.3	-116
175	-99	40	-117	3.99E+13	13.6	-117
200	-97	44	-118	9.94E+12	13.0	-118

Cu(+2a)	Extrapolated from	473.15	K	
S2O3(-2a)	Extrapolated from	473.15	K	
H(+a)	Extrapolated from	473.15	K	
SO4(-2a)	Extrapolated from	473.15	K	

Cu(+2a) + S(-2a) = CuS

T	deltaH	deltaS	deltaG	K	Log(K)	deltaG
C	kJ	J/K	kJ			kJ/mol Cu(2+)
0	-159	163	-204	9.71E+38	39.0	-204
25	-155	179	-208	2.93E+36	36.5	-208
50	-149	198	-213	2.53E+34	34.4	-213
75	-143	215	-218	5.07E+32	32.7	-216
100	-136	235	-224	2.00E+31	31.3	-224
125	-128	256	-230	1.39E+30	30.1	-230
150	-119	278	-236	1.53E+29	29.2	-236
175	-109	300	-244	2.51E+28	26.4	-244
200	-98	325	-251	5.76E+27	27.6	-251

Cu(+2a)	Extrapolated from	473.15	K	

2Cu(+2a) + 1.25S2O3(-2a) + 2.25H2O = Cu2S + 4.5H(+a) + 1.5SO4(-2a)

T	deltaH	deltaS	deltaG	K	Log(K)	deltaG
C	kJ	J/K	kJ			kJ/mol Cu(2+)
0	-104	167	-149	3.48E+28	28.5	-75
25	-122	102	-152	4.27E+26	26.6	-76
50	-126	88	-154	9.00E+24	25.0	-77
75	-130	77	-156	2.97E+23	23.5	-78
100	-133	67	-158	1.42E+22	22.2	-79
125	-132	71	-160	1.00E+21	21.0	-80
150	-133	67	-162	9.39E+19	20.0	-81
175	-134	66	-163	1.13E+19	19.1	-82
200	-133	68	-165	1.70E+18	18.2	-83

Cu(+2a)	Extrapolated from	473.15	K	
S2O3(-2a)	Extrapolated from	473.15	K	
H(+a)	Extrapolated from	473.15	K	
SO4(-2a)	Extrapolated from	473.15	K	

2. Ionic Rh precipitation without redox reactions

2Rh(+3a) + 3S2O3(-2a) + 3H2O = Rh2S3 + 6H(+a) + 3SO4(-2a)

T	deltaH	deltaS	deltaG	K	Log(K)	deltaG
C	kJ	J/K	kJ			kJ/mol Rh(3+)
0	-506	515	-647	5.13E+123	123.7	-323
25	-547	370	-657	1.34E+115	115.1	-329
50	-589	299	-665	3.74E+107	107.6	-333
75	-592	231	-672	6.94E+100	100.8	-336
100	-618	184	-677	5.96E+94	94.8	-336
125	-642	97	-680	1.79E+89	89.3	-340
150	-669	31	-682	1.51E+84	84.2	-341
175	-698	-35	-682	2.99E+79	79.5	-341
200	-726	-102	-680	1.22E+75	75.1	-340

Rh(+3a)	Extrapolated from	300	K	
S2O3(-2a)	Extrapolated from	473.15	K	
H(+a)	Extrapolated from	473.15	K	
SO4(-2a)	Extrapolated from	473.15	K	

2Rh(+3a) + 3S(-2a) = Rh2S3

T	deltaH	deltaS	deltaG	K	Log(K)	deltaG
C	kJ	J/K	kJ			kJ/mol Rh(3+)
0	-714	790	-930	6.74E+177	177.8	-465
25	-720	768	-949	2.11E+166	166.3	-475
50	-723	760	-968	3.48E+156	156.5	-484
75	-724	757	-987	1.40E+148	148.1	-494
100	-724	756	-1006	7.38E+140	140.9	-503
125	-725	754	-1025	3.17E+134	134.5	-513
150	-726	751	-1044	7.55E+126	126.9	-522
175	-728	746	-1063	7.43E+123	123.8	-531
200	-731	740	-1081	2.39E+119	119.4	-541

Rh(+3a)	Extrapolated from	300	K	

3. Ionic Rh precipitation with redox reactions

2Rh(+3a) + 1.5S2O3(-2a) + 3.5H2O = 2Rh + S + 7H(+a) + 2SO4(-2a)

T	deltaH	deltaS	deltaG	K	Log(K)	deltaG
C	kJ	J/K	kJ			kJ/mol Rh(3+)
0	-156	559	-309	1.20E+59	59.1	-154
25	-204	387	-320	1.05E+56	56.0	-160
50	-231	302	-328	1.19E+53	53.1	-164
75	-258	222	-335	1.77E+50	50.2	-167
100	-288	144	-339	3.32E+47	47.5	-170
125	-314	71	-342	7.73E+44	44.9	-171
150	-346	-7	-343	2.16E+42	42.3	-171
175	-380	-86	-342	6.87E+39	39.6	-171
200	-416	-167	-339	2.42E+37	37.4	-169

Rh(+3a)	Extrapolated from	300	K
S2O3(-2a)	Extrapolated from	473.15	K
H(+a)	Extrapolated from	473.15	K
SO4(-2a)	Extrapolated from	473.15	K

2.667Rh(+3a) + S2O3(-2a) + 5H2O = 2.667Rh + 10H(+a) + 2SO4(-2a)

T	deltaH	deltaS	deltaG	K	Log(K)	deltaG
K	kJ	J/K	kJ			kJ/mol Rh(3+)
273.15	-150	752	-355	9.68E+67	68.0	-133
298.15	-219	504	-370	6.09E+64	64.8	-139
323.15	-257	383	-381	3.65E+61	61.6	-143
348.15	-296	267	-389	2.28E+58	58.4	-148
373.15	-337	154	-394	1.53E+55	55.2	-148
398.15	-380	41	-397	1.09E+52	52.0	-149
423.15	-427	-72	-396	8.23E+48	48.9	-149
448.15	-477	-188	-393	6.42E+46	45.8	-147
473.15	-532	-308	-387	5.08E+42	42.7	-145

Rh(+3a)	Extrapolated from	300	K
S2O3(-2a)	Extrapolated from	473.15	K
H(+a)	Extrapolated from	473.15	K
SO4(-2a)	Extrapolated from	473.15	K

3Rh(+3a) + 4.125S2O3(-2a) + 4.625H2O = Rh3S4 + 9.25H(+a) + 4.25SO4(-2a)

T	deltaH	deltaS	deltaG	K	Log(K)	deltaG
C	kJ	J/K	kJ			kJ/mol Rh(3+)
0	-701	785	-918	1.40E+175	175.1	-305
25	-764	561	-881	1.50E+163	163.2	-310
50	-798	451	-944	3.94E+152	152.6	-315
75	-834	345	-954	1.34E+143	143.1	-316
100	-871	241	-881	3.66E+134	134.6	-320
125	-911	138	-966	5.45E+126	126.7	-322
150	-953	36	-968	3.29E+119	119.5	-323
175	-996	-67	-968	8.38E+112	112.8	-323
200	-1046	-171	-965	3.28E+108	108.5	-322

Rh(+3a)	Extrapolated from	300	K
S2O3(-2a)	Extrapolated from	473.15	K
H(+a)	Extrapolated from	473.15	K
SO4(-2a)	Extrapolated from	473.15	K

9.378 14.877 29.754 10.755

Rh(+3a) + 1.042S2O3(-2a) + 1.563H2O = Rh90.889 + 3.306H(+a) + 1.195SO4(-2a)

T	deltaH	deltaS	deltaG	K	Log(K)	deltaG
C	kJ	J/K	kJ			kJ/mol Rh(3+)
0	-178	276	-253	2.97E+48	48.5	-253
25	-202	192	-259	2.25E+45	45.4	-259
50	-215	149	-263	3.39E+42	42.5	-263
75	-229	108	-266	9.05E+39	40.0	-266
100	-243	67	-268	3.85E+37	37.8	-266
125	-259	27	-270	2.40E+35	35.4	-270
150	-275	-12	-270	2.06E+33	33.3	-270
175	-292	-52	-269	2.30E+31	31.4	-269
200	-311	-93	-267	3.20E+29	29.5	-267

Rh(+3a)	Extrapolated from	300	K
S2O3(-2a)	Extrapolated from	473.15	K
Rh90.889	Extrapolated from	300	K
H(+a)	Extrapolated from	473.15	K

Rh(+3a) + 1.5S(-2a) = Rh + 1.5S

T	deltaH	deltaS	deltaG	K	Log(K)	deltaG
C	kJ	J/K	kJ			kJ/mol Rh(3+)
0	-226	411	-338	5.01E+64	64.7	-338
25	-229	401	-348	1.12E+61	61.1	-348
50	-230	397	-358	8.70E+57	57.9	-358
75	-230	396	-368	1.85E+55	55.3	-368
100	-230	397	-378	8.93E+52	53.0	-378
125	-227	404	-388	6.67E+50	50.9	-388
150	-228	403	-398	1.50E+49	49.2	-398
175	-228	403	-408	4.04E+47	47.8	-408
200	-229	401	-418	1.59E+46	46.2	-418

Rh(+3a)	Extrapolated from	300	K

4. Rh^{3+} precipitation through cation substitution reaction with CuS and NIS

3CuS + 2Rh(+3a) = Rh2S3 + 3Cu(+2a)

T	deltaH	deltaS	deltaG	K	Log(K)	deltaG
C	kJ	J/K	kJ			kJ/mol Rh(3+)
0	-237	299	-318	7.37E+60	60.9	-159
25	-256	232	-325	8.34E+56	56.9	-162
50	-275	171	-330	2.14E+53	53.3	-165
75	-295	111	-333	1.06E+50	50.0	-167
100	-317	50	-335	9.18E+46	47.0	-168
125	-341	-14	-336	1.19E+44	44.1	-168
150	-369	-82	-335	2.11E+41	41.3	-167
175	-401	-155	-332	4.73E+38	38.7	-166
200	-438	-234	-327	1.25E+36	38.1	-163

Rh(+3a)	Extrapolated from	300	K
Cu(+2a)	Extrapolated from	473.15	K

3NiS + 2Rh(+3a) = 3Ni(+2a) + Rh2S3

T	deltaH	deltaS	deltaG	K	Log(K)	deltaG
C	kJ	J/K	kJ			kJ / mol Rh
0	-497	258	-567	3.15E+108	108.5	-284
25	-519	179	-573	2.25E+100	100.4	-286
50	-541	110	-576	1.48E+93	93.2	-288
75	-564	42	-578	5.80E+86	86.8	-289
100	-588	-27	-578	9.50E+80	81.0	-289
125	-616	-97	-577	4.91E+75	75.7	-288
150	-646	-171	-574	6.41E+70	70.8	-287
175	-680	-250	-568	1.76E+66	66.2	-284
200	-720	-335	-561	6.67E+61	61.9	-280

Rh(+3a)	Extrapolated from	300	K
Ni(+2a)	Extrapolated from	473.15	K

5. Rh^{3+} precipitation through cation substitution reaction with redox reactions

24Rh(+3a) + 33CuS + 4H2O = 8Rh3S4 + 33Cu(+2a) + 8H(+a) + SO4(-2a)

T C	deltaH kJ	deltaS J/K	deltaG kJ	K	Log(K)	deltaG kJ / mol Rh
0	-2645	3907	-3712	1.000E+308	308.0	-155
25	-2913	2962	-3796	1.000E+308	308.0	-158
50	-3150	2198	-3861	1.000E+308	308.0	-161
75	-3403	1445	-3906	1.000E+308	308.0	-163
100	-3680	678	-3933	1.000E+308	308.0	-164
125	-3987	-118	-3940	1.000E+308	308.0	-164
150	-4332	-957	-3927	1.000E+308	308.0	-164
175	-4723	-1855	-3892	1.000E+308	308.0	-162
200	-5170	-2825	-3833	1.000E+308	308.0	-160

Rh(+3a)	Extrapolated from	300	K	
Cu(+2a)	Extrapolated from	473.15	K	
H(+a)	Extrapolated from	473.15	K	
SO4(-2a)	Extrapolated from	473.15	K	

3Cu2S + 2Rh(+3a) = Rh2S3 + 6Cu(+a)

T C	deltaH kJ	deltaS J/K	deltaG kJ	K	Log(K)	deltaG kJ / mol Rh
0	58	643	-117	2.60E+22	22.4	-59
25	48	605	-133	1.86E+23	23.3	-66
50	35	566	-147	6.88E+23	23.8	-74
75	21	524	-161	1.49E+24	24.2	-81
100	5	480	-174	2.04E+24	24.3	-87
125	-26	399	-184	1.54E+24	24.2	-92
150	-48	345	-194	8.07E+23	23.9	-97
176	-72	289	-202	3.14E+23	23.5	-101
200	-100	228	-208	9.32E+22	23.0	-104

Rh(+3a)	Extrapolated from	300	K	
Cu(+a)	Extrapolated from	473.15	K	

Rh(+3a) + 1.5CuS = Rh + 1.5S + 1.5Cu(+2a)

T C	deltaH kJ	deltaS J/K	deltaG kJ	K	Log(K)	deltaG kJ / mol Rh
0	13	166	-33	1.66E+06	6.2	-33
25	3	133	-36	2.24E+06	6.4	-36
50	-6	103	-39	2.16E+06	6.3	-39
75	-16	73	-41	1.62E+06	6.2	-41
100	-26	45	-43	9.96E+05	6.0	-43
125	-36	20	-44	5.31E+05	5.7	-44
150	-49	-13	-44	2.50E+05	5.4	-44
175	-64	-48	-43	1.02E+06	5.0	-43
200	-82	-86	-41	3.63E+04	4.6	-41

Rh(+3a)	Extrapolated from	300	K	
Cu(+3a)	Extrapolated from	473.15	K	

6.547Rh(+3a) + 6.82CuS + 4H2O = 6.547RhS0.889 + 6.82Cu(+2a) + 8H(+a) + SO4(-2a)

T C	deltaH kJ	deltaS J/K	deltaG kJ	K	Log(K)	deltaG kJ / mol Rh
0	-551	1319	-911	1.70E+174	174.2	-139
25	-657	941	-938	2.26E+164	164.4	-143
50	-737	683	-958	8.29E+154	154.9	-146
75	-821	433	-972	7.72E+145	145.9	-149
100	-912	163	-980	1.55E+137	137.2	-150
125	-1010	-73	-981	5.75E+128	128.8	-150
150	-1119	-337	-976	3.34E+120	120.5	-149
175	-1239	-614	-964	2.63E+112	112.4	-147
200	-1375	-908	-945	2.42E+104	104.4	-144

Rh(+3a)	Extrapolated from	300	K	
Rh0.889	Extrapolated from	388	K	
Cu(+3a)	Extrapolated from	473.15	K	
H(+a)	Extrapolated from	473.15	K	
SO4(-2a)	Extrapolated from	473.15	K	

2Rh(+3a) + 4S + 4H2O = Rh2S3 + 8H(+a) + SO4(-2a)

T C	deltaH kJ	deltaS J/K	deltaG kJ	K	Log(K)	deltaG kJ/mol Rh(3+)
0	-331	536	-477	2.01E+91	91.3	-239
25	-387	335	-487	2.27E+85	85.4	-244
50	-418	237	-494	8.05E+79	79.9	-247
75	-449	143	-499	7.57E+74	74.9	-250
100	-484	47	-501	1.58E+70	70.2	-251
125	-526	-63	-501	5.93E+65	65.8	-251
150	-565	-157	-499	3.53E+61	61.5	-249
175	-608	-256	-493	3.27E+57	57.5	-247
200	-655	-357	-486	4.27E+53	53.6	-243

Rh(+3a)	Extrapolated from	300	K	
H(+a)	Extrapolated from	473.15	K	
SO4(-2a)	Extrapolated from	473.15	K	

6. Rh^{3+} precipitation through cation substitution with base metal oxides or hydroxides

Fe(OH)3 + 2Rh(+3a) = Rh2O3 + Fe(+3a) + 3H(+a)

T	deltaH	deltaS	deltaG	K	Log(K)	deltaG
C	kJ	J/K	kJ			kJ/mol Rh(3+)
0	92	390	-15	7.49E+02	2.9	-8
25	72	323	-24	1.56E+04	4.2	-12
50	53	259	-31	1.11E+05	5.0	-16
75	31	195	-37	3.43E+05	5.5	-18
100	8	131	-41	5.45E+05	5.7	-20
125	-18	65	-43	4.98E+05	5.7	-22
150	-46	-3	-44	2.86E+05	5.5	-22
175	-77	-74	-43	1.10E+05	5.0	-22
200	-111	-149	-40	2.93E+04	4.5	-20

Rh(+3a)	Extrapolated from	300	K	
Fe(+3a)	Extrapolated from	473.15	K	
H(+a)	Extrapolated from	473.15	K	

Fe2O3 + 2Rh(+3a) = Rh2O3 + 2Fe(+3a)

T	deltaH	deltaS	deltaG	K	Log(K)	deltaG
C	kJ	J/K	kJ			kJ/mol Rh(3+)
0	31	139	-7	1.79E+01	1.3	-3
25	10	63	-9	3.86E+01	1.6	-5
50	-11	-5	-10	3.81E+01	1.6	-5
75	-34	-73	-9	2.10E+01	1.3	-4
100	-59	-142	-6	7.21E+00	0.9	-3
125	-87	-214	-2	1.67E+00	0.2	-1
150	-118	-290	5	2.70E-01	-0.6	2
175	-154	-372	13	3.16E-02	-1.5	6
200	-195	-461	23	2.70E-03	-2.6	12

Rh(+3a)	Extrapolated from	300	K	
Cu(+2a)	Extrapolated from	473.15	K	

3Cu2O + 2Rh(+3a) = Rh2O3 + 6Cu(+a)

T	deltaH	deltaS	deltaG	K	Log(K)	deltaG
C	kJ	J/K	kJ			kJ/mol Rh(3+)
0	238	706	45	2.57E-09	-8.6	22
25	228	671	28	1.40E-05	-4.9	14
50	217	635	11	1.46E-02	-1.8	6
75	203	596	-4	4.02E+00	0.6	-2
100	188	554	-18	3.77E+02	2.6	-9
125	171	509	-32	1.44E+04	4.2	-16
150	151	461	-44	2.58E+05	5.4	-22
175	129	409	-55	2.39E+06	6.4	-27
200	103	353	-64	1.24E+07	7.1	-32

Rh(+3a)	Extrapolated from	300	K	
Cu(+a)	Extrapolated from	473.15	K	

1.5Cu(OH)2 + 2Rh(+3a) = Rh2O3 + 1.5Cu(+2a) + 3H(+a)

T	deltaH	deltaS	deltaG	K	Log(K)	deltaG
C	kJ	J/K	kJ			kJ/mol Rh(3+)
0	70	501	-67	7.05E+12	12.8	-34
25	52	439	-79	6.72E+13	13.8	-39
50	34	381	-89	2.59E+14	14.4	-45
75	14	322	-98	4.97E+14	14.7	-49
100	-7	263	-105	5.43E+14	14.7	-53
125	-31	202	-111	3.73E+14	14.6	-56
150	-57	139	-115	1.72E+14	14.2	-58
175	-85	73	-118	5.66E+13	13.8	-59
200	-117	5	-119	1.36E+13	13.1	-59

Rh(+3a)	Extrapolated from	300	K	
Cu(+2a)	Extrapolated from	473.15	K	
H(+a)	Extrapolated from	473.15	K	

3CuO + 2Rh(+3a) = Rh2O3 + 3Cu(+2a)

T	deltaH	deltaS	deltaG	K	Log(K)	deltaG
C	kJ	J/K	kJ			kJ/mol Rh(3+)
0	-31	353	-127	1.85E+24	24.3	-63
25	-50	286	-135	4.23E+23	23.6	-67
50	-68	226	-141	6.81E+22	22.8	-71
75	-88	167	-146	8.53E+21	21.9	-73
100	-110	106	-150	8.70E+20	20.9	-75
125	-135	42	-151	7.39E+19	19.9	-76
150	-163	-26	-152	5.26E+18	18.7	-76
175	-194	-99	-150	3.14E+17	17.5	-75
200	-231	-178	-147	1.56E+16	16.2	-73

Rh(+3a)	Extrapolated from	300	K	
Fe(+3a)	Extrapolated from	473.15	K	

7. Ferric reduction with sulfide addition

8Fe(+3a) + S2O3(-2a) + 5H2O = 8Fe(+2a) + 10H(+a) + 2SO4(-2a)

T	deltaH	deltaS	deltaG	K	Log(K)	deltaG
C	kJ	J/K	kJ			kJ/mol Fe(3+)
0	-45	1132	-354	4.85E+67	67.7	-44
25	-83	993	-379	2.65E+66	66.4	-47
50	-90	970	-404	1.78E+65	65.2	-50
75	-96	952	-428	1.47E+64	64.2	-53
100	-101	939	-451	1.50E+63	63.2	-56
125	-104	932	-475	1.89E+62	62.3	-59
150	-104	931	-496	2.95E+61	61.5	-62
175	-101	938	-521	5.77E+60	60.8	-65
200	-94	953	-545	1.44E+60	60.2	-68

Fe(+3a)	Extrapolated from	473.15	K	
S2O3(-2a)	Extrapolated from	473.15	K	
Fe(+2a)	Extrapolated from	473.15	K	
H(+a)	Extrapolated from	473.15	K	
SO4(-2a)	Extrapolated from	473.15	K	

8Fe(+3a) + S(-2a) + 4H2O = 8Fe(+2a) + 8H(+a) + SO4(-2a)

T	deltaH	deltaS	deltaG	K	Log(K)	deltaG
C	kJ	J/K	kJ			kJ/mol Fe(3+)
0	-114	1224	-448	5.31E+85	85.7	-56
25	-141	1126	-477	3.08E+83	83.5	-60
50	-142	1124	-505	3.74E+81	81.6	-63
75	-140	1127	-533	8.61E+79	79.9	-67
100	-137	1137	-561	3.47E+78	78.5	-70
125	-131	1151	-590	2.28E+77	77.4	-74
150	-123	1171	-619	2.34E+76	76.4	-77
175	-111	1198	-648	3.63E+75	75.6	-81
200	-95	1233	-679	8.33E+74	74.9	-85

Fe(+3a)	Extrapolated from	473.15	K	
Fe(+2a)	Extrapolated from	473.15	K	
H(+a)	Extrapolated from	473.15	K	
SO4(-2a)	Extrapolated from	473.15	K	

8. Ferric reduction with metal sulfide solids / precipitate

CuS + 8Fe(+3a) + 4H2O = Cu(+2a) + 8Fe(+2a) + 8H(+a) + SO4(-2a)

T	deltaH	deltaS	deltaG	K	Log(K)	deltaG
C	kJ	J/K	kJ			kJ/mol Fe(3+)
0	45	1061	-244	5.47E+46	46.7	-31
25	14	947	-268	1.05E+47	47.0	-34
50	8	927	-292	1.48E+47	47.2	-36
75	3	912	-315	1.70E+47	47.2	-39
100	-1	901	-337	1.73E+47	47.2	-42
125	-4	895	-360	1.65E+47	47.2	-45
150	-4	893	-382	1.53E+47	47.2	-48
175	-2	898	-405	1.45E+47	47.2	-51
200	3	909	-427	1.45E+47	47.2	-53

Fe(+3a)	Extrapolated from	473.15	K	
Cu(+2a)	Extrapolated from	473.15	K	
Fe(+2a)	Extrapolated from	473.15	K	
H(+a)	Extrapolated from	473.15	K	
SO4(-2a)	Extrapolated from	473.15	K	

Rh2S3 + 24Fe(+3a) + 12H2O = 2Rh(+3a) + 24Fe(+2a) + 24H(+a) + 3SO4(-2a)

T	deltaH	deltaS	deltaG	K	Log(K)	deltaG
C	kJ	J/K	kJ			kJ/mol Fe(3+)
0	372	2882	-415	2.22E+79	79.3	-17
25	298	2809	-480	1.38E+84	84.1	-20
50	298	2811	-545	1.50E+88	88.2	-23
75	303	2825	-611	4.56E+91	91.7	-25
100	313	2854	-877	5.65E+94	94.8	-28
125	331	2898	-744	3.76E+97	97.6	-31
150	357	2762	-812	1.70E+100	100.2	-34
175	394	2648	-882	6.41E+102	102.6	-37
200	446	2961	-955	2.42E+105	105.4	-40

Fe(+3a)	Extrapolated from	473.15	K	
Rh(+3a)	Extrapolated from	300	K	
Fe(+2a)	Extrapolated from	473.15	K	
H(+a)	Extrapolated from	473.15	K	
SO4(-2a)	Extrapolated from	473.15	K	

9. Thiosulphate decomposition to Sulphur and H_2S

S2O3(-2a) + H2O = H2S(g) + SO4(-2a)

T	deltaH	deltaS	deltaG	K	Log(K)	deltaG
C	kJ	J/K	kJ			kJ/mol S2O3(2-)
0	12	117	-20	5654	3.75E+00	-20
25	4	88	-22	6864	3.84E+00	-22
50	3	83	-24	7650	3.88E+00	-24
75	1	79	-26	8077	3.91E+00	-26
100	0	75	-28	8211	3.91E+00	-28
125	-1	72	-30	8116	3.91E+00	-30
150	-3	68	-32	7847	3.90E+00	-32
175	-4	65	-33	7449	3.87E+00	-33
200	-6	82	-35	6959	3.84E+00	-35

S2O3(-2a)	Extrapolated from	473.15	K	
SO4(-2a)	Extrapolated from	473.15	K	

Formula	FM	Conc.	Amount	Amount	Volume

3S2O3(-2a) + H2SO4 = 4S + H2O + 3SO4(-2a)

T	deltaH	deltaS	deltaG	K	Log(K)	deltaG
C	kJ	J/K	kJ			kJ/mol S2O3(2-)
0	-248	-80	-226	2.05E+43	4.33E+01	-75
25	-255	-103	-224	2.05E+39	3.93E+01	-75
50	-256	-106	-222	7.04E+35	3.58E+01	-74
75	-256	-107	-219	7.47E+32	3.29E+01	-73
100	-255	-104	-216	1.98E+30	3.03E+01	-72
125	-248	-86	-214	1.20E+28	2.81E+01	-71
150	-248	-84	-212	1.43E+26	2.82E+01	-71
175	-248	-82	-210	2.85E+24	2.45E+01	-70
200	-248	-80	-208	8.70E+22	2.29E+01	-69

S2O3(-2a)	Extrapolated from	473.15	K	
SO4(-2a)	Extrapolated from	473.15	K	

10. Sulphur trioxide generation

2Rh(+3a) + 3S2O3(-2a) = Rh2S3 + 3SO3(g)

T	deltaH	deltaS	deltaG	K	Log(K)	deltaG
C	kJ	J/K	kJ			kJ/mol S2O3(2-)
0	124	1247	-217	2.63E+41	4.14E+01	-72
25	137	1294	-248	3.41E+43	4.35E+01	-83
50	142	1310	-281	2.70E+45	4.54E+01	-94
75	145	1318	-314	1.26E+47	4.71E+01	-105
100	147	1323	-347	3.68E+48	4.68E+01	-116
125	149	1330	-380	7.35E+49	4.99E+01	-127
150	154	1341	-413	1.10E+51	5.10E+01	-138
175	182	1360	-447	1.34E+52	5.21E+01	-149
200	176	1389	-482	1.46E+53	5.32E+01	-161

Rh(+3a)	Extrapolated from	300	K	
S2O3(-2a)	Extrapolated from	473.15	K	

SO3(g) + H2O = H2SO4

T	deltaH	deltaS	deltaG	K	Log(K)
C	kJ	J/K	kJ		
0	-137	-165	-86	3.35E+16	1.65E+01
25	-132	-170	-82	2.12E+14	1.43E+01
50	-132	-169	-78	3.42E+12	1.25E+01
75	-132	-167	-73	1.01E+11	1.10E+01
100	-131	-166	-69	4.81E+09	9.68E+00
125	-131	-165	-65	3.39E+08	8.53E+00
150	-130	-164	-61	3.31E+07	7.52E+00
175	-130	-163	-57	4.21E+06	6.82E+00
200	-129	-162	-53	6.70E+05	5.83E+00

A.2. Eh-pH Diagrams

At the base case of 95 °C with Cu and S molality of 0.3 mol / kg (~ 20 g/l) and Rh molality of 0.001 mol/ kg (~ 100 mg/l), E^H-pH diagrams are produced for all species in the HSC Chemistry® program database and then deconstructed into dominant S-containing species, dominant Rh-containing and Cu-containing species E^H-pH in separate, less complicated diagrams.

The effect of temperature on the E^H-pH diagram is investigated by constructing combined diagrams for all species at 25 and 150 °C, as well as separating the combined diagram into S-, Cu-, and Rh- containing species diagrams.

The effect of varying molality of the S, Cu and Rh on E^H-pH diagram is demonstrated on the base case at the following molalities:

S: 0.001, 0.01 and 1 mol/kg
Cu: 0.001, 0.01 and 1 mol/kg
Rh: 0.0001, 0.001 and 0.1 mol/kg

Selecting all species in the HSC Chemistry® causes an anomaly in the E^H-pH diagrams, where the stability of the sulphate ion causes Rh and Cu metal to be stable above the respective sulfides, which is not seen in practice. Selected diagrams have been reproduced without any sulphur with oxidation state above zero, and limiting the Rh sulfide species to Rh_2S_3.

Dashed blue lines indicate areas of dominant species in solution. The region of most concern is within the pH range of 0 – 3.

The aquo or sulfato or chloro or aquo-hydroxo complexes are not in the HSC Chemistry® database; thus the pure ionic form has been used. Rh complexing would increase the stability region of the ion and reduce the driving force for the reaction.

1. Additional base case selecting all species at 95 °C

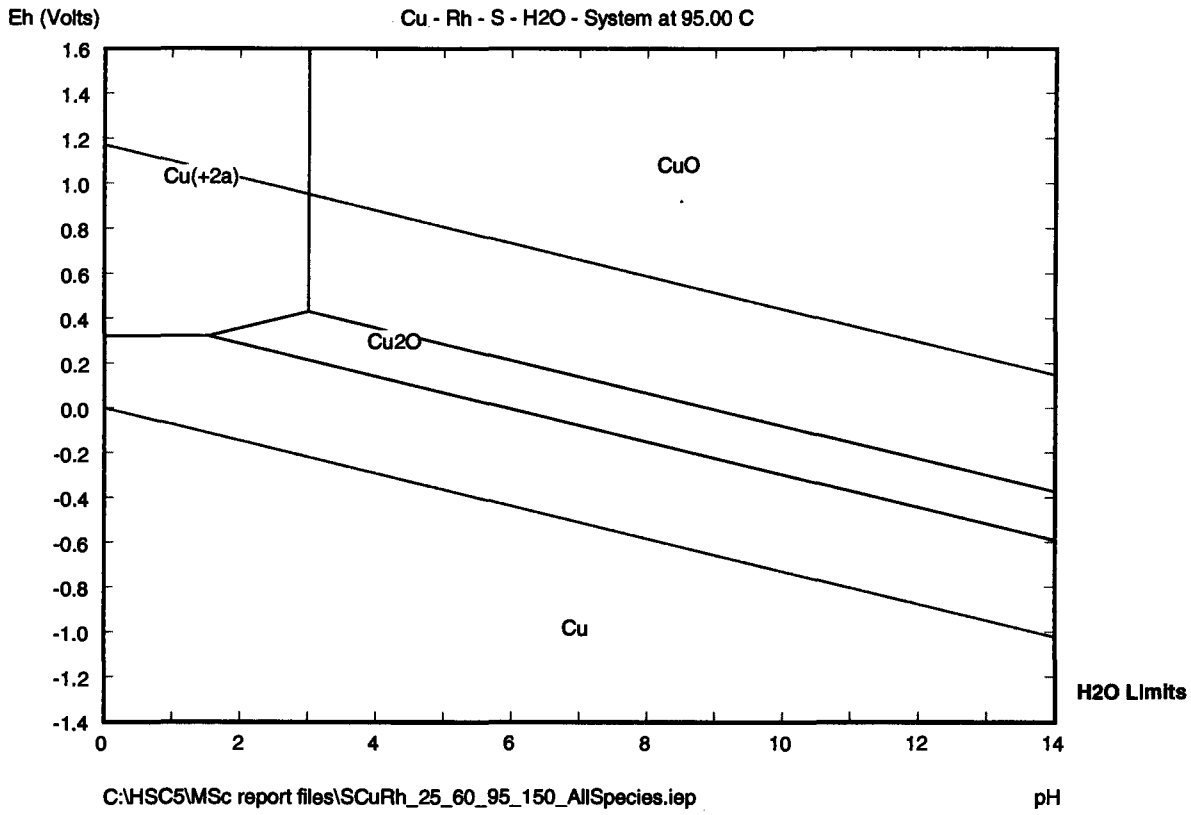

ELEMENTS	Molality	Pressure
S	3.000E-01	1.000E+00
Cu	3.000E-01	1.000E+00
Rh	1.000E-03	1.000E+00

Figure A2.1: E^H-pH diagram of S-Cu-Rh-H_2O base case for all speciation at 95 °C, only showing dominant Cu species; upon reducing the potential with sulfide-containing reducing agent, Cu^{2+} is reduced to metal, though in reality copper sulfide precipitate forms; at high oxidation potential, pH adjustment above 3 will convert Cu^{2+} to CuO, or with addition reducing agent Cu_2O.

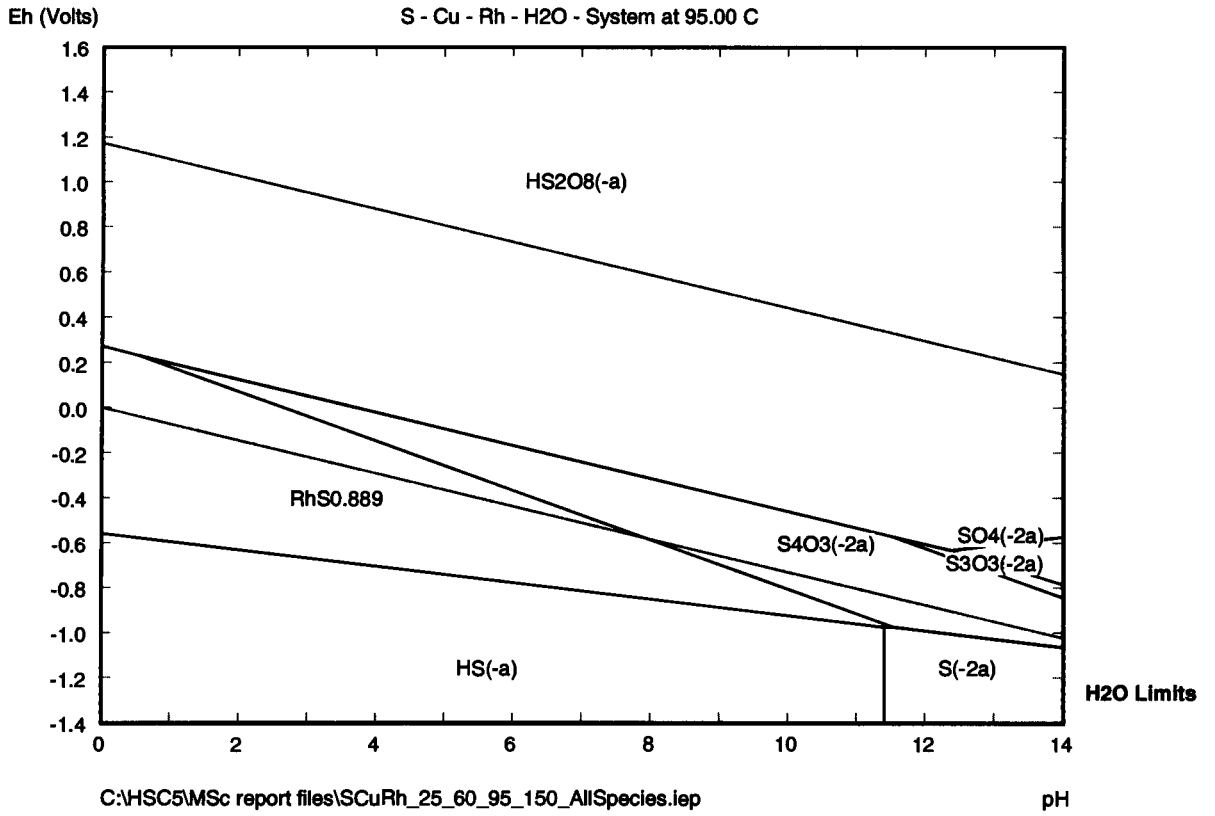

ELEMENTS	Molality	Pressure
S	3.000E-01	1.000E+00
Cu	3.000E-01	1.000E+00
Rh	1.000E-03	1.000E+00

Figure A2.2: E^H-pH diagram of S-Cu-Rh-H_2O base case system for all speciation at 95 °C, only showing dominant S speciation; sulfide is only stable at high pH, thus in this acidic system most sulfide is protonated to HS^- if the potential is low enough, otherwise it will precipitate metal sulfide or reduce metal ions to metal.

2. Additional metastable Eh-pH diagrams

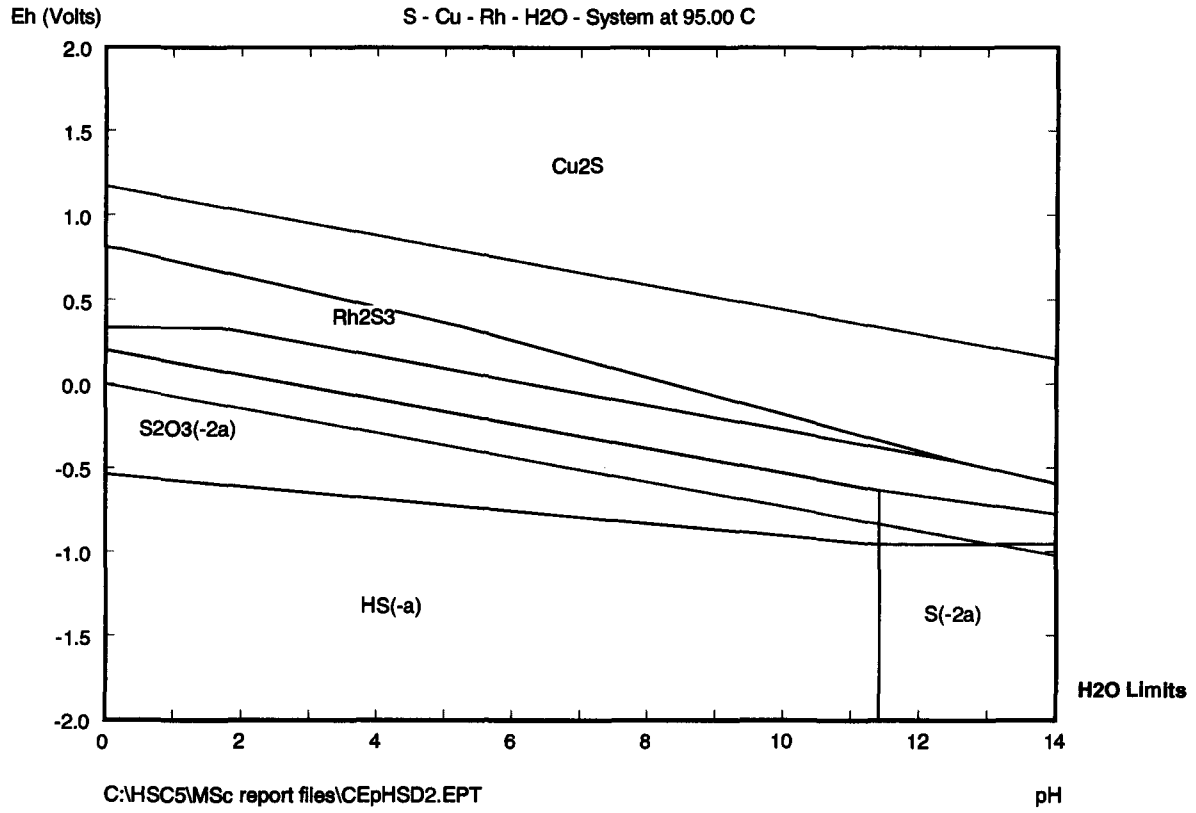

ELEMENTS	Molality	Pressure
S	3.000E-01	1.000E+00
Cu	3.000E-01	1.000E+00
Rh	1.000E-03	1.000E+00

Figure A2.3: E^H-pH diagram of S-Cu-Rh-H_2O metastable system at 95 °C showing dominant S speciation, particularly omitting species with sulphur of positive oxidation state and only including Rh_2S_3. Dashed lines indicate region of dominant ions in solution. Rh^{3+} ion is not shown to be stable, though in practice the ion complexation with water or sulphate increases stability to pH between 2 and 3.

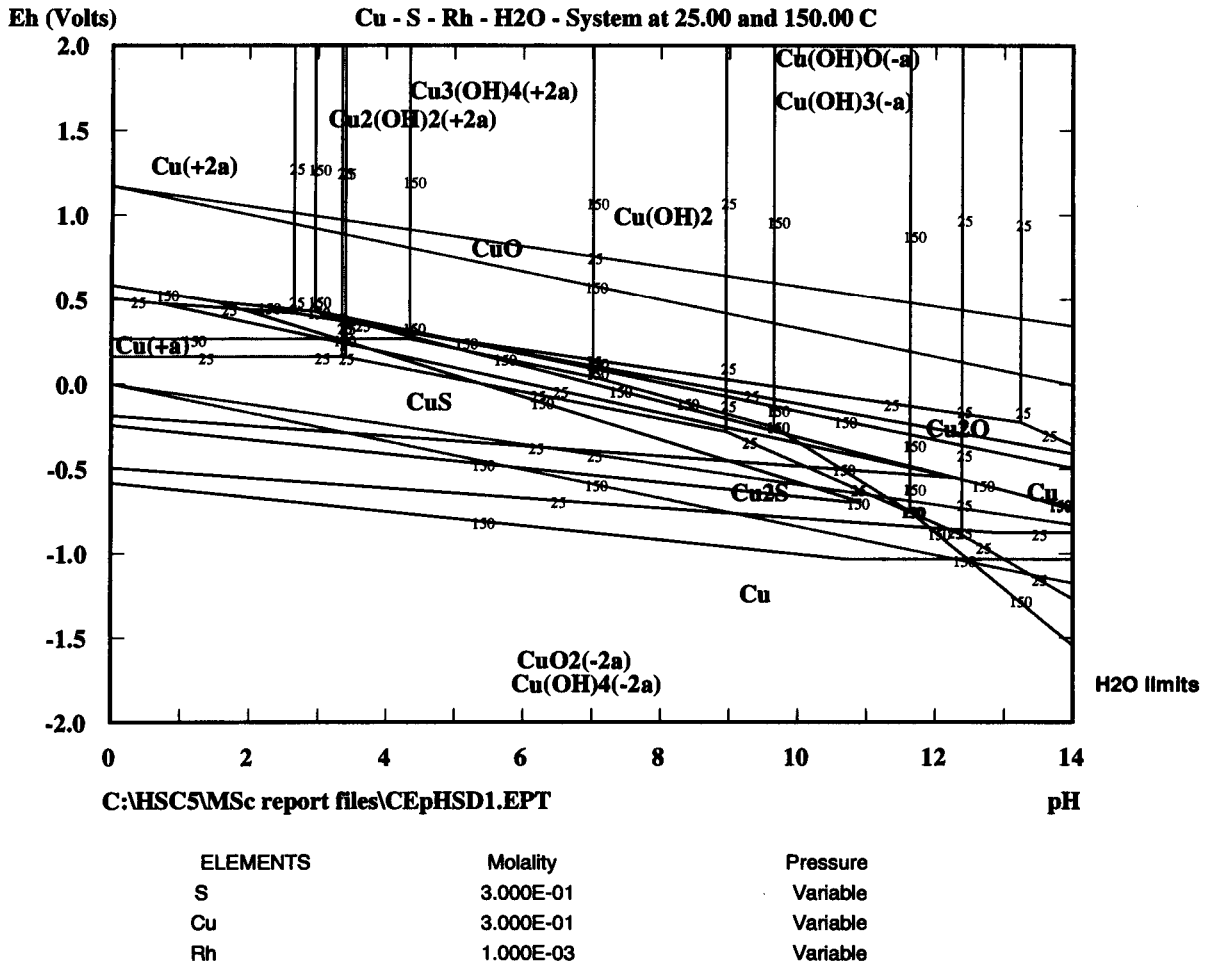

ELEMENTS	Molality	Pressure
S	3.000E-01	Variable
Cu	3.000E-01	Variable
Rh	1.000E-03	Variable

Figure A2.4: E^H-pH diagram of S-Cu-Rh-H_2O metastable system combined for 25 and 150 °C, showing effect of temperature on Cu speciation, particularly omitting species with sulphur of positive oxidation state. Dashed lines indicate region of dominant ions in solution.

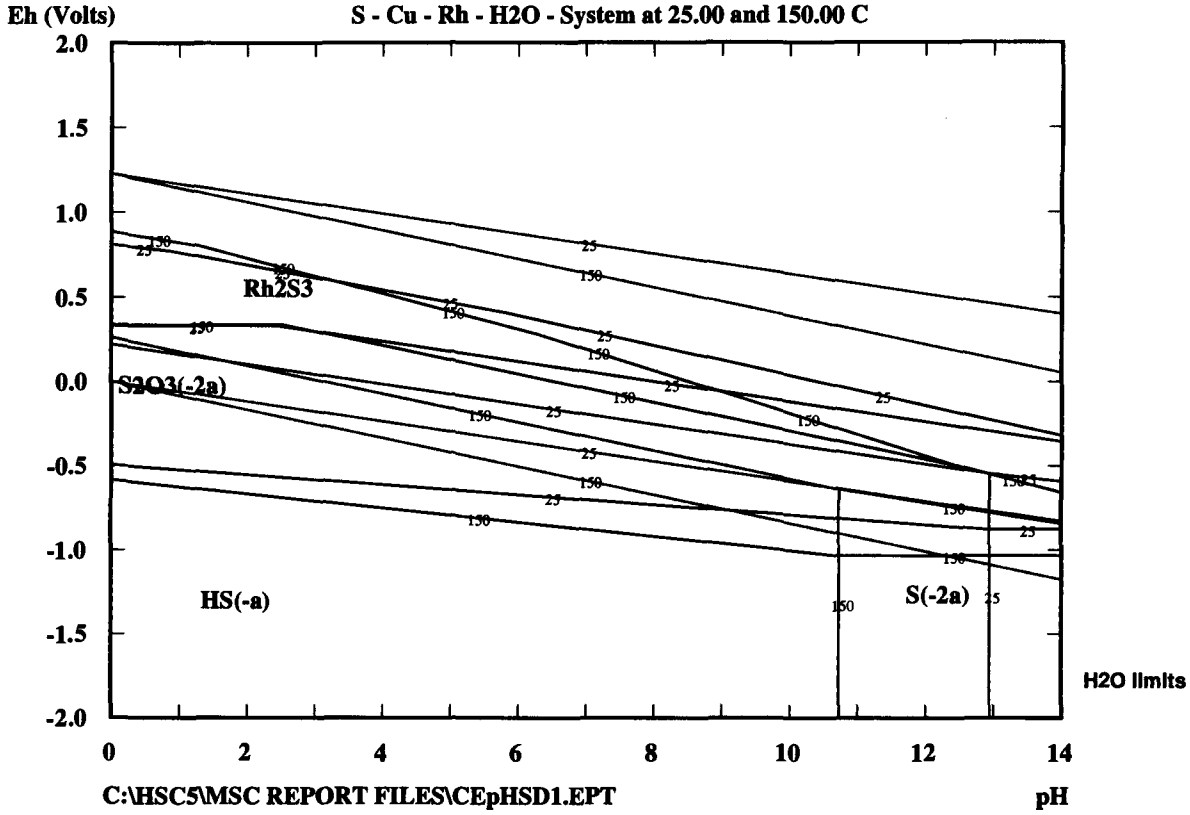

ELEMENTS	Molality	Pressure
S	3.000E-01	Variable
Cu	3.000E-01	Variable
Rh	1.000E-03	Variable

Figure A2.5: E^H-pH diagram of S-Cu-Rh-H_2O metastable system, particularly omitting species with sulphur of positive oxidation state, combined for 25 and 150 °C, showing effect of temperature on S speciation.

A.3. Equilibrium Composition Diagrams

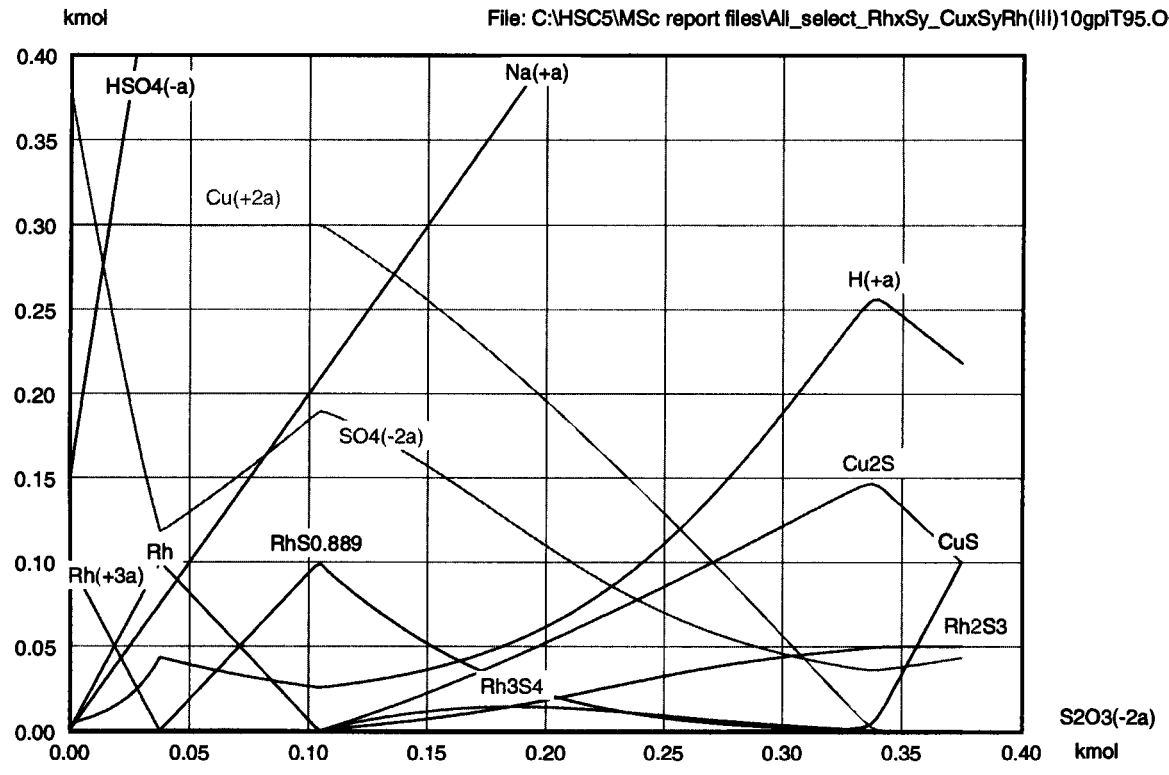

Figure A3.1: Equilibrium composition with thiosulphate addition to 10 g/l Rh containing 20 g/l Cu and 15 g/l sulphuric acid at 95 °C, showing equilibrium composition for case selecting all species; high Rh concentration allows for Rh compound progression from metal through $RhS_{0.889}$ and Rh_3S_4 to Rh_2S_3 is illustrated; Rh precipitation with sulfide is completely selective over Cu precipitation.

APPENDIX B – RESULTS

B.1. Miscellaneous

Molar Masses

Element and Compound	Molar Mass
	gmol
Cu	63.546
Ni	58.693
Fe	55.845
Rh	102.91
Pt	195.09
Pd	106.4
S	32.06
Na	22.99
K	39.098
CuS	95.606
Cu2S	159.152
Na2S2O3.5H2O	248.171
Rh2(SO4)3.xH2O	493.988
PtCl4	336.90
PdCl2	177.31
PtS2	259.21
PdS	138.46
CuSO4.5H2O	249.677
NiSO4.7H2O	280.854
FeSO4	151.901
SO4	96.056
Na2SO4	142.036
K2SO4	174.252
H2SO4	98.072
NaOH	39.997
H2O2	34.0
Rh2S3	302.00
Rh(HS)3	202.09
RhS2.3	176.64
Rh3S4	436.96
RhS1.875	163.02
RhS0.899	131.41

% Element in Cu sulphide compoun

	%S	%Cu
CuS	33.5	66.5
Cu2S	20.1	79.9

% Element in Rh compounds

	%S	%Rh
Rh2S3	31.8	68.2
Rh(HS)3	47.6	50.9
RhS2.3	41.7	58.3
Rh3S4	29.3	70.7
RhS1.875	36.9	63.1
RhS0.899	21.7	78.3

B.2. Experimental Design Details

Experimental Design – List of Tests

	Variables	Range				
1	**Rh concentration [mg/l]**	100	100	100	100	
2	**Temperature [oC]**	50	80	95	150	
3	**Acid effect [g/l]**	15	15	15	15	(Original experimental design reduced due to time and budget constraints)
4	**Reaction time [min]**	1 - 300	1 - 300	1 - 300	1 - 300	
5	**CuS form**	0 , - , +	0 , - , +	0 , - , +	0 , - , +	

CuS form	CuS -: => added from preparation step =>	add 14 g/l thiosulphate to AR quality CuSO4 solution, Solid/Liquid separation and add all solids to test "CuS - " , wash solids to remove adsorbed S(2-), HS(-) etc, dissolved Cu(2+)
	CuS +: => CuS precipitation in situ =>	add 14 g/l thiosulphate directly to test containing Cu(2+) using 15 g/l Na thiosulphate and slight excess Cu(2+)

	Base case:	0 g/l Cu(II), 100 ppm Rh(III), 15 g/l H2SO4 and 14 g/l sodium thiosulphate

Test #	Description		Temp	CuS form	Rh	Time profile (actual samples)	Mineralogy # samples	Mineralogy # samples minimum	XPS	Comments
	Feed Solution			0 g/l Cu(II)	100					AR quality synthetic solution; No Fe addition to avoid possible post precipitation
	Preliminary Tests:									
0-1	Scouting test for material generation		150	ppt in situ		None				
0-2	Rh2S3 seed production		150	0	200 mg/l					
0-3	Produce PdS (or purchase)		85-95	0	100 mg/l Pd	None				Stiochio S(2-) addn; no seed, compare to co-precipitation to measure effect of CuS on Rh pptn rate
	Kinetic Tests:									
1	Ionic Rh precipitation (seeded with PdS)		50	0	100 mg/l	0, 1, 2, 6, 12, 30, 60, 120, 180, 240, 300	1 SEM EDX			Final sample total remaining, mass bal on final only for all tests
2	Ionic Rh precipitation (seeded with PdS)		80	0	100 mg/l	0, 1, 2, 5, 10, 30, 60, 120, 180, 240	1 SEM EDX			Seed to remove induction period and compare autocatyled Rh pptn to other 2 paths ;
3	Ionic Rh precipitation (seeded with PdS)		95	0	100 mg/l	0, 1, 2, 5, 10, 30, 60, 120, 180, 240	1 SEM EDX	1 linescans	1	because fast CuS pptn can act as catalyst for Rh ionic pptn (on CuS)
4	Ionic Rh precipitation (seeded with PdS)		150	0	100 mg/l	0, 1, 2, 4, 7, 10, 20, 30, 60	1 SEM EDX	1 linescans	1	
5	Substitution reaction		50	added	100 mg/l	0, 1, 2, 5, 10, 30, 60, 90, 120, 180, 240, 290	3 SEM EDX			Inject Rh at temperature
6	Substitution reaction		80	added	100 mg/l	0, 1, 2, 5, 10, 30, 60, 90, 120, 180, 240	3 SEM EDX			Inject Rh at temperature
7	Substitution reaction		95	added	100 mg/l	0, 1, 2, 5, 10, 30, 60, 90, 120, 180, 225	3 SEM EDX	1 linescans	1	Inject Rh at temperature
8	Substitution reaction		150	added	100 mg/l	0, 1, 2, 4, 7, 13, 20, 30, 60	1 SEM EDX	1 linescans	1	Inject Rh at temperature
9	Cu and Rh co-pptn in situ		50	ppt in situ	100 mg/l	0, 1, 2, 5, 10, 30, 60, 90, 120, 180, 240, 300	3 SEM EDX			Slow CuS formation, thus Rh(III) induction probable
10	Cu and Rh co-pptn in situ		80	ppt in situ	100 mg/l	0, 1, 2, 5, 10, 30, 60, 90, 120, 180, 240	3 SEM EDX			Fast CuS pptn, thus not Rh(III) pptn induction period
11	Cu and Rh co-pptn in situ		95	ppt in situ	100 mg/l	0, 1, 2, 5, 10, 30, 60, 90, 120, 180, 240	3 SEM EDX	1 linescans	1	
12	Cu and Rh co-pptn in situ		150	ppt in situ	100 mg/l	0, 1, 2, 3, 4, 6, 7, 10, 20, 30, 60	1 SEM EDX	1 linescans	1	
	Repeat tests:									
4R	Ionic Rh precipitation (Not seeded)		150	0	100 mg/l	0, 1, 2, 4, 6, 8, 11, 15, 27				
9R	Cu and Rh co-pptn in situ		50	ppt in situ	100 mg/l	0, 1, 2, 5, 10, 30, 60, 90, 120, 180, 240				
11R	Cu and Rh co-pptn in situ		95	ppt in situ	100 mg/l					
	Additional tests:									
	Substitution reaction at high Rh concn and Rh excess		95	added	~ 1000 mg/l	60				Attempt complete Cu(II) dissolution ; indicate passivation of CuS with Rh sulphide

Test Design Details and Concentrations

Test #	Units		0-1	0-2	0-3	1	2	3	4	5a	5b	6a	6b	7a	7b	8a	8b	9	10	11	12	4 Repeat	9 Repeat	11 Repeat
Reaction type / description			Scouting coprecipitation excess S2-	Produce Rh2S3 seed stiochio S2-	Produce PdS seed stiochio S2-	Rh Ionic pptn excess S2-	Rh Ionic pptn excess S2-	Rh Ionic pptn excess S2-	Rh Ionic pptn excess S2-	CuS pptn excess S2-	Rh Substitution excess S2-	CuS pptn excess S2-	Rh Substitution excess S2-	CuS pptn excess S2-	Rh Substitution excess S2-	CuS pptn excess S2-	Rh Substitution excess S2-	co-pptn excess S2-	co-pptn excess S2-	co-pptn excess S2-	co-pptn excess S2-	Rh Ionic pptn excess S2-	co-pptn excess S2-	co-pptn excess S2-
Temperature	oC		150	150	95	50	80	95	150	50	50	80	80	95	95	150	150	50	80	95	150	150	50	95
Desired feed concentration										assuming filtration step in between														
Rh (desired - not actual)	mg/l		50	200	200	100	100	100	100	0	100	0	100	0	100	0	100	100	100	100	100	100	100	100
Cu	g/l		3	0	0	0	0	0	0	14.23	0	14.23	0	14.23	0	14.23	0	14.23	14.23	14.23	14.23	0	14.23	14.23
Ni	g/l		1	0	0	0	0	0	0	5.51	0	5.51	0	5.51	0	5.51	0	5.51	5.51	5.51	5.51	0	5.51	5.51
Fe	g/l		0	0	0	0	0	0	0	0	0	0	0	0	0	0	0	0	0	0	0	0	0	0
H2SO4	g/l		0	15	15	15	15	15	15	15	15	15	15	15	15	15	15	15	15	15	15	15	15	15
Na	g/l		0	0	0	0	0	0	0	0	0	0	0	0	0	0	0	0	0	0	0	0	0	0
K	g/l		0	1.0	1.0	1.0	1.0	1.0	1.0	1.0	1.0	1.0	1.0	1.0	1.0	1.0	1.0	1.0	1.0	1.0	1.0	1.0	1.0	1.0
pH				0.82	0.82	0.82	0.82	0.82	0.82	0.82	0.82	0.82	0.82	0.82	0.82	0.82	0.82	0.82	0.82	0.82	0.82	0.82	0.82	0.82
Desired make-up Volume	L		4.8	5.2	1	5.2	5.2	5.2	5.2	5.2	5.2	5.2	5.2	5.2	5.2	5.2	5.2	5.2	5.2	5.2	5.2	5.2	5.2	5.2
Actual make-up volume (due to water of x-stal and salt)						5.2	5.2	5.2	5.2	5.4	5.4	5.4	5.4	5.4	5.4	5.4	5.4	5.4	5.4	5.4	5.4	5.4	5.4	5.4
Volume before injection (operating volume)	L		4.6	5.0	1.0	5.0	5.0	5.0	5.0	5.0	5.0	5.0	5.0	5.0	5.0	5.0	5.0	5.0	5.0	5.0	5.0	5.0	5.0	5.0
Desired CuS concn (operating volume)	g/l		4.17	0	0	0	0	0	0	5	5	5	5	5	5	5	5	5	5	5	5	0	5	5
Mass produced (CuS) at t=0	g		20.00	0	0	0	0	0	0	25	0	25	0	25	0	25	0	25.0	25.0	25.0	25.0	0	25.0	25.0
Mass CuS added	g		0	0	0	0	0	0	0	0	25	0	25	0	25	0	25	0	0	0	0	0	0	0
sulphide/Rh(III) at t=0 / injection			80	1.5	1.5	58.1	58.1	58.1	58.1	NA	58.1	NA	58.1	NA	58.1	NA	58.1	55.8	55.8	55.8	55.8	58.1	55.8	55.8
Seed (PdS)	mg		none	none	none	25	25	25	25	none	none	none	none	none	none	none	none	none	none	none	none	none	none	none
Reagents required for make-up volume		% purity																						
Cu stiochio	g		13.3	0.0	0.0	0.0	0.0	0.0	0.0	16.6	0.0	16.6	0.0	16.6	0.0	16.6	0.0	16.6	16.6	16.6	16.6	0.0	16.6	16.6
Cu stiochio	g/l		2.8	0.0	0.0	0.0	0.0	0.0	0.0	3.2	0.0	3.2	0.0	3.2	0.0	3.2	0.0	3.2	3.2	3.2	3.2	0.0	3.2	3.2
CuSO4 stiochio			52.7	0.0	0.0	0.0	0.0	0.0	0.0	65.9	0.0	65.9	0.0	65.9	0.0	65.9	0.0	65.9	65.9	65.9	65.9	0.0	65.9	65.9
CuSO4.5H2O	g	99	57.2	0.0	0.0	0.0	0.0	0.0	0.0	293.6	0.0	293.6	0.0	293.6	0.0	293.6	0.0	293.6	293.6	293.6	293.6	0.0	293.6	293.6
NiSO4 .7H2O	g	98	23.4	0.0	0.0	0.0	0.0	0.0	0.0	139.9	0.0	139.9	0.0	139.9	0.0	139.9	0.0	139.9	139.9	139.9	139.9	0.0	139.9	139.9
FeSO4	g	99	0.00	0.00	0.00	0.00	0.00	0.00	0.00	0.00	0.00	0.00	0.00	0.00	0.00	0.00	0.00	0.00	0.00	0.00	0.00	0.00	0.00	0.00
Na2SO4	g	99	0.00	0.00	0.00	0.00	0.00	0.00	0.00	0.00	0.00	0.00	0.00	0.00	0.00	0.00	0.00	0.00	0.00	0.00	0.00	0.00	0.00	0.00
K2SO4	g	99	0.00	11.70	2.25	11.70	11.70	11.70	11.70	11.70	11.70	11.70	11.70	11.70	11.70	11.70	11.70	11.70	11.70	11.70	11.70	11.70	11.70	11.70
Reagents at temp before injection																								
Cu stiochio	g		13.3	0.0	0.0	0.0	0.0	0.0	0.0	16.6	0.0	16.6	0.0	16.6	0.0	16.6	0.0	16.6	16.6	16.6	16.6	0.0	16.6	16.6
Cu stiochio in solids	g/l		2.8	0.0	0.0	0.0	0.0	0.0	0.0	3.3	0.0	3.3	0.0	3.3	0.0	3.3	0.0	3.3	3.3	3.3	3.3	0.0	3.3	3.3
Cu stiochio			52.7	0.0	0.0	0.0	0.0	0.0	0.0	65.9	0.0	65.9	0.0	65.9	0.0	65.9	0.0	65.9	65.9	65.9	65.9	0.0	65.9	65.9
CuSO4	g	99	57.2	0.0	0.0	0.0	0.0	0.0	0.0	282.3	0.0	282.3	0.0	282.3	0.0	282.3	0.0	282.3	282.3	282.3	282.3	0.0	282.3	282.3
NiSO4	g	98	23.4	0.0	0.0	0.0	0.0	0.0	0.0	134.5	0.0	134.5	0.0	134.5	0.0	134.5	0.0	134.5	134.5	134.5	134.5	0.0	134.5	134.5
FeSO4	g	99	0.00	0.00	0.00	0.00	0.00	0.00	0.00	0.00	0.00	0.00	0.00	0.00	0.00	0.00	0.00	0.00	0.00	0.00	0.00	0.00	0.00	0.00
Na2SO4	g	99	0.00	0.00	0.00	0.00	0.00	0.00	0.00	0.00	0.00	0.00	0.00	0.00	0.00	0.00	0.00	0.00	0.00	0.00	0.00	0.00	0.00	0.00
K2SO4	g	99	0.00	22.51	4.50	22.51	22.51	22.51	22.51	22.51	22.51	22.51	22.51	22.51	22.51	22.51	22.51	22.51	22.51	22.51	22.51	22.51	22.51	22.51
Na2S2O3.5H2O for CuS	g	99	52.4	0.0	0.0	0.0	0.0	0.0	0.0	65.5	0.0	65.5	0.0	65.5	0.0	65.5	0.0	65.5	65.5	65.5	65.5	0.0	65.5	65.5
Na2S2O3.5H2O for Rh2(SO4)3	g	99	0.00	3.51	3.65	1.76	1.76	1.76	1.76	1.76	0	1.76	0	1.76	0	1.76	0	1.76	1.76	1.76	1.76	1.76	1.76	1.76
Na2S2O3.5H2O mass addn	g theoretic	99	53.308	3.513	3.654	1.757	1.757	1.757	1.757	67.306	0.000	67.306	0.000	67.306	0.000	67.306	0.000	67.306	67.306	67.306	67.306	1.757	67.306	67.306
Na2S2O3.5H2O theoretical	g/l feed		11.1	0.70	3.65	0.35	0.4	0.4	0.4	13.5	0.0	13.5	0.0	13.5	0.0	13.5	0.0	13.461	13.5	13.5	13.5	0.4	13.461	13.5
Na2S2O3.5H2O actual	g/l added		11.5	*0.70*	*3.65*	*13.5*	*13.5*	*13.5*	*13.5*	*13.5*	*0.0*	*13.5*	*0.0*	*13.5*	*0.0*	*13.5*	*0.0*	*13.5*	*13.5*	*13.5*	*13.5*	*13.5*	*13.5*	*13.5*
Na2S2O3.5H2O actual added	g		55.2	3.5	3.7	67.3	67.3	67.3	67.3	67.3	0.0	67.3	0.0	67.3	0.0	67.3	0.0	64.7	64.7	64.7	64.7	67.3	64.7	64.7
Make-up conc	g/l		500	500	500	500	500	500	500	500	500	500	500	500	500	500	500	500	500	500	500	500	500	500
Volume reagent	mL		23.0	0.0	0.0	0.0	0.0	0.0	0.0	131.1	0.0	131.1	0.0	131.1	0.0	131.1	0.0	131.1	131.1	131.1	131.1	0.0	131.1	131.1
Volume reagent set at 150 mL + water of x	mL		100	100	100	190	190	190	190	190	100	190	100	190	100	190	100	190	190	190	190	190	190	190
Actual make-up conc				35	37	354	354	354	354	354	0	354	0	354	0	354	0	341	341	341	341	354	341	341
Rh stock	g/l		10	10	10	10	10	10	10	10	10	10	10	10	10	10	10	10	10	10	10	10	10	10
Rh stock H2SO4	%		10	10	10	10	10	10	10	10	10	10	10	10	10	10	10	10	10	10	10	10	10	10
Rh mass per test (feed volume)	g			1.00	1.00	0.50	0.50	0.50	0.50	0.00	0.50	0.00	0.50	0.00	0.50	0.00	0.50	0.50	0.50	0.50	0.50	0.50	0.50	0.50
Rh mass per test (t=0 ;operating volume)	g		0.25	0.95	1.00	0.48	0.48	0.48	0.48	0.00	0.50	0.00	0.48	0.00	0.48	0.00	0.48	0.48	0.48	0.48	0.48	0.48	0.48	0.48
Rh2(SO4)3 (operating volume)	g	100	1.20	4.82	4.80	2.31	2.31	2.31	2.31	0.00	2.40	0.00	2.31	0.00	2.31	0.00	2.31	2.31	2.31	2.31	2.31	2.31	2.31	2.31
Rh2S3 formed (max)	g		0.73	2.82	2.93	1.41	1.41	1.41	1.41	0.00	1.47	0.00	1.41	0.00	1.41	0.00	1.41	1.41	1.41	1.41	1.41	1.41	1.41	1.41
Volume Rh stock soln required	mL		0.024	104.0	20.0	52.0	52.0	52.0	52.0	0.0	52.0	0.0	52.0	0.0	52.0	0.0	52.0	52.0	52.0	52.0	52.0	52.0	52.0	52.0
Volume Rh stock soln pipetted (actual)	mL		25	*100.0*	*100.0*	*50.0*	*50.0*	*50.0*	*50.0*	*0.0*	*50.0*	*0.0*	*50.0*	*0.0*	*50.0*	*0.0*	*50.0*	*50.0*	*50.0*	*50.0*	*50.0*	*50.0*	*50.0*	*50.0*
Rh actual mass added	g		0.3	1.0	1.0	0.5	0.5	0.5	0.5	0.0	0.5	0.0	0.5	0.0	0.5	0.0	0.5	0.5	0.5	0.5	0.5	0.5	0.5	0.5
Rh actual concn	mg/l		52	192	1000	96	96	96	96	0	96	0	96	0	96	0	96	96	96	96	96	96	96	96
Acid concn feed from Rh stock	g/l		0.50	2.06	2.00	1.04	1.04	1.04	1.04	0.00	1.04	0.00	1.04	0.00	1.04	0.00	1.04	1.04	1.04	1.04	1.04	1.04	1.04	1.04
Extra acid required	g	98	-2.4	66.6	13.3	74.1	74.1	74.1	74.1	79.6	74.1	79.6	74.1	79.6	74.1	79.6	74.1	74.1	74.1	74.1	74.1	74.1	74.1	74.1
Na final conc TfE	g/l		2.06	0.13	0.68	2.49	2.49	2.49	2.49	2.49	0.00	2.49	0.00	2.49	0.00	2.49	0.00	2.40	2.40	2.40	2.40	2.49	2.40	2.40
K final conc TfE	g/l		0.00	1.00	1.00	1.00	1.00	1.00	1.00	1.00	1.00	1.00	1.00	1.00	1.00	1.00	1.00	1.00	1.00	1.00	1.00	1.00	1.00	1.00
Solids g/l predicted	g/l		4.32	0.56	2.93	0.28	0.28	0.28	0.28	5.00	0.29	5.00	0.28	5.00	0.28	5.00	0.28	5.28	5.28	5.28	5.28	0.28	5.28	5.28
NaOH to neutralise acid in Rh stock	g	100	1.96	8.82	1.63	4.41	4.41	4.41	4.41	0.00	4.41	0.00	4.41	0.00	4.41	0.00	4.41	4.41	4.41	4.41	4.41	4.41	4.41	4.41
Cu leached (maximum)	mg/l										92.6		92.6		92.6		92.6							
Theoretical Rh % in CuS (100% pptn)			1.2	100.0	100.0	100.0	100.0	100.0	100.0	0.0	1.9	0.0	1.9	0.0	1.9	0.0	1.9	1.9	1.9	1.9	1.9		1.9	1.9
Excess: sulphide/Rh mass ratio				1.5	1.5	55.8	55.8	55.8	55.8		55.8		55.8		55.8		55.8	53.7	53.7	53.7	53.7		53.7	53.7
Excessive S2- in soln				0.0	0.0	0.27	0.27	0.27	0.27															
Excess: sulphide/Rh mole ratio				19	19	37	37	37	0		0		0		0		36	36	36	37	36			

Actual Conditions and Concentrations of Executed Test Runs

Test #	Units		1	2	3	4	4 Repeat	5a	5b	6a	6b	7a	7b	8a	8b	9	9 Repeat	10	11	11 Repeat	12	0-1	0-2	0-3
Reaction type / description			Rh Ionic pptn excess S2-	Rh Ionic pptn excess S2-	Rh Ionic pptn excess S2-	Rh Ionic pptn excess S2-	Rh Ionic pptn excess S2-	CuS pptn excess S2-	Rh Substitution excess S2-	CuS pptn excess S2-	Rh Substitution excess S2-	CuS pptn excess S2-	Rh Substitution excess S2-	CuS pptn excess S2-	Rh Substitution excess S2-	co-pptn excess S2-	co-pptn excess S2-	co-pptn excess S2-	co-pptn excess S2-	co-pptn excess S2-	co-pptn excess S2-	Scouting co precipitation excess S2-	Rh2S3 seed Stiochio S2-	PdS seed Stiochio S2-
Temperature	oC		50	80	95	150	150	50	50	80	80	95	95	150	150	50	50	80	95	95	150	150	150	85-95
Volumes																								
Total make-up volume	L		5.20	5.20	5.20	5.20	5.20	5.40	5.20	5.40	5.20	5.40	5.40	5.40	5.20	5.40	5.00	5.40	5.40	5.40	5.40	4.80	5.20	1.00
Volume at t=0	L		4.99	5.00	5.00	5.00	5.03	5.19	4.97	5.15	5.01	5.20	5.22	5.19	5.00	5.21	4.83	5.27	5.20	5.20	5.20	4.80	5.00	1.00
Volume injected	mL		190.0	190.0	190.0	190.0	190.0	190.0	100.0	150.0	100.0	190.0	100.0	190.0	150.0	190.0	190.0	190.0	190.0	190.0	190.0	100.0	100.0	0.0
Volume Rh stock soln pipetted (actual)	mL		50.0	50.0	50.0	50.0	50.0	0.0	50.0	0.0	50.0	0.0	50.0	0.0	50.0	50.0	50.0	50.0	50.0	50.0	50.0	50.0	100.0	100.0
Feed volume after injection before reaction	L		5.184	5.192	5.188	5.188	5.218	5.380	5.120	5.300	5.158	5.390	5.368	5.380	5.203	5.396	5.020	5.462	5.390	5.393	5.392	4.900	5.100	1.000
Masses added		% purity																						
PdS seed			25.00	25.00	25.00	25.00	none	none	none	none	none	none	none	none	none	none	none	none	none	none	none	none	none	none
CuSO4.5H20 added to make-up volume		99	0.00	0.00	0.00	0.00	0.00	293.60	0.00	293.60	0.00	293.60	0.00	293.60	0.00	293.60	293.60	293.60	293.60	293.60	293.60	38.50	0.00	0.00
NiSO4 added to make-up volume		98	0.00	0.00	0.00	0.00	0.00	139.90	0.00	139.90	0.00	139.90	0.00	139.90	0.00	139.90	139.90	139.90	139.90	139.90	139.90	12.91	0.00	0.00
FeSO4 added to make-up volume		99	0.00	0.00	0.00	0.00	0.00	0.00	0.00	0.00	0.00	0.00	0.00	0.00	0.00	0.00	0.00	0.00	0.00	0.00	0.00	0.00	0.00	0.00
K2SO4 added to make-up volume		99	11.70	11.70	11.70	11.70	11.70	11.70	11.70	11.70	11.70	11.70	11.70	11.70	11.70	11.70	11.70	11.70	11.70	11.70	11.70	0.00	2.25	0.00
Na2S2O3.5H2O added at t=0		98	67.31	67.31	67.31	67.31	67.31	67.31	0.00	67.31	0.00	67.31	0.00	67.31	0.00	64.72	64.72	64.72	64.72	64.72	64.72	55.20	3.65	0.30
H2SO4 to make-up		98	74.07	74.07	74.07	74.07	74.07	76.30	77.37	76.30	74.12	76.30	74.12	79.59	74.07	74.07	74.07	74.07	74.07	74.07	74.07	0.00	100.00	0.00
Rh		100	500	500	500	500	500	0	500	0	500	0	500	0	500	500	500	500	500	500	500	500	1000	1000
Acid in Rh			5	5	5	5	5	0	5	0	5	0	5	0	5	5	5	5	5	5	5	5	10	10
Feed Make-up Concentrations:																								
Cu	mg/l		0	0	0	0	0	13700	0	13700	0	13700	0	13700	0	13700	14796	13700	13700	13700	13700	1916	0	0
Ni	mg/l		0	0	0	0	0	5306	0	5306	0	5306	0	5306	0	5305	5730	5306	5306	5306	5306	551	0	0
Fe	mg/l		0	0	0	0	0	0	0	0	0	0	0	0	0	0	0	0	0	0	0	0	0	0
K	mg/l		1000	1000	1000	1000	1000	983	1000	983	1000	983	983	983	1000	963	1040	983	983	983	983	0	192	0
H2SO4	g/l		14.0	14.0	14.0	14.0	14.0	13.8	14.8	13.8	14.0	13.8	13.5	14.4	14.0	13.4	14.5	13.4	13.4	13.4	13.4	0.0	18.8	0.0
Solids	g/l		0.00	0.00	0.00	0.00	0.00	0.00	4.81	0.00	4.81	0.00	4.63	0.00	4.81	0.00	0.00	0.00	0.00	0.00	0.00	0.00	0.00	0.00
Rh (measured prior to injection and dilu	mg/l		98.9	93.8	96.9	98.2	102.0	0.0	96.2	0.0	96.2	0.0	92.8	0.0	96.2	103.0	111.0	104.0	102.0	94.8	92.6	104.2	173.0	1000.0
Na to be added	g/l		2350	2350	2350	2350	2350	2263	0	2263	0	2263	0	2263	0	2176	2350	2176	2176	2176	2176	2088	128	54
Concentrations after injection before reaction:																								
Cu	g/l		0	0	0	0	0	13216	0	13312	0	13217	0	13216	0	13217	14236	13223	13217	13217	13217	1877	0	0
Ni	g/l		0	0	0	0	0	5118	0	5156	0	5119	0	5118	0	5119	5513	5121	5119	5119	5119	540	0	0
Fe	g/l		0.00	0.00	0.00	0.00	0.00	0.00	0.00	0.00	0.00	0.00	0.00	0.00	0.00	0.00	0.00	0.00	0.00	0.00	0.00	0.00	0.00	0.00
K	mg/l		983	963	963	983	983	929	971	936	971	929	936	929	962	929	1001	929	929	929	929	0	189	0
Na	g/l		2264	2264	2264	2264	2265	2183	0	2199	0	2183	0	2183	0	2099	2261	2100	2099	2099	2099	2045	125	54
H2SO4	g/l		14.41	14.41	14.41	14.41	14.41	13.36	15.13	13.46	14.53	13.36	14.01	13.93	14.36	13.90	14.96	13.89	13.90	13.90	13.90	1.02	20.44	10.00
Rh	mg/l		95.3	90.2	93.4	92.6	98.3	0.0	93.3	0.0	93.4	0.0	90.0	0.0	92.5	99.4	106.8	100.4	98.4	91.5	89.3	102.0	189.6	1000.0
Solids	g/l		0.28	0.26	0.27	0.27	0.00	0.00	4.67	0.00	4.67	0.00	4.50	0.00	4.62	0.00	0.00	0.00	0.00	0.00	0.00	0.00	0.00	0.00
Dilution factor			0.96	0.963	0.963	0.963	0.964	0.971	0.971	0.971	0.971	0.972	0.972	0.972	0.962	0.965	0.962	0.965	0.965	0.965	0.965			
Final filtrate 5a-8a	mg/l							10012		10060		10019		10012										

B.3. Solid and Solution Assays

1. Solids Assays

Solids assay list with replicate and repeat analyses

Sample #	Solid Concentration Cu (%)	Ni (%)	S (%)	Na (%)	K (%)	Rh (%)	Sum %	Comment
Rh/0-2/245/S1	NR	NR	55.5	0.05	0.15	16.10		
Rh/0-2/245/S1 rep				0.05	0.14	16.64		
Rh/0-2/245/S1 avg	Fe contamination		55.5	0.05	0.145	16.37		
Rh/1307/1/ 240/S1-Insuff	i.s.	i.s.	i.s.	i.s.	i.s.			
Rh/1307/1/ 300/S2	< 0.05	< 0.05	91.4	NR	NR	1.08	92	
Rh/1307/1/ 300/S2 rep						1.08		
Rh/1/300/S1 repeat	0.07	NR	98.2	NR	NR	1.59	100	
Rh/1/300/S1 repeat rep						1.40		
Rh/1307/1/ 300/S2 avg	0.06	< 0.05	94.8	NR	NR	1.27	96	
1207/2/ 180/S1-Insuff	i.s.	i.s.	i.s.	i.s.	i.s.			
1207/2/ 240/S2			80.6	0.31	0.03	2.89	84	stats & mass bal;#1-#4 S>90%
1207/2/ 240/S2				0.32	0.03	2.81		
Rh/2/240/S repeat	0.19		94.9			3.77		
Rh/2/240/S repeat rep.			94.9					
Rh/1207/2/ 240/S2 avg	0.19	NR	94.9	0.32	0.03	3.16	99	
1107/3/ 180/S2-Insuff	i.s.		i.s.		i.s.			
Rh/1107/3/ 240/S1	2.42	NR	79.1	NR	NR	3.36		stats & mass bal;#1-#4 S>90%
Rh/1107/3/ 240/S1 rep						3.11		
Rh/3/240/S3 repeat	2.25		91.8			4.70	99	
Rh/3/240/S3 repeat rep.						4.72		
Rh/1107/3/ 240/S1 avg	2.34	NR	91.8	NR	NR	3.97	96	0.74% std dev on Rh
Rh/2107/4/60/S1	N.R.	N.R.	N.R.	N.R.	N.R.	N.R.		
Rh/1508/ 4R/S1	NR	NR	95.2	NR	NR	2.18	97	
Rh/2806/5b/ TO/S1	i.s.	NR	25.8	NR	NR	0.01		
2806/5b/ 290/S2	41.5		25.8			0.36	68	Cu very low; no S precipitation
2806/5b/ 290/S2	42.0					0.37		
Rh/5b/290/S repeat	33.5		25.3			0.50		
Rh/5b/ 290/S2 avg	39.0	NR	25.6	NR	NR	0.41	65	Cu very low;
Rh/0307/6b/TO/S1	64.3	NR	28.1	NR	NR	< 0.05		
0307/6b/TO/S1						< 0.05		
Rh/0307/6b/TO/S1 avg	64.3	NR	28.1	NR	NR	< 0.05	92	
0307/6b/ 240/S2	48	NR	27.6			0.87	72	feed and repeat correspond
0307/6b/ 240/S2 rep.						0.94		stats, mineralogy & mass bal
Rh/6b/240/S repeat	61.9	NR	27.2	NR	NR	1.02	90	
Rh/6b/ 240/S2 avg	61.9	NR	27.5	NR	NR	0.94	90	
Rh/2306/7b/ t0/S	NR	NR	NR	NR	NR	NR		
Rh/2306/7b/ 225/S			28.2	0.01	0.02	1.22		
2306/7b/ 225/S dup	i.s.		29.3			1.08		
Rh/7b/225/S repeat	64.2		28.5			1.45	94	
Rh/7b/ 225/S avg	64.2	NR	28.7	0.01	0.02	1.25	94	
Rh/1907/6b/ 0/S1	42.8	0.05	NR	NR	NR	NR		
1907/8b/ 0/S1-Insuff			i.s.		i.s.			
1907/8b/ 60/S2	42.6	< 0.05	33.9	NR	0.01	2.31		stats, mineralogy & mass bal
1907/8b/ 60/S2 rep	44.7	< 0.05			0.01	1.98		stats, mineralogy & mass bal
Rh/8b/60/S repeat	58.7		34.0	NR	NR	2.33	95	
Rh/8b/60/S repeat rep.	58.4							
Rh/8b/ 60/S2 avg	58.6	< 0.05	34.0	NR	0.01	2.21	95	
0607/9/ 30/S1	i.s.	i.s.	22.7		i.s.			
0607/9/ 300/S2	62.9	0.07	27.8			0.828		
0607/9/ 300/S2 rep	62.9	0.09				0.795		
Rh/9/300/S repeat	58.1	NR	33.3	NR	NR	1.004	67	stats, mineralogy & mass balance
Rh/9/ 300/S2 avg	62.9	0.08	30.6	NR	NR	0.811	94	
Rh/1508/ 9R/S2	69.2		26.7			0.209		
Rh/1508/ 9R/S2						0.216		
Rh/1508/ 9R/S2 avg	69.2	NR	26.7	NR	NR	0.213	96	
0507/10/ 2/S1	i.s.	i.s.	23.9		i.s.			
0507/10/ 240/S2	62.1	0.07	32.7	NR	0.03	0.795	96	
0507/10/ 240/S2						0.760		
Rh/10/240/S repeat	59.0		31.6			0.922		
Rh/10/ 240/S2 avg	60.6	0.07	32.2	NR	0.0	0.826	94	
0407/11/ 1/S1								
Rh/0407/11/240/S2	42.7	0.07	32.1	0.22	0.02	0.98	76	stats, mineralogy & mass balance
0407/11/240/S2 rep			32.1			0.93		
Rh/11/240/S repeat	58.8	NR	30.9	NR	NR	1.24		
Rh/11/240/S repeat rep.	58.3	NR	30.8	NR	NR			
Rh//11/240/S2 avg	58.6	0.07	31.5	0.22	0.02	1.05	91	
Rh/11R/240/ S1	64.9	0.05	31.0	NR	NR	0.68		
Rh/11R/240/ S1 rep	64.2	0.05	31.0	NR	NR	0.92		
Rh/11R/240/ S1 avg	64.6	0.1	31.0	NR	NR	0.90	97	
Rh/2007/12/ 1/S1	42.6	< 0.05	i.s.	NR	NR	i.s.		
Rh/2007/12/ 60/S2	44.6	< 0.05	29.6	NR	NR	1.94		mineralogy & mass balance
Rh/12/60/S repeat	64.3	NR	30.3	NR	NR	1.82	100	Mass balance
Rh/12/60/S avg	64.3	< 0.05	30.0	NR	NR	1.94	96	

Note:
i.s. = insufficient solid mass for analysis
= analysis disregarded for reasons stated in "Comments" column.
stats => statistical outlier mineralogy => CuS shown in previous test work for similar conditions
mass balance => disregarding value improves overall mass balance and accountability; sum of assays closer to 100%

Solids assay finalised values used in study

Testing Cu outliers for significance for exclusion in finalised list above

x_1	x_2	$(x_1-x_{1,ave})^2$	$(x_2-x_{2,ave})^2$
64.3	43	1.44	0.00
61.9			

Average x_i	63.1	43.0
n_i	2	1
s_i	1.697	
S	1.697	
t	9.671	
DOF	1	
Significance	93.44	two-sided
95% confidence limits	2.35	
Significance	**98.7**	**one-sided**
90% confidence limits	1.97	

x_1	x_2	$(x_1-x_{1,ave})^2$	$(x_2-x_{2,ave})^2$
64.3	46.5	5.65	0.00
61.9		0.00	
64.2		5.18	
58.7		10.39	
58.4		12.41	
62.9		0.95	
62.9		0.95	
69.2		52.95	
62.1		0.03	
59.0		8.54	
58.8		9.75	
58.3		13.13	
64.3		5.65	

Average x_i	61.9	46.5
n_i	13	1
s_i	3.235	
S	3.235	
t	4.594	
DOF	12	
Significance	99.94	two-sided
95% confidence limits	1.76	
Significance	100.0	one-sided
90% confidence limits	1.48	

Testing Sulphur outliers for significance for exclusion

x_1	x_2	$(x_1-x_{1,ave})^2$	$(x_2-x_{2,ave})^2$
91.4	79.1	9.00	0.00
98.2			
94.9			
94.9			
91.8			
95.2			

Average x_i	94.4	79.1
n_i	5	1
s_i	2.765	
S	2.765	
t	5.052	
DOF	4	
Significance	99.28	two-sided
95% confidence limits	2.42	
Significance	**99.6**	**one-sided**
90% confidence limits	2.03	

x_1	x_2	$(x_1-x_{1,ave})^2$	$(x_2-x_{2,ave})^2$
94.9	80.6	0.00	0.00
94.89			

Average x_i	94.9	80.6
n_i	2	1
s_i	0.007	
S	0.007	
t	1650.644	
DOF	1	
Significance	99.96	two-sided
95% confidence limits	0.01	
Significance	**100.0**	**one-sided**
90% confidence limits	0.01	

Finalised solids assay summary list

Sample #	Solid Concentration							Comment
	Cu (%)	Ni (%)	S (%)	Na (%)	K (%)	Rh (%)	Sum (%)	
Rh/1307/1/ 300/S2 avg	*0.05*	*0.05*	94.8	NR	NR	1.27	96	
Rh/1207/2/ 240/S2 avg	0.19	NR	94.9	0.32	0.03	3.16	99	
Rh/1107/3/ 240/S1 avg	2.34	NR	91.8	NR	NR	3.97	98	
Rh/2107/4/60/S1	N.R.	N.R.	N.R.	N.R.	N.R.	N.R.		
Rh/1508/ 4R/S1	NR	NR	95.2	NR	NR	2.18	97	
Rh/2806/5b/ TO/S1	i.s.	NR	25.8	NR	NR	0.01	26	
Rh/5b/ 290/S2 avg	39.0	NR	25.6	NR	NR	0.41	65	
Rh/0307/6b/TO/S1 avg	64.3	NR	28.1	NR	NR	*0.05*	92	
Rh/6b/ 240/S2 avg	61.9	NR	27.5	NR	NR	0.94	90	
Rh/2306/7b/ t0/S	NR	NR	NR	NR	NR	0.03		Rh avg of 5b and 6b t=0
Rh/7b/ 225/S avg	64.2	NR	28.7	0.01	0.02	1.25	94	
Rh/1907/8b/ 0/S1	58.6	0.05	34.0	NR	NR	0.03	93	Assume 8b final Cu ; Rh avg 5b& 6b
Rh/8b/ 60/S2 avg	58.6	*0.05*	34.0	NR	0.01	2.21	95	
Rh/9/ 300/S2 avg	62.9	0.08	30.6	NR	NR	0.81	94	
Rh/1508/ 9R/S2 avg	69.2	NR	26.7	NR	NR	0.21	96	
Rh/10/ 240/S2 avg	60.6	0.07	32.2	NR	0.03	0.83	94	
Rh//11/240/S2 avg	58.6	0.07	31.5	0.22	0.02	1.05	91	
Rh/11R/240/ S1 avg	64.6	0.05	31.0	NR	NR	0.90	97	
Rh/12/60/S avg	64.3	*0.05*	30.0	NR	NR	1.94	96	
	= < that value							

2. Solution Assays

Solution assay list with replicate and repeat analyses

Sample # / Rh'date/test #'time/Sample#	Time min	Solution concentration Cu (mg/l)	Ni (g/l)	H2SO4 (g/l)	Na (mg/l)	K (mg/l)	Rh (mg/l)	Comments OR Standard deviation on Rh assay
FEED1 soln				16.8	< 1	977	173	
Feed1 soln replicate				16.6				
FEED1 avg		NR	NR	16.6	< 1	977	173	
Rh'0-2/0 min (feed @ 150 oC)	0	NR	NR	16.7	< 1	999	179	
Rh'0-2/2 min	2.4	NR	NR	16	163	964	101	
Rh'0-2/5 min	5	NR	NR	15.7	119	974	99	
Rh'0-2/10 min	10	NR	NR	15.6	111	998	100	
Rh'0-2/30 min				15.6	117	987	100	
Rh'0-2/30 min dup						995		
Rh'0-2/30 min avg	30	NR	NR	15.6	117	991	100	
Rh'0-2/60 min	60	NR	NR	15.6	115	991	81	
Rh'0-2/90 min	90	NR	NR	15.2	114	975	65	
Rh'0-2/120 min	120	NR	NR	15.3	117	977	64	
Rh'0-2/180 min	180	NR	NR	14.9	117	996	51	
Rh'0-2/240min				14.8	115	990	63	
Rh'0-2/240dup							65	
Rh'0-2/240 avg	240	NR	Fe(mg/l)	14.8	115	990	64	1.3
Rh'0-2/245			105	15.1	549	990	0.2	
Rh'0-2/245 dup					553			
Rh'0-2/245 avg	245	NR	105	15.1	551	990	0.2	
Rh'0-1/ no samples								
Rh'0-3/ no samples								
Rh'1307/1/ 0/L1	0	7.6	8.68	15.5	NR	1189	96	
Rh'1307/1/ 0/L1 repeat				15.4			101.8	
Rh'1307/1/ 0/L1 avg	0	7.5	8.7	15.4	NR	1189.0	98.9	4.1
Rh'1307/1/ 1/L2		NR	NR	12.1	NR	1144	70.8	
Rh'1307/1/ 1/L2 rep				12.1		1136	67.5	
Rh'1307/1/ 1/L2 avg	1	NR	NR	12.1	NR	1140	69.2	2.3
Rh'1307/1/ 2/L3	2	NR	NR	12.2	NR	1156	79.2	
Rh'1307/1/ 6/L4	6	NR	NR	11.6	NR	1161	79.0	
Rh'1307/1/ 6/L4 repeat							72.7	post-pptn ignor repeat result
Rh'1307/1/ 6/L4 avg	6	NR	NR	11.6	NR	1161	79.0	4.5
Rh'1307/1/ 12/L5	12	NR	NR	11.4	NR	1144	71.7	
Rh'1307/1/ 12/L5 repeat							65.5	post-pptn ignor repeat result
Rh'1307/1/ 12/L5 avg	12	NR	NR	11.4	NR	1144	71.7	4.4
Rh'1307/1/ 30/L6	30	NR	NR	11.6	NR	1139	73.7	
Rh'1307/1/ 60/L7	60	NR	NR	11.7	NR	1156	71.4	
Rh'1307/1/ 90/L8	90	NR	NR	11.6	NR	1153	67.9	
Rh'1307/1/ 120/L9	120	NR	NR	11.7	NR	1256	67.2	
Rh'1307/1/ 180/L10		NR	NR	11.5	NR	1271	64.7	
Rh'1307/1/ 180/L10 rep						1264		
Rh'1307/1/ 180/L10 avg	180	NR	NR	11.6	NR	1267	64.7	
Rh'1307/1/ 240/L11	240	< 2	8.7	11.4	NR	1177	63.5	
Rh'Rh'1307/1/ 300/L12		< 2	8.7	10.9	NR	1243	56.8	
Rh'1307/1/ 300/L12 rep		< 2	8.7	10.9			63.5	
Rh'1307/1/ 300/L12 repeat							64.9	
Rh'1307/1/ 300/L12 avg	300	< 2	8.7	10.9	NR	1243	65.1	1.7
Rh'1207/2/ 0/L1		8.9	8.7	15.9	NR	1170	92.5	
Rh'1207/2/ 0/L1 rep				15.1			94.7	
Rh'1207/2/ 0/L1 avg	0	9.9	8.7	15.5	NR	1170	93.6	1.6
Rh'1207/2/ 1/L2		< 2	8.7	12.7		1121	77.2	
Rh'1207/2/ 1/L2 rep		< 2	8.7	12.7			65.0	
Rh'1207/2/ 1/L2 avg	1	< 2	8.7	12.7	NR	1121	71.1	8.6
Rh'1207/2/ 2/L3	2	NR	NR	12.1	NR	1126	70.8	
Rh'1207/2/ 2/L3 repeat							68.0	
Rh'1207/2/ 2/L3 avg	2	NR	NR	12.1	NR	1126	69.4	2.0
Rh'1207/2/ 5/L4	5	NR	NR	10.4	NR	1113	73.0	
Rh'1207/2/ 5/L4 repeat							68.0	
Rh'1207/2/ 5/L4 avg	5	NR	NR	10.4	NR	1113	70.8	3.5
Rh'1207/2/ 10/L5	10	NR	NR	11.9	NR	1117	55.1	
Rh'1207/2/ 10/L5 repeat							60.3	
Rh'1207/2/ 10/L5 avg	10	NR	NR	11.9	NR	1117	59.2	1.6
Rh'1207/2/ 30/L6	30	NR	NR	11.4	NR	1107	60.4	
Rh'1207/2/ 60/L7	60	NR	NR	11.6	NR	1120	49.5	
Rh'1207/2/ 90/L8				11.5		1127	43.9	
Rh'1207/2/ 90/L8 rep							44.8	
Rh'1207/2/ 90/L8 avg	90	NR	NR	11.5	NR	1127	44.4	0.6
Rh'1207/2/ 120/L9				11.4		1117	43.4	
Rh'1207/2/ 120/L9 rep						1124		
Rh'1207/2/ 120/L9 avg	120	NR	NR	11.4	NR	1121	43.4	
Rh'1207/2/ 180/L10	180	< 2	8.7	11.3	NR	1126	39.5	
Rh'1207/2/ 180/L10 repeat							42.5	
Rh'1207/2/ 180/L10 avg	180	< 2	8.7	11.3	NR	1126	41.0	2.1
Rh'1207/2/ 240/L11	240	< 2	8.7	11.3		1131	39.2	
Rh'1207/2/ 240/L11 rep			8.7	11.3		1129	36.4	
Rh'1207/2/ 240/L11 repeat							37.1	
Rh'1207/2/ 240/L11 avg	240	< 2	8.68	11.3	NR	1130	38.6	2.1
Rh'1107/3/ 0/L1	0	36	NR	15.7	64	1191	80.5	
Rh'1107/3/ 0/L1 repeat							103.2	
Rh'1107/3/ 0/L1 avg	0	36	NR	16.7	NR	1191	96.9	9.0
Rh'1107/3/ 1/L2	1	NR	NR	12.7	NR	1114	62.4	
Rh'1107/3/ 2/L3	2	NR	NR	13.3	NR	1115	52.5	
Rh'1107/3/ 5/L4	5	NR	NR	11.9	NR	1101	50.6	
Rh'1107/3/ 18/L6	10	NR	NR	11.4	NR	1096	41.6	
Rh'1107/3/ 30/L6	30	NR	NR	11.8	NR	1119	41.1	
Rh'1107/3/ 60/L7				11.9		1128	32.2	
Rh'1107/3/ 60/L7 rep				11.6				
Rh'1107/3/ 60/L7 avg	60	NR	NR	11.8	NR	1128	32.2	
Rh'1107/3/ 90/L8	90	NR	NR	11.4	NR	1132	31.3	
Rh'1107/3/ 120/L9		NR	NR	11.3	NR	1146	26.2	
1107/3/ 120/L9 rep							29.6	
1107/3/ 120/L9 avg	120	NR	NR	11.3	NR	1143	27.9	2.4
Rh'1107/3/ 180/L10	180	< 2	NR		2363	1169	24.9	
Rh'1107/3/ 180/L10 repeat				11.8			27.9	
Rh'1107/3/ 180/L10 avg	180	< 2	NR	11.6	2363	1199	26.4	2.1
Rh'1107/3/ 240/L11		< 2	NR	12.7	2446	1138	22.6	
Rh'Rh'1107/3/ 240/L11 rep				11.9		1135	24.8	
Rh'1107/3/ 240/L11 avg	240	< 2	NR	12.3	2446	1137	23.7	1.5
Rh'2107/4/ 0/L1	0	77.9	NR	15.8	8.5	1222	25.6	
Rh'2107/4/ 0/L1 repeat							28.0	
Rh'2107/4/ 0/L1 avg	0	77.9	NR	15.6	9.5	1222	26.8	1.7
Rh'2107/4/ 1/L2	1	NR	NR	11.3	2599	1182	1.2	
Rh'2107/4/ 2/L3	2	NR	NR	10.9	NR	1171	0.6	
Rh'2107/4/ 4/L4				10.6		1196	0.4	
Rh'2107/4/ 4/L4 rep				11.1			0.4	
Rh'2107/4/ 4/L4 avg	4	NR	NR	11.0	NR	1196	0.4	0.0
Rh'2107/4/ 7/L5	7	NR	NR	10.9	NR	1192	0.2	
Rh'2107/4/ 18/L6	18	NR	NR	11.2	NR	1224	0.1	
Rh'2107/4/ 20/L7	20	NR	NR	10.9	NR	1180	< 0.05	
Rh'2107/4/ 30/L6	30	NR	NR	11.0	NR	1201	< 0.05	
Rh'2107/4/ 60/L9		< 2	NR	11.5	2698	1284	< 0.05	
Rh'2107/4/ 60/L9 rep						1272		
Rh'2107/4/ 60/L9 avg	60	< 2	NR	11.5	2698	1288	< 0.05	
Rh'1008/4R/ 0/L1	0	4.2	< 2	17.7	10	965	102.0	
Rh'1008/4R/ 1/L2				11.5	2561	891	40.0	
Rh'1008/4R/ 1/L2 rep						962		
Rh'1008/4R/ 1/L2 avg	1	NR	NR	11.5	2561	927	40.0	
Rh'1008/4R/ 2/L3							27.5	
Rh'1008/4R/ 2/L3 rep							27.7	
Rh'1008/4R/ 2/L3 avg	2	NR	NR	NR	NR	NR	27.6	0.1
Rh'1008/4R/ 4/L4	4	NR	NR	12.4	NR	NR	14.2	
Rh'1008/4R/ 6/L5	6	NR	NR	12.4	NR	NR	8.9	
Rh'1008/4R/ 8/L6	8	NR	NR	12.4	NR	NR	4.5	
Rh'1008/4R/ 11/L7	11	NR	NR	12.6	NR	NR	2.2	
Rh'1008/4R/ 15/L8				12.2	NR	NR	0.8	
Rh'1008/4R/ 15/L8 rep				12.1				
Rh'1008/4R/ 15/L8 avg	15	NR	NR	12.2	NR	NR	0.8	
Rh'1008/4R/ 27/L9		< 2	< 2	12.3	2582	972	0.1	
Rh'1008/4R/ 27/L9		< 2	< 2		2584		< 0.05	
Rh'1008/4R/ 27/L9 avg	27	< 2	< 2	12.3	2583	972	< 0.1	0.0

		Solution concentration						
Sample #	Time	Cu	Ni	H_2SO_4	Na	K	Rh	Comments OR Standard deviation
Rh/date/test #/time/Sample#	min	(mg/l)	(g/l)	(g/l)	(mg/l)	(mg/l)	(mg/l)	on Rh assay
Rh/2306/5a/t0/L1		13291	5929	16.7	24	965	0.3	
Rh/2306/5a/t0/L1 rep						962		
Rh/2306/5a/t0/L1 avg	0	13291	5929	16.7	24	964	0.3	
Rh/2306/6a/t0/L2		12813	5814	16.4	18	920	0.2	
Rh/2306/6a/t0/L2 rep				17.1	18			
Rh/2306/6a/t0/L2 avg	0	12813	5814	16.8	18	920	0.2	
Rh/2306/7a/to/L3		14123	5872	16.9	11	942	0.3	
Rh/2306/7a/to/L3 rep		14107						
Rh/2306/7a/to/L3 avg	0	14115	5872	16.9	11	942	0.3	
Rh/ /8a/0/L1	0	NR	NR	NR	NR	NR	NR	
Rh/8a/0/L8	0	14040	7057	16.0	NR	NR	0.05	
Rh/8a/0/L6		14054	7038					
Rh/8a/0/L6 avg	0	14047	7048	16.0			0.05	
Rh/2306/5a/filt/L4	80	10515	5891	18.5	2724	931	0.2	
Rh/2306/6a/filt/L5	20	11492	5806	18.3	2421	899	0.2	
Rh/2306/7a/filt/L6	15	10675	6155	19.0	2480	915	0.3	
Rh/8a/filt/L	10	NR	NR	NR	NR	NR	NR	
Rh/2806/5b/TO/ L1	0	35.9	NR	15.0	9	991	0.2	
Rh/Rh estimate after injection	0.01							Calculated Rh feed value
Rh/2806/5b/ 1/ L2		32.5		16.4	12	908	116	no sample flush, thus Rh contamination caused spike
Rh/2806/5b/ 1/ L2 repeat		32.6					137	
Rh/2806/5b/ 1/ L2 avg	1	32.6	NR	16.4	12	908		guesstimate
Rh/2806/5b/ 2/L3		34.0		16.6	11	959	100	no sample flush, thus Rh contamination caused spike
Rh/2806/5b/ 2/L3						963	118	
Rh/2806/5b/ 2/L3 avg	2	34.0	NR	16.8	11	961		guesstimate
Rh/2806/5b/ 5/L4	5	33.2	NR	16.2	12	936	88	
Rh/2806/5b/ 5/L4 repeat							104	
Rh/2806/5b/ 5/L4 avg	5	33.2	NR	16.2	12	936	96	
Rh/2806/5b/ 10/L5	10	35.8	NR	16.2	12	929	92	
Rh/2806/5b/ 10/L5 repeat							98	
Rh/2806/5b/ 10/L5 avg	10	35.8	NR	16.2	12	929	95	4.2
Rh/2806/5b/ 30/L8	30	36.0	NR	16.4	10	932	94	
Rh/Rh/2806/5b/ 60/L7	60	34.3	NR	16.5	10	944	86	
Rh/2806/5b/ 90/L8	90	35.2	NR	16.5	10	910	84	
Rh/2806/5b/ 120/L9	120	35.8	NR	16.4	10	929	87	
Rh/2806/5b/ 160/L10	180	35.7	NR	16.6	10	949	77	
Rh/2806/5b/ 240/L11		34.3		16.2	11	922	77	
Rh/2806/5b/ 240/L11		33.2		16.8				
Rh/2806/5b/ 240/L11 avg	240	33.8	NR	16.5	11	922	77	
Rh/2806/5b/ 290/L12		33.2		14.7	11	925	82	
Rh/2806/5b/ 290/L12					11		79	
Rh/2806/5b/ 290/L12 avg	290	33.2	NR	14.7	11	925	80	1.7
Rh/0307/6b/tOL1		87.7		13.7	3	994	0.1	
Rh/0307/6b/tOL1		87.6						
Rh/0307/6b/tOL1 avg	0	87.7	NR	13.7	3	994	0.1	
Rh estimate after injection	0.01							Calculated Rh feed value
Rh/0307/6b/ 1/L2		87.4		15.9	6	956	106.0	small sample flush, some contamination
Rh/0307/6b/ 1/L2				15.9			93.5	
Rh/0307/6b/ 1/L2 avg	1	87.4	NR	15.9	6	956	99.8	
Rh/0307/6b/ 2/L3	2	88.4	NR	15.5	NR	953	77.9	
Rh/0307/6b/ 2/L3 repeat							103.9	
Rh/0307/6b/ 2/L3 avg	2	88.4	NR	15.5	NR	953	90.9	18.4
Rh/0307/6b/ 5/L4	5	90.5	NR	15.3	NR	946	82.2	
Rh/0307/6b/ 5/L4 repeat							83.9	
Rh/0307/6b/ 5/L4 avg	5	90.5	NR	15.3	NR	946	83.1	1.2
Rh/Rh/0307/6b/ 10/L5	10	92	NR	15.1	NR	940	75.1	
Rh/Rh/0307/6b/ 10/L5 repeat							93.9	
Rh/Rh/0307/6b/ 10/L5 avg	10	92	NR	15.1	NR	940	84.5	13.3
Rh/0307/6b/ 30/L6	30	95.6	NR	15.2	NR	960	85.4	
Rh/0307/6b/ 30/L6 repeat							85.2	
Rh/0307/6b/ 30/L6 avg	30	95.6	NR	15.2	NR	960	85.3	0.1
Rh/0307/6b/ 60/L7	60	96.4	NR	15.5	NR	970	65.0	
Rh/0307/6b/ 90/L8		96.3		15.6		959	70.7	
Rh/0307/6b/ 90/L8						975	71.1	
Rh/0307/6b/ 90/L8 avg	90	96.3	NR	15.6	NR	967	70.9	0.3
Rh/0307/6b/ 120/L9	180	94.8	NR	15.5	NR	965	62.6	
Rh/0307/6b/ 160/L10		96.4		15.7		960	63.0	
Rh/0307/6b/ 180/L10		96.9						
Rh/0307/6b/ 160/L10 avg	240	96.7	NR	15.7	NR	960	63.0	
Rh/0307/6b/ 240/L11	290	90.4	NR	15.8	6	977	61.5	
			42 mL sampler flush on 7b					
Rh/2806/7b/t0/L1	0	116	NR	15.5	8	939	< 0.05	
Rh estimate after injection	0.01							Calculated Rh feed value
Rh/2806/7b/1/L2		107	NR	16.6	8	858	75.5	
Rh/2806/7b/1/L2 rep						860	96.5	Standard deviation on Rh
Rh/2806/7b/1/L2 avg	1	107	NR	16.6	8	859	96.0	14.8
Rh/2806/7b/2/L3		106		16.1	7	878	88.0	
Rh/2806/7b/2/L3 rep		106					70.0	
Rh/2806/7b/2/L3 avg	2	106	NR	16.1	7	878	89.0	1.4
Rh/2806/7b/5/L4	5	117	NR	16.7	8	882	83.4	
Rh/2806/7b/10/L5	10	118	NR	16.6	8	898	86.3	
Rh/2806/7b/30/L6		117		16.8	8	895	58.5	
Rh/2806/7b/30/L6 rep					8			
Rh/2806/7b/30/L6 avg	30	117	NR	16.8	8	895	58.5	
Rh/2806/7b/60/L7	60	118	NR	17.7	8	890	56.2	
Rh/2806/7b/90/L8		127		17.4	7	901	54.7	
Rh/2806/7b/90/L8 rep							55.2	
Rh/2806/7b/90/L8 avg	90	127	NR	17.4	7	901	55.0	0.4
Rh/2806/7b/120/L11		116		17.0	8	884	52.0	
Rh/2806/7b/120/L11 rep		117						
Rh/2806/7b/120/L11 avg	120	117	NR	17.0	8	884	52.0	
Rh/2806/7b/180/L9		121		17.3	7	909	51.3	
Rh/2806/7b/180/L9 rep				17.5		909		
Rh/2806/7b/180/L9 avg	160	121	NR	17.4	7	909	51.3	
Rh/2806/7b/225/L10	225	113	NR	17.9	6	904	49.7	
1907/8b/ 0/L1		76.3	NR	15.6	12	1192	< 0.05	
1907/8b/ 0/L1 rep		75.9	NR					
1907/8b/ 0/L1 avg	0	76.1	NR	15.6	12	1192	< 0.05	
Rh estimate after injection	0.01						92.5	
1907/8b/ 1/L2	1	96.3	NR	16.4	13	1152	35.0	
1907/8b/ 2/L3				16.6		1172	16.8	
1907/8b/ 2/L3 rep							18.1	
1907/8b/ 2/L3 avg	2	NR	NR	15.6	NR	1172	16.5	0.5
1907/8b/ 4/L4	4	NR	NR	16.2	NR	1155	4.6	
1907/8b/ 7/L5				16.5	NR	1157	1.2	
1907/8b/ 7/L5 rep				16.5	NR			
1907/8b/ 7/L5 avg	7	NR	NR	16.5	NR	1157	1.2	
1907/8b/ 13/L6	13	NR	NR	16.6	NR	1163	0.7	
1907/8b/ 20/L7	20	NR	NR	16.5	NR	1184	0.5	
1907/8b/ 30/L8	30	NR	NR	16.6	NR	1166	0.4	
1907/8b/ 60/L9		111	NR	17.5	12	1279	0.06	
1907/8b/ 60/L9 rep				18.3		1292	0.11	
1907/8b/ 60/L9 avg	60	111	NR	17.9	12	1286	0.08	0.04

Sample #		Solution concentration							
Rh/date/test #/time/Sample#	Time min	Cu (mg/l)	Ni (g/l)	H2SO4 (g/l)	Na (mg/l)	K (mg/l)	Rh (mg/l)	Comments OR Standard deviation on Rh assay
Rh/0607/9/ 0/ L1	0	13405	5657	16.1	22	1123	103.0	
Rh/0607/9/ 1/L2	1	12060	5632	17.9	2270	1060	57.0	
Rh/0607/9/ 1/L2 repeat							51.9	
Rh/0607/9/ 1/L2 avg	1	12060	5632	17.9	2270	1060	54.5	3.6
Rh/0607/9/ 2/L3	2	11442	5414	17.8	NR	1096	63.6	
Rh/0607/9/ 2/L3 repeat							61.6	
Rh/0607/9/ 2/L3 avg	2	11442	5414	17.8	NR	1096	62.6	1.4
Rh/0607/9/ 5/L4	5	11471	5358	15.4	NR	1078	53.9	
Rh/0607/9/ 5/L4 repeat							62.2	
Rh/0607/9/ 5/L4 avg	5	11471	5358	15.4	NR	1078	58.1	5.9
Rh/0607/9/ 10/L5	10	11325	5342	17.2	NR	1061	58.4	
Rh/0607/9/ 10/L5 repeat							63.8	
Rh/0607/9/ 10/L5 avg	10	11325	5342	17.2	NR	1061	61.1	3.8
Rh/0607/9/ 30/L6	30	10724	5449	17.8	NR	1080	61.5	
Rh/0607/9/ 30/L6 repeat							64.2	
Rh/0607/9/ 30/L6 avg	30	10724	5449	17.8	NR	1080	62.9	1.9
0607/9/ 60/L7		10442	5389	18.1	NR	1084	58.3	
0607/9/ 60/L7		10412	5387					
Rh/0607/9/ 60/L7 avg	60	10427	5388	18.1	NR	1084	58.3	
0607/9/ 90/L8		9658	5048	17.5		1033	54.3	
0607/9/ 90/L8							51.4	
Rh/0607/9/ 90/L8 avg	90	9658	5048	17.5	NR	1096	52.9	2.1
Rh/0607/9/ 120/L9	120	9762	5364	18.2	NR	1096	61.2	
0607/9/ 180/L10		10804	5537	18.7	NR	1131	51.3	
0607/9/ 180/L10				18.2				
Rh/0607/9/ 180/L10 avg	180	10804	5537	18.5	NR	1131	51.3	
Rh/0607/9/ 240/L11	240	10180	5401	18	1969	1067	58.2	
0607/9/ 300/L12		10989	5562	18.4	2268	1101	56.1	
0607/9/ 300/L12 rep							53.5	
0607/9/ 300/L12 repeat							55.9	
Rh/0607/9/ 300/L12 avg	300	10989	5562	18.4	2268	1101	55.2	1.4
Rh/1407/9R/ 0/L1		13531	5727	16.0	31	1229	111.0	
Rh/1407/9R/ 0/L1 rep		13568	5761					
Rh/1407/9R/ 0/L1 avg	0	13595	5744	16.0	31	1229	111.0	
Rh/1407/9R/ 2/L2		12752	5648	15.6	2729	1189	92.1	
Rh/1407/9R/ 2/L2 rep						1185	90.8	
Rh/1407/9R/ 2/L2 avg	2	12752	5648	15.6	2729	1187	91.5	
Rh/1407/9R/ 5/L3	5	12410	NR	15.7	NR	NR	92.5	
Rh/1407/9R/ 9/L4	9	12299	NR	15.7	NR	NR	91.6	
Rh/1407/9R/ 14/L5	14	12305	NR	15.5	NR	NR	*107	Discard 107 using MB, stats.
Rh/1407/9R/ 14/L5 repeat							89.0	
Rh/1407/9R/ 14/L5 avg	14	12305	NR	15.5	NR	NR	89.0	
Rh/1407/9R/ 20/L6	20	12082	NR	15.6	NR	NR	86.0	
Rh/1407/9R/ 30/L7		11781		16.8			86.7	
Rh/1407/9R/ 30/L7 rep				16.4				
Rh/1407/9R/ 30/L7 avg	30	11781	NR	16.6	NR	NR	86.7	
Rh/1407/9R/ 60/L8	60	10956	NR	17.1	NR	NR	98.6	
Rh/1407/9R/ 60/L8 repeat							94.1	
Rh/1407/9R/ 60/L8 avg	60	10956	NR	17.1	NR	NR	96.9	3.9
Rh/1407/9R/ 90/L8		10873		17.5			94.2	
Rh/1407/9R/ 90/L9		10748						
Rh/1407/9R/ 90/L9 avg	90	10811	NR	17.5	NR	NR	94.2	
Rh/1407/9R/ 120/L10	120	10860	NR	17.3	NR	NR	89.0	
Rh/1407/9R/ 180/L11		10753	5686	17.6	2561	1175	89.7	
Rh/1407/9R/ 180/L11					2542		97.7	
Rh/1407/9R/ 180/L11 avg	180	10753	5686	17.6	2552	1175	95.7	2.8
Rh/1407/9R/ 240/L12	240	10861	5677	17.8	2485	1178	90.6	
0507/10/ 0/L1		13265	5737	18.5		1158	106	
0507/10/ 0/L1 rep				15.7		1141	102.2	
Rh/0507/10/ 0/L1 avg	0	13265	5737	16.1	NR	1150	104.1	2.7
0507/10/ 1/L2		11006	5537	17.2		1078	70.8	
0507/10/ 1/L2 rep							70.2	
0507/10/ 1/L2 repeat							75.4	
Rh/0507/10/ 1/L2 avg	1	11006	5537	17.2	NR	1078	72.1	2.5
0507/10/ 2/L3		10900	5602	17.6		1096	75	
0507/10/ 2/L3 rep						1091	77.7	
Rh/0507/10/ 2/L3 avg	2	10900	5602	17.5	NR	1093	76.9	2.9
Rh/0507/10/ 5/L4	5	10706	5485	17.8	NR	1084	84	
Rh/0507/10/ 5/L4 repeat							79.1	
Rh/0507/10/ 5/L4 avg	5	10706	5485	17.8	NR	1084	81.6	3.7
Rh/0507/10/ 10/L5	10	10692	5713	18.1	NR	1090	73.7	
Rh/0507/10/ 30/L6	30	10486	5714	18.4	NR	1121	71.9	
Rh/0507/10/ 30/L6 repeat							74.0	
Rh/0507/10/ 30/L6 avg	30	10486	5714	18.4	NR	1121	73.0	1.1
0507/10/ 60/L7		10197	5626	18.1	NR	1096	87.8	
0507/10/ 60/L7 rep		10185	5651					
Rh/0507/10/ 60/L7 avg	60	10175	5639	19.1	NR	1096	87.8	
Rh/0507/10/ 90/L9	90	9615	5516	19.4	NR	1104	89.2	
Rh/0507/10/ 120/L9	120	9607	5627	19.6	NR	1089	80.3	
0507/10/ 180/L10		9693	5570	20.1		1096	89.4	
0507/10/ 180/L10 rep								
Rh/0507/10/ 180/L10 avg	180	9693	5570	20.1	NR	1096	89.4	
0507/10/ 240/L11		9076	5527	20.3		1109	56.7	
0507/10/ 240/L11 rep		9037	5529			1110	57.2	
Rh/0507/10/ 240/L11 avg	240	9056	5528	20.3	NR	1110	57.0	0.4
0407/11/ 0/L1		13782	6233	16.4	16	1052	102	
0407/11/ 0/L1 rep		13796	6224					
Rh/0407/11/ 0/L1 avg	0	13789	6229	16.4	16	1052	102	
0407/11/ 1/L2		10428	5445	"20.1"	2467	950	78.5	acid ignorred
0407/11/ 1/L2 rep				16.1	2497		75.1	
0407/11/ 1/L2 repeat							81.5	
Rh/0407/11/ 1/L2 avg	1	10428	5448	16.1	2482	950	78.7	3.3
Rh/0407/11/ 2/L3	2	11279	5855	18.1	NR	986	78.5	
0407/11/ 5/L4		10867	5667	16.2	NR	982	80.7	
0407/11/ 5/L4 rep		10855	5659			995	86.3	
Rh/0407/11/ 5/L4 avg	5	10861	5663	16.2	NR	988.5	82.0	1.8
0407/11/ 10/L5		11019	5754	18.7		1004	79.5	
0407/11/ 10/L5 rep				19.4			76.6	
Rh/0407/11/ 10/L5 avg	10	11019	5754	19.1	NR	1004	78.1	2.1
Rh/0407/11/ 30/L6	30	10450	5781	20.2	NR	984	79.3	
Rh/0407/11/ 60/L7	60	10070	5621	20.7	NR	986	80.6	
Rh/0407/11/ 90/L8	90	9974	5625	21.6	NR	970	46.1	
Rh/0407/11/ 120/L9	120	9997	5663	21.5	NR	978	49.5	
Rh/0407/11/ 120/L9 repeat							52.6	
Rh/0407/11/ 120/L9 avg	120	9997	5663	21.5	NR	978	51.1	2.2
0407/11/ 180/L10		10006	5689	21.4		980	41.6	
0407/11/ 180/L10 rep							42.7	
Rh/0407/11/ 180/L10 avg	180	10006	5689	21.4	NR	980	42.2	0.8
Rh/0407/11/ 240/L11	240	9867	5662	21.6	2282	971	44.2	
Rh/0407/11/ 240/L11 repeat				21.7			43.9	
Rh/0407/11/ 240/L11 avg	240	9867	5662	21.7	2282	971	44.1	0.2
2107/11R/ 0/L1		12952	5575	14.8	18	1100	56.2	
2107/11R/ 0/L1 rep		13156	5582	15.1	17	1114	89.4	
2107/11R/ 0/L1 avg	0	13054	5579	15.0	18	1107	94.8	
2107/11R/ 1/L2	1	10386	NR	16.4	NR	NR	81.5	
2107/11R/ 2/L3	2	10419	NR	16.2	NR	NR	80.8	
2107/11R/ 5/L4	5	10438	NR	16.8	NR	NR	79.2	
2107/11R/ 10/L5	10	10321	NR	17.5	NR	NR	76.3	
2107/11R/ 20/L6	20	10062	NR	20.0	NR	NR	70.1	
2107/11R/ 30/L7	30	9838	NR	20.6	NR	NR	64.1	
2107/11R/ 60/L8	60	9729	NR	19.8	NR	NR	58.6	
2107/11R/ 120/L8		9822	5494	20.0	2264	1088	51.2	
2107/11R/ 120/L8 rep		9836	5466	19.7	2281	1089	52.9	
2107/11R/ 120/L8 avg	120	9829	5475	19.9	2273	1080.5	52.1	1.2
2007/12/ 0/L1	0	13228	5756	15.1	16	1016	81.9	
2007/12/ 0/L1 repeat	0			15.1			87.9	
2007/12/ 0/L1	0	13228	5756	15.1	16	1016	84.9	4.2
2007/12/ 1/L2		9869	5564	19.8	2271	1336	28.4	
2007/12/ 1/L2 rep						1353		
2007/12/ 1/L2 avg	1	9869	5564	19.8	2271	1345	20.4	
2007/12/ 2/L3	2	8668	4861	18.2	NR	1134	15.9	
2007/12/ 5/L4	3	10328	5822	21.2	NR	1138	12.5	
2007/12/ 4/L5		10807	6027	20.8	NR	1128	9.5	
2007/12/ 4/L5 rep							0.7	
2007/12/ 4/L5 avg	4	10807	6027	20.8	NR	1128	9.6	0.2
2007/12/ 6/L6	6	10266	5884	20.8	NR	1134	6.2	
2007/12/ 7/L7	7	10043	5756	20.9	NR	1096	4.8	
2007/12/ 10/L5	10	9967	5758	21.1	NR	1115	3.5	
2007/12/ 15/L9		9834	5706	20.5		1139	2.7	
2007/12/ 15/L9 rep		9870	5693	20.8				
2007/12/ 15/L9 avg	15	9852	5700	20.7	NR	1139	2.7	
2007/12/ 80/L10	20	9967	5691	20.1	NR	1200	2.0	
2007/12/ 30/L11		9631	5964	20.8	2236	1188	1.8	
2007/12/ 30/L11 rep							1.6	
2007/12/ 30/L11 avg	30	9631	5964	20.8	2236	1188	1.5	0.1
2007/12/ 80/L12		10513	5925	22.1	2369	1257	0.1	
2007/12/ 80/L12 rep		10482	5926				0.2	
2007/12/ 60/L12 avg	60	10498	5627	22.1	2369	1257	0.1	0.04

Notation:
rep = replicate — occurred on random elements performed in duplicate on the same sample at the same time
repeat = sample repeated to confirm results; sample analysed a long period later
avg = average of sample, replicates and repeats

Feed solution assay summary list

Sample #	Time	Solution concentration					
		Cu	Ni	H2SO4	Na	K	Rh
	min	(mg/l)	(mg/l)	(g/l)	(mg/l)	(mg/l)	(mg/l)
Theoretical Calculated feed concentrations (after reagent injection (thiosulphate or Rh(III), before reaction)							
#1-#4	t=0	0	0	14.4	2264	963	92.6
#5a	t=0	13216	5118	13.4	2183	929	0.0
#6a	t=0	13312	5156	13.5	2199	936	0.0
#7a	t=0	13217	5119	13.4	2183	929	0.0
#8a	t=0	13216	5118	13.9	2183	929	0.0
#5b	t=0	0	0	15.1	0	971	93.3
#6b	t=0	0	0	14.5	0	971	93.4
#7b	t=0	0	0	14.0	0	936	90.0
#8b	t=0	0	0	14.4	0	962	92.5
#9	t=0	13217	5119	13.9	2099	929	89.3
#9R	t=0	14236	5513	15.0	2261	1001	96.2
#10	t=0	13223	5121	13.9	2100	929	89.4
#11	t=0	13217	5119	13.9	2099	929	89.3
#11R	t=0	13217	5119	13.9	2099	929	89.3
#12	t=0	13217	5119	13.9	2099	929	89.3
Measured feed concentrations (before reagent injection)							
Rh/1307/1/ 0/L1	0	8	9	15.4	NR	1189	98.9
Rh/1207/2/ 0/L1 avg	0	9	9	15.5	NR	1170	93.6
Rh/1107/3/ 0/L1 avg	0	36	NR	16.7	NR	1191	96.9
Rh/2107/4/ 0/L1 avg	0	78	NR	15.8	10	1222	26.8
Rh/1008/4R/ 0/L1	0	4	< 2	17.7	10	965	102
Rh/2306/5a/t0/L1 avg	0	13291	5929	16.7	24	964	0.3
Rh/2306/6a/t0/L2 avg	0	12813	5614	16.8	18	920	0.2
Rh/2306/7a/to/L3 avg	0	14115	5872	16.9	11	942	0.3
Rh/8a/0/L6 avg	0	14047	7048	18.0	NR	NR	0.05
Rh/2806/5b/TO/ L1	0	36	NR	15.0	9	991	0.2
Rh/0307/6b/tO/L1 avg	0	88	NR	13.7	3	994	0.1
Rh/2806/7b/t0/L1	0	116	NR	15.5	8	939	< 0.05
1907/8b/ 0/L1 avg	0	76	NR	15.6	12	1192	< 0.05
Rh/0607/9/ 0/ L1	0	13405	5657	16.1	22	1123	103
Rh/1407/9R/ 0/L1 avg	0	13595	5744	16.0	31	1229	111
Rh/0507/10/ 0/L1 avg	0	13265	*5737*	16.1	NR	1150	104
Rh/0407/11/ 0/L1 avg	0	13789	6229	16.4	16	1052	102
2107/11R/ 0/L1 avg	0	12952	5575	14.8	18	1100	96.2
2007/12/ 0/L1	0	13226	5756	15.1	16	1016	81.5
Measured feed concentrations (after injection before reaction)							
Rh/1307/1/ 0/L1	0	7	8	14.9	NR	1145	95.3
Rh/1207/2/ 0/L1 avg	0	9	8	14.9	NR	1127	90.2
Rh/1107/3/ 0/L1 avg	0	35	NR	16.1	NR	1147	93.3
Rh/2107/4/ 0/L1 avg	0	75	NR	15.2	9	1177	25.8
Rh/1008/4R/ 0/L1	0	4	< 2	17.1	10	931	98.4
Rh/2306/5a/t0/L1 avg	0	12902	5755	16.2	24	935	0.3
Rh/2306/6a/t0/L2 avg	0	12450	5649	16.3	17	894	0.2
Rh/2306/7a/to/L3 avg	0	13705	5701	16.4	10	915	0.3
Rh/8a/0/L6 avg	0	13552	6799	15.4	NR	NR	0.0
Rh/2806/5b/TO/ L1	0	35	NR	14.6	9	963	0.2
Rh/0307/6b/tO/L1 avg	0	85	NR	13.2	3	959	0.1
Rh/2806/7b/t0/L1	0	112	NR	14.9	7	903	< 0.05
1907/8b/ 0/L1 avg	0	73	NR	15.1	11	1150	< 0.05
Rh/0607/9/ 0/ L1	0	12939	5460	15.5	21	1084	99.4
Rh/1407/9R/ 0/L1 avg	0	13115	5542	15.4	30	1186	107.1
Rh/0507/10/ 0/L1 avg	0	12798	*5535*	15.5	NR	1109	100.4
Rh/0407/11/ 0/L1 avg	0	13287	6002	15.8	15	1014	98.3
2107/11R/ 0/L1 avg	0	12462	5364	14.2	17	1058	92.6
2007/12/ 0/L1	0	12762	5553	14.6	15	980	78.6

Finalised solution assay summary list used in comparative kinetic study

Sample #	Time	Solution concentration					
		Cu	Ni	H2SO4	Mn	K	Rh
	min	(mg/l)	(mg/l)	(g/l)	(mg/l)	(mg/l)	(mg/l)
Rh/1307/1/ 0/L1	0	7	8	14.9	66	1145	92.6
Rh/1307/1/ 1/L2 avg	1	NR	NR	12.1	NR	1140	84.4
Rh/1307/1/ 2/L3	2	NR	NR	12.2	NR	1156	83.7
Rh/1307/1/ 5/L4	5	NR	NR	11.6	NR	1161	79.8
Rh/1307/1/ 12/L5 avg	12	NR	NR	11.4	NR	1144	77.7
Rh/1307/1/ 30/L6	30	NR	NR	11.8	NR	1139	76.1
Rh/1307/1/ 60/L7	60	NR	NR	11.7	NR	1156	75.4
Rh/1307/1/ 90/L8	90	NR	NR	11.6	NR	1153	75.2
Rh/1307/1/ 120/L9	120	NR	NR	11.7	NR	1256	75.2
Rh/1307/1/ 180/L10 avg	180	NR	NR	11.6	NR	1207	74.4
Rh/1307/1/ 240/L11	240	< 2	9	11.4	NR	1177	74.4
Rh/1307/1/ 300/L12 avg	300	2	9	10.9	2264	1243	74.3
Rh/1207/2/ 0/L1 avg	0	9	8	14.9	71	1127	92.6
Rh/1207/2/ 1/L2 avg	1	< 2	9	12.7	NR	1121	60.8
Rh/1207/2/ 2/L3 avg	2	NR	NR	12.1	NR	1126	54.6
Rh/1207/2/ 5/L4 avg	5	NR	NR	10.4	NR	1113	51.4
Rh/1207/2/ 10/L5 avg	10	NR	NR	11.9	NR	1117	48.8
Rh/1207/2/ 30/L6	30	NR	NR	11.4	NR	1107	47.2
Rh/1207/2/ 60/L7	60	NR	NR	11.6	NR	1120	47.4
Rh/1207/2/ 90/L8 avg	90	NR	NR	11.5	NR	1127	46.2
Rh/1207/2/ 120/L9 avg	120	NR	NR	11.4	NR	1121	45.8
Rh/1207/2/ 180/L10 avg	180	< 2	8.7	11.3	NR	1126	46.6
Rh/1207/2/ 240/L11 avg	240	2	8.7	11.3	2284	1130	46.4
Rh/1107/3/ 0/L1 avg	0	35	NR	16	77	1147	92.6
Rh/1107/3/ 1/L2	1	NR	NR	12.7	NR	1114	40.4
Rh/1107/3/ 2/L3	2	NR	NR	13.3	NR	1116	40.4
Rh/1107/3/ 5/L4	5	NR	NR	11.9	NR	1101	39.0
Rh/1107/3/ 10/L5	10	NR	NR	11.4	NR	1096	36.8
Rh/1107/3/ 30/L6	30	NR	NR	11.8	NR	1119	34.1
Rh/1107/3/ 60/L7 avg	60	NR	NR	11.8	NR	1126	32.3
Rh/1107/3/ 90/L8	90	NR	NR	11.4	NR	1132	34.1
1107/3/ 120/L9 avg	120	NR	NR	11.3	NR	1146	32.7
Rh/1107/3/ 180/L10 avg	180	< 2	NR	11.8	2363	1169	32.6
Rh/1107/3/ 240/L11 avg	240	2	NR	12.3	2446	1137	32.7
Rh/2107/4/ 0/L1 avg	0	75	NR	15.2	9	1177	25.8
Rh/2107/4/ 1/L2	1	NR	NR	11.3	2500	1182	1.2
Rh/2107/4/ 2/L3	2	NR	NR	10.9	NR	1171	0.6
Rh/2107/4/ 4/L4 avg	4	NR	NR	11.0	NR	1195	0.4
Rh/2107/4/ 7/L5	7	NR	NR	10.9	NR	1192	0.2
Rh/2107/4/ 10/L6	10	NR	NR	11.2	NR	1224	0.1
Rh/2107/4/ 20/L7	20	NR	NR	10.9	NR	1180	0.05
Rh/2107/4/ 30/L8	30	NR	NR	11.0	NR	1201	0.05
Rh/2107/4/ 60/L9 avg	60	2	NR	11.5	2898	1208	0.05
Rh/1008/4R/ 0/L1	0	4	< 2	17	10	931	92.6
Rh1008/4R/ 1/L2 avg	1	NR	NR	11.9	2581	927	10.0
Rh/1008/4R/ 2/L3 avg	2	NR	NR	NR	NR	955	2.6
Rh/1008/4R/ 4/L4	4	NR	NR	12.4	NR	955	1.2
Rh/1008/4R/ 6/L5	6	NR	NR	12.4	NR	955	0.9
Rh/1008/4R/ 8/L6	8	NR	NR	12.4	NR	955	0.5
Rh/1008/4R/ 11/L7	11	NR	NR	12.6	NR	955	0.2
Rh/1008/4R/ 15/L8 avg	15	NR	NR	12.15	NR	955	0.8
Rh/1008/4R/ 27/L9 avg	27	< 2	< 2	12.3	2563	972	0.05

Sample #	Time	Solution concentration					
	min	Cu (mg/l)	Ni (mg/l)	H2SO4 (g/l)	Na (mg/l)	K (mg/l)	Rh (mg/l)
Rh/2306/5a/10/L1 avg	0	12802	5929	17	24	964	0.0
Rh/2306/5a/filt/L4	80	10515	5891	18.5	2724	931	0.2
Rh/2306/6a/10/L2 avg	0	12450	5849	16	17	894	0.0
Rh/2306/6a/filt/L5	20	11492	5806	18.3	2421	899	0.2
Rh/2306/7a/10/L3 avg	0	13705	5701	16	10	915	0.0
Rh/2306/7a/filt/L6	15	10875	6155	19.0	2480	915	0.3
Rh/8a/0/L6 avg	0	13705	5701	16	10	915	0.0
Rh/8a/filt/L	10	NR	NR	NR	NR	NR	NR
Rh/2806/5b/T0/ L1	0	34.9	NR	14.6	8.7	963.3	93.3
Rh/Rh estimate after injection	0.01						96.2
Rh/2806/5b/ 1/ L2 avg	1	32.6	NR	16.4	12.4	908	96.0
Rh/2806/5b/ 2/L3 avg	2	34.0	NR	16.6	10.6	961	96.0
Rh/2806/5b/ 5/L4 avg	5	33.2	NR	16.2	12	936	96.1
Rh/2806/5b/ 10/L5 avg	10	35.8	NR	16.2	12	929	95.0
Rh/2806/5b/ 30/L6	30	36.0	NR	16.4	10	932	94.4
Rh/Rh/2806/5b/ 60/L7	60	34.3	NR	16.5	10	944	85.6
Rh/2806/5b/ 90/L8	90	35.2	NR	16.5	10	910	84.1
Rh/2806/5b/ 120/L9	120	35.8	NR	16.4	10	929	87.0
Rh/2806/5b/ 180/L10	180	35.7	NR	16.6	10	949	76.9
Rh/2806/5b/ 240/L11 avg	240	33.8	NR	16.5	11	922	76.9
Rh/2806/5b/ 290/L12 avg	290	33.2	NR	14.7	11	925	80.3
Rh/0307/6b/10/L1 avg	0	85	NR	13.2	3	959	94.4
Rh estimate after injection	0.01						93.4
Rh/0307/6b/ 1/L2 avg	1	87.4	NR	15.9	6	956	92.0
Rh/0307/6b/ 2/L3 avg	2	88.4	NR	15.5	NR	953	90.9
Rh/0307/6b/ 5/L4 avg	5	90.5	NR	15.3	NR	946	83.1
Rh/Rh/0307/6b/ 10/L5 avg	10	92.0	NR	15.1	NR	940	84.5
Rh/0307/6b/ 30/L6 avg	30	95.6	NR	15.2	NR	960	85.3
Rh/0307/6b/ 60/L7	60	96.4	NR	15.5	NR	970	65.0
Rh/0307/6b/ 90/L8 avg	90	96.3	NR	15.6	NR	967	70.9
Rh/0307/6b/ 120/L9	180	94.8	NR	15.5	NR	965	62.6
Rh/0307/6b/ 180/L10 avg	240	96.7	NR	15.7	NR	960	63.0
Rh/0307/6b/ 240/L11	290	90.4	NR	15.8	5	977	61.5
Rh/2806/7b/10/L1	0	112	NR	14.9	7	903	90.0
Rh estimate after injection	0.01						90.0
Rh/2806/7b/1/L2 avg	1	107	NR	16.6	8	859	86.0
Rh/2806/7b/2/L3 avg	2	105	NR	16.1	7	878	69.0
Rh/2806/7b/5/L4	5	117	NR	16.7	8	862	63.4
Rh/2806/7b/10/L5	10	118	NR	16.6	8	898	66.3
Rh/2806/7b/30/L6 avg	30	117	NR	16.8	8	895	58.5
Rh/2806/7b/60/L7	60	118	NR	17.7	8	890	56.2
Rh/2806/7b/90/L8 avg	90	127	NR	17.4	7	901	55.0
Rh/2806/7b/120/L11 avg	120	117	NR	17.0	8	884	52.0
Rh/2806/7b/180/L9 avg	180	121	NR	17.4	7	909	51.3
Rh/2806/7b/225/L10	225	113	NR	17.9	6	904	49.7
1907/8b/ 0/L1 avg	0	73	NR	15.1	11	1150	92.5
Rh estimate after injection	0.01					1192	92.5
1907/8b/ 1/L2	1	98	NR	16.4	13	1152	35.0
1907/8b/ 2/L3 avg	2	NR	NR	16.6	NR	1172	18.5
1907/8b/ 4/L4	4	NR	NR	16.2	NR	1155	4.6
1907/8b/ 7/L5 avg	7	NR	NR	16.5	NR	1157	1.2
1907/8b/ 13/L6	13	NR	NR	16.6	NR	1163	0.7
1907/8b/ 20/L7	20	NR	NR	16.5	NR	1164	0.5
1907/8b/ 30/L8	30	NR	NR	16.6	NR	1166	0.4
1907/8b/ 60/L9 avg	60	111	NR	17.9	12	1286	0.1

Sample #	Time min	Solution concentration					
		Ca (mg/l)	Mg (mg/l)	Mg/Ca	Na (mg/l)	Sr (ug/l)	Fe (mg/l)
[illegible]	[illegible]	12911	5118	13.8	2239	923	39.2
[illegible]	1	12935	5234	17.9	2270	1052	89.3
[illegible]	2	12938	5414	17.8	NR	1039	90.5
[illegible]	5	12931	5357	18.4	NR	1078	98.8
[illegible]	10	12934	5344	17.9	NR	1061	97.3
[illegible]	30	12575	5448	17.6	NR	1064	94.1
[illegible]	60	12683	5385	18.1	NR	1054	92.8
[illegible]	90	12743	5048	17.5	NR	1033	82.1
[illegible]	120	10707	5354	18.2	NR	1084	89.6
[illegible]	180	10745	5537	18.5	NR	1151	80.9
[illegible]	240	8560	5401	18.0	1969	2087	60.3
[illegible]	300	10858	5607	18.4	2568	1137	58.1
[illegible]	0	13115	5542	15.4	30	1186	97.0
[illegible]	2	13170	5644	16.0	2723	1187	97.0
[illegible]	5	13115	NR	16.7	NR	NR	97.0
[illegible]	10	13115	NR	16.7	NR	NR	96.7
[illegible]	30	13058	NR	16.9	NR	NR	96.4
[illegible]	60	12926	NR	16.6	NR	NR	95.8
[illegible]	90	12787	NR	16.8	NR	NR	94.4
[illegible]	120	12281	NR	17.1	NR	NR	91.9
[illegible]	180	11512	NR	17.5	NR	NR	91.3
[illegible]	240	11026	NR	17.3	NR	NR	90.6
[illegible]	300	11172	5686	17.6	2553	1175	91.9
[illegible]	360	11513	5677	17.8	2486	1179	91.8
[illegible]	0	13736	5536	15.5	19	1109	89.5
[illegible]	1	10914	5587	17.2	NR	1078	65.9
[illegible]	2	10612	5632	17.6	NR	1098	64.0
[illegible]	5	10617	5485	17.6	NR	1064	64.7
[illegible]	10	12088	5715	19.1	NR	1090	63.3
[illegible]	30	10404	5714	18.4	NR	1121	58.5
[illegible]	60	10956	5639	19.5	NR	1098	57.3
[illegible]	90	10068	5618	19.4	NR	1104	55.4
[illegible]	120	9563	5627	19.6	NR	1080	51.4
[illegible]	180	9924	5670	20.1	NR	1096	48.7
[illegible]	240		5628	20.2		1110	
[illegible]	0	13567	6002	15.6	15	1014	89.3
[illegible]	1	11267	5448	16.1	2482	950	89.5
[illegible]	2	10744	5655	18.1	NR	998	48.2
[illegible]	5	11194	5666	18.2	NR	989	55.7
[illegible]	10	11010	5754	19.1	NR	1004	53.4
[illegible]	30	10309	5781	20.2	NR	984	42.2
[illegible]	60	10184	5621	20.7	NR	985	40.6
[illegible]	90	9830	5625	21.6	NR	970	36.5
[illegible]	120	10156	5663	21.5	NR	978	36.5
[illegible]	180	10072	5688	21.4	NR	980	38.6
[illegible]	240	10110	5662	21.4	2283	971	35.2
[illegible]	0	13452	5864	14.3	17	1058	89.3
[illegible]	1	11683	NR	16	NR	NR	72.5
[illegible]	2	10613	NR	16	NR	NR	62.9
[illegible]	5	10634	NR	16.8	NR	NR	67.1
[illegible]	10	10029	NR	17.5	NR	NR	58.0
[illegible]	20	9803	NR	20.0	NR	NR	53.3
[illegible]	30	9572	NR	20.6	NR	NR	50.1
[illegible]	60	9214	NR	19.6	NR	NR	42.2
[illegible]	120	9369	5478	19.9	2275	1091	47.3
[illegible]	0	13747	5555	14.6	15	960	89.2
[illegible]	1	9817	5564	18.6	2271	1545	28.4
[illegible]	2	9597	4981	18.2	NR	1134	15.3
[illegible]	5	9503	5022	21.2	NR	1138	12.5
[illegible]	10	9543	5027	20.6	NR	1126	9.6
[illegible]	60	9533	5684	20.8	NR	1134	6.7
[illegible]	90	9542	5795	20.9	NR	1095	4.9
[illegible]	120	9520	5758	21.1	NR	1115	3.8
[illegible]	180	9579	5700	20.7	NR	1139	2.7
[illegible]	240	9516	5691	20.1	NR	1210	2.0
[illegible]	300	9458	5964	20.6	2348	1186	1.3
[illegible]	600	9430	5807	22.1	2359	1257	0.1

Sample #	Time min	Solution concentration					
		Ca (mg/l)	Mg (mg/l)	Mg/Ca	Na (mg/l)	Sr (ug/l)	Fe (mg/l)
Miscellaneous tests:							
FEED1 avg	0	NR	NR	16.8	1	977	170
Pfe/0-2/C min (feed @ 150 uC:	0.01	NR	NR	16.7	1	998	179
Pfe/0-2/2 min	2.4	NR	NR	18	183	964	107
Pfe/0-2/5 min	5	NR	NR	15.7	115	974	99
Pfe/0-2/10 min	10	NR	NR	16.6	113	998	93.5
Pfe/0-2/30 min avg	30	NR	NR	15.8	117	991	99.8
Pfe/0-2/60 min	60	NR	NR	15.6	116	991	81.1
Pfe/0-2/90 min	90	NR	NR	15.2	114	975	65.1
Pfe/0-2/120 min	120	NR	NR	15.3	117	977	63.8
Pfe/0-2/180 min	180	NR	NR	14.9	117	996	60.9
Pfe/0-2/240 avg	240	NR	Fe(mg/l)	14.8	115	990	63.9
Pfe/0-2/245 avg	245	NR	105	15.1	553	990	0.2
0-1 and 0-3 data not available							

Note:
[illegible] sub to no [illegible]
calculated estimate
[illegible] (values are measured concentration)
NR no results / not required / not analysed

3. Statistics on Assays and Comparisons

1. Solution Assay Standard Deviations

		Solution concentration			Low	High					
	Time	Cu	Ni	H2SO4	Rh	Rh			Comments		
	min	(mg/l)	(g/l)	(g/l)	(mg/l)	(mg/l)					
Rh/1407/9R/ 240/L12	240	10861	5677	17.8	22.6	90.8			original sample analysed previous month		
Rh-L1	240	11285	6717	18.8	25.0	93.6					
Rh-L2	240	11122	6501	18.0	22.9	95.7					
Rh-L2 rep	240	11151	6511	17.6	25.8						
Rh-L3	240	11285	6613	17.8	24.8	89.2					
Rh-L4	240	11509	6482	17.5	25.4	91.8					
Rh-L5	240	11518	6627	17.6	24.8	93.1					
Rh-L5 rep	240					*98.4*			*outlier assay*		
Descriptive Statistics									Eliminate original	Eliminate outlier	Eliminate original&outlier
Mean		11247	6447	17.9	24.5	93.2			93.6	92.4	92.7
Standard Error		87	132	0.2	0.5	1.2			1.3	0.9	1.1
Median		11285	6511	17.8	24.8	93.1			93.4	92.5	93.1
Mode		11285	#N/A	17.8	25	#N/A			#N/A	#N/A	#N/A
Standard Deviation		231	350	0.4	1.2	3.1			3.2	2.3	2.4
Sample Variance		53135	122332	0.2	1.5	9.5			10.1	5.2	5.8
Kurtosis		-0.0009	5.777	4.026	-0.865	0.021			0.199	-0.212	0.719
Skewness		-0.431	-2.321	1.916	-0.884	0.562			0.223	0.089	-0.435
Range		657	1040	1.3	3.2	9.2			9.2	6.5	6.5
Minimum		10861	5677	17.5	22.6	89.2			89.2	89.2	89.2
Maximum		11518	6717	18.8	25.8	98.4			98.4	95.7	95.7
Sum		78731	45128	125.1	171	653			562	554	463
Count		7	7	7	7	7			6	6	5
Largest(1)		11518	6717	18.8	25.8	98.4			98.4	95.7	95.7
Smallest(1)		10861	5677	17.5	22.6	89.2			89.2	89.2	89.2
Confidence Level(95.0%)		213	323	0.41	1.1	2.9			2.6	2.4	2.3
Confidence Level(90.0%)		169	257	0.32	0.9	2.3				1.9	
Std dev. % on mean		2.0			5.0	3.3			3.4	2.5	2.6
Rel. error		***0.020***	***0.054***	***0.025***	***0.050***	***0.033***			0.034	0.025	0.026

2. Average and Standard deviations for Rh element analysed in replicate (two analyses)

Rh - Low concentration			Rh - Medium concentration			Rh - High concentration		
Average	Std dev.	Std dev. / Avg %	Average	Std dev.	Std dev. / Avg %	Average	Std dev.	Std dev. / Avg %
			9.6	0.2	1.6			
0.4	0.01	2.0	18.5	0.5	2.7	70.5	3.5	5.0
0.1	0.04	53.0	23.7	1.6	6.6	70.9	0.3	0.4
0.1	0.04	30.3	26.4	2.1	8.0	71.1	8.6	12.1
1.5	0.06	4.2	26.8	1.7	6.3	72.1	2.8	3.9
			27.6	0.1	0.5	73.0	1.1	1.6
			27.9	2.4	8.6	79.0	4.5	5.6
			35.6	2.1	5.8	76.9	2.9	3.7
			41.0	2.1	5.2	78.1	2.1	2.6
			42.2	0.8	1.8	78.7	3.3	4.2
			44.1	0.2	0.5	80.3	1.7	2.1
			44.4	0.6	1.4	80	1.7	2.1
			51.1	2.2	4.3	81.6	3.7	4.5
			52.9	2.1	3.9	84.5	13.3	15.7
			54.5	3.6	6.6	84.9	4.2	5.0
			55.0	0.4	0.6	85.3	0.1	0.2
			55.2	1.4	2.6	86.0	14.8	17.3
			57.0	0.4	0.6	83.1	1.2	1.4
			58.1	5.9	10.1	93.6	1.6	1.7
			59.2	1.6	2.6	94.1	3.9	4.1
			61.1	3.8	6.2	94.1	3.9	4.1
			62.6	1.4	2.3	95	4.2	4.4
			62.9	1.9	3.0	95.7	2.8	3.0
			63.9	1.3	2.1	95.7	2.8	3.0
			65.1	1.7	2.5	98.9	4.1	4.1
			71.7	4.4	6.1	104.1	2.7	2.6
			69.0	1.4	2.0			
			69.2	2.3	3.3			
			69.4	2.0	2.9			
Average								
0.5	0.04	***22.4***	50	1.9	***3.9***	84	3.8	***4.6***
Std dev of std dev	0.02			1.3			3.5	

3. Average and Standard deviations for other element analysed in replicate (two analyses)

	Cu			Ni			H2SO4			Na			K		
Conc (mg/l)	Average	Std dev.	Std dev. / Avg %	Average	Std dev.	Std dev. / Avg %	Average	Std dev.	Std dev. / Avg %	Average	Std dev.	Std dev. / Avg %	Average	Std dev.	Std dev. / Avg %
Low	33	0.1	0.2	9	0.0	0.0	10.9	0.1	1.0	7.6	0.1	1.2	859	1	0.2
	33	1.0	3.0				11.8	0.2	1.8	11.1	0.3	2.5	909		
	97	0.4	0.4				12.1			17.9	0.1	0.8	927	50	5.4
	106	0.7	0.7				12.2	0.1	0.6				961	3	0.3
	117	0.7	0.6				12.3	0.6	4.7				964	2	0.2
							12.7						967	11	1.2
Count	5						6			3			6		
Average	77	0.6	1.0				12.0	0.2	2.0	12	0	1.5	931	14	1.5
High	9852	25	0.3	5388	1	0.0	15.0	0.2	1.4	551	2.8	0.5	989	9	0.9
	10175	32	0.3	5528	1	0.0	15.1	0.0	0.2				991	6	0.6
	10412	199	1.9	5639	18	0.3	15.8						1093	3	0.3
	10482	694	6.6	5663	6	0.1	15.4	0.1	0.6				1110	1	0.1
	10748	59	0.5	5700	9	0.2	15.5	0.6	3.6				1121	5	0.4
	10865	270	2.5	5744	24	0.4	15.9						1130	2	0.2
				5927	2	0.0	16.1	0.6	3.5				1137	2	0.2
	13595	104	0.8	6229	6	0.1	16.5						1140	6	0.5
	13789	10	0.1	7048	13	0.2	16.5	0.4	2.6				1150	12	1.0
	14047	10	0.1				16.6	0.3	1.7				1187	3	0.2
	14115	11	0.1				16.8	0.5	3.0						
							17.4	0.1	0.8	2482	21.2	0.9	1267	5	0.4
							17.9	0.6	3.2	2552	13.4	0.5	1268	6	0.4
							18.5	0.4	1.9	2583	1.4	0.1	1286	9	0.7
							19.1	0.5	2.6				1345	12	0.9
							19.9	0.2	1.1						
							20.7	0.2	1.0						
							21.7	0.1	0.3						
							19.3	0.3	2.1		12	0.5		8.0	0.6
								0.2			10			3.2	
Count	10			9			19			4			14		
Average	11808	141	1.3	5874	9	0.1	17.2	0.3	1.9	2042	6	0.9	1158	8	0.7

4. Average and Standard deviations for Solid Assays repeats

Cu			S			Rh		
Average	Std dev.	Std dev. / Avg %	Average	Std dev.	Std dev. / Avg %	Average	Std dev.	Std dev. / Avg %
39.0	4.8	12.2	25.6	0.3	1.1	0.2	0.005	2
58.6	0.2	0.4	28.7	0.6	2.0	0.4	0.1	19
58.6	0.4	0.6	30.0	0.5	1.7	0.8	0.1	14
60.6	2.2	3.6	30.6	3.9	12.7	0.8	0.1	10
62.9	0.0	0.0	31.5	0.7	2.3	0.9	0.1	8
			94.9	0.0	0.0	1.0	0.2	16
						1.2	0.2	15
						1.3	0.3	21
						2.2	0.2	9
						3.2	0.5	17
						4.0	0.9	22
						16.4	0.4	2
Average	1.5	3.4		1.0	3.3		0.2	13

5. Comparative statistics using T-Test

	High Rh concn comparison		Medium conc comparison		Low Rh conc comparison		Very Low Rh conc comparison	
Total relative error	0.086		0.063		0.12		0.3	
Average x_i	90.0	85.7	50	48.4	20	16.2	0.25	0.1
n_i	25	25	29	29	4	4	2	3
s_i	7.7	7.4	3	3	2	2	0.08	0.03
S pooled	8		3		2.2		0.05	
t	2.012		2.028		2.461		3.303	
DOF	48		56		6		3	
Significance (two-sided)	95.0		95.3		95.1		95.4	
Significance (one-sided)	97.5		97.6		97.5		97.7	
95% confidence limits	3.0		1.1		2.1		0.1	
90% confidence limits	2.5		0.9		1.8		0.1	
Difference @95%	4		2		4		0.2	

B.4. Log sheets, Assays and Mass Balance Tables

Miscellaneous:

0-2 Rh_2S_3 seed production
0-3 Produce PdS (Pd mg/l)

Kinetic tests:

1 Ionic Rh precipitation
2 Ionic Rh precipitation
3 Ionic Rh precipitation
4 Ionic Rh precipitation
4R Ionic Rh precipitation repeat

5a CuS precipitation
5b Substitution reaction
6a CuS precipitation
6b Substitution reaction
7a CuS precipitation
7b Substitution reaction
8a CuS precipitation
8b Substitution reaction

9 Cu and Rh co-precipitation *in situ*
9R Cu and Rh co-precipitation *in situ* repeat
10 Cu and Rh co-precipitation *in situ*
11 Cu and Rh co-precipitation *in situ*
11R Cu and Rh co-precipitation *in situ* repeat
12 Cu and Rh co-precipitation *in situ*

Table of final solution and calculated solution concentrations

Test # :	0-2	
Test description:	Stoichiometric sulphide addition to make Rh ppt seed.	
Conditions:		
Temperature	150	oC
Make-up Volume	5.200	L
Volume before injection (operating volume)	5.000	L
Seed (Rh sulphide)	0	mg
CuSO4	0.00	g
NiSO4	0.00	g
FeSO4	0.00	g
K2SO4	11.71	g
Na2S2O3.5H2O actaul added	3.51	g
Volume reagent set at	100	mL
Volume Rh stock soln pipetted (actual)	100	mL
H2SO4	68.56	g

Time	Temp	Pressure	Agitator	Sample	Filter paper	FP + solids	Net Dry	[Solid]		pH	Redox	Observations
(min)	oC	kPa	rpm	Volume	g	g	mass g	g/l			mV	
Feed				100								light yellow solution
												micropore discolouration with brown ppt, solution
0	150	690 stm+N2	530	100	0.129	0.129	0.00	0		NA	NA	same yelow
												too soon too sample due to injector/sampler change-
1	150	690 stm+N2			NA	NA	NA	NA		NA	NA	over
2.40	150	690 stm+N2		100	0.129	0.152	0.023	0.23		NA	NA	black ppt, soln slightly brown
5	150	690 stm+N2	520	90	0.122	0.158	0.036	0.40		NA	NA	max. black ppt (visual),
10	150	690 stm+N2	536	100	0.130	0.154	0.024	0.24		NA	NA	black ppt, soln slightly brown
30	150	690 stm+N2		90	0.129	0.151	0.022	0.24		NA	NA	black ppt, soln slightly brown
												black ppt, soln going darker with time, slight H2S
60	150	690 stm+N2		105	0.123	0.144	0.021	0.20		NA	NA	smell,possible corrosion induced
90	150	690 stm+N2	527	100	0.127	0.161	0.034	0.34		NA	NA	black ppt, soln going darker with time
120	150	690 stm+N2		100	0.127	0.154	0.027	0.27		NA	NA	black ppt, soln going darker with time
180	150	690 stm+N2	547	95	0.125	0.157	0.032	0.34		NA	NA	black ppt, soln going darker with time
240	150	690 stm+N2	527	100	0.123	0.151	0.028	0.28		NA	NA	black ppt, soln darkest brown soln
242												Added 10.5 g Na2S2O3.5H2O
247												Cooldown after 5 min at 150 oC
249	137											
250	127		536									
251	117											
252	108		537									
254	100											90% of sample forced out of sampler at 85 oC
265	filtration			4120	14.78	16.83	2.06	0.50				Pressure filtration started, clear, colourless solution
												SO2 smell from soln, <1mm cake thickness, some
												fines passing
												(fines collected on millipore) , double expected mass
												due to Fe contamination

Comments:

100 mL sample easy filtration on millipore, total sample filtration on millipore very slow, performed on 5 millipore papers
solids repulped formed large flocs.
Strong SO2 was not detected upon venting as in first scouting test.
316L shaft possible cause S2- lost to SO2, what is SO2 partial pressure at 150 oC

Test # : 0-3
Test description: Stoichiometric sulphide addition to make PdS ppt seed (slight excess Pd).

Conditions Bench top magnetic stirrer with heating

Temperature		85-95	oC
Make-up Volume		1.000	L
Volume before injection (operating volume)		1.000	L
Seed (Rh sulphide)		none	mg
CuSO4		0.00	g
NiSO4		0.00	g
FeSO4		0.00	g
K2SO4		1.00	g
Na2S2O3.5H2O actaul added		0.30	g excess of 0.3 g assuming Pd(II)
Volume Pd stock soln pipetted (actual)		100	mL
H2SO4		0.00	g

Time	Temp	Pressure	Agitator	Sample	Filter paper	FP + solids	Net Dry	[Solid]	pH	Redox	Observations
(min)	oC	kPa	rpm	Volume	mg	mg	mass mg	g/l		mV	
Feed				100							
0	85-95	90 stm+N2	530	100			0.00	0	NA	NA	light orange solution
0.1	85-95										Solution colours darkens immediately
0.50	85-95										black ppt, soln almost clear
5	85-95	90 stm+N2	520	90	122	158	36	0.40	NA	NA	max. black ppt, clear soln, large flocs (visual),
60	85-95	90 stm+N2	536	100	130.000	154.000	24	0.24	NA	NA	black ppt, clear soln, flocs
60-90											solid / liquid separation and cake washing
0	Add ~10 ml PdCl2 soln to ensure no excess sulphide										slight orange colour to solution
60	85-95										visually clear soln
											easilty filterable, seems crystalline
											possibly some shiny alloy? Or refective xstals

Comments:
All Pd(II) precipitated within 5 min . Flashed back within 30 sec. Darkening of solution probably due to complexing or primary nucleation.
Flashed black within 30 sec.
Switching off magnetic stirrer showed that large flocs formed.

Test # : 1
Test description: Ionic precipitation of Rh from pure synthetic solutions containing no Cu(II)

Conditions:

Temperature	50 oC	
Make-up Volume	5.200 L	(incl. Rh soln)
Volume before injection (operating volume)	4.984 L	
Seed (Pd sulphide)	25 mg	
CuSO4.5H20 added to make-up volume	0.00 g	
NiSO4 added to make-up volume	0.00 g	
FeSO4 added to make-up volume	0.00 g	
K2SO4 added to make-up volume	11.70 g	
Na2S2O3.5H2O added at t=0	67.31 g	
Volume reagent set at	190 mL	
Volume Rh stock soln pipetted (actual)	50 mL	
H2SO4 to make-up	74.07 g	

Time (min)	Temp oC	Pressure kPa	Agitator rpm	Sample Volume	Filter paper g	FP + solids g	Net Dry mass g	[Solid] g/l	[Solid] S g/l	[Solid] Rh2S3 g/l	Redox mV	Observations
Feed			375	40				measured	calc'd	calc'd		
0	50		374	168	122	125	3	0.02	0.00	0		34 ml flush; milky
1	50		375	152	127	225	98	0.84	3.62	0.012	214	milky beige; very poor filtration;
2	50		374	98	124	193	69	0.70	3.49	0.020	220	wash water extremely slow filtration
6	50		368	106	123	230	107	1.01	4.27	0.020	224	
12	50		364	100	126	243	117	1.17	4.54	0.031	239	
30	50		364	114	126	274	148	1.30	4.01	0.028	244	milky tea colour; filtrate clear
60	50		350	94	125	252	127	1.35	4.14	0.031	243	
90	50		346	100	125	262	137	1.37	4.27	0.036	245	
120	50		338	100	124	261	137	1.37	4.14	0.037	250	
180	50		338	96	124	261	137	1.43	4.27	0.041	243	
240	50		334	482	249	940	691	1.43	4.54	0.043		strong milk coffee colour
300	50.0			3310	192615	197370	4755	1.44	5.19	0.040		slow filtration relative to # 2 and 3, dark brown
		splash over		100								
		flush at t= 1		34								
Volume balance shortage				298								
		Vf / Vo %		84								

Comments:

Slight SO2smell initially,but significantly less than test # 2 and 3.
Post-pptn in all samples
Filtrate samples have strong SO2 smell.
Solids are brown
Filtration and precipitate darkness increased with reaction time.

S [g/l] calculated from acid consumption
Rh2S3 [g/l] calculated from Rh soln
[Rh] mg/l calculated from Rh in solids, assuming final Rh % across the profile

Average solution and solid assays with Mass Balance Test #: 1

Sample #	Time (min)		Cu (mg/l)	Ni (mg/l)	H2SO4 (g/l)	Na (mg/l)	K (mg/l)	Rh (mg/l)	Rh calc'd (mg/l)	Redox Ag/AgCl mV	
			Solution concentration								
Rh/1307/1/ 0/L1	0		7	8	14.9	66	1145	92.6	92.6		
Rh/1307/1/ 1/L2 avg	1		NR	NR	12.1	NR	1140	84.4	84.4	214	Rh solution concn calcualted from solids mass profil
Rh/1307/1/ 2/L3	2		NR	NR	12.2	NR	1156	79.2	83.7	220	assuming Rh % in solids of final sample
Rh/1307/1/ 6/L4	6		NR	NR	11.8	NR	1161	79.0	79.8	224	
Rh/1307/1/ 12/L5 avg	12		NR	NR	11.4	NR	1144	71.7	77.7	239	
Rh/1307/1/ 30/L6	30		NR	NR	11.8	NR	1139	73.7	76.1	244	
Rh/1307/1/ 60/L7	60		NR	NR	11.7	NR	1156	71.4	75.4	243	
Rh/1307/1/ 90/L8	90		NR	NR	11.6	NR	1153	67.9	75.2	245	
Rh/1307/1/ 120/L9	120		NR	NR	11.7	NR	1256	67.2	75.2	250	
Rh/1307/1/ 180/L10 avg	180		NR	NR	11.6	NR	1267	84.7	74.4	243	
Rh/1307/1/ 240/L11	240		< 2	9	11.4	NR	1177	53.5	74.4		
Rh/1307/1/ 300/L12 avg	300		2	9	10.9	2264	1243	65.1	74.3		

Sample #	Time (min)		Cu %	Ni %	S %	Na ppm	K ppm	Rh %	Concn g/L	
			Solid concentration							
	240								0.02	
Rh/1307/1/ 300/S2 avg	300		0.05	0.05	84.8	NR	NR	1.27	1.43	

Mass balance: Amount removed (mmol/l)			Cu	Ni	H2SO4	Na	K	Rh soln	Rh solids	
Solution basis (mmol/L)	1				26.2			0.06	0.06	
	2				27.2			0.13	0.09	
	6				33.3			0.13	0.13	
	12				35.4			0.20	0.14	
	30				31.3			0.18	0.16	
	60				32.3			0.21	0.17	
	90				33.3			0.24	0.17	
	120				32.3			0.25	0.17	
	180				33.3			0.27	0.18	
	240		0.08	0.0	35.4			0.28	0.18	
	300		0.08	0.0	40.5	-95.6		0.27	0.18	

Solid basis (mmol/L)			Cu	Ni	S	Na	K	Rh		
	300		0.01	0.01	42.4			0.18		
Stiochiometry (soln basis)				Acid / S	Acid / Na	S / Na		Rh / acid		2 mol Na for 1 mol Na2S2O3.5H20
Mole ratios %										Na = Na2S2O3.5H20
100% required	300			95.5	85	89		0.66		S =elemental S or S(2-)
										100% is a 1:1 mole ratio
Accountability (per litre)								Rh		
=100-(soln-solid)/soln%	300							66.3		% mol Rh removed from soln / Rh in solids
= (mol Rh in soln+solids @t=final) / (Rh @ t=0) %								90.0		total accountability
Solution concentrations calculated	0		7	8	14.9	85.5	1145	98		
from solid mass and assay	240		7					74		

Acid balance

Feed	mmol/l			151.6	85.6				
Acid generated from MeS precipitation	mmol/l	0.08					0.40		
Acid consumed (elemental S: Total S - MeS)	mmol/l			10.1					
Acid concentration predicted	mmol/l			142.0					
Acid concentration predicted	g/l			13.9					
Accountability (t=final) (actual-pred.)/actual%				-27.8					

Test # : 2

Test description: Ionic precipitation of Rh from pure synthetic solutions containing no Cu(II)

Conditions:

Temperature	80 oC	
Make-up Volume	5.200 L	(incl. Rh soln)
Volume before injection (operating volume)	5.002 L	
Seed (Pd sulphide)	25 mg	
CuSO4.5H20 added to make-up volume	0.00 g	
NISO4 added to make-up volume	0.00 g	
FeSO4 added to make-up volume	0.00 g	
K2SO4 added to make-up volume	11.70 g	
Na2S2O3.5H2O added at t=0	67.31 g	
Volume reagent set at	190 mL	
Volume Rh stock soln pipetted (actual)	50 mL	
H2SO4 to make-up	74.07 g	

Time (min)	Temp oC	Pressure kPa	Agitator rpm	Sample Volume	Filter paper mg	FP + solids mg	Net Dry mass mg	[Solid] g/l	[Solid] g/l S	[Solid] Rh2S3	Redox mV	Observations
Feed				40	122	127	5	0.13	calc'd	calc'd		flush
0	80		401	158	126	132	6	0.04	0.00	0	393	slightest discolouration of filter paper; strong SO2 smell
1	80			120	124	245	121	1.01	2.92	0.032	206	colloidal light milky brown; poor filtration
2	80		380	96	125	240	115	1.20	3.70	0.034	214	colloidal light milky brown; better filtration
5	80			118	126	280	154	1.31	5.93	0.032	220	filtration ok,slurry darkening.
10	80		369	104	124	269	145	1.39	3.97	0.049	224	
30	80			116	124	291	167	1.44	4.62	0.047	239	brown slurry
60	80			134	126	318	192	1.43	4.36	0.063	244	darker brown slurry, clear filtrate ,fast filtration
90	80		353	96	126	270	144	1.47	4.49	0.071	243	darker brown slurry, clear filtrate ,fast filtration
120	80		360	118	121	298	177	1.50	4.62	0.072	245	darker brown slurry, clear filtrate ,fast filtration
180	80		365	96	120	260	140	1.46	4.75	0.076	250	darker brown slurry, clear filtrate ,fast filtration
240	80			3950	192741	198520	5779	1.46	4.75	0.034	243	Darkest slurry and precipitate. Slight SO2 smell.
		splash over		100								
		flush at t= 1		34								
Volume balance shortage				108								
		Vf / Vo %		76								

Comments:

Precipiate got darker with time and filtration improved with time. Filtrate decreased in colour to almost clear.

Post precipitation in t= 1, t=2 and t = 5 min.
Strong SO2 smell initially. Slight SO2smell in final filtrate.

S [g/l] calculated from acid consumption
Rh2S3 [g/l] calculated from Rh soln
[Rh] mg/l calculated from Rh in solids, assuming final Rh % across the profile

Average solution and solid assays with Mass Balance — Test #: 2

Solution concentration

Sample #	Time (min)		Cu (mg/l)	Ni (mg/l)	H2SO4 (g/l)	Na (mg/l)	K (mg/l)	Rh (mg/l)	Rh calc'd (mg/l)	Redox Ag/AgCl mV	
Rh/1207/2/ 0/L1 avg	0		9	8	14.9	11	1127	92.6	92.6		
Rh/1207/2/ 1/L2 avg	1		< 2	9	12.7	NR	1121	71.1	60.8	206	
Rh/1207/2/ 2/L3 avg	2		NR	NR	12.1	NR	1126	69.4	54.8	214	
Rh/1207/2/ 5/L4 avg	5		NR	NR	10.4	NR	1113	70.5	51.4	220	
Rh/1207/2/ 10/L5 avg	10		NR	NR	11.9	NR	1117	59.2	48.6	224	
Rh/1207/2/ 30/L6	30		NR	NR	11.4	NR	1107	60.4	47.2	239	
Rh/1207/2/ 60/L7	60		NR	NR	11.6	NR	1120	49.5	47.4	244	
Rh/1207/2/ 90/L8 avg	90		NR	NR	11.5	NR	1127	44.4	46.2	243	
Rh/1207/2/ 120/L9 avg	120		NR	NR	11.4	NR	1121	43.4	45.3	245	
Rh/1207/2/ 180/L10 avg	180		< 2	9	11.3	NR	1126	41.0	46.6	250	
Rh/1207/2/ 240/L11 avg	240		2	9	11.3	2264	1130	35.6	46.4		

Solid concentration

Sample #	Time (min)		Cu %	Ni %	S %	Na ppm	K ppm	Rh %		Concn g/L
Rh/1207/2/ 240/S2 avg	240		0.19	NR	94.9	0.315	0.0	3.16		1.46

Mass balance: Amount removed (mmol/l)

Solution basis (mmol/L)		Cu	Ni	H2SO4	Na	K	Rh soln	Rh solids
	1			22.8			0.21	0.31
	2			28.9			0.23	0.37
	5			46.2			0.22	0.40
	10			30.9			0.32	0.43
	30			36.0			0.31	0.44
	60			34.0			0.42	0.44
	90			35.0			0.47	0.45
	120			36.0			0.48	0.46
	180	0.10	0.0	37.0			0.50	0.45
	240	0.10	0.0	37.0	-96.0	-0.1	0.55	0.45

Solid basis (mmol/L)		Cu	Ni	S	Na	K	Rh
	240	0.04		43.3	0.2	0.0	0.45

Stiochiometry (soln basis)			Acid / S	Acid / Na	S / Na		Rh / acid
Mole ratios %	240		85.5	76	88		1.50

Na = Na2S2O3.5H20
S =elemental S or S(2-)
100% is a 1:1 mole ratio

Accountability		Rh
=100-(soln-solid)/soln%	240	80.9
= (mol Rh in soln+solids @ t=final) / (Rh @ t=0) %		88.2
Solution concentrations	0	93
calculated from solid	240	46

Acid balance

Feed	mmol/l			152.3	0.0				
Acid generated from MeS precipitatio	mmol/l	0.10					0.83		
Acid consumed (elemental S: Total S	mmol/l			10.7					
Acid concentration predicted	mmol/l			141.6					
Acid concentration predicted	g/l			13.9					
Accountability (t=final) (actual-pred.)/actual%				-22.9					

Test # :	3
Test description:	Ionic precipitation of Rh from pure synthetic solutions containing no Cu(ii)

Conditions:

Temperature	95 oC	
Make-up Volume	5.200 L	(incl. Rh soln)
Volume before injection (operating volume)	4.998 L	
Seed (Pd sulphide)	25 mg	
CuSO4.5H20 added to make-up volume	0.00 g	
NiSO4 added to make-up volume	0.00 g	
FeSO4 added to make-up volume	0.00 g	
K2SO4 added to make-up volume	11.70 g	
Na2S2O3.5H2O added at t=0	67.31 g	
Volume reagent set at	190 mL	
Volume Rh stock soln pipetted (actual)	50 mL	
H2SO4 to make-up	74.07 g	

Time (min)	Temp oC	Pressure kPa	Agitator rpm	Sample Volume	Filter paper mg	FP + solids mg	Net Dry mass mg	[Solid] g/l	[Solid] g/l S	[Solid] Rh2S3	Redox mV	Observations
Feed				66				measured	calc'd	calc'd		flush
0	95		411	136	125	128	3	0.02	0.00	0	433	slightest discolouration of filter paper; strong SO2 smell
1	95		410	130	126	297	171	1.32	4.43	0.044	230	sampler flushed at t=30; colloidal light milky brown; poor filtration
2	95		411	108	9156	9298	142	1.31	3.65	0.059	235	colloidal light milky brown; better filtration
5	95		413	108	9162	9305	143	1.35	5.48	0.062	238	filtration ok,slurry darkening.
10	95		413	98	125	260	135	1.41	6.13	0.075	252	
30	95		401	110	9159	9321	162	1.47	5.61	0.076	262	brown slurry
60	95		403	102	9037	9192	155	1.52	5.67	0.089	270	darker brown slurry, clear filtrate ,fast filtration
90	95		395	114	126	294	168	1.47	6.13	0.090	275	darker brown slurry, clear filtrate ,fast filtration
120	95		400	108	126	289	163	1.51	6.26	0.095	285	darker brown slurry, clear filtrate ,fast filtration
180	95		398	98	125	273	148	1.51		0.097	303	darker brown slurry, clear filtrate ,fast filtration
240	95		337	3950	192613	198570	5957	1.51	4.97	0.101	297	Darkest slurry and precipitate. Slight SO2 smell.
		splash over		100								
		flush at t= 1		30.0								
Volume balance shortage				136								
		Vf / Vo %		76								

Comments:

Precipiate got darker with time and filtration improved with time. Filtrate decreased in colour to almost clear.

Post precipitation in t= 1 and t=2 min.
Strong SO2 smell initially. Slight SO2smell in final filtrate.

S [g/l] calculated from acid consumption
Rh2S3 [g/l] calculated from Rh soln
[Rh] mg/l calculated from Rh in solids, assuming final Rh % across the profile

Average solution and solid assays with Mass Balance — Test #: 3

Sample #	Time (min)		Cu (mg/l)	Ni (mg/l)	H2SO4 (g/l)	Na (mg/l)	K (mg/l)	Rh (mg/l)	Rh calc'd (mg/l)	Redox Ag/AgCl mV
Rh/1107/3/ 0/L1 avg	0		35	NR	16.1	11	1147	92.6	92.6	433
Rh/1107/3/ 1/L2	1		NR	NR	12.7	NR	1114	62.4	40.4	230
Rh/1107/3/ 2/L3	2		NR	NR	13.3	NR	1116	52.5	40.4	235
Rh/1107/3/ 5/L4	5		NR	NR	11.9	NR	1101	50.6	39.0	238
Rh/1107/3/ 10/L5	10		NR	NR	11.4	NR	1096	41.8	36.8	252
Rh/1107/3/ 30/L6	30		NR	NR	11.8	NR	1119	41.1	34.1	262
Rh/1107/3/ 60/L7 avg	60		NR	NR	11.8	NR	1128	32.2	32.3	270
Rh/1107/3/ 90/L8	90		NR	NR	11.4	NR	1132	31.3	34.1	275
1107/3/ 120/L9 avg	120		NR	NR	11.3	NR	1146	27.9	32.7	285
Rh/1107/3/ 180/L10 avg	180		< 2	NR	11.8	2363	1169	26.4	32.6	303
Rh/1107/3/ 240/L11 avg	240		2	NR	12.3	2446	1137	23.7	32.7	

Solid concentration

Sample #	Time (min)		Cu %	Ni %	S %	Na ppm	K ppm	Rh %		Conc g/L
Rh/1107/3/ 240/S1 avg	240		2.335	NR	91.8	NR	NR	3.97		1.51

Mass balance: Amount removed (mmol/l)			Cu	Ni	H2SO4	Na	K	Rh	Rh solids
Solution basis (mmol/L)	1				34.6			0.29	0.51
	2				28.4			0.39	0.51
	5				42.7			0.41	0.52
	10				47.8			0.49	0.54
	30				43.7			0.50	0.57
	60				44.2			0.59	0.59
	90				47.8			0.60	0.57
	120				48.8			0.63	0.58
	180		0.51		44.2			0.64	0.58
	240		0.51		38.7	-105.9		0.67	0.58

Solid basis (mmol/L)			Cu	Ni	S	Na	K	Rh		
	240		0.55		43.2			0.58		
Stoichiometry (soln basis)				Acid / S	Acid / Na	S / Na		Rh / acid		
Mole ratios %	240			89.7	73	62		1.73		Na = Na2S2O3.5H20 S =elemental S or S(2-) 100% is a 1:1 mole ratio
Accountability								Rh		
=100-(soln-solid)/soln%	240							86.9		
= (mol Rh in soln+solids @ t=final) / (Rh @ t=0) %								90.3		
Solution concentrations	0		34.7		16.1	11	1147	98		
calculated from solid	240		-0.5					33		

Acid balance

Feed	mmol/l			164.0	0.0				
Acid generated from MeS precipitation	mmol/l	0.51					1.00		
Acid consumed (elemental S: Total S	mmol/l			9.3					
Acid concentration predicted	mmol/l			156.3					
Acid concentration predicted	g/l			15.3					
Accountability (t=final) (actual-pred.)/actual%				-24.7					

Test # :		4	
Test description:	Ionic precipitation of Rh from pure synthetic solutions containing no Cu(II)		
Conditions:			
Temperature		150 oC	
Make-up Volume		5.200 L	(incl. Rh soln)
Volume before injection (operating volume)		4.998 L	
Seed (Pd sulphide)		25 mg	
CuSO4.5H20 added to make-up volume		0.00 g	
NiSO4 added to make-up volume		0.00 g	
FeSO4 added to make-up volume		0.00 g	
K2SO4 added to make-up volume		11.70 g	
Na2S2O3.5H2O added at t=0		67.31 g	
Volume reagent set at		190 mL	
Volume Rh stock soln pipetted (actual)		50 mL	
H2SO4 to make-up		74.07 g	

Time	Temp	Pressure	Agitator	Sample	Filter paper	FP + solids	Net Dry	[Solid]	[Solid]	[Solid]	Redox	Observations
(min)	oC	kPa	rpm	Volume	mg	mg	mass mg	g/l	g/l S	Rh2S3	mV	
0				90				measured	calc'd	calc'd		Feed flush
0	150	~500	414	112				unknown	0	0	424	No solids visible; H2S and SO2/SO3 smell.
1	150	~500	416	102				unknown	5.13	0.036	276	Colourless solution indicating complete Rh pptn
2	150	~500	414	100				unknown	5.65	0.037	274	
4	150	~500	414	98				unknown	5.59	0.037	323	Precipiate formed on PV internals and walls.
7	150	~500		100				unknown	5.65	0.038	285	
10	150	~500		108				unknown	5.26	0.038	300	
20	150	~500		120				unknown	5.65	0.038	294	
30	150	~500		100				unknown	5.52	0.038	299	
60	150	~500	415	4240				unknown	4.74	0.038	368	
		splash over		100								
		flush at t= 1		0								
Volume balance shortage				120								
		Vf / Vo %		82								

Comments:
Crystalline Rh precipitate formed on PV internals and walls.

Recommendation:
Repeat #4, but add Rh at 150 oC, sample for Rh concentration and then inject thiosulphate!

S [g/l] calculated from acid consumption
Rh2S3 [g/l] calculated from Rh soln
[Rh] mg/l calculated from Rh in solids, assuming final Rh % across the profile

Average solution and solid assays with Mass Balance — Test #: 4

Solution concentration

Sample #	Time		Cu	Ni	H2SO4	Na	K	Rh	Rh calc'd	Redox Ag/AgCl
	(min)		(mg/l)	(mg/l)	(g/l)	(mg/l)	(mg/l)	(mg/l)	(mg/l)	mV
Rh/2107/4/ 0/L1 avg	0		75.04707	NR	15.2	9	1177	25.8		424
Rh/2107/4/ 1/L2	1		NR	NR	11.3	2599	1182	1.2		276
Rh/2107/4/ 2/L3	2		NR	NR	10.9	NR	1171	0.6		274
Rh/2107/4/ 4/L4 avg	4		NR	NR	11.0	NR	1196	0.4		323
Rh/2107/4/ 7/L5	7		NR	NR	10.9	NR	1192	0.2		285
Rh/2107/4/ 10/L6	10		NR	NR	11.2	NR	1224	0.1		300
Rh/2107/4/ 20/L7	20		NR	NR	10.9	NR	1180	0.1		294
Rh/2107/4/ 30/L8	30		NR	NR	11.0	NR	1201	0.1		299
Rh/2107/4/ 60/L9 avg	60		2	NR	11.6	2698	1268	0.1		368

Solid concentration

Sample #	Time		Cu	Ni	S	Na	K	Rh		Concn
	(min)		%	%	%	ppm	ppm	%		g/L
Rh/2107/4/60/S1	60		N.R.	N.R.	N.R.	N.R.	N.R.	N.R.		unknown

Mass balance: Amount removed	(mmol/l)	Cu	Ni	H2SO4	Na	K	Rh
Solution basis (mmol/L)	1			40.0			0.24
	2			44.1			0.24
	4			43.6			0.25
	7			44.1			0.25
	10			41.0			0.25
	20			44.1			0.25
	30			43.0			0.25
	60	1.1		36.9	-117		0.25

Solid basis (mmol/L)		Cu	Ni	S	Na	K	Rh		
	60						N.R.		
Stiochiometry (soln basis)			Acid / S	Acid / Na	S / Na		Rh / acid		
Mole ratios %	60			63			0.68		Na = Na2S2O3.5H20 S =elemental S or S(2-) 100% is a 1:1 mole ratio
Accountability							Rh		
=100-(soln-solid)/soln%	60								
= (mol Rh in soln+solids @ t=final) / (Rh @ t=0) %									
Solution concentrations	0	75.0		15.2	9.1520617	1177	26		
calculated from solid mass	0	75.0							

Acid balance

Feed	mmol/l							
Acid generated from MeS precipitation	mmol/l							
Acid consumed (elemental S: Total S - M	mmol/l							
Acid concentration predicted	mmol/l							
Acid concentration predicted	g/l			NR				
Accountability (t=final) (actual-pred.)/actual	%			NR				

Test # :		4R
Test description:	Ionic precipitation of Rh from pure synthetic solutions containing no Cu(II)	

Conditions:

Temperature	150 oC	
Make-up Volume	5.200 L	(incl. Rh soln and chaser)
Volume before injection (operating volume)	5.026 L	
Seed (Pd sulphide)	none mg	
CuSO4.5H2O added to make-up volume	0.00 g	
NiSO4 added to make-up volume	0.00 g	
FeSO4 added to make-up volume	0.00 g	
K2SO4 added to make-up volume	11.70 g	
Na2S2O3.5H2O added at t=0	67.31 g	
Volume reagent set at	190 mL	
Volume Rh stock soln pipetted (actual)	50 mL	
H2SO4 to make-up	74.07 g	

Time (min)	Temp oC	Pressure kPa	Agitator rpm	Sample Volume	Filter paper mg	FP + solids mg	Net Dry mass mg	[Solid] g/l	[Solid] g/l S	[Solid] Rh2S3	Redox mV	Observations
0				74				measured	calc'd	calc'd		Feed flush before Rh injection
0	150		405	98	120	124	4	0.04	0.00	0	403	H2S and SO2/SO3 smell.; brown ppt, flocculated
1	150		406	106	121	270	149	1.41	7.29	0.077	234	fast filtration (sample 1 and 2 possibly swapped),
2	150		406	100	120	271	151	1.51		0.095	218	t=1 and t=2 showed post pptn; H2S smell;
4	150		405	106	119	276	157	1.48	6.11	0.115	253	Clear filtrate; darkbrown/black ppt
6	150		405	106	120	270	150	1.42	6.11	0.123	270	black ppt
8	150		405	102	121	266	145	1.42	6.11	0.129	274	black ppt
11	150		405	112	120	280	160	1.43	5.85	0.139	283	black ppt
15	150		405	100	120	260	140	1.40	6.44	0.135	282	black ppt
27	150		402	3695	362	6506	6144	1.66	6.24	0.136	278	SO2/SO3 smell;
												black ppt, crystalline, very high bulk density, very electrostatic
		splash over		100								
		flush at t= 1		54								
		H2O lost to flash/boiling										
Volume balance shortage				637								
Final volume / initial volume		Vf / Vo %		71								

Comments:
Crystalline Rh precipitate formed on PV internals and walls.

Recommendation:
Repeat #4, but add Rh at 150 oC, sample for Rh concentration and then inject thiosulphate!

S [g/l] calculated from acid consumption
Rh2S3 [g/l] calculated from Rh soln
[Rh] mg/l calculated from Rh in solids, assuming final Rh % across the profile

Average solution and solid assays with Mass Balance — Test #: 4R

Solution concentration

Sample #	Time (min)		Cu (mg/l)	Ni (mg/l)	H2SO4 (g/l)	Na (mg/l)	K (mg/l)	Rh (mg/l)	Rh calc'd (mg/l)	Redox Ag/AgCl mV	
Rh/1008/4R/ 0/L1	0		4.05167266	< 2	17.1	10	931	92.6	92.6	403	
Rh1008/4R/ 1/L2 avg	1		NR	NR	11.5	2581	927	40.0	62.0	234	
Rh/1008/4R/ 2/L3 avg	2		NR	NR	NR	NR	955	27.8	59.7	218	
Rh/1008/4R/ 4/L4	4		NR	NR	12.4	NR	955	14.2	60.4	253	
Rh/1008/4R/ 6/L5	6		NR	NR	12.4	NR	955	8.9	61.8	270	
Rh/1008/4R/ 8/L6	8		NR	NR	12.4	NR	955	4.5	61.7	274	
Rh/1008/4R/ 11/L7	11		NR	NR	12.6	NR	955	2.2	61.5	283	
Rh/1008/4R/ 15/L8 avg	15		NR	NR	12.2	NR	955	0.8	62.1	282	
Rh/1008/4R/ 27/L9 avg	27		< 2	< 2	12.3	2583	972	0.1	56.4	278	

Solid concentration

Sample #	Time (min)		Cu %	Ni %	S %	Na ppm	K ppm	Rh %		Concn g/L	
Rh/1508/ 4R/S1	27		NR	NR	95.2	NR	NR	2.18		1.66	Poor Rh accountability due to solids precipitation on internals of PV

Mass balance: Amount removed (mmol/l)

Solution basis (mmol/L)			Cu	Ni	H2SO4	Na	K	Rh		
	1				56.8			0.51		
	2							0.63		
	4				47.7			0.76		
	6				47.7			0.81		
	8				47.7			0.86		
	11				45.6			0.88		
	15				50.2			0.89		
	27		0.0	0.0	48.7	-111.9		0.90		

Solid basis (mmol/L)			Cu	Ni	S	Na	K	Rh			
	27		NR	NR	49.4	NR	NR	0.35			

Stiochiometry (soln basis)				Acid / S	Acid / Na	S / Na		Rh / acid			
Mole ratios %	27			98.6	87	88		1.85			Na = Na2S2O3.5H2O S =elemental S or S(2-) 100% is a 1:1 mole ratio

Accountability											
=100-(soln-solid)/soln%	27							39.1			
= (mol Rh in soln+solids @ t=final) / (Rh @ t=0) %								39.2			
Solution concentrations calculated	0		4.1	< 2	17.1	9.84684015	931	93			
from solid mass and assay	0		NR	NR		NR	NR	56			

Acid balance (solution assays and S in solid)

Feed	mmol/l			174.1	111.9			
Acid generated from MeS precipitation	mmol/l	0.03					1.35	
Acid consumed (elemental S: Total S - MeS)	mmol/l			11.0				
Acid concentration predicted	mmol/l			184.5				
Acid concentration predicted	g/l			18.1				
Accountability (t=final) (actual-pred.)/actual%				-31.2				

Test # :	5a
Test description:	CuS formation for substitution reaction

Conditions:

Temperature	50 oC	
Make-up Volume	5.400 L	
Volume before injection (operating volume)	5.190 L	
Seed (Pd sulphide)	none mg	
CuSO4.5H20 added to make-up volume	293.60 g	
NiSO4 added to make-up volume	139.90 g	
FeSO4 added to make-up volume	0.00 g	
K2SO4 added to make-up volume	11.70 g	
Na2S2O3.5H2O added at t=0	67.31 g	
Volume reagent set at	190 mL	
Volume Rh stock soln pipetted (actual)	0.00 mL	
H2SO4 to make-up	76.30 g	(adjusted for pH 2 water in error;should have been 79 g for 15 g/l)

Time (min)	Temp oC	Pressure kPa	Agitator rpm	Sample Volume	Filter paper mg	FP + solids mg	Net Dry mass mg	[Solid] g/l	[Solid] g/l CuS	Redox mV	Observations
Feed 1				100				measured	calc'd		
Feed 2 (t=0)	35		450	110							
0	35										inject 190 mL (67.3 g thiosulphate)
10	35			10							clear green solution;no ppt; increase temperature set point to 50 oC
35	41		470	10							
39	51		470								
45	50		470								
58	50		470								
62	50		470	10							
75	50		470								
78	50		470								10.6 g/l Cu onn AA
88	50		470								9.7 g/l Cu onn AA
129	50		470	10							10.2 g/l Cu onn AA; reaction stopped
144	50		470					2.88	3.59		sample at 10 min turining colloidal brown
											(days laters ppt still brown ; not black
											Solids measured in 5 b feed sample

Comments:
10 min sample and subsequent samples were heating on magnetic stirrer at 50 oC to make required CuS ppt.
heating 1st sample >40 oC for 5 min , precipitation occurred from mercy green to greeny brwon, brown and then black The precipitate was added backto the bulk solids to maintain CuS mass.
Cake repulped in pH 2 watrer, refiltered and stored in pH2 water at room temperature for days before part (b) of test.
25 ml lost to slurry lost over PV sleeve.

Average solution and solid assays with Mass Balance — Test #: 5a

Sample #	Time (min)		Solution concentration Cu (mg/l)	Ni (mg/l)	H2SO4 (g/l)	Na (mg/l)	K (mg/l)	Rh (mg/l)	Redox Ag/AgCl mV
Rh/2306/5a/t0/L1 avg	0		12902	5929	16.7	24	964	0.0	
Rh/2306/5a/fil/L4	80		10515	5891	16.5	2724	931	0.2	

Sample #	Time (min)		Solid concentration Cu %	Ni %	S %	Na ppm	K ppm	Rh %	Concn g/L
Rh/2806/5b/ TO/S1	80		i.s.	NR	25.8	NR	NR	0.01	2.88

Mass balance: Amount removed	(mmol/l)		Cu	Ni	H2SO4	Na	K	Rh
Solution basis (mmol/L)	80		37.6	0.65	-16.4	-117.4		0.00
Solid basis (mmol/L)	80				23.2			0.00

Stiochiometry (soln basis)			Cu / Na	Cu soln / S	Acid / Na	S / Na	Cu / Acid	Rh / acid	
Mole ratios %	80		64	162	31	39	205	0.01	2 mol Na for 1 mol Na2S2O3.5H20 Na = Na2S2O3.5H20 S =elemental S or S(2-) 100% is a 1:1 mole ratio

Accountability								Rh	
=100-(soln-solid)/soln%	80								
Solution concentrations	0		12902	5929	16.7	24	964	0	
calculated from solid mass	80								

Acid balance (solution assays and S in solid)							
Feed	mmol/l			170.3	117.4		
Acid generated from MeS precipitation	mmol/l	37.56					0.00
Acid consumed (elemental S: Total S - MeS)	mmol/l			0.0			
Acid concentration predicted	mmol/l			207.8			
Acid concentration predicted	g/l			20.4			
Accountability (t=final) (actual-pred.)/actual%				-10.2			

Test # :	5b
Test description:	Substitution reaction of Rh(III) with CuS at temperature

Conditions:

Temperature	50 oC
Make-up Volume	5.200 L
Volume before injection (operating volume)	4.970 L
Seed (Pd sulphide)	none mg
CuSO4.5H20 added to make-up volume	0.00 g
NiSO4 added to make-up volume	0.00 g
FeSO4 added to make-up volume	0.00 g
K2SO4 added to make-up volume	11.70 g
Na2S2O3.5H2O added at t=0	0.00 g
Volume reagent set at	100 mL
Volume Rh stock soln pipetted (actual)	50.00 mL
H2SO4 to make-up	74.05 g

Time (min)	Temp oC	Pressure kPa	Agitator rpm	Sample Volume	Filter paper mg	FP + solids mg	Net Dry mass mg	[Solid] g/l		Redox mV	Observations
0				20				measured			~20 mL lost to floor;
0	50	atm	430	210	347	952	605	2.88		546	reagents injeted 50 mL 10 g/l + 100 mL water chaser
1	50		400	98	126	409	283	2.89		488	light yellow solution
2	50		397	106	127	443	316	2.98		509	light yellow solution
5	50		397	100	125	441	316	3.16		453	light yellow solution
10	50		397	100	124	412	288	2.88		460	light yellow solution; getting slightly lihter with time
30	50		393	116	251	617	366	3.16		439	light yellow solution; getting slightly lihter with time
60	50		397	126	126	502	376	2.98		452	light yellow solution; getting slightly lihter with time
90	50		391	120	126	489	363	3.03		440	light yellow solution; getting slightly lihter with time
120	50		409	120	126	509	383	3.19		434	light yellow solution; getting slightly lihter with time
180	50		410	110	125	473	348	3.16		424	light yellow solution; getting slightly lihter with time
240	50		413	106	126	448	322	3.04		402	light yellow solution; getting slightly lihter with time
290	50		405	3800	101262	112858	11596	3.05		407	
		splash over		100							
											NB: t=1 sample was not flushed prior to the sample,
Volume balance shortage				116							thus Rh contamination would have occurred to greater extent.
Final volume / initial volume		Vf / Vo %		73							

Comments:
~5 mL diluted Rh(III) not added (stuck to walls of injector)

Bulk volume of treated precipitate is significantly reduced.

Average solution and solid assays with Mass Balance — Test #: 5b

Solution concentration

Sample #	Time (min)		Cu (mg/l)	Ni (mg/l)	H2SO4 (g/l)	Na (mg/l)	K (mg/l)	Rh (mg/l)	Redox Ag/AgCl mV	
Rh/2806/5b/TO/ L1	0		34.896833	NR	14.6	9	963	93.3		
Rh/Rh estimate after injectior	0.01							96.2	546	Calculated feed concentration
Rh/2806/5b/ 1/ L2 avg	1		33	NR	16.4	12	908	98.0	488	Guess value as sample was contaminated
Rh/2806/5b/ 2/L3 avg	2		34	NR	16.6	11	981	98.0	509	Guess value as sample was contaminated
Rh/2806/5b/ 5/L4 avg	5		33	NR	16.2	12	936	98.1	453	
Rh/2806/5b/ 10/L5 avg	10		36	NR	16.2	12	929	95.0	460	
Rh/2806/5b/ 30/L6	30		36	NR	16.4	10	932	94.4	439	Ignor 104 mg repeat analysis as it does not fit trend
Rh/Rh/2806/5b/ 60/L7	60		34	NR	16.5	10	944	85.6	452	
Rh/2806/5b/ 90/L8	90		35	NR	16.5	10	910	84.1	440	
Rh/2806/5b/ 120/L9	120		36	NR	16.4	10	929	87.0	434	
Rh/2806/5b/ 160/L10	180		36	NR	16.6	10	949	76.9	424	
Rh/2806/5b/ 240/L11 avg	240		34	NR	16.5	11.1	922	76.9	402	
Rh/2806/5b/ 290/L12 avg	290		33	NR	14.7	11.1	925	80.3	407	

Solid concentration

Sample #	Time (min)		Cu %	Ni %	S %	Na ppm	K ppm	Rh %	Concn g/L	
Rh/2806/5b/ TO/S1	0		i.s.	NR	25.8	NR	NR	0.01	2.88	
Rh/5b/ 290/S2 avg	290		39.0	NR	25.55	NR	NR	0.41	3.05	

Mass balance: Amount removed (mmol/l)			Cu	Ni	H2SO4	Na	K	Rh		
Solution basis (mmol/L)	0									
	0									
	1		0.04		-18.5			0.00		
	2		0.01		-20.6			0.00		
	5		0.03		-16.5			0.00		
	10		-0.01		-16.5			0.01		
	30		-0.02		-18.5			0.02		
	80		0.01		-19.6			0.10		
	90		0.00		-19.6			0.12		
	120		-0.01		-18.5			0.09		
	180		-0.01		-20.6			0.19		
	240		0.02		-19.6			0.19		
	290		0.03		-1.2			0.15		
Solid basis (mmol/L)			Cu	Ni	S	Na	K	Rh		
	0		i.s.		23.2			0.0		
	290		18.73		24.3			0.12		
Difference (mmol/L)	290		#VALUE!		-1.1			-0.12		
Stiochiometry (soln basis)			Cu / Rh	Cu soln / S	(Cu+Rh) / S (solids)			Rh / acid		
Mole ratios %										Na = Na2S2O3.5H20
	290		17		77.5			12.7		S =elemental S or S(2-)
Expected			150		100			0.0		100% is a 1:1 mole ratio
Accountability								Rh		
=100-(soln-solid)/soln%	290							79.1		
= (mol Rh in soln+solids @t=final) / (Rh @ t=0) %								96.5		
Solution concentrations	0		34.9	NR	14.6	8.7485097	963	98		
calculated from solid mass	290							84		

Acid balance (solution assays and S in solid)

Feed	mmol/l
Acid generated from MeS precipitation	mmol/l
Acid consumed (elemental S: Total S - M	mmol/l
Acid concentration predicted	mmol/l
Acid concentration predicted	g/l
Accountability (t=final) (actual-pred.)/actual	%

Test # :		6a
Test description:	CuS formation for substitution reaction	
Conditions:		
Temperature	80	oC
Make-up Volume	5.400	L
Volume before injection (operating volume)	5.150	L
Seed (Pd sulphide)	none	mg
CuSO4.5H20 added to make-up volume	293.60	g
NISO4 added to make-up volume	139.90	g
FeSO4 added to make-up volume	0.00	g
K2SO4 added to make-up volume	11.70	g
Na2S2O3.5H2O added at t=0	67.31	g
Volume reagent set at	150	mL
Volume Rh stock soln pipetted (actual)	0.00	mL
H2SO4 to make-up	76.30	g (adjusted for pH 2 water in error;should have been 79 g fo

Time	Temp	Pressure	Agitator	Sample	Filter paper	FP + solids	Net Dry	[Solid]	[Solid]	Redox	Observations
(min)	oC	kPa	rpm	Volume	mg	mg	mass mg	g/l	g/l CuS	mV	
feed				250				measured	calc'd	426 / 434	50 ml used to flush sampler
0	80		450								inject reagents
1	80		430								
2	80										
3	80										black slurry; [Cu(II)]=9.8 g/l on AA
11	80										black slurry; [Cu(II)]=10.6 g/l on AA
18	80		421								
20	80							3.58	1.44	396	start cooling

Comments:

approx 25 ml lost tp PV sleeve due to priming etc

redox measured on filtrates days later

Average solution and solid assays with Mass Balance Test #: 6a

			Solution concentration						Redox
Sample #	Time		Cu	Ni	H2SO4	Na	K	Rh	Ag/AgCl
	(min)		(mg/l)	(mg/l)	(g/l)	(mg/l)	(mg/l)	(mg/l)	mV
Rh/2306/6a/t0/L2 avg	0		12450	5649	16.3	17	894	0.0	
Rh/2306/6a/filt/L5	20		11492	5806	16.3	2421	899	0.2	

			Solid concentration						
Sample #	Time		Cu	Ni	S	Na	K	Rh	Concn
	(min)		%	%	%	ppm	ppm	%	g/L
Rh/0307/6b/TO/S1 avg	20		64	NR	28.1	NR	NR	0.05	3.58

Mass balance: Amount removed (mmol/l)			Cu	Ni	H2SO4	Na	K	Rh	
Solution basis (mmol/L)									
	20		15.08	-2.67	-20.6	-104.6		0.00	
Solid basis (mmol/L)			Cu	Ni	S	Na	K	Rh	
	20		36.21		31.36			0.02	
Stiochiometry (soln basis)			Cu / Na	Cu / S	Acid / Na	S / Na	Cu / Acid	Rh / acid	
Mole ratios %	20		29	115	39	60	73	0.01	Na = Na2S2O3.5H20 S =elemental S or S(2-) 100% is a 1:1 mole ratio
Accountability								Rh	
=100-(soln-solid)/soln%	20		240.1						
= (mol Rh in soln+solids @ t=final) / (Rh @ t=0) *			110.8						
Solution concentrations	0		12450	5649	16.3	17	894	0	
calculated from solid	20		10150						

Acid balance (solution assays and S in solid)								
Feed	mmol/l			166.0	104.6			
Acid generated from MeS precipitatio	mmol/l	15.08					0.00	
Acid consumed (elemental S: Total S	mmol/l			0.0				
Acid concentration predicted	mmol/l			181.0				
Acid concentration predicted	g/l			17.8				
Accountability (t=final) (actual-pred.)/	actual%			3.0				

Test # :	6b
Test description:	Substitution reaction of Rh(III) with CuS at temperature

Conditions:

Temperature	80 oC
Make-up Volume	5.200 L
Volume before injection (operating volume)	5.008 L
Seed (Pd sulphide)	none mg
CuSO4.5H20 added to make-up volume	0 g
NiSO4 added to make-up volume	0 g
FeSO4 added to make-up volume	0 g
K2SO4 added to make-up volume	11.70473 g
Na2S2O3.5H2O added at t=0	0 g
Volume reagent set at	100 mL
Volume Rh stock soln pipetted (actual)	50 mL
H2SO4 to make-up	70.8 g

Time	Temp	Pressure	Agitator	Sample	Filter paper	FP + solids	Net Dry	[Solid]		Redox	Observations
(min)	oC	kPa	rpm	Volume	mg	mg	mass mg	g/l		mV	
0	80	atm	420	192	4414	5101	687	3.58		527	
1	80		418	100			305	3.05		545	
2	80		418	100	127	438	311	3.11		481	
5	80		416	94	127	418	291	3.10		495	
10	80		419	98	127	430	303	3.09		489	
30	80		410	110	4578	4938	360	3.27		540	
60	80		409	110			355	3.23		562	
90	80		407	94	127	431	304	3.23		570	
120	80		390	96	126	440	314	3.20		542	
180	80		380	94	128	400	272	2.89		554	Solids sample dropped, mass approximate.
240	80		380	4200	13200	26977	13777	3.28		440	
		splash over		100							
Volume balance shortage				-40							
Final volume / initial volume		Vf / Vo %		81							

Comments:

t=1 sample not flushed prior to sample; probably biased with higher Rh concn due to Rh on walls of sample system.

Slight H2S smell (but not on filtrates). Possibly from splash over and sulphides being heated.

Average solution and solid assays with Mass Balance Test #: 6b

Sample #	Time		Cu	Ni	H2SO4	Na	K	Rh	Redox Ag/AgCl	
	(min)		(mg/l)	(mg/l)	(g/l)	(mg/l)	(mg/l)	(mg/l)	mV	
Rh/0307/6b/tO/L1 avg	0		85	NR	13.2	3	959	93.4		
Rh estimate after injection	0.01							93.4	527	
Rh/0307/6b/ 1/L2 avg	1		87	NR	15.9	6	956	*92.0*	545	guesstimate due to contamination
Rh/0307/6b/ 2/L3 avg	2		88	NR	15.5	NR	953	90.9	481	
Rh/0307/6b/ 5/L4 avg	5		91	NR	15.3	NR	946	83.1	495	
Rh/Rh/0307/6b/ 10/L5 avg	10		92	NR	15.1	NR	940	84.5	489	
Rh/0307/6b/ 30/L6 avg	30		96	NR	15.2	NR	960	85.3	540	
Rh/0307/6b/ 60/L7	60		96	NR	15.5	NR	970	65.0	562	
Rh/0307/6b/ 90/L8 avg	90		98	NR	15.6	NR	967	70.9	570	
Rh/0307/6b/ 120/L9	180		95	NR	15.5	NR	965	62.6	542	
Rh/0307/6b/ 180/L10 avg	240		97	NR	15.7	NR	960	63.0	554	
Rh/0307/6b/ 240/L11	290		90	NR	15.8	5.38	977	61.5	440	

Sample #	Time		Cu	Ni	S	Na	K	Rh	Concn	
	(min)		%	%	%	ppm	ppm	%	g/L	
Rh/0307/6b/TO/S1 avg	0		84.3	NR	28.1	NR	NR	0.05	3.58	
Rh/6b/ 240/S2 avg	290		61.9	NR	27.5	NR	NR	0.94	3.28	

Mass balance: Amount removed	(mmol/l)		Cu	Ni	H2SO4	Na	K	Rh		
Solution basis (mmol/L)	0									
	0									
	1		-0.04		-27.4			0.01		
	2		-0.06		-23.3			0.02		
	5		-0.09		-21.2			0.10		
	10		-0.12		-19.2			0.09		
	30		-0.17		-20.2			0.08		
	60		-0.19		-23.3			0.28		
	90		-0.22		-24.3			0.22		
	180		-0.16		-23.3			0.30		
	240		-0.19		-25.3			0.29		
	290		-0.09		-26.3			0.31		
Solid basis (mmol/L)			Cu	Ni	S	Na	K	Rh		
	0		36.2		31.4			0.02		
	290		32.0		28.1			0.30		
Difference (mmol/L)	290		4.3		3.2			-0.28		
Stiochiometry (soln basis)			Cu / Rh		(Cu+Rh) / S (solids)			Rh / acid		
Mole ratios %	290		30		114.6			1.2		Na = Na2S2O3.5H20 S =elemental S or S(2-)
Expected			150		100					100% is a 1:1 mole ratio
Accountability								Rh		
=100-(soln-solid)/soln%	290		-4623.5					97.1		
= (mol Rh in soln+solids @ t=final) / (Rh @ t=0) %			426.5					99		
Solution concentrations	0		84.6	NR	13.2	3.260632	959	93		
calculated from solid mass	0		355					62		

Acid balance (solution assays and S in solid)

Feed	mmol/l	
Acid generated from MeS precipitation	mmol/l	
Acid consumed (elemental S: Total S - M	mmol/l	
Acid concentration predicted	mmol/l	
Acid concentration predicted	g/l	
Accountability (t=final) (actual-pred.)/actual	%	

Test # : 7a
Test description: CuS formation for substitution reaction

Conditions:

Temperature	95 oC	
Make-up Volume	5.400 L	
Volume before injection (operating volume)	5.200 L	
Seed (Pd sulphide)	none mg	
CuSO4.5H20 added to make-up volume	293.60 g	
NiSO4 added to make-up volume	139.90 g	
FeSO4 added to make-up volume	0.00 g	
K2SO4 added to make-up volume	11.70 g	
Na2S2O3.5H2O added at t=0	67.31 g	
Volume reagent set at	190 mL	
Volume Rh stock soln pipetted (actual)	0.00 mL	
H2SO4 to make-up	76.30 g	(adjusted for pH 2 water in error;should have been 79 g for 15

Time (min)	Temp oC	Pressure kPa	Agitator rpm	Sample Volume	Filter paper mg	FP + solids mg	Net Dry mass mg	[Solid] g/l	[Solid] g/l CuS	Redox mV	Observations
feed1				100				measured	calc'd		
feed2 t=0				100							inject 190 ml of reagents
10	95.0		450					3.26	4.26		

Comments:
wet mass: 500 ml pH2 water + beaker + solids = 698.4 g

very high bulk density of solids
140 mL bed volume

Average solution and solid assays with Mass Balance Test #: 7a

Solution concentration

Sample #	Time (min)		Cu (mg/l)	Ni (mg/l)	H2SO4 (g/l)	Na (mg/l)	K (mg/l)	Rh (mg/l)	Redox Ag/AgCl mV	
Rh/2306/7a/to/L3 avg	0		13705	5701	16.4	10	915	0.0		
Rh/2306/7a/filt/L6	15		10875	6155	19.0	2480	915	0.3		

Solid concentration

Sample #	Time (min)		Cu %	Ni %	S %	Na ppm	K ppm	Rh %	Concn g/L	
Rh/2306/7b/ t0/S	15		NR	NR	NR	NR	NR	0.03	3.26	

Mass balance: Amount removed (mmol/l)			Cu	Ni	H2SO4	Na	K	Rh		
Solution basis (mmol/L)	15		44.53	-7.73	-26.4	-107.4		0.00		
Solid basis (mmol/L)	15		Cu	Ni	S	Na	K	Rh		
Stiochiometry (soln basis)			Cu / Na	Cu / S	Acid / Na	S / Na	Cu / Acid	Rh / acid		
Mole ratios %	15		83		49		169	0.01		Na = Na2S2O3.5H20 S =elemental S or S(2-) 100% is a 1:1 mole ratio
Accountability								Rh		
=100-(soln-solid)/soln% = (mol Rh in soln+solids @t=final) / (Rh @ t=0) %	15									
Solution concentrations calculated from solid	0 15		13705	5701	16.4	10	915	0		

Acid balance (solution assays and S in solid)		
Feed	mmol/l	
Acid generated from MeS precipitatio	mmol/l	
Acid consumed (elemental S: Total S	mmol/l	
Acid concentration predicted	mmol/l	
Acid concentration predicted	g/l	
Accountability (t=final) (actual-pred.)/actual%		

Test # :	7b
Test description:	Substitution reaction of Rh(III) with CuS at temperature

Conditions:

Temperature	95 oC
Make-up Volume	5.400 L
Volume before injection (operating volume)	5.218 L
Seed (Pd sulphide)	none mg
CuSO4.5H20 added to make-up volume	0.00 g
NiSO4 added to make-up volume	0.00 g
FeSO4 added to make-up volume	0.00 g
K2SO4 added to make-up volume	11.70 g
Na2S2O3.5H2O added at t=0	0.00 g
Volume reagent set at	100 mL
Volume Rh stock soln pipetted (actual)	50.00 mL
H2SO4 to make-up	70.80 g

Time	Temp	Pressure	Agitator	Sample	Filter paper	FP + solids	Net Dry	[Solid]		Redox	Observations
(min)	oC	kPa	rpm	Volume	mg	mg	mass mg	g/l		mV	
feed1			470								clear, colourless solution
feed2 (t=o)	95		470	182	482	1076	594	3.26		474	inject brown Rh(iii) soln, chased by 100 mL water
1	95		470	98	241	535	294	3.00		429	light yellow solution
2	95		470	110	239	583	344	3.13		427	light yellow solution
5	95		470	98	242	546	304	3.10		425	light yellow solution
10	95		465	100	1295	1607	312	3.12		422	light yellow solution
30	95		460	102	241	586	345	3.38		424	light yellow solution
60	95		465	110	239	593	354	3.22		423	light yellow solution
90	95		470	110	241	602	361	3.28		423	light yellow solution
120	95		465	110	241	618	377	3.43		424	[Cu(ii)] = 120 mg/l on AA
180	95		465	110	118	486	368	3.35		419	[Cu(ii)] = 120 mg/l on AA
225	95		470							415	start cooling
230											filtrate sample at 225 min
250				4000	96280	111850	13570	3.39			start bulph filtration at 230 min
		splash over		100							
Volume balance shortage				320							
Final volume / initial volume		Vf / Vo %		74							

Comments:
solids repulped in pH 2 water added up front, so some additional aging of ppt expected.
NB: feed sample to check solution reduced the S(2-) content and thus te3st 9-12 sulphide additon must be reduced accordingly
Redox measured on filtrate days later
Couple of mL of Rh was not injected.
t=1 sample not flushed prior to sample; probably biased with higher Rh concn due to Rh on walls of sample system.

Average solution and solid assays with Mass Balance — Test #: 7b

			Solution concentration						Redox	
Sample #	Time		Cu	Ni	H2SO4	Na	K	Rh	Ag/AgCl	
	(min)		(mg/l)	(mg/l)	(g/l)	(mg/l)	(mg/l)	(mg/l)	mV	
Rh/2806/7b/t0/L1	0		112	NR	14.9	7	903	90.0		
Rh estimate after injection	0.01		0					90.0	474	
Rh/2806/7b/1/L2 avg	1		107	NR	18.6	8	859	86.0	429	
Rh/2806/7b/2/L3 avg	2		106	NR	18.1	7	878	69.0	427	
Rh/2806/7b/5/L4	5		117	NR	16.7	8	862	63.4	425	
Rh/2806/7b/10/L5	10		118	NR	16.6	8	898	66.3	422	
Rh/2806/7b/30/L6 avg	30		117	NR	16.8	8	895	58.5	424	
Rh/2806/7b/60/L7	60		118	NR	17.7	8	890	56.2	423	
Rh/2806/7b/90/L8 avg	90		127	NR	17.4	7	901	55.0	423	
Rh/2806/7b/120/L11 avg	120		117	NR	17.0	8	884	52.0	424	
Rh/2806/7b/180/L9 avg	180		121	NR	17.4	7	909	51.3	419	
Rh/2806/7b/225/L10	225		113	NR	17.9	6	904	49.7	415	

		Solid concentration						
Sample #	Time	Cu	Ni	S	Na	K	Rh	Concn
	(min)	%	%	%	ppm	ppm	%	g/L
Rh/2306/7b/ t0/S	0	NR	NR	NR	NR	NR	0.03	3.26
Rh/7b/ 225/S avg	225	64.2	NR	28.7	0.01	0.02	1.25	3.39

Mass balance: Amount removed	(mmol/l)	Cu	Ni	H2SO4	Na	K	Rh
Solution basis (mmol/L)	0						
	0						
	1	0.07		-17.3			0.04
	2	0.09		-12.2			0.20
	5	-0.09		-18.3			0.26
	10	-0.10		-17.3			0.23
	30	-0.09		-19.3			0.31
	60	-0.10		-26.5			0.33
	90	-0.24		-25.4			0.34
	120	-0.06		-21.4			0.37
	180	-0.15		-25.4			0.38
	225	-0.02		-30.5			0.39

Solid basis (mmol/L)		Cu	Ni	S	Na	K	Rh	
	0	NR					0.0	
	225	34.27		30.3	0.0	0.0	0.41	
Difference (mmol/L)	225	#VALUE!					0.41	
Stiochiometry (soln basis)		Cu / Rh	Cu / S	(Cu+Rh) / S (solids)			Rh / acid	
Mole ratios %								Na = Na2S2O3.5H20
	180	6	113	114.3			1.5	S =elemental S or S(2-)
Expected		150						100% is a 1:1 mole ratio
Accountability							Rh	
=100-(soln-solid)/soln%	225						105.2	
= (mol Rh in soln+solids @t=final) / (Rh @ t=0) %		#VALUE!					102	
Solution concentrations	0	112		14.9	7.336708	903	90	
calculated from solid mass	0						48	

Acid balance (solution assays and S in solid)	
Feed	mmol/l
Acid generated from MeS precipitation	mmol/l
Acid consumed (elemental S: Total S - M	mmol/l
Acid concentration predicted	mmol/l
Acid concentration predicted	g/l
Accountability (t=final) (actual-pred.)/actual%	

Test # :											8a
Test description:	CuS formation for substitution reaction										
Conditions:											
Temperature											150 oC
Make-up Volume											5.400 L
Volume before injection (operating volume)											5.190 L
Seed (Pd sulphide)											none mg
CuSO4.5H20 added to make-up volume											293.60 g
NiSO4 added to make-up volume											139.90 g
FeSO4 added to make-up volume											0.00 g
K2SO4 added to make-up volume											11.70 g
Na2S2O3.5H2O added at t=0											67.31 g
Volume reagent set at											190 mL
Volume Rh stock soln pipetted (actual)											0.00 mL
H2SO4 to make-up											79.59 g

Time	Temp	Pressure	Agitator	Sample	Filter paper	FP + solids	Net Dry	[Solid]	[Solid]	Redox	Observations
(min)	oC	kPa	rpm	Volume	g	g	mass g	g/l	g/l CuS	mV	
feed1				90				measured	calc'd		Sampler flush; slight brown on filter paper,
feed2 (t=o)	148		400	120							Less brown colour of filter paper on feed
1	151.0		395								
2	150		384								
5	150		387								
10	150		385	900							No SO2 smell. Flashes off during sampling.
20				4000				5.13	#VALUE!		cooling and shutdown
											Bulk filtration
											Brown ppt is Rh2S3 from previous test.

Comments:
Assume 100% Cu precipitation with thiosulphate, as no breakdown of reagent to form SO2/SO3.

Average solution and solid assays with Mass Balance								Test #:	8a	
	Solution concentration								Redox	
Sample #	Time		Cu	Ni	H2SO4	Na	K	Rh	Ag/AgCl	
	(min)		(mg/l)	(mg/l)	(g/l)	(mg/l)	(mg/l)	(mg/l)	mV	
Rh/8a/0/L6 avg	0		13705	5701	16	10	915	0.0		
Rh/8a/fiit/L	10		NR	NR	NR	NR	NR	NR		
	Solid concentration									
Sample #	Time		Cu	Ni	S	Na	K	Rh	Concn	
	(min)		%	%	%	ppm	ppm	%	g/L	
	0									
Rh/1907/8b/ 0/S1	10		59	0.05	33.95	NR	NR	0.03	5.13	
Mass balance: Amount removed	(mmol/l)		Cu	Ni	H2SO4	Na	K	Rh		
Solution basis (mmol/L)										
	10		NR	NR	NR	NR	NR	NR		
Solid basis (mmol/L)			Cu	Ni	S	Na	K	Rh		
	10		47.2	0.04	54.30					
Stiochiometry (soln basis)			Cu / Na	Cu / S	Acid / Na	S / Na				
Mole ratios %	10									Na = Na2S2O3.5H20 S =elemental S or S(2-) 100% is a 1:1 mole ratio
Accountability								Rh		
=100-(soln-solid)/soln%	10									
Solution concentrations calculated from solid	0 10		13705	5701	16.4	10	915	0		
Acid balance (solution assays and S in solid)										
Feed		mmol/l								
Acid generated from MeS precipitatio		mmol/l								
Acid consumed (elemental S: Total S		mmol/l								
Acid concentration predicted		mmol/l								
Acid concentration predicted		g/l								
Accountability (t=final) (actual-pred.)/		actual%								

Test # : 8b
Test description: Substitution reaction of Rh(III) with CuS at temperature

Conditions:

Temperature	150 oC
Make-up Volume	5.200 L
Volume before injection (operating volume)	5.003 L
Seed (Pd sulphide)	none mg
CuSO4.5H20 added to make-up volume	0.00 g
NiSO4 added to make-up volume	0.00 g
FeSO4 added to make-up volume	0.00 g
K2SO4 added to make-up volume	11.70 g
Na2S2O3.5H2O added at t=0	0.00 g
Volume reagent set at	150 mL
Volume Rh stock soln pipetted (actual)	50.00 mL
H2SO4 to make-up	74.07 g

Time (min)	Temp oC	Pressure kPa	Agitator rpm	Sample Volume	Filter paper g	FP + solids g	Net Dry mass g	[Solid] g/l		Redox mV	Observations
feed1				25							feed flush
feed2 (t=o)	150		358	172	124	1006	882	5.13		463	50 mL sample flush at 30 sec, black ppt
1	150		331	98	127	570	443	4.52		435	No H2S or SO2 smells
2	150		281	100	125	588	463	4.63		436	
4	150		547	94	122	521	399	4.24		448	possible solids lost
7	150		545	94	123	533	410	4.36		456	
13	150		552	98	127	550	423	4.32		416	
20	150		410	100	127	566	439	4.39		439	
30	150		410	98	125	560	435	4.44		440	solids lost
60	150		410	4330	192738	213140	20402	4.71		420	
		flush for t=1		50.0							
		splash over		100							
Volume balance shortage				41							
Final volume / initial volum		Vf / Vo %		83							

Comments:
Same amount of Rh not injected at 5b-7b

Solids diluted with 200 mL Rh solution injection
No H2S or other smells

Average solution and solid assays with Mass Balance Test #: 8b

Solution concentration

Sample #	Time (min)		Cu (mg/l)	Ni (mg/l)	H2SO4 (g/l)	Na (mg/l)	K (mg/l)	Rh (mg/l)	Redox Ag/AgCl mV	
1907/8b/ 0/L1 avg	0		73	NR	15.1	11	1150	92.5		
Rh estimate after injection	0.01							92.5	463	
1907/8b/ 1/L2	1		98	NR	16.4	13	1152	35.0	435	
1907/8b/ 2/L3 avg	2		NR	NR	16.6	NR	1172	16.5	436	
1907/8b/ 4/L4	4		NR	NR	16.2	NR	1155	4.6	448	
1907/8b/ 7/L5 avg	7		NR	NR	16.5	NR	1157	1.2	456	
1907/8b/ 13/L6	13		NR	NR	16.6	NR	1163	0.7	416	
1907/8b/ 20/L7	20		NR	NR	16.5	NR	1164	0.5	439	
1907/8b/ 30/L8	30		NR	NR	16.6	NR	1166	0.4	440	
1907/8b/ 60/L9 avg	60		111	NR	17.9	12	1286	0.1	420	

Solid concentration

Sample #	Time (min)		Cu %	Ni %	S %	Na ppm	K ppm	Rh %	Concn g/L	
Rh/1907/8b/ 0/S1	0		58.6	0.05	34.0	NR	NR	0.02	5.13	assumed
Rh/8b/ 60/S2 avg	60		58.6	0.05	34.0	NR	0.0	2.21	4.71	

Mass balance: Amount removed (mmol/l)

Solution basis (mmol/L)		Cu	Ni	H2SO4	Na	K	Rh
	0						
	0.01						
	1	-0.36		-13.8			0.56
	2			-15.8			0.72
	4			-11.7			0.85
	7			-14.8			0.89
	13			-15.8			0.89
	20			-14.8			0.89
	30			-15.8			0.89
	60	-0.59		-29.1	0.5		0.90

Solid basis (mmol/L)		Cu	Ni	S	Na	K	Rh
	0	NR		54.3			0.01
	60	43.4		49.9			1.01
Difference (mmol/L)	60	NR		4.4			-1.00

Stiochiometry (soln basis)		Cu / Rh	Cu / S	(Cu+Rh) / S (solids)			Rh / acid	
Mole ratios %								Na = Na2S2O3.5H20
	60	66	87	89			3.1	S =elemental S or S(2-)
Expected		150						100% is a 1:1 mole ratio

Accountability								
=100-(soln-solid)/soln%	60						112.7	
= (mol Rh in soln+solids @t=final) / (Rh @ t=0) %							112.7	

Solution concentrations	0	73.4	NR	15.1	11.09507	1150	92		
calculated from solid	0						-12		

Acid balance (solution assays and S in solid)

Feed	mmol/l							
Acid generated from MeS precipitatio	mmol/l							
Acid consumed (elemental S: Total S	mmol/l							
Acid concentration predicted	mmol/l							
Acid concentration predicted	g/l							
Accountability (t=final) (actual-pred./actual%								

Test # : 9
Test description: Co-precipitation of Cu(II) and Rh(III)

Conditions:

Temperature	50	oC
Make-up Volume	5.400	L
Volume before Injection (operating volume)	5.206	L
Seed (Pd sulphide)	none mg	
CuSO4.5H20 added to make-up volume	293.60	g
NiSO4 added to make-up volume	139.90	g
FeSO4 added to make-up volume	0.00	g
K2SO4 added to make-up volume	11.70	g
Na2S2O3.5H2O added at t=0	64.72	g
Volume reagent set at	190	mL
Volume Rh stock soln pipetted (actual)	50.00	mL
H2SO4 to make-up	74.07	g

Time	Temp	Pressure	Agitator	Sample	Filter paper	FP + solids	Net Dry	[Solid]	[Solid]	[Solid]	Redox	Redox	Observations
(min)	oC	kPa	rpm	Volume	mg	mg	mass mg	g/l	g/l CuS	g/l Rh2S3	repeat	mV	
feed1				20				measured	calc'd	calc'd			flush sampler
feed2 (t=o)	50		380	174	9197	9198	0.0	0.00	0.00	0.00	415	281	
1	50			98	9177	9171	0.0	0.00	1.32	0.051		251	no pptn,solution turned darker colour
2	50		379	100	9175	9160	0.0	0.00	2.25	0.039		259	dark brown/blacksolution, insignificant solids on paper
5	50		375	104	9155	9162	7.0	0.07	2.21	0.046		258	dark brown ppt, black/grey after drying
10	50		385	106	9161	9219	58	0.55	2.43	0.041		265	black ppt, clear blue/green solution as per other tests
30	50		392	134	9162	9577	415	3.10	3.33	0.039	386	279	
60	50		405	122	9186	9589	403	3.30	3.78	0.046	382	280	
90	50		400	98	9161	9490	329	3.36	3.76	0.054	382	281	
120	50		390	100	9167	9497	330	3.30	4.78	0.041	382	283	
180	50		392	114	9179	9587	408	3.58	3.21	0.056	383	313	
240	50			94	9167	9504	337	3.59	4.15	0.046	380	392	
300				4100	192270	208080	15810	3.86	2.93	0.050	370	376	
		splash over		100									
Volume balance shortage				126									
Final volume / initial volume		Vf / Vo %		76									

Comments:
Solids [g/l] calculkated from Cu and Rh precipitation as CuS and Rh2S3

Average solution and solid assays with Mass Balance Test #: 9

	Solution concentration										Redox	
Sample #	Time	Cu calc'd	Cu	Ni	H2SO4	Na	K	Rh	Rh calc'd		Ag/AgCl	
	(min)	(mg/l)	(mg/l)	(mg/l)	(g/l)	(mg/l)	(mg/l)	(mg/l)	(mg/l)		mV	
Rh/0607/9/ 0/ L1	0	12939	12939	5119	13.9	2099	929	89.3	89.3		415	
Rh/0607/9/ 1/L2 avg	1	12939	12080	5632	17.9	2270	1060	64.5	89.3			
Rh/0607/9/ 2/L3 avg	2	12939	11442	6414	17.8	NR	1088	62.6	89.3			
Rh/0607/9/ 5/L4 avg	5	12894	11471	5358	18.4	NR	1078	58.1	88.8			
Rh/0607/9/ 10/L5 avg	10	12575	11325	5342	17.2	NR	1061	61.1	64.9			
Rh/0607/9/ 30/L6 avg	30	10880	10724	5449	17.5	NR	1080	62.9	64.2			
Rh/0607/9/ 60/L7 avg	60	10743	10427	5388	18.1	NR	1084	58.3	62.6		382	
Rh/0607/9/ 90/L8 avg	90	10707	10442	5048	17.5	NR	1033	52.9	62.1		382	
Rh/0607/9/ 120/L9	120	10745	9762	5354	18.2	NR	1068	61.2	62.6		382	
Rh/0607/9/ 180/L10 avg	180	10560	10804	5537	18.5	NR	1131	51.3	60.3		383	
Rh/0607/9/ 240/L11	240	10556	10180	5401	18.0	1989	1087	58.2	60.3		380	
Rh/0607/9/ 300/L12 avg	300	10376	10989	5562	18.4	2268	1101	55.2	58.1		370	

	Solid concentration										
Sample #	Time		Cu	Ni	S	Na	K	Rh			Concn
	(min)		%	%	%	ppm	ppm	%			g/L
Rh/9/ 300/S2 avg	300		62.9	0.08	30.55	NR	NR	0.81			3.86
Mass balance: Amount removed	(mmol/l)		Cu	Ni	H2SO4	Na	K	Rh	Rh solids		
Solution basis (mmol/L)	1		13.8	-8.7	-40.8			0.34	0.00		
	2		23.6	-5.0	-39.8			0.26	0.00		
	5		23.1	-4.1	-45.9			0.30	0.01		
	10		25.4	-3.8	-33.7			0.27	0.04		
	30		34.9	-5.6	-36.7			0.26	0.24		
	60		39.5	-4.6	-42.9			0.30	0.26		
	90		39.3	1.2	-36.7			0.35	0.26		
	120		50.0	-4.0	-43.9			0.27	0.26		
	180		33.6	-7.1	-46.4			0.37	0.28		
	240		43.4	-4.8	-41.8	6		0.30	0.28		
	300		30.7	-7.5	-45.9	-7		0.33	0.30		
Solid basis (mmol/L)			Cu	Ni	S	Na	K	Rh			
	300		38.2	0.05	36.7			0.30			
Stiochiometry (soln basis)			(Cu+Rh)/Na 2S2O3	(Cu+Rh) / Acid	(Cu+Rh) / S (solids)	Acid / Na	S / Na				
Mole ratios %	300	solution	846	68		1253					Na = Na2S2O3.5H20
		solids	1050		105		1002				S =elemental S or S(2-)
											100% is a 1:1 mole ratio
Accountability								Rh			
=100-(soln-solid)/soln%	300		124.4					91.5			
= (mol Rh in soln+solids @t=final) / (Rh @ t=0) %			104					98.7			
Solution concentrations	0		12939	5119	13.9	2099	929	89			
calculated from solid mass	240		10513	5116			929	58			

Acid balance (solution assays and S in solid)									
Feed	mmol/l			141.7	7.3				
Acid generated from MeS precipitation	mmol/l	30.68					0.50		
Acid consumed (elemental S: Total S -	mmol/l			0.0					
Acid concentration predicted	mmol/l			172.9					
Acid concentration predicted	g/l			17.0					
Accountability (t=final) (actual-pred.)/actual%				6.8					

Test # :													9R
Test description:		Co-precipitation of Cu(II) and Rh(III)											
Conditions:													
Temperature												50	oC
Make-up Volume												5.000	L
Volume before injection (operating volume)												4.830	L
Seed (Pd sulphide)												none	mg
CuSO4.5H20 added to make-up volume												293.60	g
NiSO4 added to make-up volume												139.90	g
FeSO4 added to make-up volume												0.00	g
K2SO4 added to make-up volume												11.70	g
Na2S2O3.5H2O added at t=0												64.72	g
Volume reagent set at												190	mL
Volume Rh stock soln pipetted (actual)												50.00	mL
H2SO4 to make-up												74.07	g

Time	Temp	Pressure	Agitator	Sample	Filter paper	FP + solids	Net Dry	[Solid]	[Solid]	[Solid]	Redox	Observations
(min)	oC	kPa	rpm	Volume	mg	mg	mass mg	g/l	g/l CuS	g/l Rh2S3	mV	
								measured	calc'd	calc'd		
feed1				70								
feed2 (t=o)	50			100			0.0	0.00	0.00	0.00	??	70 mL flush after Rh injection
2	50		403	138	123	129	0.0	0.00	0.55	0.006	251	
5	50		404	122	124	129	0.0	0.00	1.06	0.007	250	murcy green, brown ppt; filtrate purple colour
9	50		404	130	121	138	17	0.13	1.23	0.006	251	ppt gets darker with time and slurry darker
14	50		404	88	123	148	25	0.28	1.22	0.012	253	cake washing of t=2-120 washed out brown filtrate/slurry
20	50		406	116	127	194	67	0.58	1.55	0.016	253	
30	50		406	104	126	255	129	1.24	2.01	0.002	256	clear filtrate at 30 min, black ppt; clear cake washing
60	50		402	102	125	371	246	2.41	3.25	0.000	275	
90	50		403	104	127	407	280	2.69	3.47	0.004	280	
120	50		401	130	123	503	380	2.92	3.89	0.012	284	
180	50		398	124	123	422	299	2.41	3.55	0.002	285	
240			398	3700	10428	19427	8999	2.43	3.39	0.009	285	
		splash over		100								
		flush at t= 1		70								brown ppts turned black after drying in air
Volume balance shortage				-8								
Final volume / initial volume		Vf / Vo %		74								

Comments:
No H2S smell or SO2 smel
t= 1- 20 filter cake washing washed out a brown filtrate/slurry
Brown ppt turned to balck colour upon atmospheric drying
Post filtration pptn occurred on t=2-20. Clear Cu/Ni filtrate from t= 30 onwards.

Average solution and solid assays with Mass Balance — Test #: 9R

			Solution concentration								Redox
Sample #	Time	Cu calc'd	Cu	Ni	H2SO4	Na	K	Rh	Rh calc'd	Ag/AgCl
	(min)	(mg/l)	(mg/l)	(mg/l)	(g/l)	(mg/l)	(mg/l)	(mg/l)	(mg/l)	mV
Rh/1407/9R/ 0/L1 avg	0	13115	13115	5542	15.4	30	1186	97.0	97.0	
Rh/1407/9R/ 2/L2 avg	2	13115	12752	5648	15.6	2729	1187	91.5	97.0	251
Rh/1407/9R/ 5/L3	5	13115	12410	NR	15.7	NR	NR	92.5	97.0	250
Rh/1407/9R/ 9/L4	9	13028	12299	NR	15.7	NR	NR	91.6	96.7	251
Rh/1407/9R/ 14/L5 avg	14	12926	12305	NR	15.5	NR	NR	89.0	96.4	253
Rh/1407/9R/ 20/L6	20	12731	12082	NR	16.6	NR	NR	86.0	95.8	253
Rh/1407/9R/ 30/L7 avg	30	12291	11781	NR	16.6	NR	NR	95.7	94.4	256
Rh/1407/9R/ 60/L8 avg	60	11512	10956	NR	17.1	NR	NR	96.9	91.9	275
Rh/1407/9R/ 90/L9 avg	90	11326	10611	NR	17.5	NR	NR	94.2	91.3	280
Rh/1407/9R/ 120/L10	120	11172	10660	NR	17.3	NR	NR	89.0	90.8	284
Rh/1407/9R/ 180/L11 avg	180	11513	10753	5686	17.6	2552	1175	95.7	91.9	285
Rh/1407/9R/ 240/L12	240	11499	10861	5677	17.8	2485	1178	90.8	91.8	285
		Calculated Cu g/l based on pure CuS in solids								

		Solid concentration							
Sample #	Time	Cu	Ni	S	Na	K	Rh		Concn
	(min)	%	%	%	ppm	ppm	%		g/L
Rh/1508/ 9R/S2 avg	240	69.2	NR	26.7	NR	NR	0.21		2.43

Mass balance: Amount removed	(mmol/l)		Cu	Ni	H2SO4	Na	K	Rh	Rh solids		
Solution basis (mmol/L)	2		5.7	-1.8	-1.7			0.05	0.00		
	5		11.1		-2.7			0.04	0.00		
	9		12.8		-2.7			0.05	0.00		
	14		12.8		-0.7			0.06	0.01		
	20		16.3		-11.9			0.11	0.01		
	30		21.0		-11.9			0.01	0.03		
	60		34.0		-17.0			0.00	0.05		
	90		36.3		-21.0			0.03	0.06		
	120		38.6		-19.0			0.08	0.06		
	180		37.2	-2.5	-22.1	-110		0.01	0.05		
	240		35.5	-2.3	-24.1	-107		0.06	0.05		
Solid basis (mmol/L)			Cu	Ni	S	Na	K	Rh			
	240		26.5	NR	20.3			0.05			
Stiochiometry (soln basis)			(Cu+Rh)/Na 2S2O3	(Cu+Rh) / Acid	(Cu+Rh) / S (solids)	Acid / Na	S / Na				2 mol Na for 1 mol Na2S2O3.5H20
Mole ratios %	240	solution	67	147		45					Na = Na2S2O3.5H20
		solids	50		131		38				S =elemental S or S(2-)
											100% is a 1:1 mole ratio
Accountability								Rh			
=100-(soln-solid)/soln%	240		74.7					83.4			
= (mol Rh in soln+solids @t=final) / (Rh @ t=0) %			96					96.9			
	0		13115	5542	15.4	30	1186	97			
Solution concentrations calculated from solid mass and assay	180		11432	NR				92			
Acid balance (solution assays and S in solid)											
Feed		mmol/l			157.4	106.8					
Acid generated from MeS precipitation		mmol/l	35.47					0.09			
Acid consumed (elemental S: Total S - MeS)		mmol/l			0.0						
Acid concentration predicted		mmol/l			193.0						
Acid concentration predicted		g/l			18.9						
Accountability (t=final) (actual-pred.)/actual%					-8.1						

Test # :												10
Test description:	Co-precipitation of Cu(II) and Rh(III)											
Conditions:												
Temperature												80 oC
Make-up Volume												5.400 L
Volume before injection (operating volume)												5.272 L
Seed (Pd sulphide)												none mg
CuSO4.5H20 added to make-up volume												293.80 g
NiSO4 added to make-up volume												139.90 g
FeSO4 added to make-up volume												0.00 g
K2SO4 added to make-up volume												11.70 g
Na2S2O3.5H2O added at t=0												64.72 g
Volume reagent set at												190 mL
Volume Rh stock soln pipetted (actual)												50.00 mL
H2SO4 to make-up												74.07 g

Time	Temp	Preesure	Agitator	Sample	Filter paper	FP + solids	Net Dry	[Solid]	[Solid]	[Solid]	Redox	Observations
(min)	oC	kPa	rpm	Volume	mg	mg	mass mg	g/l	g/l CuS	g/l Rh2S3	mV	
feed1				28				measured	calc'd	calc'd		flush sampler
feed2 (t=0)	80		40	100	9159	9185	6	0.06	0.00	0.00	433	feed soln clean (some dicoloration)
1	80		389	102	9191	9480	289	2.83	2.70	0.034	276	At 50 sec, flush sample dark brown ppt;t-1 min black pp
2	80		392	106	9170	9487	317	2.99	2.85	0.036	402	
5	80		392	96	9169	9455	286	2.98	3.15	0.036	400	
10	80		385	110	9192	9540	348	3.16	2.72	0.038	400	
30	80		387	108	9193	9582	389	3.60	3.48	0.044	401	
60	80		380	102	9168	9558	390	3.82	3.95	0.046	401	
90	80		387	94	9185	9551	366	4.11	4.79	0.050	400	
120	80			110	9157	9689	532	4.84	4.80	0.059	399	
180	80			106	9181	9703	522	4.92	4.67	0.060	403	
240	80			4100			no result	no result			397	
		splash over		150								
			flush	20								
Volume balance shortage				258								
Final volume / initial volume		Vf / Vo %		76								

Comments:

At t =1min,solution filtrate darker blue, less opaque, refilter t=1 sample At 35 min, no solids visible. Add H2O2 to 10 mL subsample,brown ppt formed.
Add H2O2 to filtrate of t = 240 min ; no pptn occurred.
Filtrate samples showing dicolourartion / post -pptn were analused for the total stream by first performing a solids digestion with nitric acid.
t = 2 min sample shows no post pptn or filtrate disclouration, indicating complete CuS pptn.

Average solution and solid assays with Mass Balance Test #: 10

	Solution concentration									Redox
Sample #	Time	Cu calc'd	Cu	Ni	H2SO4	Na	K	Rh	Rh calc'd	Ag/AgCl
	(min)	(mg/l)	(mg/l)	(mg/l)	(g/l)	(mg/l)	(mg/l)	(mg/l)	(mg/l)	mV
Rh/0507/10/ 0/L1 avg	0	12798	12798	5535	15.5	11	1109	89.3	89.3	433
Rh/0507/10/ 1/L2 avg	1	10814	11006	5587	17.2	NR	1078	85.9	85.9	276
Rh/0507/10/ 2/L3 avg	2	10810	10900	5602	17.5	NR	1093	64.6	64.6	402
Rh/0507/10/ 5/L4 avg	5	10817	10706	5485	17.8	NR	1084	64.7	64.7	400
Rh/0507/10/ 10/L5	10	10695	10992	5713	18.1	NR	1090	83.2	63.2	400
Rh/0507/10/ 30/L6 avg	30	10404	10486	5714	18.4	NR	1121	59.6	59.8	401
Rh/0507/10/ 60/L7 avg	80	10256	10175	5639	19.1	NR	1098	57.8	57.8	401
Rh/0507/10/ 90/L8	90	10068	9815	5516	19.4	NR	1104	55.4	55.4	400
Rh/0507/10/ 120/L9	120	9583	9607	5627	19.8	NR	1089	49.4	49.4	399
Rh/0507/10/ 180/L10 avg	180	9524	9693	5570	20.1	NR	1096	48.7	48.7	403
Rh/0507/10/ 240/L11 avg	240		9058	5528	20.3	2280	1110	0.0		397

	Solid concentration									
Sample #	Time		Cu	Ni	S	Na	K	Rh		Concn
	(min)		%	%	%	ppm	ppm	%		g/L
Rh/10/ 240/S2 avg	0		80.55	0.07	32.15	NR	0.0	0.83		4.92

Mass balance: Amount removed (mmol/l)			Cu	Ni	H2SO4	Na	K	Rh	Rh solids
Solution basis (mmol/L)	1		28	-1	-17.0			0.23	0.23
	2		30	-1	-20.1			0.24	0.24
	5		33	1	-23.1			0.24	0.24
	10		26	-3	-26.2			0.25	0.25
	30		36	-3	-29.2			0.29	0.29
	60		41	-2	-36.4			0.31	0.31
	90		50	0	-39.4			0.33	0.33
	120		50	-2	-41.5			0.38	0.39
	180		49	-1	-46.6			0.40	0.40
	240		59	0	-46.6	-99		0.87	
Solid basis (mmol/L)			Cu	Ni	S	Na	K	Rh	
	240		47	0.06	49.4	#VALUE!	0.0	0.40	
Stiochiometry (soln basis)			(Cu+Rh) / Na2S2O3	(Cu+Rh) / Acid	(Cu+Rh) / S (solids)	Acid / Na	S / Na		
Mole ratios %		Basis:							Na = Na2S2O3.5H20
	240	solution	121	123		99			S =elemental S or S(2-)
		solids	97		96		100		100% is a 1:1 mole ratio
Accountability								Rh	
=100-(soln-solid)/soln%	0		79.7	50.4				45.5	
= (mol Rh in soln+solids @t=final) / (Rh @ t=0) %			94	100				45.5	
Solution concentrations	0		12798	5535	15.5	11	1109	89	
calculated from solid mass	240		9816	5531				49	

Acid balance (solution assays and S in solid)									
Feed	mmol/l			158.4	98.7				
Acid generated from MeS precipitation	mmol/l	58.86					1.30		
Acid consumed (elemental S: Total S - MeS	mmol/l			0.0					
Acid concentration predicted	mmol/l			218.5					
Acid concentration predicted	g/l			21.4					
Accountability (t=final) (actual-pred.)/actual%				-9.3					Some S precipitation ?

Test # :												11
Test description:	Co-precipitation of Cu(II) and Rh(III)											
Conditions:												
Temperature												95 oC
Make-up Volume												5.400 L
Volume before injection (operating volume)												5.200 L
Seed (Pd sulphide)												none mg
CuSO4.5H20 added to make-up volume												293.60 g
NiSO4 added to make-up volume												139.90 g
FeSO4 added to make-up volume												0.00 g
K2SO4 added to make-up volume												11.70 g
Na2S2O3.5H2O added at t=0												64.72 g
Volume reagent set at												190 mL
Volume Rh stock soln pipetted (actual)												50.00 mL
H2SO4 to make-up												74.07 g

Time	Temp	Pressure	Agitator	Sample	Filter paper	FP + solids	Net Dry	[Solid]	[Solid]	[Solid]	Redox	Observations
(min)	oC	kPa	rpm	Volume	mg	mg	mass mg	g/l	g/l CuS	g/l Rh2S3	mV	
feed1								measured	calc'd	calc'd		
feed2 (t=0)	95			200	124	130	8	0.03	0.00	0.00	434	
1	95		395	134	9169	9552	383	2.86	4.30	0.044	390	
2	95		393	115	9182	9622	440	3.83	3.02	0.059	387	
5	95		935	92	9180	9475	295	3.21	3.82	0.049	395	
10	95		390	94	9048	9370	322	3.43	3.41	0.053	400	
30	95		387	108	9186	9651	485	4.49	4.27	0.069	401	
60	95		385	93	9173	9629	456	4.65	4.84	0.072	403	
90	95		375	108	9174	9718	544	5.04	4.96	0.078	401	
120	95			108	9022	9515	493	4.65	4.95	0.072	474	
180	95		386	92	9177	9622	445	4.84	4.94	0.074	400	
240	95		385	4200	192394	212470	20078	4.78	4.93	0.074	401	
		splash over		100								
Volume balance shortage				143								
Final volume / initial volume		Vf / Vo %		78								

Comments:

Average solution and solid assays with Mass Balance Test #: 11

		Solution concentration								Redox	
Sample #	Time	Cu calc'd	Cu	Ni	H2SO4	Na	K	Rh	Rh calc'd	Ag/AgCl	
	(min)	(mg/l)	(mg/l)	(mg/l)	(g/l)	(mg/l)	(mg/l)	(mg/l)	(mg/l)	mV	
Rh/0407/11/ 0/L1 avg	0	13287	13287	6002	15.8	15	1014	89.3	89.3	434	
Rh/0407/11/ 1/L2 avg	1	11387	10428	5448	16.1	2482	950	59.3	59.3	390	
Rh/0407/11/ 2/L3	2	10744	11279	5855	18.1	NR	998	49.2	49.2	387	
Rh/0407/11/ 5/L4 avg	5	11156	10881	5663	18.2	NR	989	55.7	55.7	395	
Rh/0407/11/ 10/L5 avg	10	11010	11019	5754	19.1	NR	1004	53.4	53.4	400	
Rh/0407/11/ 30/L6	30	10302	10450	5781	20.2	NR	984	42.2	42.2	401	
Rh/0407/11/ 60/L7	60	10194	10070	5621	20.7	NR	985	40.5	40.5	403	
Rh/0407/11/ 90/L8	90	9939	9974	5625	21.6	NR	970	36.5	36.5	401	
Rh/0407/11/ 120/L9 avg	120	10193	9997	5663	21.5	NR	978	40.5	40.5	474	
Rh/0407/11/ 180/L10 avg	160	10072	10006	5689	21.4	NR	980	38.8	38.6	400	
Rh/0407/11/ 240/L11 avg	240	10110	9987	5662	21.7	2282	971	39.2	39.2	401	

		Solid concentration							
Sample #	Time	Cu	Ni	S	Na	K	Rh		Concn
	(min)	%	%	%	ppm	ppm	%		g/L
Rh//11/240/S2 avg	240	58.6	0.07	31.475	0.22	0.0	1.05		4.78

Mass balance: Amount removed	(mmol/l)	Cu	Ni	H2SO4	Na	K	Rh	Rh solids
Solution basis (mmol/L)	1	45	9	-3.0			0.29	0.29
	2	32	2	-23.4			0.39	0.39
	5	38	6	-24.4			0.33	0.33
	10	36	4	-33.1			0.35	0.35
	30	45	4	-44.8			0.46	0.46
	60	51	8	-49.9			0.47	0.47
	90	52	6	-59.1			0.51	0.51
	120	52	6	-58.1			0.47	0.47
	180	52	5	-57.1			0.49	0.49
	240	52	8	-59.6	-99		0.49	0.49

Solid basis (mmol/L)		Cu	Ni	S	Na	K	Rh		
	240	44	0.06	46.9	0.5	0.0	0.49		
Stiochiometry (soln basis)		(Cu+Rh) / Na2S2O3	(Cu+Rh) / Acid	(Cu+Rh) / S (solids)	Acid / Na	S / Na			
Mole ratios %	Basis:								Na = Na2S2O3.5H20
	240 solution	106	89		121				S =elemental S or S(2-
	solids	90		95		95			100% is a 1:1 mole rati
Accountability							Rh		
=100-(soln-solid)/soln%	240	64.8	1.0				100.0		
= (mol Rh in soln+solids @t=final) / (Rh @ t=0) %		96	94				100.0		
Solution concentrations	0	13287	6002	15.8	15	1014	89		
calculated from solid mass	240	10488	5998				39		

Acid balance (solution assays and S in solid)									
Feed	mmol/l			181.1	93.6				
Acid generated from MeS precipitation	mmol/l	51.93					0.73		
Acid consumed (elemental S: Total S - MeS)	mmol/l			0.0					
Acid concentration predicted	mmol/l			213.8					
Acid concentration predicted	g/l			21.0					
Accountability (t=final) (actual-pred.)/actual%				2.5					Some S precipitation ?

Test # : 11R
Test description: Co-precipitation of Cu(II) and Rh(III)

Conditions:

Temperature	0 oC
Make-up Volume	5.400 L
Volume before injection (operating volume)	5.203 L
Seed (Pd sulphide)	none mg
CuSO4.5H20 added to make-up volume	293.60 g
NiSO4 added to make-up volume	139.90 g
FeSO4 added to make-up volume	0.00 g
K2SO4 added to make-up volume	11.70 g
Na2S2O3.5H2O added at t=0	84.72 g
Volume reagent set at	190.00 mL
Volume Rh stock soln pipetted (actual)	50.00 mL
H2SO4 to make-up	74.07 g

Time	Temp	Pressure	Agitator	Sample	Filter paper	FP + solids	Net Dry	[Solid]	[Solid]	[Solid]	Redox	Observations
(min)	oC	kPa	rpm	Volume	mg	mg	mass mg	g/l	g/l CuS	g/l Rh2S3	mV	
feed1				97				measured	calc'd	calc'd		
feed2 (t=o)	95			100	119	130	11	0.11	0.00	0.00		
1	95		404	119	120	263	143	1.20	3.11	0.011		
2	95		404	88	126	384	258	2.93	3.07	0.013		
5	95		405	98	122	418	296	3.02	3.04	0.015		
10	95		405	97	122	448	326	3.36	3.22	0.019		
20	95		400	117	121	588	467	3.99	3.61	0.028		
30	95			120	121	643	522	4.35	3.95	0.037		
60	95			97	123	597	474	4.89	4.11	0.045		
120	95		405	4500	9425	30366	20941	4.65	3.96	0.055		
		flush at t =1		78								
		splash over		100								
Volume balance shortage				-21								
Final volume / initial volume		Vf / Vo %		83								

Comments:

Average solution and solid assays with Mass Balance Test #: 11R

		Solution concentration								Redox	
Sample #	Time	Cu calc'd	Cu	Ni	H2SO4	Na	K	Rh	Rh calc'd	Ag/AgCl	
	(min)	(mg/l)	(mg/l)	(mg/l)	(g/l)	(mg/l)	(mg/l)	(mg/l)	(mg/l)	mV	
2107/11R/ 0/L1 avg	0	12462	12462	5364	14.2	17	1058	89.3	89.3		
2107/11R/ 1/L2	1	11663	10396	NR	16.4	NR	NR	81.5	78.5		
2107/11R/ 2/L3	2	10513	10419	NR	16.2	NR	NR	80.8	62.9		
2107/11R/ 5/L4	5	10454	10438	NR	16.8	NR	NR	79.2	62.1		
2107/11R/ 10/L5	10	10228	10321	NR	17.5	NR	NR	76.3	59.0		
2107/11R/ 20/L6	20	9809	10062	NR	20.0	NR	NR	70.1	53.3		
2107/11R/ 30/L7	30	9570	9838	NR	20.5	NR	NR	64.1	50.1		
2107/11R/ 60/L8	60	9214	9729	NR	19.6	NR	NR	58.6	45.2		
2107/11R/ 120/L8 avg	120	9369	9829	5475	19.9	2273	1091	52.1	47.3		

		Solid concentration							
Sample #	Time		Cu	Ni	S	Na	K	Rh		Concn
	(min)		%	%	%	ppm	ppm	%		g/L
Rh/11R/240/ S1 avg	120		64.6	0.05	31.0	NR	NR	0.90		4.65

Mass balance: Amount removed	(mmol/l)		Cu	Ni	H2SO4	Na	K	Rh	Rh solids		
Solution basis (mmol/L)	1		33		-22.0			0.08	0.11		
	2		32		-20.0			0.08	0.26		
	5		32		-26.1			0.10	0.26		
	10		34		-33.2			0.13	0.29		
	20		38		-58.7			0.19	0.35		
	30		41		-63.8			0.25	0.38		
	80		43		-56.7			0.30	0.43		
	f 20		41	-2	-57.2	-98		0.36	0.41		
Solid basis (mmol/L)			Cu	Ni	S	Na	K	Rh			
	120		47	0.04	45.0			0.41	0.41		
Stiochiometry (soln basis)			(Cu+Rh) / Na2S2O3	(Cu+Rh) / Acid	(Cu+Rh) / S (solids)	Acid / Na	S / Na				
Mole ratios %		Basis:									Na = Na2S2O3.5H20
-)	120	solution	85	73		117					S =elemental S or S(2-)
io		solids	97		108		92				100% is a 1:1 mole ratio
Accountability								Rh			
=100-(soln-solid)/soln%	120		114.1					113			
= (mol Rh in soln+solids @ t=final) / (Rh @ t=0) %			108.0					105			
Solution concentrations	0		12462	5364	14.2	17	1058	89			
calculated from solid mass and	0		9458	5362				47			

Acid balance (solution assays and S in solid)									
Feed	mmol/l			145.2	0.0				
Acid generated from MeS precipitation	mmol/l	0.00					0.00		
Acid consumed (elemental S: Total S - MeS)	mmol/l			0.0					
Acid concentration predicted	mmol/l			145.2					
Acid concentration predicted	g/l			14.2					
Accountability (t=final) (actual-pred.)/actual%				28.3					Some S precipitation ?

Test # :	12
Test description:	Co-precipitation of Cu(II) and Rh(III)

Conditions:

Temperature	150 oC
Make-up Volume	5.400 L
Volume before injection (operating volume)	5.202 L
Seed (Pd sulphide)	none mg
CuSO4.5H20 added to make-up volume	293.60 g
NiSO4 added to make-up volume	139.90 g
FeSO4 added to make-up volume	0.00 g
K2SO4 added to make-up volume	11.70 g
Na2S2O3.5H2O added at t=0	64.72 g
Volume reagent set at	190 mL
Volume Rh stock soln pipetted (actual)	50.00 mL
H2SO4 to make-up	74.07 g

Time (min)	Temp oC	Pressure kPa	Agitator rpm	Sample Volume	Filter paper mg	FP + solids mg	Net Dry mass mg	[Solid] g/l measured	[Solid] g/l CuS calc'd	[Solid] g/l Rh2S3 calc'd	Redox mV	Observations
feed1				100								flush
feed2 (t=o)	150			98	123	129	6	0.06	0.00	0.00		
1	150			102	250	702	452	4.43	4.35	0.089		indicative solids g/l
2	150			102	126	612	486	4.76	5.86	0.108		indicative solids g/l
3	150		540	102	127	611	484	4.75	3.66	0.113	540	indicative solids g/l
4	150		537	102	125	619	494	4.64	2.94	0.117	537	indicative solids g/l
6	150		544	100	122	607	485	4.85	3.73	0.122	544	indicative solids g/l
7	150		548	106	125	638	513	4.64	4.09	0.124	548	indicative solids g/l
10	150		551	106	124	641	517	4.88	4.17	0.126	551	indicative solids g/l
15	150		552	104	127	636	509	4.89	4.38	0.127	552	indicative solids g/l
20	150		560	100	124	612	488	4.88	4.21	0.128	560	indicative solids g/l
30	150		562	102	125	632	507	4.97	4.86	0.129	562	indicative solids g/l
60	150		405	4175	201806	222735	20929	5.01	3.41	0.131	405	accurate g/l
		splash over		100	(evaporated)							
Volume balance shortage				91								
Final volume / initial volume		Vf / Vo %		77								

Comments:
No H2S or SO2 smell, thus all reagents consumed in precipitation.
Solids g/l indicative (slightly on low side) due to not removing soloids from millipore glass, as there was insufficient time available.

Average solution and solid assays with Mass Balance — Test #: 12

Solution concentration

Sample #	Time (min)	* Cu calc'd (mg/l)	Cu (mg/l)	Ni (mg/l)	H2SO4 (g/l)	Na (mg/l)	K (mg/l)	Rh (mg/l)	Rh calc'd (mg/l)	Redox Ag/AgCl mV	
2007/12/ 0/L1	0	12762	12762	5553	14.6	15	980	89.3	89.3		
2007/12/ 1/L2 avg	1	9817	9869	5564	19.8	2271	1345	28.4	3.2		* Cu calculated assumes pure CuS in the solids
2007/12/ 2/L3	2	9595	8869	4961	18.2	NR	1134	15.9	-3.3		
2007/12/ 3/L4	3	9608	10328	5922	21.2	NR	1138	12.5	-2.9	540	
2007/12/ 4/L5 avg	4	9543	10807	6027	20.8	NR	1128	9.6	-4.8	537	
2007/12/ 6/L6	6	9538	10286	5884	20.8	NR	1134	6.2	-4.9	544	
2007/12/ 7/L7	7	9545	10043	5756	20.9	NR	1095	4.9	-4.7	548	
2007/12/ 10/L8	10	9520	9987	5758	21.1	NR	1115	3.5	-5.5	551	
2007/12/ 15/L9 avg	15	9509	9852	5700	20.7	NR	1139	2.7	-5.8	552	
2007/12/ 20/L10	20	9518	9967	5691	20.1	NR	1200	2.0	-5.5	560	
2007/12/ 30/L11 avg	30	9458	9531	5964	20.8	2236	1188	1.5	-7.3	562	
2007/12/ 60/L12 avg	60	9430	10498	5927	22.1	2369	1257	0.1	-8.1	405	

Solid concentration

Sample #	Time (min)		Cu %	Ni %	S %	Na ppm	K ppm	Rh %		Concn g/L	
Rh/12/60/S avg	60		64.3	0.05	29.95	NR	NR	1.94		5.01	
Mass balance: Amount removed (mmol/l)			Cu	Ni	H2SO4	Na	K	Rh			
Solution basis (mmol/L)	1		46	0	-53.3	-98.1		0.59			
	2		61	10	-37.0			0.71			
	3		38	-6	-67.6			0.75			
	4		31	-8	-63.5			0.78			
	6		39	-6	-63.5			0.81			
	7		43	-3	-64.6			0.82			
	10		44	-3	-66.6			0.89			
	15		46	-2	-62.0			0.64			
	20		44	-2	-56.4			0.85			
	30		51	-7	-63.5	-97		0.85			
	60		36	-6	-76.8	-102		0.87			
Solid basis (mmol/L)			Cu	Ni	S	Na	K	Rh			
	0		0	0.0	0.0	0.0	0.0	0.0			
	60		51	0.04	46.8	NR	NR	0.96			
Stiochiometry (soln basis)			(Cu+Rh) / Na	(Cu+Rh) / Acid	(Cu+Rh) / S (solids)	Acid / Na	S / Na				
Mole ratios %	60	Basis: solution	71	48		150					Na = Na2S2O3.5H20
		solids	101		110		91				S =elemental S or S(2-)
Accountability								Rh			100% is a 1:1 mole ratio
=100-(soln-solid)/soln%	60		142.3					109.2			
= (mol Rh in soln+solids @t=final) / (Rh @ t=0) %			107.5	107				109			
Solution concentrations calculated from solid mass and assay	0		12762	5553	14.6	15	980	89			
	60		9539					-8			

Acid balance (solution assays and S in solid)

Feed	mmol/l			148.5	102.4		
Acid generated from MeS precipitation	mmol/l	35.64				1.30	
Acid consumed (elemental S: Total S - MeS)	mmol/l			0.0			
Acid concentration predicted	mmol/l			185.5			
Acid concentration predicted	g/l			18.2			
Accountability (t=final) (actual-pred.)/actual%				11.9			

B.5. Leach Profiles

1. Summary of predicted and measured concentration values

Table B.5.1: Summary of Rh precipitation concentration results (solids basis)

		Rh concentration [mg/l]								
Reaction Path	oC	Feed t=0	t=1	t=2	t= ~5	t= ~10	t= ~30	t= 60	t= 120	t=240 (or final)
#1 ionic (solids)	50	93	*84*	*84*	80	78	76	75	75	74
#2	80	93	61	55	51	49	47	47	45	46
#3	95	93	40	40	39	37	34	32	33	33
#4R	150	93	40	28	14.2	2.9	0.1	0.1	0.1	0.05
#5b substitution	50	96	*96*	*96*	96	95	94	86	87	80
#6b	80	93	92	91	83	85	85	65	63	62
#7b	95	90	86	89	63	66	59	56	52	50
#8b	150	92	35	18	4.8	1.2	0.4	0.1	0.1	0.1
#9 co-precipitation (soli	50	89	89	89	89	85	64	63	82	63
#9R (solids)	50	97	97	97	97	97	94	92	91	92
#10	80	89	*66*	*65*	65	63	80	58	49	
#11	95	89	*59*	*65*	56	53	42	41	41	39
#11R	95	89	78	63	82	59	50	45	47	
#11 avg	95	89	89	64	59	56	46	43	44	39
#12	150	89	28	18	10	3.5	1.5	0.1	0.1	0.1

Table B.5.2: Summary of Rh precipitation extent for all reaction systems (solution basis)

		Rh concentration [mg/l]								
Reaction Path	oC	Feed t=0	t=1	t=2	t= ~5	t= ~10	t= ~30	t= 60	t= 120	t=240 (or final)
#1 ionic (solids)	50	93	*84*	*84*	80	78	78	75	75	74
#2	80	93	71	89	71	59	60	50	43	36
#3	95	93	62	53	51	42	41	32	28	24
#4R	150	93	40	28	14.2	2.9	0.1	0.1	0.1	0.05
#5b substitution	50	96	*126*	*109*	96	95	94	86	87	80
#6b	80	93	92	91	83	85	85	65	63	62
#7b	95	90	86	69	63	66	59	56	52	50
#8b	150	92	35	18	4.6	1.2	0.4	0.1	0.1	0.1
#9 co-precipitation (soli	50	89	89	89	89	85	64	63	62	63
#9R (solids)	50	97	97	97	97	97	94	92	91	92
#10	80	89	*72*	*77*	82	74	73	68	60	
#11	95	89	*79*	*77*	82	78	70	61	51	44
#11R	95	89	82	81	79	78	64	59	52	
#11 avg	95	89	80	79	81	77	67	60	52	44
#12	150	89	28	18	10	3.5	1.5	0.1	0.1	0.1

Note: - *problem with time profile due to contamination and post precipitation*
- *replaced 126 and 109 with 96 mg/l (same as fed and t=5 min)*
- calculated feed concentration at t = 0 are used in calculations to compensate for the varying dilution effect
- #1, #9 and #9R on caculated from solids basis due to post precipitation

t=1: #1-4; inject thiosulphate at temp and t=0
1st sample more precipitation because thiosulphate in sampler (even though it was washed)
or due to post precipitation

#5b-#8b inject Rh at temp
1st sample [Rh] higher that expected due to Rh contamination of 1st sample

#9-#12 inject thiosulphate at temp and t=0
1st sample more precipitation because thiosulphate in sampler (even though it was washed)
or due to post precipitation

Concentration profiles are as expected from t = 5 min onwards

Table B.5.3: Summary of Cu precipitation extent for all reaction systems (solids basis)

Test #	Temp	Rh concentration [mg/l]							
	°C	1 min	2 min	~5 min	10 min	30 min	60 min	120 min	240 min
Co-precipitation system									
#9 *	50	12939	12939	12939	12939	12894	12575	10880	10707
#9R *	50	13115	13115	13115	13115	13115	12731	12291	11326
#10	80	12798	10914	10810	10817	10695	10404	10256	9583
#11	95	13287	11387	10744	11156	11010	10302	10194	
#11R	95	12462	11663	10513	10454	10228	9809	9570	9369
#12	150	12762	9817	9595	9541	9520	9458	9430	

Table B.5.4: Summary of Cu precipitation extent for all reaction systems (solution basis)

Test #	Temp	Rh concentration [mg/l]							
	°C	1 min	2 min	~5 min	10 min	30 min	60 min	120 min	240 min
Co-precipitation system									
#9 *	50	12939	12939	12939	12939	12894	12575	10880	10707
#9R *	50	13115	13115	13115	13115	13115	12731	12291	11326
#10	80	12798	11006	10900	10706	10992	10486	10175	9607
#11	95	13287	10428	11279	10881	11019	10450	10070	
#11R	95	12462	10396	10419	10438	10321	10062	9838	9829
#12	150	12762	9869	8869	10547	9987	9531	10498	

Table B.5.5: Final solution comparison of measured concentration and calculated concentration using solids precipitation profile

Test #	Final solution (mg/l)		Final solution (mg/l)		Used in study (mg/l)	
	Measured concn	Calc from solids	Measured concn	Calc from solids		
	Rh	Rh	Cu	Cu	Rh	Cu
1	65.1	74.3	--	--	74.3	--
2	35.6	46.4	--	--	46.4	--
3	23.7	32.7	--	--	32.7	--
4R	0.1	56.4	--	--	0.1	--
5b	80.3	--	--	--	80.3	--
6b	61.5	--	--	--	61.5	--
7b	49.7	--	--	--	49.7	--
8b	0.1	--	--	--	0.1	--
9	55.2	55.6	10990	10380	55.6	10380
9R	90.8	91.8	10860	11500	91.8	11500
10	57.0	48.7	9060	9520	48.7	9520
11	44.1	39.2	9990	10110	39.2	10110
11R	52.1	47.3	9830	9370	47.3	9370
12	0.1	-8.1	10500	9430	0.1	9430

Table B.5.6: Order of precipitation extent for final solution comparison of Rh precipitation extent on solution and solids

Test #	Final precipitation extent		Final precipitation extent	
	Measured on solution	Order of X	Calculated on solids	Order of X
	Rh	1 slowest; 12 fastest	Rh	1 slowest; 12 fastest
1	20	3	20	3
2	62	8	50	▮
3	74	9	65	9
4R	100	10-12	100	10-12
5b	17	2	17	2
6b	34	4	34	4
7b	45	6	45	■
8b	100	10-12	100	10-12
9R	5	1	5	1
10	36	5	45	■
11 avg	47	7	52	▮
12	100	10-12	100	10-12

This shows that the comparative precipitation extent between the solution basis and solid basis is very similar. Where the order did change, the difference between the actual precipitation extents is negligible i.e. the relative order does not really change.

2. Calculation of precipitation extent and reaction rates over middle period: (pseudo first order kinetics at 150 °C; logarithmic fit at 50 - 95 °C)

Sample #	Time	X Rh	X Cu	X Cu	RATE	d/dt(Xrh)	RATE d/dt [Rh] =	X Rh calc	[Rh] calc
					1st order	= const / t	[Rh]o d/dt(Xrh)		
	min			normalised to 25% max	-r Rh= k [Rh]	/ min	mg / min / ltr		mg/l
Rh/2306/5a/t0/L1 avg	0								
Rh/2306/5a/filt/L4	80								
Rh/2306/6a/t0/L2 avg	0								
Rh/2306/6a/filt/L5	20								
Rh/2306/7a/to/L3 avg	0								
Rh/2306/7a/filt/L6	15								
Rh/8a/0/L6 avg	0								
Rh/8a/filt/L	10								
Rh/2806/5b/TO/ L1	0								
Rh/Rh estimate after injection	0.01	0.000			ln(t) slope	0.053	ln(t) y-int	-0.112	
Rh/2806/5b/ 1/ L2 avg	1	0.002				0.05287	5.086	0.00	96.0
Rh/2806/5b/ 2/L3 avg	2	0.002				0.02644	2.543	0.00	96.0
Rh/2806/5b/ 5/L4 avg	5	0.002				0.01057	1.017	0.00	96.1
Rh/2806/5b/ 10/L5 avg	10	0.013				0.00529	0.509	0.01	95.0
Rh/2806/5b/ 30/L6	30	0.019				0.00176	0.170	0.07	89.6
Rh/Rh/2806/5b/ 60/L7	60	0.110				0.00088	0.085	0.10	86.1
Rh/2806/5b/ 90/L8	90	0.126				0.00059	0.057	0.13	84.0
Rh/2806/5b/ 120/L9	120	0.096				0.00044	0.042	0.14	82.6
Rh/2806/5b/ 180/L10	180	0.201				0.00029	0.028	0.16	80.5
Rh/2806/5b/ 240/L11 avg	240	0.201				0.00022	0.021	0.18	79.1
Rh/2806/5b/ 290/L12 avg	290	0.165				0.00018	0.018	0.19	78.1
Rh/0307/6b/tO/L1 avg	0				ln(t) slope	0.060	ln(t) y-int	-0.012	
Rh estimate after injection	0.01	0.000							
Rh/0307/6b/ 1/L2 avg	1	0.015				0.06026	5.625	-0.01	94.5
Rh/0307/6b/ 2/L3 avg	2	0.026				0.03013	2.813	0.03	90.6
Rh/0307/6b/ 5/L4 avg	5	0.110				0.01205	1.125	0.08	85.5
Rh/Rh/0307/6b/ 10/L5 avg	10	0.095				0.00603	0.563	0.13	81.6
Rh/0307/6b/ 30/L6 avg	30	0.086				0.00201	0.188	0.19	75.4
Rh/0307/6b/ 60/L7	60	0.304				0.00100	0.094	0.23	71.5
Rh/0307/6b/ 90/L8 avg	90	0.241				0.00067	0.063	0.26	69.2
Rh/0307/6b/ 120/L9	180	0.329				0.00033	0.031	0.30	65.3
Rh/0307/6b/ 180/L10 avg	240	0.325				0.00025	0.023	0.32	63.7
Rh/0307/6b/ 240/L11	290	0.341				0.00021	0.019	0.33	62.6
Rh/2806/7b/t0/L1	0				ln(t) slope	0.060	ln(t) y-int	0.135	
Rh estimate after injection	0.01	0.000							
Rh/2806/7b/1/L2 avg	1	0.045				0.05991	5.392	0.13	77.9
Rh/2806/7b/2/L3 avg	2	0.233				0.02995	2.696	0.18	74.1
Rh/2806/7b/5/L4	5	0.296				0.01198	1.078	0.23	69.2
Rh/2806/7b/10/L5	10	0.263				0.00599	0.539	0.27	65.5
Rh/2806/7b/30/L6 avg	30	0.350				0.00200	0.180	0.34	59.5
Rh/2806/7b/60/L7	60	0.376				0.00100	0.090	0.38	55.8
Rh/2806/7b/90/L8 avg	90	0.389				0.00067	0.060	0.40	53.6
Rh/2806/7b/120/L11 avg	120	0.422				0.00050	0.045	0.42	52.1
Rh/2806/7b/180/L9 avg	180	0.430				0.00033	0.030	0.45	49.9
Rh/2806/7b/225/L10	225	0.448				0.00027	0.024	0.46	48.7
					k overall (middle period)				
1907/8b/ 0/L1 avg	0				0.564	ln(t) slope	0.148	ln(t) y-int	0.676
Rh estimate after injection	0.01	0.000							
1907/8b/ 1/L2	1	0.621			19.74	0.14754	13.642	0.68	35.0
1907/8b/ 2/L3 avg	2	0.800			10.40	0.07377	6.821	0.78	18.5
1907/8b/ 4/L4	4	0.950			2.61	0.03689	3.410	0.88	4.6
1907/8b/ 7/L5 avg	7	0.987			0.68	0.02108	1.949	0.96	1.2
1907/8b/ 13/L6	13	0.992			0.41	0.01135	1.049	1.05	0.7
1907/8b/ 20/L7	20	0.995			0.28	0.00738	0.682	1.12	0.5
1907/8b/ 30/L8	30	0.995			0.25	0.00492	0.455	1.18	0.4
1907/8b/ 60/L9 avg	60	0.999			0.05	0.00246	0.227	1.28	0.1

Sample #	Time	X Rh	X Cu	X Cu	RATE		d/dt(Xrh)	RATE d/dt [Rh] =		
					1st order		= const / t	[Rh]o d/dt(Xrh)	X Rh calc	[Rh] calc
	min			normalised to 25% max	-r Rh= k [Rh]		/ min	mg / min / ltr		mg/l
Rh/0607/9/ 0/ L1	0	0.000	0.00	0.00						
Rh/0607/9/ 1/L2 avg	1	0.000	0.00	0.00						
Rh/0607/9/ 2/L3 avg	2	0.000	0.00	0.00						
Rh/0607/9/ 5/L4 avg	5	0.006	0.00	0.00						
Rh/0607/9/ 10/L5 avg	10	0.050	0.00	0.01						
Rh/0607/9/ 30/L6 avg	30	0.281	0.03	0.11						
Rh/0607/9/ 60/L7 avg	60	0.300	0.16	0.61						
Rh/0607/9/ 90/L8 avg	90	0.305	0.17	0.65						
Rh/0607/9/ 120/L9	120	0.299	0.17	0.66						
Rh/0607/9/ 180/L10 avg	180	0.325	0.17	0.65						
Rh/0607/9/ 240/L11	240	0.325	0.18	0.70						
Rh/0607/9/ 300/L12 avg	300	0.350	0.18	0.71						
Rh/1407/9R/ 0/L1 avg	0	0.000	0.00	0.00		ln(t) slope	0.023	ln(t) y-int	-0.05	
Rh/1407/9R/ 2/L2 avg	2	0.000	0.00	0.00			0.01143	1.11	-0.04	100.4
Rh/1407/9R/ 5/L3	5	0.000	0.00	0.00			0.00457	0.44	-0.01	98.4
Rh/1407/9R/ 9/L4	9	0.003	0.00	0.00			0.00254	0.25	0.00	97.1
Rh/1407/9R/ 14/L5 avg	14	0.006	0.01	0.03			0.00163	0.16	0.01	96.1
Rh/1407/9R/ 20/L6	20	0.013	0.01	0.06			0.00114	0.11	0.02	95.3
Rh/1407/9R/ 30/L7 avg	30	0.027	0.03	0.11			0.00076	0.07	0.03	94.4
Rh/1407/9R/ 60/L8 avg	60	0.053	0.06	0.24			0.00038	0.04	0.04	92.9
Rh/1407/9R/ 90/L9 avg	90	0.059	0.12	0.47			0.00025	0.02	0.05	92.0
Rh/1407/9R/ 120/L10	120	0.064	0.14	0.52			0.00019	0.02	0.06	91.3
Rh/1407/9R/ 180/L11 avg	180	0.053	0.15	0.57			0.00013	0.01	0.07	90.4
Rh/1407/9R/ 240/L12	240	0.053	0.12	0.47			0.00010	0.01	0.07	89.8
Rh/0507/10/ 0/L1 avg	0	0.000	0.00	0.00		ln(t) slope	0.032	ln(t) y-int	0.24	
Rh/0507/10/ 1/L2 avg	1	0.262	0.15	0.56			0.03232	2.89	0.24	67.8
Rh/0507/10/ 2/L3 avg	2	0.276	0.16	0.59			0.01616	1.44	0.26	65.8
Rh/0507/10/ 5/L4 avg	5	0.275	0.15	0.59			0.00646	0.58	0.29	63.2
Rh/0507/10/ 10/L5	10	0.292	0.16	0.63			0.00323	0.29	0.32	61.2
Rh/0507/10/ 30/L6 avg	30	0.333	0.19	0.72			0.00108	0.10	0.35	58.0
Rh/0507/10/ 60/L7 avg	60	0.353	0.20	0.76			0.00054	0.05	0.37	56.0
Rh/0507/10/ 90/L8	90	0.380	0.21	0.82			0.00036	0.03	0.39	54.8
Rh/0507/10/ 120/L9	120	0.447	0.25	0.96			0.00027	0.02	0.40	54.0
Rh/0507/10/ 180/L10 avg	180	0.455	0.26	0.98			0.00018	0.02	0.41	52.8
Rh/0507/10/ 240/L11 avg	240									
Rh/0407/11/ 0/L1 avg	0	0.000	0.00	0.00		ln(t) slope	0.043	ln(t) y-int	0.35	
Rh/0407/11/ 1/L2 avg	1	0.336	0.14	0.55			0.04261	3.81	0.35	57.7
Rh/0407/11/ 2/L3	2	0.449	0.19	0.73			0.02131	1.90	0.38	55.1
Rh/0407/11/ 5/L4 avg	5	0.377	0.16	0.61			0.00852	0.76	0.42	51.6
Rh/0407/11/ 10/L5 avg	10	0.402	0.17	0.66			0.00426	0.38	0.45	49.0
Rh/0407/11/ 30/L6	30	0.527	0.22	0.86			0.00142	0.13	0.50	44.8
Rh/0407/11/ 60/L7	60	0.546	0.23	0.89			0.00071	0.06	0.53	42.1
Rh/0407/11/ 90/L8	90	0.592	0.25	0.97			0.00047	0.04	0.55	40.6
Rh/0407/11/ 120/L9 avg	120	0.546	0.23	0.89			0.00036	0.03	0.56	39.5
Rh/0407/11/ 180/L10 avg	180	0.568	0.24	0.93			0.00024	0.02	0.58	38.0
Rh/0407/11/ 240/L11 avg	240	0.561	0.24	0.92			0.00018	0.02	0.59	36.9
2107/11R/ 0/L1 avg	0	0.000	0.00	0.00		ln(t) slope	0.069	ln(t) y-int	0.19	
2107/11R/ 1/L2	1	0.121	0.06	0.25			0.06897	6.16	0.19	72.6
2107/11R/ 2/L3	2	0.296	0.16	0.60			0.03449	3.08	0.23	68.3
2107/11R/ 5/L4	5	0.305	0.16	0.62			0.01379	1.23	0.30	62.7
2107/11R/ 10/L5	10	0.340	0.18	0.69			0.00690	0.62	0.35	58.4
2107/11R/ 20/L6	20	0.403	0.21	0.82			0.00345	0.31	0.39	54.2
2107/11R/ 30/L7	30	0.439	0.23	0.89			0.00230	0.21	0.42	51.7
2107/11R/ 60/L8	60	0.494	0.26	1.00			0.00115	0.10	0.47	47.4
2107/11R/ 120/L8 avg	120	0.470	0.25	0.95			0.00057	0.05	0.52	43.1
					k overall (middle period)					
2007/12/ 0/L1	0	0.000	0.00	0.00	0.24	ln(t) slope	0.060	ln(t) y-int	0.81	
2007/12/ 1/L2 avg	1	0.682	0.23	0.88	6.72		0.05973	5.34	0.81	28.40
2007/12/ 2/L3	2	0.822	0.25	0.95	3.76		0.02987	2.67	0.85	15.90
2007/12/ 3/L4	3	0.860	0.25	0.95	2.96		0.01991	1.78	0.87	12.50
2007/12/ 4/L5 avg	4	0.893	0.25	0.97	2.26		0.01493	1.33	0.89	9.56
2007/12/ 6/L6	6	0.931	0.25	0.97	1.46		0.00996	0.89	0.91	6.17
2007/12/ 7/L7	7	0.946	0.25	0.97	1.15		0.00853	0.76	0.92	4.85
2007/12/ 10/L8	10	0.961	0.25	0.97	0.83		0.00597	0.53	0.94	3.52
2007/12/ 15/L9 avg	15	0.970	0.25	0.98	0.63		0.00398	0.36	0.97	2.65
2007/12/ 20/L10	20	0.978	0.25	0.97	0.46		0.00299	0.27	0.98	1.95
2007/12/ 30/L11 avg	30	0.983	0.26	0.99	0.36		0.00199	0.18	1.01	1.51
2007/12/ 60/L12 avg	60	0.998	0.26	1.00	0.03		0.00100	0.09	1.05	0.14

3. Precipitation profile graphical illustrations

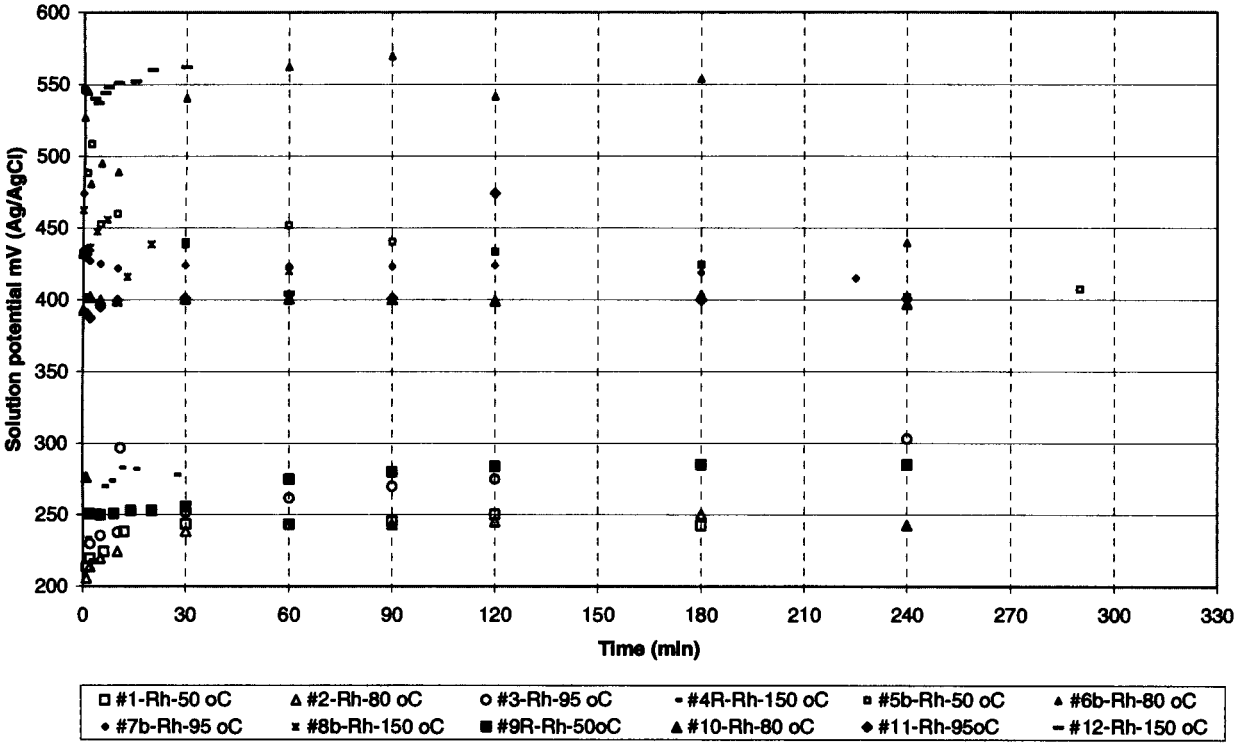

Figure B.5.1: Redox profile comparison of precipitation profiles of various reaction paths

4. Kinetics of systems on concentration basis

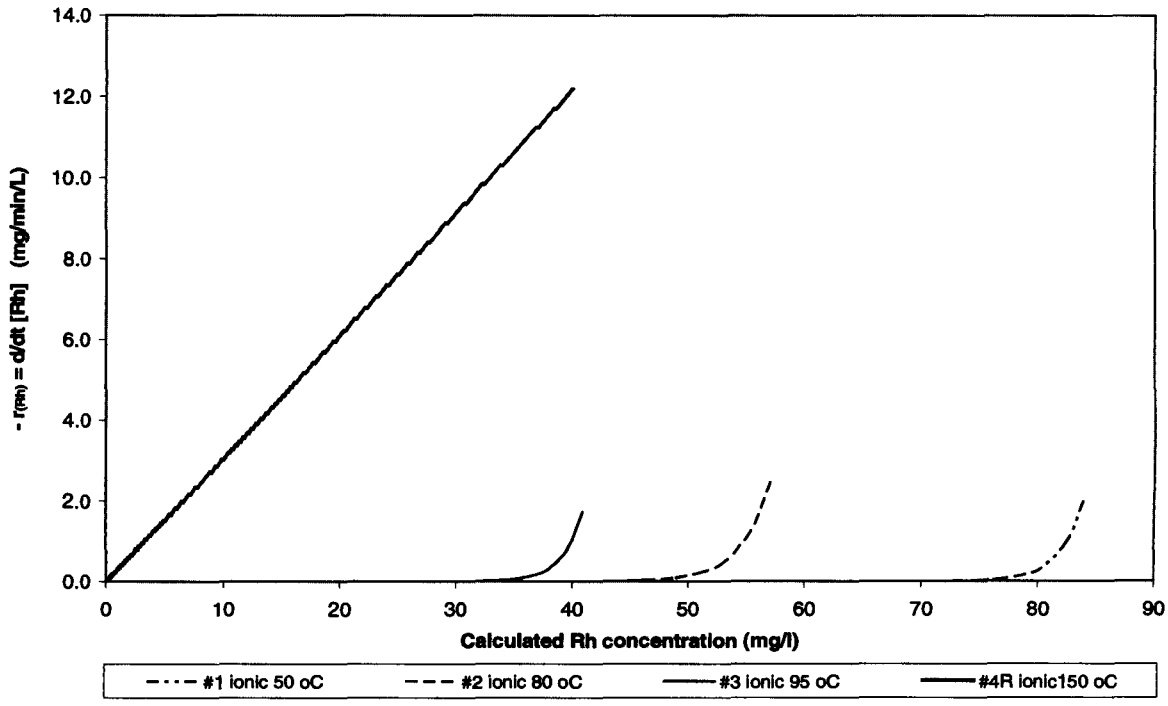

Figure B.5.6a: Comparison of calculated Rh precipitation rates for ionic reaction system Rh over the middle period over 50 -150 °C, showing that the rate is fairly independent of temperature at atmospheric temperatures and increases significantly at 150 °C; rates tend towards zero precipitation prior to completion, showing passivation of the elemental sulfur occurring at atmospheric temperatures.

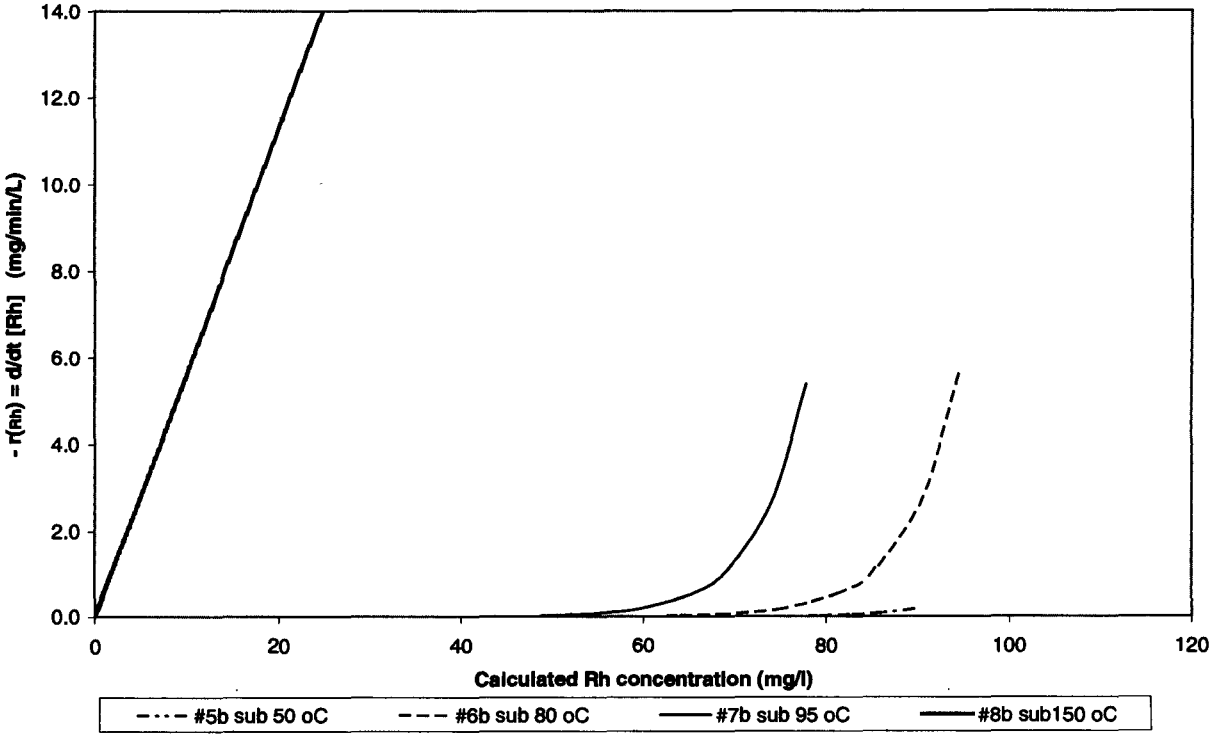

Figure B.5.6b: Comparison of calculated Rh precipitation rates for substitution reaction system Rh over the middle period over 50 -150 °C, showing that the rate is fairly independent of temperature at atmospheric temperatures and

increases significantly at 150 °C; rates tend towards zero precipitation prior to completion, showing passivation of the CuS occurring at atmospheric temperatures.

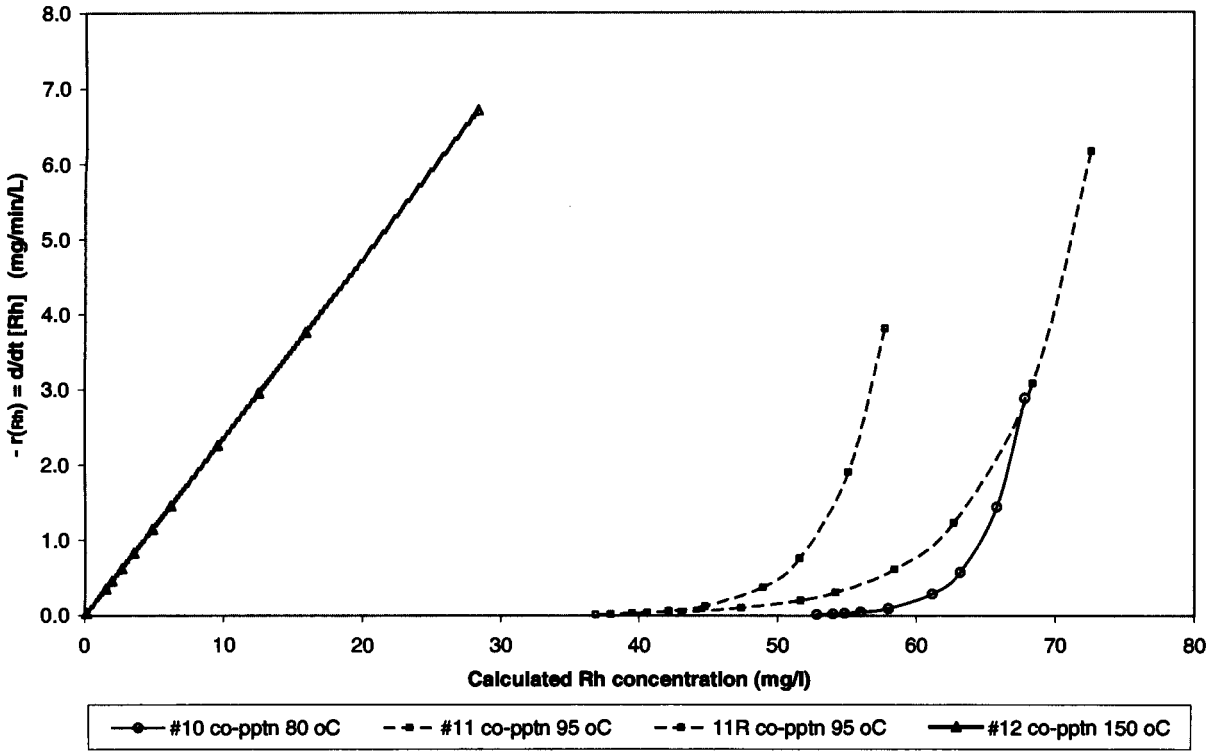

Figure B.5.6c Comparison of calculated Rh precipitation rates for co-precipitation reaction system over 50 -150 °C over the middle period, showing that the rate increases with increasing temperature; though the rates converge with increasing precipitation.

B.6. Kinetic Modelling

1. Kinetic calculation data (solids basis)

			Rhodium				Rhodium				Rhodium		Copper	
		Conversion	First order kinetics	Second order kinetics		Conversion	First order kinetics	Second order kinetics		Conversion	First order kinetics	Second order kinetics	1st order	2nd order
Test #	Time	X a	-ln(Ca/Cao)	1/Ca	Test #	Time	X a	-ln(Ca/Cao)	1/Ca	Test #	Time	X a	-ln(Ca/Cao)	1/Ca	-ln(Ca/Cao)	1/Ca
	min	Not norm.	Not norm.	Not norm.		min	Not norm.	Not norm.	Not norm.		min	Not norm.	Not norm.	Not norm.	Not norm.	Not norm.
1	0	0.000	0.000	0.0108	5b	0	0.000	0.000	0.0104	9	0	0.000		0.0112		7.73E-05
	1	0.089	0.093	0.0118		1	0.002	0.002	0.0104		1	0.000	0.000	0.0112	0.000	7.73E-05
	2	0.097	0.102	0.0120		2	0.002	0.002	0.0104		2	0.000	0.000	0.0112	0.000	7.73E-05
	6	0.139	0.150	0.0125		5	0.002	0.002	0.0104		5	0.006	0.006	0.0113	0.000	7.73E-05
	12	0.161	0.176	0.0129		10	0.013	0.013	0.0105		10	0.050	0.051	0.0118	0.003	7.76E-05
	30	0.179	0.197	0.0131		30	0.019	0.019	0.0106		30	0.281	0.330	0.0156	0.029	7.95E-05
	60	0.186	0.206	0.0133		60	0.110	0.117	0.0117		60	0.300	0.356	0.0160	0.173	9.19E-05
	90	0.189	0.209	0.0133		90	0.126	0.134	0.0119		90	0.305	0.363	0.0161	0.186	9.31E-05
	120	0.189	0.209	0.0133		120	0.098	0.101	0.0115		120	0.299	0.356	0.0160	0.189	9.34E-05
	180	0.196	0.219	0.0134		180	0.201	0.224	0.0130		180	0.325	0.393	0.0166	0.186	9.31E-05
	240	0.197	0.220	0.0134		240	0.201	0.224	0.0130		240	0.325	0.393	0.0166	0.203	9.47E-05
	300	0.198	0.220	0.0135		290	0.165	0.181	0.0125		300	0.350	0.431	0.0172	0.204	9.47E-05
2	0	0.000	0.000	0.0108	6b	0	0.000	0.000	0.0107	9R	0	0.000	0.000	0.0103		7.62E-05
	1	0.344	0.421	0.0164		1	0.015	0.015	0.0109		2	0.000	0.000	0.0103	0.000	7.62E-05
	2	0.408	0.525	0.0182		2	0.026	0.027	0.0110		5	0.000	0.000	0.0103	0.000	7.62E-05
	5	0.445	0.588	0.0194		5	0.110	0.117	0.0120		9	0.003	0.003	0.0103	0.000	7.62E-05
	10	0.475	0.645	0.0206		10	0.095	0.100	0.0118		14	0.006	0.006	0.0104	0.007	7.68E-05
	30	0.491	0.675	0.0212		30	0.086	0.090	0.0117		20	0.013	0.013	0.0104	0.015	7.74E-05
	60	0.488	0.670	0.0211		60	0.304	0.362	0.0154		30	0.027	0.028	0.0106	0.030	7.85E-05
	90	0.501	0.695	0.0216		90	0.241	0.275	0.0141		60	0.010	0.054	0.0109	0.065	8.14E-05
	120	0.511	0.716	0.0221		180	0.329	0.400	0.0160		90	0.010	0.081	0.0110	0.130	8.69E-05
	180	0.497	0.687	0.0215		240	0.325	0.393	0.0159		120	0.010	0.086	0.0110	0.147	8.83E-05
	240	0.499	0.690	0.0215		290	0.341	0.417	0.0163		180	0.010	0.054	0.0109	0.160	8.95E-05
											240	0.010	0.055	0.0108	0.130	8.69E-05
3	0	0.000	0.000	0.0108	7b	0	0.000	0.000	0.0111	10	0	0.000	0.000	0.0112		7.81E-05
	1	0.564	0.831	0.0246		1	0.045	0.046	0.0116		1	0.262	0.304	0.0152	0.159	9.16E-05
	2	0.564	0.830	0.0246		2	0.233	0.266	0.0145		2	0.276	0.323	0.0155	0.169	9.25E-05
	5	0.579	0.864	0.0256		5	0.296	0.350	0.0158		5	0.275	0.322	0.0154	0.168	9.24E-05
	10	0.603	0.924	0.0272		10	0.263	0.306	0.0151		10	0.292	0.346	0.0158	0.179	9.35E-05
	30	0.632	0.999	0.0293		30	0.350	0.431	0.0171		30	0.333	0.405	0.0168	0.207	9.81E-05
	60	0.652	1.055	0.0310		60	0.376	0.471	0.0178		60	0.353	0.436	0.0173	0.221	9.75E-05
	90	0.632	1.000	0.0293		90	0.389	0.493	0.0182		90	0.360	0.477	0.0180	0.240	9.93E-05
	120	0.647	1.042	0.0306		120	0.422	0.549	0.0192		120	0.447	0.592	0.0202	0.289	1.04E-04
	180	0.648	1.044	0.0307		180	0.430	0.562	0.0195		180	0.455	0.607	0.0205	0.295	1.05E-04
	240	0.647	1.041	0.0306		225	0.448	0.594	0.0201		240					
4	0	0.000	0.000	0.04	8b	0	0.000	0.000	0.0108	11	0	0.000	0.000	0.0112		7.53E-05
	1	0.954	3.086	0.85		1	0.621	0.971	0.0288		1	0.336	0.409	0.0169	0.154	8.78E-05
	2	0.976	3.713	1.59		2	0.800	1.612	0.0542		2	0.449	0.597	0.0203	0.212	9.31E-05
	4	0.986	4.287	2.82		4	0.950	2.996	0.2165		5	0.377	0.473	0.0180	0.175	8.96E-05
	7	0.994	5.084	5.25		7	0.987	4.336	0.8264		10	0.402	0.515	0.0187	0.188	9.08E-05
	10	0.997	5.659	11.11		13	0.992	4.841	1.3699		30	0.527	0.749	0.0237	0.254	9.71E-05
	20	0.998		20.00		20	0.995	5.240	2.0408		60	0.546	0.791	0.0247	0.265	9.81E-05
						30	0.995	5.348	2.2727		90	0.592	0.895	0.0274	0.290	1.01E-04
4R	0	0.000	0.000	0.011		60	0.999	7.052	12.5000		120	0.546	0.790	0.0247	0.265	9.81E-05
	1	0.568	0.840	0.03							180	0.566	0.839	0.0259	0.277	9.93E-05
	2	0.702	1.211	0.04							240	0.561	0.824	0.0255	0.273	9.89E-05
	4	0.847	1.875	0.07						11R	0	0.000	0.000	0.0112		8.02E-05
	6	0.904	2.340	0.11							1	0.121	0.129	0.0127	0.066	8.57E-05
	8	0.951	3.022	0.22							2	0.296	0.351	0.0159	0.170	9.51E-05
	11	0.977	3.763	0.47							5	0.305	0.364	0.0161	0.176	9.57E-05
	15	0.992	4.816	1.33							10	0.340	0.415	0.0169	0.198	9.78E-05
	27	0.999	7.524	20.00							20	0.403	0.516	0.0188	0.239	1.02E-04
											30	0.439	0.579	0.0200	0.264	1.04E-04
											60	0.494	0.681	0.0221	0.302	1.09E-04
											120	0.470	0.635	0.0211	0.285	1.07E-04
										12	0	0.000		0.0112		7.84E-05
											1	0.682	1.146	0.0352	0.262	1.02E-04
											2	0.822	1.726	0.0629	0.285	1.04E-04
											3	0.860	1.957	0.0800	0.284	1.04E-04
											4	0.893	2.235	0.1046	0.291	1.05E-04
											6	0.951	2.673	0.1621	0.291	1.05E-04
											7	0.946	2.913	0.2062	0.290	1.05E-04
											10	0.961	3.234	0.2841	0.293	1.05E-04
											15	0.970	3.518	0.3774	0.294	1.05E-04
											20	0.978	3.825	0.5128	0.293	1.05E-04
											30	0.983	4.084	0.6645	0.300	1.08E-04
											60	0.998	6.458	7.1429	0.303	1.08E-04

2. Kinetic calculation data (solution basis)

			Rhodium					Rhodium					Rhodium		Copper	
		Conversion	First order kinetics	Second order kinetics			Conversion	First order kinetics	Second order kinetics			Conversion	First order kinetics	Second order kinetics	1st order	2nd order
Test #	Time min	X a Not norm.	-ln(Ca/Cao) Not norm.	1/Ca Not norm.	Test #	Time min	X a Not norm.	-ln(Ca/Cao) Not norm.	1/Ca Not norm.	Test #	Time min	X a Not norm.	-ln(Ca/Cao) Not norm.	1/Ca Not norm.	-ln(Ca/Cao) Not norm.	1/Ca Not norm.
1	0	0.000	0.000	0.0108	5b	0	0.000	0.000	0.0104	9	0	0.000		0.0112		7.73E-05
	1	0.089	0.093	0.0118		1	0.002	0.002	0.0104		1	0.000	0.000	0.0112	0.000	7.73E-05
	2	0.097	0.102	0.0120		2	0.002	0.002	0.0104		2	0.000	0.000	0.0112	0.000	7.73E-05
	6	0.139	0.150	0.0125		5	0.002	0.002	0.0104		5	0.006	0.006	0.0113	0.000	7.73E-05
	12	0.161	0.176	0.0129		10	0.013	0.013	0.0105		10	0.050	0.051	0.0118	0.003	7.76E-05
	30	0.179	0.197	0.0131		30	0.019	0.019	0.0106		30	0.281	0.330	0.0156	0.029	7.95E-05
	60	0.186	0.206	0.0133		60	0.110	0.117	0.0117		60	0.300	0.356	0.0160	0.173	9.19E-05
	90	0.189	0.209	0.0133		90	0.126	0.134	0.0119		90	0.305	0.363	0.0161	0.186	9.31E-05
	120	0.189	0.209	0.0133		120	0.096	0.101	0.0115		120	0.299	0.356	0.0160	0.189	9.34E-05
	180	0.196	0.219	0.0134		180	0.201	0.224	0.0130		160	0.325	0.393	0.0166	0.186	9.31E-05
	240	0.197	0.220	0.0134		240	0.201	0.224	0.0130		240	0.325	0.393	0.0166	0.203	9.47E-05
	300	0.198	0.220	0.0135		290	0.165	0.181	0.0125		300	0.350	0.431	0.0172	0.204	9.47E-05
2	0	0.000	0.000	0.0108	6b	0	0.000	0.000	0.0107	9R	0	0.000	0.000	0.0103		7.62E-05
	1	0.232	0.265	0.0141		1	0.015	0.015	0.0109		2	0.000	0.000	0.0103	0.000	7.62E-05
	2	0.251	0.289	0.0144		2	0.026	0.027	0.0110		5	0.000	0.000	0.0103	0.000	7.62E-05
	5	0.239	0.273	0.0142		5	0.110	0.117	0.0120		9	0.003	0.003	0.0103	0.000	7.62E-05
	10	0.361	0.448	0.0169		10	0.095	0.100	0.0118		14	0.006	0.006	0.0104	0.007	7.68E-05
	30	0.348	0.428	0.0166		30	0.086	0.090	0.0117		20	0.013	0.013	0.0104	0.015	7.74E-05
	60	0.466	0.627	0.0202		60	0.304	0.362	0.0154		30	0.027	0.028	0.0106	0.030	7.85E-05
	90	0.521	0.736	0.0225		90	0.241	0.275	0.0141		60	0.010	0.054	0.0109	0.065	8.14E-05
	120	0.531	0.758	0.0230		180	0.329	0.400	0.0160		90	0.059	0.061	0.0110	0.130	8.69E-05
	180	0.557	0.815	0.0244		240	0.325	0.393	0.0159		120	0.064	0.066	0.0110	0.147	8.83E-05
	240	0.616	0.958	0.0281		290	0.341	0.417	0.0163		160	0.053	0.054	0.0109	0.160	8.95E-05
											240	0.053	0.055	0.0109	0.130	8.69E-05
3	0	0.000	0.000	0.0108	7b	0	0.000	0.000	0.0111	10	0	0.000	0.000	0.0112		7.81E-05
	1	0.326	0.395	0.0160		1	0.045	0.046	0.0116		1	0.193	0.214	0.0139	0.151	9.09E-05
	2	0.433	0.568	0.0190		2	0.233	0.266	0.0145		2	0.140	0.151	0.0130	0.160	9.17E-05
	5	0.454	0.605	0.0196		5	0.296	0.350	0.0158		5	0.087	0.091	0.0123	0.178	9.34E-05
	10	0.549	0.796	0.0239		10	0.263	0.306	0.0151		10	0.175	0.192	0.0136	0.152	9.10E-05
	30	0.556	0.813	0.0243		30	0.350	0.431	0.0171		30	0.183	0.203	0.0137	0.199	9.54E-05
	60	0.652	1.057	0.0311		60	0.376	0.471	0.0178		60	0.241	0.276	0.0147	0.229	9.83E-05
	90	0.662	1.085	0.0619		90	0.389	0.493	0.0182		90	0.337	0.411	0.0169	0.286	1.04E-04
	120	0.699	1.200	0.0358		120	0.422	0.549	0.0192		120	0.325	0.393	0.0166	0.287	1.04E-04
	180	0.715	1.255	0.0379		180	0.430	0.562	0.0195		160	0.402	0.515	0.0187	0.278	1.03E-04
	240	0.744	1.363	0.0422		225	0.448	0.594	0.0201		240					
4	0	0.000	0.000	0.04	8b	0	0.000	0.000	0.0108	11	0	0.000	0.000	0.0112		7.53E-05
	1	0.954	3.086	0.85		1	0.621	0.971	0.0286		1	0.119	0.127	0.0127	0.242	9.59E-05
	2	0.976	3.713	1.59		2	0.800	1.612	0.0542		2	0.118	0.125	0.0127	0.164	8.87E-05
	4	0.986	4.287	2.82		4	0.950	2.996	0.2165		5	0.082	0.086	0.0122	0.200	9.19E-05
	7	0.994	5.084	6.25		7	0.987	4.336	0.8264		10	0.126	0.135	0.0128	0.187	9.08E-05
	10	0.997	5.659	11.11		13	0.992	4.841	1.3699		30	0.213	0.240	0.0142	0.240	9.57E-05
	20	0.998		20.00		20	0.995	5.240	2.0408		60	0.322	0.388	0.0165	0.277	9.93E-05
						30	0.995	5.348	2.2727		90	0.484	0.662	0.0217	0.287	1.00E-04
4R	0	0.000	0.000	0.011		60	0.999	7.052	12.5000		120	0.429	0.560	0.0196	0.284	1.00E-04
	1	0.568	0.840	0.03							180	0.528	0.751	0.0237	0.284	9.99E-05
	2	0.702	1.211	0.04							240	0.507	0.707	0.0227	0.286	1.00E-04
	4	0.847	1.875	0.07						11R	0	0.000	0.000	0.0112		8.02E-05
	6	0.904	2.340	0.11							1	0.088	0.092	0.0123	0.181	9.62E-05
	8	0.951	3.022	0.22							2	0.096	0.100	0.0124	0.179	9.60E-05
	11	0.977	3.763	0.47							5	0.113	0.120	0.0126	0.177	9.58E-05
	15	0.992	4.816	1.33							10	0.146	0.158	0.0131	0.188	9.69E-05
	27	0.999	7.524	20.00							20	0.215	0.242	0.0143	0.214	9.94E-05
											30	0.282	0.332	0.0156	0.236	1.02E-04
											60	0.344	0.422	0.0171	0.248	1.03E-04
					11avg	0	0.000		0.011		120	0.417	0.540	0.0192	0.237	1.02E-04
						1	0.103	0.109	0.012							
						2	0.107	0.113	0.013	12	0	0.000		0.0112		7.84E-05
						5	0.098	0.103	0.012		1	0.682	1.146	0.0352	0.257	1.01E-04
						10	0.136	0.146	0.013		2	0.822	1.726	0.0629	0.364	1.13E-04
						30	0.248	0.286	0.014		3	0.860	1.967	0.0800	0.212	9.68E-05
						60	0.333	0.405	0.016		4	0.893	2.235	0.1046	0.166	9.25E-05
						120	0.423	0.550	0.019		6	0.931	2.673	0.1621	0.216	9.72E-05
											7	0.946	2.913	0.2062	0.240	9.98E-05
											10	0.901	3.234	0.2841	0.245	1.00E-04
											15	0.970	3.518	0.3774	0.259	1.02E-04
											20	0.978	3.825	0.5128	0.247	1.00E-04
											30	0.983	4.084	0.6645	0.292	1.05E-04
											60	0.998	6.458	7.1429	0.195	9.53E-05

3. Comparison of pseudo first order and second order models over middle period

Temperature	ionic 95 initial	ionic 95 middle	ionic 80 initial	ionic 80 middle	ionic 50 initial	ionic 50 middle	substitution 95 initial	substitution 95 middle	substitution 60 initial	substitution 60 middle	substitution 50 initial	substitution 50 middle	co-precipitation 95 initial	co-precipitation 95 middle	co-precipitation 80 initial	co-precipitation 80 middle	co-precipitation 50 initial	co-precipitation 50 middle	ionic 150 initial	ionic 150 middle	substitution 150 initial	substitution 150 middle	co-pptn 150 initial	co-pptn 150 middle 1sr order	co-pptn 150 middle 2nd order
Measured k1 initial and middle	8.31E-01	0.00153	4.21E-01	1.17E-03	9.29E-02	2.06E-04	4.55E-02	2.10E-03	1.46E-02	1.79E-03	2.08E-03	1.12E-03	4.09E-01	2.66E-03	3.04E-01	2.14E-03	3.24E-01	5.51E-04	8.40E-01	0.284	9.71E-01	0.564	1.15E+00	0.236	0.00
k1 used adapted to fit data	8.31E-01	0.00153	4.21E-01	8.18E-04	9.29E-02	2.08E-04	1.20E-01	2.10E-03	1.46E-02	1.79E-03	2.08E-03	1.12E-03	4.09E-01	2.66E-03	3.04E-01	2.14E-03	3.24E-01	5.51E-04	8.40E-01	0.284	9.71E-01	0.564	1.10E+00	0.236	0.1800
[Rh]0 mg/l	93	93	93	93	93	93	90.0	90.0	93.4	93.4	96.2	96.2	89.3	89.3	89.3	89.3	97.0	97.0	93	93	93	93	93	93	93
[Rh]0 pseudo (measured)		40.4		49.2		76.9		66.7		86.8		95.2		53.6		65.9		59.6		32.4		35.1		17.8	92.6
Shift time	0	1.00	0	1.5	0	2.0	0	2.5	0	5	0	5	0	1.25	0	1.00	0	1.5	0	1.25	0	1.00	0	1.50	1.7
Actual Time (mn)	conversion																		conversion						
0	0.01		0.00		0.00		0.00		0.00		0.00		0.00		0.00		0.00		0.01		0.01		0.01		
0.2	0.15		0.08		0.02		0.02		0.00		0.00		0.08		0.06		0.06		0.15		0.18		0.20		
0.4	0.28		0.15		0.04		0.66		0.01		0.00		0.15		0.11		0.12		0.29		0.32		0.36		
0.6	0.39		0.22		0.06		0.07		0.01		0.00		0.22		0.17		0.18		0.40		0.44		0.48		
0.8	0.49		0.29		0.07		0.09		0.01		0.00		0.28		0.22		0.23		0.49		0.54		0.59		
1	0.56	0.564	0.34		0.09		0.11		0.01		0.00		0.34		0.26	0.262	0.23		0.57	0.62	0.62		0.67		
1.25		0.564	0.41		0.11		0.14		0.02		0.00		0.40	0.400		0.262	0.33		0.65	0.65	0.67		0.75		
1.5		0.565	0.47	0.468	0.13		0.16		0.02		0.00			0.401		0.263	0.39	0.385		0.67	0.71		0.81	0.81	
1.75		0.565		0.468	0.15		0.19		0.03		0.00			0.401		0.263		0.385		0.70	0.75			0.82	0.00
2		0.565		0.468	0.17	0.170	0.21		0.03		0.00			0.401		0.263		0.385		0.72	0.78			0.83	0.80
2.25		0.566		0.469		0.170	0.24		0.03		0.00			0.402		0.264		0.385		0.74	0.81			0.84	0.89
2.5		0.565		0.469		0.170	0.269	0.259	0.04		0.01			0.402		0.264		0.386		0.75	0.84			0.85	0.92
3		0.566		0.469		0.170		0.260	0.04		0.01			0.403		0.265		0.386		0.79	0.88			0.87	0.95
4		0.566		0.469		0.170		0.262	0.06		0.01			0.405		0.267		0.386		0.84	0.93			0.89	0.97
5		0.567		0.470		0.170		0.263	0.07	0.071	0.01	0.010		0.406		0.268		0.386		0.88	0.96			0.92	0.98
6		0.568		0.470		0.170		0.265		0.072		0.011		0.408		0.270		0.387		0.91	0.98			0.95	0.98
7		0.568		0.471		0.170		0.266		0.074		0.013		0.409		0.271		0.387		0.93	0.99			0.95	0.98
8		0.569		0.471		0.171		0.266		0.076		0.014		0.411		0.273		0.387		0.95	0.99			0.96	0.99
9		0.570		0.471		0.171		0.269		0.077		0.015		0.412		0.274		0.388		0.96	1.00			0.97	0.99
10		0.570		0.472		0.171		0.271		0.079		0.016		0.414		0.276		0.388		0.97	1.00			0.97	0.99
15		0.573		0.474		0.172		0.278		0.087		0.021		0.422		0.284		0.390		0.99	1.00			0.99	0.98
20		0.577		0.476		0.173		0.286		0.095		0.027		0.429		0.291		0.391		1.00	1.00			1.00	0.99
25		0.580		0.478		0.174		0.293		0.103		0.032		0.437		0.299		0.393		1.00	1.00			1.00	0.99
30		0.583		0.480		0.174		0.301		0.111		0.038		0.444		0.306		0.395		1.00	1.00			1.00	0.99
35		0.586		0.483		0.175		0.308		0.119		0.043		0.452		0.314		0.396		1.00	1.00			1.00	0.99
40		0.589		0.486		0.176		0.315		0.127		0.049		0.459		0.321		0.398		1.00	1.00			1.00	0.99
45		0.593		0.487		0.177		0.323		0.135		0.054		0.466		0.328		0.400		1.00	1.00			1.00	0.99
50		0.595		0.489		0.178		0.330		0.142		0.059		0.473		0.335		0.401		1.00	1.00			1.00	0.99
55		0.599		0.491		0.179		0.337		0.150		0.064		0.480		0.342		0.403		1.00	1.00			1.00	0.99
60		0.602		0.493		0.180		0.344		0.158		0.070		0.487		0.349		0.405		1.00	1.00			1.00	0.99
65		0.605		0.495		0.180		0.350		0.165		0.075		0.494		0.356		0.406		1.00	1.00			1.00	0.99
70		0.608		0.497		0.181		0.357		0.172		0.080		0.500		0.363		0.408		1.00	1.00			1.00	0.99
75		0.611		0.498		0.182		0.364		0.180		0.085		0.507		0.370		0.410		1.00	1.00			1.00	0.99
80		0.614		0.501		0.183		0.371		0.187		0.090		0.513		0.376		0.411		1.00	1.00			1.00	0.99
85		0.617		0.503		0.184		0.377		0.194		0.095		0.520		0.383		0.413		1.00	1.00			1.00	0.99
90		0.620		0.505		0.185		0.384		0.202		0.100		0.526		0.390		0.414		1.00	1.00			1.00	0.99
95		0.622		0.507		0.185		0.390		0.209		0.106		0.532		0.396		0.416		1.00	1.00			1.00	0.99
100		0.625		0.509		0.186		0.397		0.216		0.111		0.539		0.403		0.418		1.00	1.00			1.00	0.99
105		0.628		0.511		0.187		0.403		0.223		0.116		0.545		0.409		0.419		1.00	1.00			1.00	0.99
110		0.631		0.513		0.188		0.409		0.230		0.120		0.551		0.415		0.421		1.00	1.00			1.00	0.99
115		0.634		0.515		0.189		0.415		0.236		0.125		0.557		0.421		0.422		1.00	1.00			1.00	0.99
120		0.637		0.517		0.190		0.421		0.243		0.130		0.562		0.427		0.424		1.00	1.00			1.00	0.99
125		0.639		0.519		0.191		0.428		0.250		0.135		0.568		0.434		0.426		1.00	1.00			1.00	1.00
130		0.642		0.521		0.191		0.434		0.257		0.140		0.574		0.440		0.427		1.00	1.00			1.00	1.00
135		0.645		0.523		0.192		0.439		0.263		0.145		0.580		0.446		0.429		1.00	1.00			1.00	1.00
140		0.647		0.525		0.193		0.445		0.270		0.150		0.585		0.451		0.430		1.00	1.00			1.00	1.00
145		0.650		0.527		0.194		0.451		0.276		0.154		0.591		0.457		0.432		1.00	1.00			1.00	1.00
150		0.653		0.529		0.195		0.457		0.283		0.159		0.595		0.463		0.434		1.00	1.00			1.00	1.00
155		0.656		0.531		0.196		0.463		0.289		0.164		0.601		0.469		0.435		1.00	1.00			1.00	1.00
160		0.658		0.533		0.196		0.468		0.295		0.169		0.607		0.474		0.437		1.00	1.00			1.00	1.00
165		0.661		0.535		0.197		0.474		0.302		0.173		0.612		0.480		0.438		1.00	1.00			1.00	1.00
170		0.663		0.537		0.198		0.479		0.308		0.178		0.617		0.485		0.440		1.00	1.00			1.00	1.00
175		0.666		0.539		0.199		0.485		0.314		0.182		0.622		0.491		0.441		1.00	1.00			1.00	1.00
180		0.668		0.540		0.200		0.490		0.320		0.187		0.627		0.496		0.443		1.00	1.00			1.00	1.00
185		0.671		0.542		0.201		0.496		0.326		0.192		0.632		0.502		0.444		1.00	1.00			1.00	1.00
190		0.673		0.544		0.201		0.501		0.332		0.196		0.637		0.507		0.446		1.00	1.00			1.00	1.00
195		0.676		0.546		0.202		0.506		0.338		0.201		0.641		0.512		0.447		1.00	1.00			1.00	1.00
200		0.678		0.548		0.203		0.511		0.344		0.206		0.646		0.517		0.449		1.00	1.00			1.00	1.00
205		0.681		0.550		0.204		0.516		0.350		0.210		0.651		0.523		0.450		1.00	1.00			1.00	1.00
210		0.683		0.552		0.205		0.521		0.356		0.214		0.655		0.528		0.452		1.00	1.00			1.00	1.00
215		0.686		0.553		0.206		0.526		0.361		0.218		0.660		0.533		0.453		1.00	1.00			1.00	1.00
220		0.688		0.555		0.206		0.531		0.367		0.223		0.664		0.538		0.455		1.00	1.00			1.00	1.00
225		0.690		0.557		0.207		0.536		0.373		0.227		0.669		0.542		0.456		1.00	1.00			1.00	1.00
230		0.693		0.559		0.208		0.541		0.378		0.231		0.673		0.547		0.458		1.00	1.00			1.00	1.00
235		0.695		0.561		0.209		0.546		0.384		0.236		0.678		0.552		0.459		1.00	1.00			1.00	1.00
240		0.697		0.562		0.210		0.551		0.389		0.240		0.682		0.557		0.461		1.00	1.00			1.00	1.00
245		0.700		0.564		0.210		0.555		0.395		0.244		0.686		0.562		0.462		1.00	1.00			1.00	1.00
250		0.702		0.566		0.211		0.560		0.400		0.249		0.690		0.566		0.464		1.00	1.00			1.00	1.00
255		0.704		0.568		0.212		0.565		0.406		0.253		0.694		0.571		0.465		1.00	1.00			1.00	1.00
260		0.706		0.570		0.213		0.569		0.411		0.257		0.698		0.575		0.467		1.00	1.00			1.08	1.00
265		0.709		0.571		0.214		0.574		0.416		0.261		0.702		0.580		0.468		1.00	1.00			1.60	1.00
270		0.711		0.573		0.215		0.578		0.421		0.265		0.706		0.584		0.470		1.00	1.00			1.08	1.00
275		0.713		0.575		0.215		0.582		0.426		0.269		0.710		0.589		0.471		1.00	1.00			1.00	1.00
280		0.715		0.577		0.216		0.587		0.431		0.273		0.714		0.593		0.473		1.00	1.00			1.00	1.00
285		0.717		0.578		0.217		0.591		0.436		0.277		0.718		0.598		0.474		1.00	1.00			1.00	1.00
290		0.720		0.580		0.218		0.595		0.441		0.282		0.721		0.602		0.476		1.00	1.00			1.00	1.00
295		0.722		0.582		0.219		0.600		0.446		0.286		0.725		0.606		0.477		1.00	1.00			1.00	1.00
300		0.724		0.583		0.219		0.604		0.451		0.290		0.729		0.610		0.478		1.00	1.00			1.00	1.00
305		0.726		0.585		0.220		0.608		0.456		0.294		0.732		0.614		0.480		1.00	1.00			1.00	1.00
310		0.728		0.587		0.221		0.612		0.461		0.297		0.736		0.618		0.481		1.00	1.00			1.00	1.00
315		0.730		0.589		0.222		0.616		0.466		0.301		0.739		0.622		0.483		1.00	1.00			1.00	1.00
320		0.732		0.590		0.223		0.620		0.470		0.305		0.743		0.627		0.484		1.00	1.00			1.00	1.00
325		0.734		0.592		0.223		0.624		0.476		0.309		0.746		0.630		0.486		1.00	1.00			1.08	1.00
330		0.736		0.594		0.224		0.628		0.480		0.313		0.749		0.634		0.487		1.00	1.00			1.00	1.00
335		0.738		0.595		0.225		0.632		0.484		0.317		0.753		0.638		0.488		1.00	1.00			1.00	1.00
340		0.740		0.597		0.226		0.636		0.489		0.321		0.756		0.642		0.490		1.00	1.00			1.00	1.00
345		0.742		0.598		0.227		0.640		0.494		0.325		0.759		0.646		0.491		1.00	1.00			1.00	1.00
350		0.744		0.600		0.228		0.643		0.498		0.328		0.762		0.650		0.493		1.00	1.00			1.00	1.00
355		0.746		0.602		0.228		0.647		0.503		0.332		0.766		0.653		0.494		1.00	1.00			1.00	1.00
360		0.748		0.603		0.229		0.651		0.507		0.336		0.769		0.657		0.495		1.00	1.00			1.00	1.00
365		0.750		0.605		0.230		0.655		0.511		0.340		0.772		0.661		0.497		1.00	1.00			1.00	1.00
370		0.752		0.607		0.231		0.658		0.516		0.343		0.775		0.664		0.498		1.00	1.00			1.60	1.00
375		0.754		0.608		0.232		0.662		0.520		0.347		0.778		0.668		0.500		1.00	1.00			1.08	1.00
380		0.756		0.610		0.232		0.665		0.524		0.351		0.781		0.671		0.501		1.00	1.00			1.00	1.00
385		0.757		0.611		0.233		0.669		0.529		0.354		0.783		0.675		0.502		1.00	1.00			1.00	1.00
390		0.759		0.613		0.234		0.672		0.533		0.358		0.786		0.678		0.504		1.00	1.00			1.00	1.00
395		0.761		0.614		0.235		0.676		0.537		0.361		0.789		0.682		0.505		1.00	1.00			1.00	1.00
400		0.763		0.616		0.236		0.679		0.541		0.365		0.792		0.685		0.506		1.00	1.00			1.00	1.00
405		0.765		0.618		0.236		0.682		0.545		0.369		0.795		0.689		0.508		1.00	1.00			1.00	1.00
410		0.767		0.619		0.237		0.686		0.549		0.372		0.797		0.692		0.509		1.00	1.00			1.00	1.00
415		0.768		0.621		0.238		0.689		0.553		0.376		0.800		0.696		0.511		1.00	1.00			1.00	1.00
420		0.770		0.622		0.239		0.692		0.557		0.379		0.803		0.698		0.512		1.00	1.00			1.00	1.00

4. Modelling rate constant to Arrhenius relationship

Using initial rates to fit Arrhenius constants over 50 – 150 °C (E_a and k_o)

Temp	Ionic	Substitution		Co-precipitation					
	A		B		C				
1/T	ln(k)	1/T	ln(k)	1/T	ln(k)	Statistic	A	B	C
						N	4	4	5
0.0031	-2.37593	0.0031	-6.1748	0.0031	-6.9073	Σ X	0.01	0.01	0.01
0.0028	-0.86511	0.0028	-4.2234	0.0031	-7.6004	Mean X	0.00	0.00	0.00
0.0027	-0.18555	0.0027	-3.0896	0.0028	-1.1920	Σ Y	-3.60	-13.52	-16.46
0.0024	-0.17467	0.0024	-0.0290	0.0027	-0.8941	Mean Y	-0.9003	-3.3792	-3.2915
						Σ x^2	0.00	0.00	0.00
				0.0024	0.1363	Σ y^2	3.2161	19.8358	53.5451
						Σ xy	-0.0008	-0.0023	-0.0040
						Pool s^2			
						Ao =	7.17E+00	19.9074	2.69E+01
						V(Ao)=	0.00E+00	0.0000	0.00E+00
						A1 =	-2.932E+03	-8460	-1.071E+04
						V(A1)=	0.00E+00	0.0000	0.00E+00
						R(A) =	-8.60E-01	-9.99E-01	-8.91E-01
						t(A) =	-2.3824	-30.2343	-3.4029
						D.f.(A) =	2	2	3
						p(t{A}) =	0.1401	0.0011	0.0424

Using initial rates to fit Arrhenius constants over 50 – 95 °C

Temp	Ionic	Substitution		Co-precipitation					
	A		B		C				
1/T	ln(k)	1/T	ln(k)	1/T	ln(k)	Statistic	A	B	C
						N	3	3	4
0.0031	-2.37593	0.0031	-6.1748	0.0031	-6.9073	Σ X	0.01	0.01	0.01
0.0028	-0.86511	0.0028	-4.2234	0.0031	-7.6004	Mean X	0.00	0.00	0.00
0.0027	-0.18555	0.0027	-3.0896	0.0028	-1.1920	Σ Y	-3.43	-13.49	-16.59
				0.0027	-0.8941	Mean Y	-1.1422	-4.4959	-4.1484
						Σ x^2	0.00	0.00	0.00
						Σ y^2	2.5140	4.8708	38.8582
						Σ xy	-0.0004	-0.0006	-0.0020
						Pool s^2			
						Ao =	1.55E+01	18.6281	4.96E+01
						V(Ao)=	0.00E+00	0.0000	0.00E+00
						A1 =	-5.8E+03	-8023	-1.833E+04
						V(A1)=	0.00E+00	0.0000	0.00E+00
						R(A) =	-1.00E+00	-9.98E-01	-9.75E-01
						t(A) =	-173.2295	-14.3352	-6.1432
						D.f.(A) =	1	1	2
						p(t{A}) =	0.0037	0.0443	0.0255

Using initial rates to fit Arrhenius constants over 95 – 150 °C

Temp	Ionic	Substitution		Co-precipitation					
	A		B		C		A	B	C
1/T	ln(k)	1/T	ln(k)	1/T	ln(k)	Statistic			
						N	2	2	2
						Σ X	0.01	0.01	0.01
						Mean X	0.00	0.00	0.00
0.0027	-0.18555	0.0027	-3.0896	0.0027	-0.8941	Σ Y	-0.36	-3.12	-0.76
0.0024	-0.17467	0.0024	-0.0290	0.0024	0.1363	Mean Y	-0.1801	-1.5593	-0.3789
						Σ x^2	0.00	0.00	0.00
						Σ y^2	0.0001	4.6836	0.5308
						Σ xy	0.0000	-0.0005	-0.0002
						Pool s^2			
						Ao =	-1.02E-01	20.4490	7.03E+00
						V(Ao)=	0.00E+00	0.0000	0.00E+00
						A1 =	-3.077E+01	-8662	-2.916E+03
						V(A1)=	0.00E+00	0.0000	0.00E+00
						R(A) =	-1.00E+00	-1.00E+00	-1.00E+00
						t(A) =	0.0000	0.0000	0.0000
						D.f.(A) =	0	0	0
						p(t{A}) =	#NUM!	#NUM!	#NUM!

Arrhenius constants fit over 50 – 150 °C for middle period using pseudo kinetics

Temp	Ionic		Substitution		Co-precipitation					
	A		B		C					
1/T	ln(k)	1/T	ln(k)	1/T	ln(k)	Statistic		A	B	C
						N		4	4	4
0.0031	0.00021	0.0031	0.0011	0.0031	0.0006	ΣX		0.01	0.01	0.01
0.0028	0.00117	0.0028	0.0018	0.0028	0.0021	Mean X		0.00	0.00	0.00
0.0027	0.00153	0.0027	0.0021	0.0027	0.0027	ΣY		0.29	0.57	0.24
0.0024	0.28351	0.0024	0.5639	0.0024	0.2364	Mean Y		0.0716	0.1422	0.0604
						Σx^2		0.00	0.00	0.00
						Σy^2		0.0599	0.2371	0.0413
						Σxy		-0.0001	-0.0002	-0.0001
						Pool s^2				
						Ao =		1.17E+00	2.3192	9.73E-01
						V(Ao)=		0.00E+00	0.0000	0.00E+00
						A1 =		-3.982E+02	-791	-3.315E+02
						V(A1)=		0.00E+00	0.0000	0.00E+00
						R(A) =		-8.55E-01	-8.54E-01	-8.57E-01
						t(A) =		-2.3328	-2.3198	-2.3523
						D.f.(A) =		2	2	2
						p(t|A|) =		0.1449	0.1462	0.1430

Arrhenius constants fit over 50 – 95 °C for middle period using pseudo kinetics

	Ionic		Substitution		Co-precipitation					
	A		B		C					
1/T	ln(k)	1/T	ln(k)	1/T	ln(k)	Statistic		A	B	C
						N		3	3	3
0.0031	0.00021	0.0031	0.0011	0.0031	0.0006	ΣX		0.01	0.01	0.01
0.0028	0.00117	0.0028	0.0018	0.0028	0.0021	Mean X		0.00	0.00	0.00
0.0027	0.00153	0.0027	0.0021	0.0027	0.0027	ΣY		0.00	0.01	0.01
						Mean Y		0.0010	0.0017	0.0018
						Σx^2		0.00	0.00	0.00
						Σy^2		0.0000	0.0000	0.0000
						Σxy		0.0000	0.0000	0.0000
						Pool s^2				
						Ao =		1.11E-02	0.0091	1.80E-02
						V(Ao)=		0.00E+00	0.0000	0.00E+00
						A1 =		-3.51E+00	-3	-5.642E+00
						V(A1)=		0.00E+00	0.0000	0.00E+00
						R(A) =		-9.99E-01	-1.00E+00	-9.98E-01
						t(A) =		-26.8553	-45.7829	-15.9146
						D.f.(A) =		1	1	1
						p(t|A|) =		0.0237	0.0139	0.0399

Arrhenius constants fit over 95 – 150 °C for middle period using pseudo kinetics

Ionic		Substitution		Co-precipitation		Statistic			
	A		B		C		A	B	C
1/T	ln(k)	1/T	ln(k)	1/T	ln(k)				
						N	2	2	2
						Σ X	0.01	0.01	0.01
						Mean X	0.00	0.00	0.00
0.0027	0.00153	0.0027	0.0021	0.0027	0.0027	Σ Y	0.29	0.57	0.24
0.0024	0.28351	0.0024	0.5639	0.0024	0.2364	Mean Y	0.1425	0.2830	0.1196
						Σ x^2	0.00	0.00	0.00
						Σ y^2	0.0398	0.1578	0.0273
						Σ xy	0.0000	-0.0001	0.0000
						Pool s^2			
						Ao =	2.17E+00	4.3243	1.80E+00
						V(Ao)=	0.00E+00	0.0000	0.00E+00
						A1 =	-7.99E+02	-1591	-6.622E+02
						V(A1)=	0.00E+00	0.0000	0.00E+00
						R(A) =	-1.00E+00	-1.00E+00	-1.00E+00
						t(A) =	#NUM!	#NUM!	#NUM!
						D.f.(A) =	0	0	0
						p(t{A}) =	#NUM!	#NUM!	#NUM!

Cu precipitation: Arrhenius fit for co-precipitation initial rate constant over 50 – 150 °C

50 - 150 oC		50 - 95 oC		95 - 150 oC					
Temp	recipitation	Co-precipitation		Co-precipitation					
	A		B		C				
1/T	ln(k)	1/T	ln(k)	1/T	ln(k)	Statistic	A	B	C
						N	4	3	2
						Σ X	0.01	0.01	0.01
0.0031	-7.60040	0.0031	-7.6004			Mean X	0.00	0.00	0.00
0.0028	-1.83774	0.0028	-1.8377			Σ Y	-12.64	-11.31	-3.21
0.0027	-1.86890	0.0027	-1.8689	0.0027	-1.8689	Mean Y	-3.1612	-3.7690	-1.6034
0.0024	-1.33790			0.0024	-1.3379	Σ x^2	0.00	0.00	0.00
						Σ y^2	26.4525	22.0198	0.1410
						Σ xy	-0.0022	-0.0012	-0.0001
						Ao =	1.85E+01	43.2154	2.21E+00
						V(Ao)=	0.00E+00	0.0000	0.00E+00
						A1 =	-7.85E+03	-16302	-1.50E+03
						V(A1)=	0.00E+00	0.0000	0.00E+00
						R(A) =	-8.03E-01	-9.53E-01	-1.00E+00
						t(A) =	-1.9058	-3.1562	0.0000
						D.f.(A) =	2	1	0
						p(t{A}) =	0.1969	0.1953	#NUM!

5. Rh Modelling data

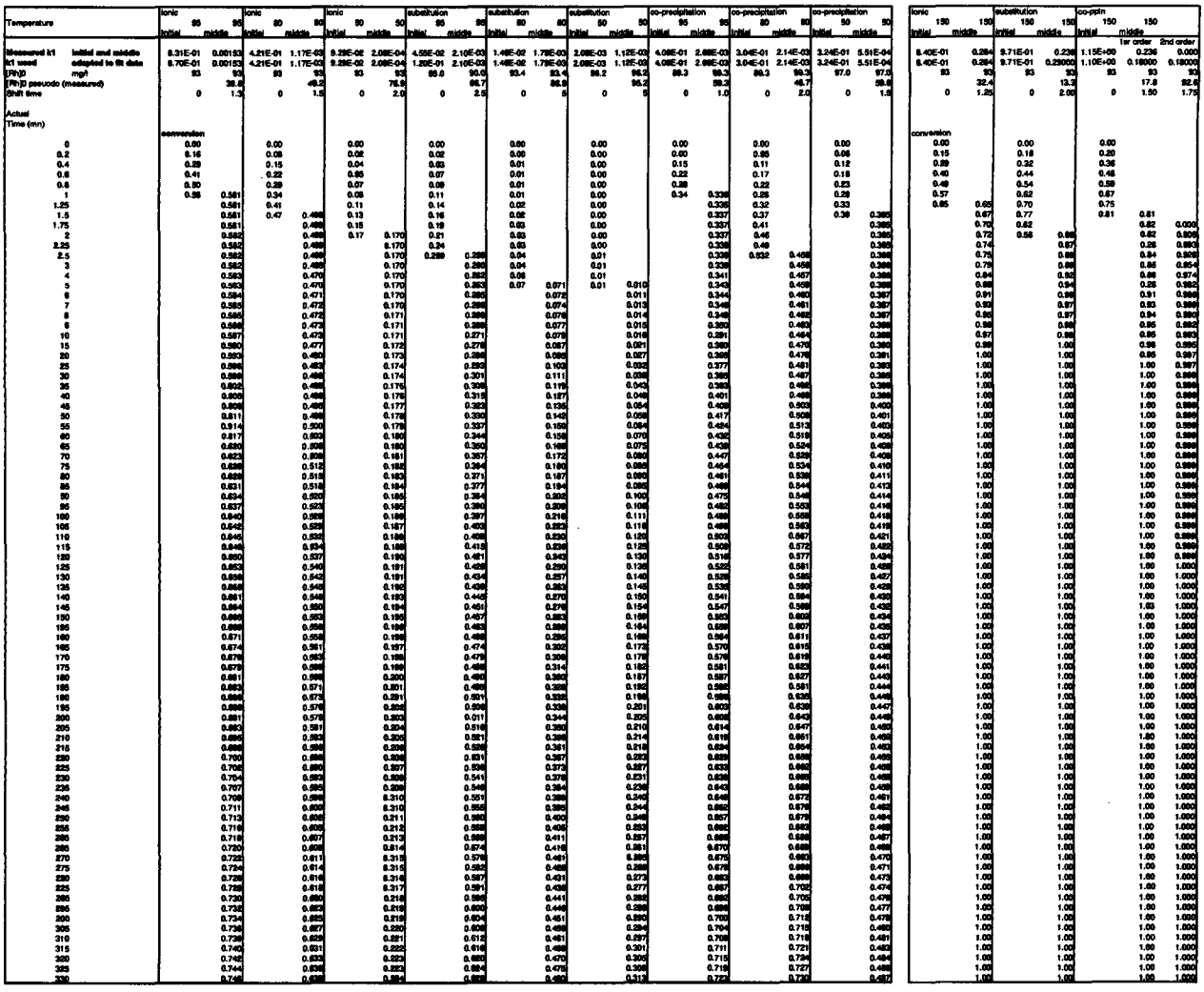

Logarithmic fit constants of X_{Rh} vs time

	X_{Rh} = a ln(t) + b	
	a	b
#1	0.021	0.0939
#2	0.027	0.383
#3	0.019	0.558
#4R	0.146	0.627
#5b	0.053	-0.112
#6b	0.060	-0.012
#7b	0.060	0.135
#8b	0.148	0.676
#9R	0.023	-0.051
#10	0.032	0.241
#11	0.043	0.354
#11R	0.069	0.187
#12	0.060	0.81

B.7. Individual and comparative results using solution basis

#1, 9 and 9R are calculated on solids basis due to excessive post-precipitation.

Table B8.1: Summary of Rh precipitation extent for all reaction systems (solution basis)

Test #	Temp	Rh precipitation extent [%]							
	°C	1 min	2 min	~5 min	10 min	30 min	60 min	120 min	240 min
Ionic system (solids basis)									
#1 *	50	9	10	14	16	18	19	19	20
#2	80	23	25	24	36	35	47	53	62
#3	95	33	43	45	55	56	65	70	74
#4R	150	57	70	85	97	100	100	100	100
Substitution system (solution basis)									
#5b	50	0	0	0	1	2	11	10	17
#6b	80	1	3	11	9	9	30	33	34
#7b	95	4	23	30	26	35	38	42	45
#8b	150	62	80	95	99	100	100	100	100
Co-precipitation system (solids basis)									
#9 *	50	0	0	1	5	28	30	30	30
#9R *	50	0	0	0	0	3	5	6	5
#10	80	19	14	9	17	18	24	32	36
#11	95	12	14	8	13	21	32	43	51
#11R	95	9	10	11	15	28	34	42	NR
#12	150	68	82	89	96	98	100	100	100

Note: * profiles calculated using precipitated Rh in solids profile due to post precipitation in samples (see section 6.1.3)

Calculation of initial rate constant

	change in mmol	[Rh]/[Rh]o	-ln([Rh]/[TI	TIME	slope k measure	ln(k)	[S2O3(2-)] [CuS]o	k of rxn	ln k of rxn
1	0.08	0.91	0.09	1	0.093	-2.376	49.24	0.0019	-6.2727
2	0.21	0.77	0.26	1	0.265	-1.330	49.24	0.0054	-5.2266
3	0.29	0.67	0.40	1	0.395	-0.929	49.24	0.0080	-4.8255
4R	0.51	0.43	0.84	1	0.840	-0.175	49.24	0.0171	-4.0714
5b	0.00	1.00	0.00	1	0.002	-6.175	50.3	0.0000	-10.0926
6b	0.01	0.99	0.01	1	0.015	-4.223	50.3	0.0003	-8.1411
7b	0.04	0.96	0.05	1	0.046	-3.090	48.4	0.0009	-6.9696
8b	0.56	0.38	0.97	1	0.971	-0.029	50.3	0.0193	-3.9467
9	0.00	1.00	0.001	1	0.001	-6.907	45.7	0.0000	-10.7285
9R	0.00	1.00	0.00	2	0.001	-7.600	45.66	0.0000	-11.4216
10	0.17	0.88	0.13	1	0.127	-2.066	49.18	0.0026	-5.9612
11	0.10	0.88	0.13	1	0.127	-2.066	45.68	0.0028	-5.8874
11R	0.08	0.91	0.09	1	0.092	-2.389	45.66	0.0020	-6.2098
12	0.59	0.32	1.15	1	1.146	0.136	45.66	0.0251	-3.6849

Calculation of activation energy and frequency factor

Temp	Ionic		Sub				
1/T	ln(k)	1/T	ln(k)	Statistic	A: n	B: t	Total
				N	4	4	8
0.0031	-2.37593	0.0031	-6.1748	Σ X	0.01	0.01	0.022011417
0.0028	-1.32983	0.0028	-4.2234	Mean X	0.00	0.00	0.00
0.0027	-0.92876	0.0027	-3.0896	Σ Y	-4.81	-13.52	-18.3260
0.0024	-0.17467	0.0024	-0.0290	Mean Y	-1.2023	-3.3792	-2.2908
				Σ x^2	0.00	0.00	0.00
				Σ y^2	2.5245	19.8358	31.8382
				Σ xy	-0.0008	-0.0023	-0.0032
				Pool s^2			
				Ao =	6.98E+00	19.9167	
				V(Ao)=	0.00E+00	0.0000	
				A1 =	-2.98E+03	-8466.85	
				V(A1)=	0.00E+00	0.0000	
				R(A) =	-9.84E-01	t(A) =	-7.7933
				D.f.(A) =	2	p(t[A]) =	0.0161
				R(B) =	-9.99E-01	t(B) =	-30.2533
				D.f.(B) =	2	p(t[B]) =	0.0011
				ko	1.08E+03	4.46E+08	
				Ea (kJ)	25	70	

APPENDIX C – LITERATURE

Additional details and comments of key papers referenced:

Barken, V.Sh. and Greiver T,N. , *"Coprecipitation of platinum metals with iron hydroxide"*, Russian Journal of Inorganic Chemistry , 22 (8), 1977. Translated from Zhurnal Neorganicheskoi Khimii, 22, 2197-2203 , 1977.

Barken and Gravier studied the effect of pH, temperature, iron-metal ratio and contact of PGM co-precipitation with iron hydroxide in sulfate and sulfate-chloride solutions. Almost complete PGM co-precipitation occurred at specific conditions. Precipitation occurred through isomorphism, but complicated by the formation of hydroxosulfatoaquo- or hydroxochloroaquo- complexes. Iron (III) facilitates the extensive hydrolysis of all the PGMs, except Pt, thus Pt can be separated from the other PGMs through oxidation in the presence of Fe(III).

The Rhodium Removal Section in RBMR could be optimised by operating with $Fe(OH)_3$ alone at elevated temperature and eliminate the undesired sulphur addition.

Mc George, B. , *"Recovery of PGMs from MC Plant process liquors"*, Amplats Internal Refining Conference , RBMR Library, (2000).
(Edited Abstract)

Thioform, a mixture of sodium formate and sodium thiosulphate, removed Rhodium in base metal sulphate liquors from 10 – 30 mg/l down to 5 mg/l at 90 – 95 °C. At least 90 minutes reaction time is required for effective Rh removal. 1 – 5 % of the total Cu co-precipitates as a copper sulfide, and insignificant Ni and Fe precipitation occurs. This is a significant improvement on the caustic addition process that produced an average Rh concentration of 10 mg/l. Temperature has the dominant effect on PGM removal efficiency. Rh was reduced to 0 – 3 mg/l at 150 °C under a nitrogen atmosphere at half the atmospheric thioform requirement. Rh precipitation extent and selectivity decreased with gentle mixing when compared to excessive agitation (10 – 1100 rpm), showing mass transfer limitations could occur. PGM precipitation extent and selectivity was not improved by splitting the reagent addition into multiple additions. Precipitation kinetics increase significantly at elevated temperatures, where less than 1 minute is required to achieve 0.1 mg/l Rh at 170 °C. Thioform addition at atmospheric conditions was successfully retrofitted into the current Rh removal section and increased the first pass recovery substantially. A pipe reactor will improve Rh precipitation extent to obtain complete recovery from the Pressure Vessel Liquor stream.

Myasoedova, G.V., Malofeeva, O.P., Shvoeva, E.V., Illarionova, S.B., Savvin, S.B. and Zolotov. Yu. A. V.I. Vernadskii Institute of Geochemistry and Analytical Chemistry, Academy of Sciences of the USSR. Translated from Zhural Analiticheskoi Khimii, Vol. 32, No.4, pp. 645-649, (1977).

Myasoedova *et al.* (1977) developed a pre-concentration technique for group concentration of PGMs for subsequent analysis by instruments through the combined co-precipitation on CuS, thereby separating the PGMs from large amounts of Ni, Co, Fe, Ca, Mg, Al etc., followed by the CuS-PGM precipitate dissolution and separating the PGMs from the Cu by adsorbing the PGMs on a chelate resin. Rh and Ir precipitation was improved to 90% by using a mixed collector, namely, CuS and 2-mercaptobenzothiazole. If the solution to be analysed is low in Cu (<1 g/l) then Cu salt has to be added to bring it up to this level. Depending on the solution, only CuS co-precipitation or the sorption on a chelate could be used.

Pavlenko, L.I., Malofeeva, G.I., Simonova, L.V. and Andryyushchenko, O.Yu. V.I. Vernadskii Institute of Geochemistry and Analytical Chemistry, Academy of Sciences of the USSR. Translated from Zhural Analiticheskoi Khimii, Vol. 29, No.6, pp. 1122-1129, (1974).

Pavlenko *et al.* (1974) developed an analytical procedure for pre-concentrating PGMs from base metal sulphate solutions in chloride media containing low PGM concentration prior to analysis. Hydrogen sulfide previously used for sulfide carrier precipitation was replaced with thioacetamide (TAA) (2%) addition. Sulfuric acid was added to break down the PGM-TAA complexes. Cu in solution was added to provide CuS precipitation and the solution was boiled for 15 min to allow

coagulation of the precipitate. A large number of different inorganic sulfides exhibiting the opposite properties (acidic or basic) to the PGM sulfides were tested.

Pshenitsyn, N.K. and Prokof'yeva, Zhural Neoganicheskoi Khimii (J. of Inorganic Chem.), Vol. III. No.4, (1958), pp. 996-1001. English translation.

Pshenisyn and Prokof'yeva (1958) investigated the use of thiourea for qualitative separation of PGMs from solutions, particularly Rh and Ir. PGM complexing with thiourea occurred. Upon heating selective PGM sulfide precipitation occurred through hydrolysis at elevated temperatures between 120 –190 °C or in solution of concentrated sulfuric acid. Low concentrations of Fe, Ni and Se did not interfere with the analytical method, while Cu, Pb and Sn were partially co-precipitated.

Konig *et al.* from Degussa has patented a novel substituted thiourea, which acts as a selective bulk precipitant for PGMs, thus giving a clean precious metal concentrate for subsequent processing.

Roy, T.K., *"Preparing nickel and cobalt concentrates."*, Ind. Eng. Chem., 53 (1961): 559-566.

Roy (1961) studied the kinetics of Co and Ni precipitation in the development of a process using hydrogen sulfide. Roy showed the catalytic effect of seeding the Ni precipitation with finely powdered metallic Ni or Fe and recycled MeS product. The seeding effect was less pronounced at temperatures greater than 120 °C, but an explanation for this was not offered. It is probably due to more or faster primary nucleation occurring at elevated temperatures, thus negating the need for an initial seed. In the initial precipitation phase the reaction was independent of Ni concentration (zero order) and probably limited by the mass transfer of H_2S to the solution. After the bulk of the Ni and Co was precipitated, the reaction then switched to first order kinetics, and Roy suggested that it was probably limited by transfer of Ni^{2+} to the sulfide surface, because significantly faster kinetics was observed in the turbulent pipe reactor pilot plant compared to the initial, agitated batch reactor tests and 4-stage CSTR in series, where the same precipitation extent was achieved in the pipe reactor within 5 – 10 % of the residence time.

Shorikov, Yu. S., Orlov, A.M. and Kornyushina, S.N. , State scientific research and planning institute for the rear earth industry. , Translate from: Zhural Prikladnoi Khimii, Vol. 59, No.3, pp. 496-499, (1986).

Shorikov *et al.* (1986) investigated the sulfide precipitation of Rh, Ru and Ir from chloride solutions as containing 2-500 mg/l PGMs at 100 °C using sulfur dissolved in 1% caustic solution. The sulfur solution contained largely polysulfides (NaS_x) with 50 g sulfur per litre, which retained its activity for at least 3 weeks. Direct extraction of Ru into sulfide precipitate from a synthetic solution not containing base metals was 99.3 - 99.7 % for 60 – 90 min reaction time, 80 -100 °C operating temperature and S:Ru of 29 - 32 on molar basis. The initial and final terminal pH had a significant effect precipitation extent. The extraction extent increases significantly with increasing Ru concentration, though a terminal Ru concentration between 0.5 - 0.7 was achieved in all tests. Similar results were achieved over a wide range of chloride salt concentrations. Direct Rh precipitation maximum was 80%, while Ir was only 40%, which is in line with the decreasing solubilities: Ir_2S_3 > Rh_2S_3 > RuS_2. The transfer of PGMs to soluble thio salts (e.g. $[RuS_3]_n^{2-}$) is primarily a function of terminal pH, which in turn is a function of initial pH. Significant reduction in metal transfer to precipitate occurs if pH > 2-3 due to the complexing in solution. Acidification decomposes the thio salts, which precipitate sulfides and sulfur.

This critical paper highlights the fact that direct precipitation of PGMs to their sulfides does occur without the co-precipitation of base metal sulfides [there were no base metals present] and that the required terminal acid concentration is paramount to break down the thio-PGM complexes. This complexing with sulfide (or sulfites and thiosulfates if sodium thiosulfate is added) would have to be taken into consideration in the mechanism. Increasing the temperature would increase the decomposition rate of these complexes. Unfortunately, this acid also digests the thiosulphate to elemental sulphur. The reaction times were similar to that of PGM co-precipitation on CuS. Elemental S dissolved in 1% caustic should be considered as a possible reagent for Rh removal from PVL, as it most likely would be considerably cheaper than Na_2S or $Na_2S_2O_3$.

Additional references

References related to this study that were reviewed, but not referenced, are provided below:

General co-precipitation with sulfides

Kortly, S., and Sucha, L., *"Handbook of Chemical Equilabria in Analytical Chemistry."* Ellis Horwood, Chichester, UK (1985).

Williams, R., Yocom, P.N., and Stofko, F.S., *"Preparation and properties of spherical zinc sulfide particles."* J. Colloid Interface Sci., 106 (1985):388-398.

Copper sulfide precipitate

Shea, D., and Helz, G.R. , Geochemica et Cosmochimica Acta Vol. 52 p1815-1825, Pergamon Press, 1988.

Saito, S., Kishi, H., Nie, K. and Nakamaru, H, Physical review B, Vol.55, No.21 (June 1997).
Volkov, A.V.; Moskvina, M.A.; Volynskii, A.L.; Bakeev, N.F.; Polymer Science, Ser.A, Vol.40 No.9, 1998 p. 893-900.

Haram S.K., Mahadeshwar A.R. and Dixit S.G., Adsorption Science and technology, 1998, Vol.16 pp. 667-677.

Woods, R. , Yoon, R.H. , and Young, C.A. , *"Eh-pH diagrams for stable and metastable phases in the copper-sulphur-water system"*, Int. J. of Minerals Processing, 20 (1987) 109-120 , Elsevier Science Publishers B.V.

Young, C.A. , Dahlgren E.J. and Robins, R.G. , *"The solubility of copper sulfides under reducing conditions."*, Hydrometallurgy , 68 , p. 23-31 , 2003.

Chemistry and Thermodynamics

Shukla, S. K. and M. Lederer, *"The study of rhodium(III) complexes by paper electrophoresis and ion exchange chromatography: IV. The solution chemistry of rhodium sulphates"*, *Journal of the Less Common Metals, Volume 1, Issue 4, August 1959, Pages 255-262.*

Cabri, L.J. (editor), *Platinum-Group Elements: Mineralogy, Geology, Recovery*, CIM Special Vol. 23, Chapter 2.

Zhilyaev, A.N. and Fomina, T.A., *"Chemistry of the Platinum-Metal sulfate complexes"*, Russian J. of Coordination chemistry, Vol. 23. No.8, 1997, pp.525-542. Translated from Koordinatsionnaya Khimiya, Vol. 23. No.8, 1997, pp.563-581.

Krauss, F. and Umbach, H., Z. Anorg. Chem., 1929, vol. 180 p. 149. In: Zhilyaev, A.N. and Fomina, T.A., Russian J. of Coordination chemistry, Vol. 23. No.8, 1997, pp.525-542.

Reid, F.H., *Trans. Inst. Metal Finish.*, 1959, vol.36, p.74

Rhodes, E.C., *Chem. Ind.*, 1956, vol.75, p. 1292.

Bol'shakov, K.A., Sinitsyn, N.M., Borisov, V.V., and Borbat, V.F., *Dolk. Akad. Nauk USSR*, 1969, vol. 188, no.4, p. 815

Wagman D.D, Evans, W.H., Parker, V.B. Halow, I., Bailey, S.M. and Schumm, R.H. , *"Selected values of chemical thermodynamic properties"*, Technical note 270-4 , U.S. government printing office , 1969.

Barner, H.E. and Scheuerman, R.V. , Handbook on thermochemical data for compounds and aqueous species , Wiley-Interscience publication , 1978.

Mills, K.C. , *"Thermodynamic data for inorganic sulfides, selenides and tellurides"* , Published by Butterworth & Co (Publishers) Ltd , 1974.

McDonald,J.E. and Cobble, J.W., *J. Phys. Chem.*, 66, 791 (1962).

Base metal pressure leaching and PGM refining

Hofirek Z., *"Application of "non-oxidising" pressure leach as a key stage for reduction of sodium sulphate production in Ni/Cu matte refining"* , Alta Conference, 2002.

Ni pressure leaching and PGM refining

Cosmochimica Acta, Volume 62, Issue 15, August 1998, Pages 2643-2671.

PGM chemistry and precipitation processes

Leshch I.Yu. et al. , *"Autoclave method for the purification of copper solutions with the use of elemental sulphur"* , Tr-inta Gipronickel, Vosproyy tecknologii,vyp.38,1968,126-139

Benguerel, E., Demopoulos. G.P. and Harris, G.B., Solution chemistry and separation of Rhodium(III) from chloride solutions: a critical review. (no reference) 1993.

Benguerel, E., Demopoulos. G.P. , "A radically new solvent extraction process for Rh recovery" , In: Rhodium/sampling and analysis, ed. Kaltenbach, R.C., and Manziek, L., IPMI, New York, pp. 147-158, (1992)

Sassani D. C. and E. L. , *"Shock Solubility and transport of platinum-group elements in supercritical fluids: summary and estimates of thermodynamic properties for ruthenium, rhodium, palladium, and platinum solids, aqueous ions, and complexes to 1000°C and 5 kbar"* , *Geochimica et*

Ginzburg S.I. Ezerskaya, N.A., Profof'eva, I.V., et al , *"Analytical chemistry of platinum group metals"*, Nuaka, 1972

Bol'shakov, K.A., Sinitsyn, N.M., Borisov, V.V., and Borbat, V.F., *Dolk. Akad. Nauk USSR*, 1969, vol. 188, no.4, p. 815.

McPartlin, M., and Mason, R., Chem. Comm., 16, 1967.